UNIVERSIDADE DE LISBOA
INSTITUTO SUPERIOR TÉCNICO

Characterization of the Vdelta1+ T Cell Receptor repertoire during early and adult human life: implication of clonal diversity for cancer immunotherapy

Biagio Di Lorenzo

Supervisor: Doctor Bruno Miguel de Carvalho e Silva Santos

Co-supervisor: Doctor Cláudia Alexandra Martins Lobato da Silva

Thesis approved in public session to obtain the PhD Degree in BioEngineering

Jury final classification: Pass with distinction

2019

UNIVERSIDADE DE LISBOA
INSTITUTO SUPERIOR TÉCNICO

Characterization of the Vdelta1+ T Cell Receptor repertoire during early and adult human life: implication of clonal diversity for cancer immunotherapy

Biagio Di Lorenzo

Supervisor: Doctor Bruno Miguel de Carvalho e Silva Santos

Co-supervisor: Doctor Cláudia Alexandra Martins Lobato da Silva

Thesis approved in public session to obtain the PhD Degree in BioEngineering

Jury final classification: Pass with distinction

Jury

Chairperson: Doctor Joaquim Manuel Sampaio Cabral, Instituto Superior Técnico, Universidade de Lisboa
Members of the Committee:

Doctor Benjamin Ernest Willcox, Institute of Immunology and Immunotherapy, University of Birmingham, UK
Doctor Joaquim Manuel Sampaio Cabral, Instituto Superior Técnico, Universidade de Lisboa
Doctor Luís Ricardo Simões da Silva Graça, Faculdade de Medicina, Universidade de Lisboa
Doctor Bruno Miguel de Carvalho e Silva Santos, Faculdade de Medicina, Universidade de Lisboa
Doctor Sérgio Jerónimo Rodrigues Dias, Faculdade de Medicina, Universidade de Lisboa
Doctor Alexandre Valentim Xavier Mourão do Carmo, Instituto de Biologia Molecular e Celular

FUNDING INSTITUTIONS:

FCT scholarship PD/BD/105880/2014

2019

Resumo

As células T γδ desempenham funções importantes na interface entre o sistema imune inato e o adaptativo. Em humanos, a recombinação V(D)J e a expansão devida a antigénios ambientais resultam em dois subtipos principais de células T γδ: as células T Vγ9Vδ2, o subtipo predominante no sangue periférico (PB); e as células T Vδ1^{+}, o subtipo dominante no timo pós-natal e nos tecidos periféricos (e o segundo mais abundante no PB). Embora muito tenha sido dissecado na biologia de células T Vγ9Vδ2, sabe-se muito menos sobre o repertório, reconhecimento e ativação das células T Vδ1^{+}. Durante o meu projeto de doutoramento, abordámos essas questões usando uma combinação de ensaios genéticos, bioquímicos e imunológicos.

Primeiro, aplicamos *Next Generation Sequencing* (NGS) a timócitos Vδ1^{+} altamente purificados (FACS). A caracterização do repertório revelou aspectos até agora desconhecidos no que diz respeito aos repertórios *TRG* e *TRD* rearranjados e expressos por estes timócitos. O nosso estudo constitui um recurso que fornece novos dados e qualifica conclusões prévias sobre o repertório do receptor de células T (TCR) γδ tímicas humanas.Em seguida, explorámos o potencial imunoterapêutico das células PB Vδ1^{+}. Usando o nosso protocolo de grau clínico desenvolvido recentemente para expansão e diferenciação de células *Delta One T* (DOT), descobrimos que elas são altamente citotóxicas contra amostras primárias de leucemia mielóide aguda (AML) e linhas celulares, incluindo células selecionadas para resistência a quimioterapia, sugerindo uma ampla capacidade de reconhecimento. A injeção de células DOT *in vivo* reduziu a carga de AML no sangue e órgãos de múltiplos modelos de xenoenxerto de AML humana e prolongou significativamente a sobrevivência dos animais, sem qualquer toxicidade perceptível, fornecendo a *proof-of-concept* para a aplicação de células DOT no tratamento de AML. Finalmente, graças a uma abordagem bioquímica desenvolvida em colaboração com o laboratório de Julie Dechanet-Mérville, fornecemos novos conhecimentos sobre os mecanismos de reconhecimento de células tumorais por células T γδ, apoiando um novo modelo de trabalho no qual a indução de complexos CD3-TCR permite aos múltiplos Vδ1^{+} γδTCR reconhecer uma molécula do tipo "superantígénio" na superfície da célula-alvo, sem envolvimento da região CDR3, superando assim a necessidade de ligandos específicos para clones. Isto abre novos caminhos para a investigação num esforço conjunto e contínuo com nossos colaboradores.

No geral, a minha tese de doutoramento desvendou vários novos aspectos da biologia da célula T γδ Vδ1^{+}, desde o seu desenvolvimento no timo humano até ao seu potencial terapêutico contra células tumorais, destacando assim a sua importância dentro do sistema imunológico humano.

Palavras-chave: células T γδ; análise de repertórios γδTCR tímicos; clonalidade do TCR γδ; DOT targeting de AML; identificação de ligandos

Summary

γδ T-cells play important roles at the interface between the innate and the adaptive immune systems. In humans, V(D)J recombination and expansions due to environmental antigens result in two major subsets of γδ T-cells: Vγ9Vδ2 T-cells, the predominant subtype in the peripheral blood (PB); and Vδ1$^+$ T-cells, the dominant one in post-natal thymus and in peripheral tissues (and second most abundant in PB). Whereas a lot has been dissected in Vγ9Vδ2 T-cell biology, much less is known about the repertoire, recognition and activation of Vδ1$^+$ T-cells. During my PhD project, we addressed these issues using a combination of genetic, biochemical and immunological assays.

First, we applied Next Generation Sequencing (NGS) to highly (FACS-)purified Vδ1$^+$ thymocytes. Their repertoire characterization revealed unsuspected aspects of thymic rearranged and expressed *TRG* and *TRD* repertoires. Our study constitutes a resource providing new data and qualifying previous conclusions on the TCR repertoire of human thymic γδ T-cells.

We next explored the immunotherapeutic potential of PB Vδ1$^+$ T-cells. Using our recently developed clinical-grade protocol for expansion and differentiation of "Delta One T" (DOT)-cells, we found them to be highly cytotoxic against acute myeloid leukemia (AML) primary samples and cell lines, including cells selected for resistance to standard chemotherapy, suggesting a broad recognition domain. Transfer of DOT-cells *in vivo* reduced AML load in the blood and target organs of multiple human AML xenograft models; and significantly prolonged host survival, without any noticeable toxicity, thus providing the proof-of-concept for DOT-cell application in AML treatment.

Finally, thanks to a biochemical approach designed in collaboration with the Dechanet-Mérville laboratory, we provided new insights into the mechanisms of tumour cell recognition by γδ T-cells, supporting a novel working model in which inducing CD3-TCR complex clustering enables multiple Vδ1$^+$ γδTCRs to recognize a "superantigen"-like molecule on the target cell surface, with no involvement of the CDR3 region, and thereby overcoming the need of clonal-specific ligands. This opens new avenues for investigation in a joint and continued effort with our collaborators.

Overall, my PhD thesis unravelled various new aspects of Vδ1$^+$ γδ T-cell biology, from their development in the human thymus to their therapeutic potential against tumour cells, thus highlighting their importance within the human immune system.

Keywords:

γδ T cells; analysis of thymic γδTCR repertoires; γδTCR clonality; DOT cell targeting of AML; ligand identification

Acknowledgments

I am grateful to a number of people without whose support this stage of my personal and scientific life would not have been possible. Indeed, four years abroad are much more than a PhD.

First of all, I want to thank Bruno Silva-Santos. I am not starting from him just because he has been my supervisor, but because he was able to transmit me his enthusiasm for science during this last three years I spent in his lab. And this was essential to me, because he allowed me to keep my interest and focus for science, to successfully finish my research projects and to reach many important achievements. He is not only the lab head, but an excellent leader, mentor and friend as well. I always found him very attentive to the needs of his lab members (me included) and very supportive, even when I told him that it was time for me to hang up my pipette and gloves and to try to do science in a different way.

I was honoured to have Bruno as supervisor, but I also have to state that this work is also the result of the vibrant and amazing scientific community I found in Lisbon and abroad.

Indeed, I want to thank..

.. Claudia Lobato da Silva from IST, my co-supervisor: beside being a really smart scientist, she supported me all along and especially during the first year at the MIT-Portugal Program, helping me to find my place in Bruno's lab;

.. Luis Graça, Sergio Dias, João Barata from IMM for their scientific contribution. They were always available for discussion and willing to help;

.. Pedro Fernandes from IGC. He gave me his support and motivation to do something that I was trying to avoid so far: bioinformatics;

..Julie Dechanet-Mérville from the University of Bordeaux: she gave a big contribution to my research project, being always present for scientific discussion and hosting me during six months in her lab;

.. David Vermijlen from the Université Libre de Bruxelles and Immo Printz from the Hannover Medical School: their scientific contribution and their collaboration were essential for the development of my PhD projects.

And I was extremely lucky to do my research project in Bruno's lab. It would be impossible to thank one by one all the great people I have met during my stay in the lab: Ana, André, Anita, Carolina C, Carolina J, Daniel C, Daniel I, Francisco, Gina, Gisela, Hakan, Helena, Hiroshi, Julie, Karine, Miguel, Natacha, Nina, Paula, Pedro, Sergio, Sofia, Tiago, all the Master's students and visiting people. I shared most of my time in Lisbon with them and I can truly say they are great people beside being great scientists.

However, I want to give a special thanks to Tiago, Andre, Paula, Helena and Miguel. They were my family in Lisbon. It was so hard to say them goodbye, but we have that kind of friendship that cannot be damaged by the time and the distance. Thanks as well for turning on the PC in the lab and allowing me to work remotely from Italy on my thesis and on the revisions for the papers!!! Thanks to Debanjan, Ines, Daniel P, Susana, Luis F: they were part of my Lisbon family and it is also thanks to their support and friendship that I enjoyed my time in Lisbon.

I want also to thank the whole community at IMM, where I met a lot of nice, friendly and motivated people.

Thanks to Paola Tieppo from David Vermijlen's lab and Sarina Ravens from Immo Prinz's lab for their technical and scientific.

Thanks to Julie Dechanet-Mérville's lab, especially to Sonia Netzer and Vincent Pitard (because I learnt a lot from them) and to Angela Pappalardo (because it was good to have an Italian friend in the lab!).

Thanks to the water polo teams of Estádio Universitario de Lisboa and of Saint Bruno in Bordeaux.

Thanks to the MIT-Portugal People and colleagues!

Thanks FCT for funding.

Grazie agli amici imperdibili, che ci sono sempre anche se ci sente e ci si incontra poco, soprattutto Nicola e Aisha, che mi avete visto crescere come persona e scienziato, da studente universitario fino a (quasi) dottorato.

Voglio anche ringraziare di cuore il Gruppo di Italiani che ho incontrato a Bordeaux e specialmente i miei amici siciliani Nadia e Giovanni: tutti voi avete contribuito alla mia permanenza in città!

Un grazie speciale a Sonia, alla nostra amicizia nata a Bordeaux e che pian piano si è trasformata in qualcosa di diverso, più grande e più forte nonostante la distanza e le difficoltà che essa comporti. Grazie per starmi vicino, confortarmi e darmi modo di confrontarmi, per tutte le esperienze e viaggi che abbiamo condiviso e che vogliamo condividere.

Grazie a Mamma, a Papozzo e a Cri, i miei punti di riferimento da sempre e che non smetto mai di ringraziare.

Grazie a Skype e WhatsApp che ci hanno permesso di stare vicino anche a migliaia di chilometri di distanza!

I also want to thank all the people with whom I shared bad and good experiences during these last four years of my life. All of them contributed to making me the person I am now.

Index

Index of figures

Index of tables

List of abbreviations

ACT	Adoptive cell therapy
ADCC	Antibody-dependent cellular cytotoxicity
AHR	Aryl hydrocarbon receptor
AIDS	Acquired immunodeficiency syndrome
AML	Acute myeloid leukaemia
APC	Antigen presenting cell
BATF	Basic leucine zipper transcription factor
BCG	Bacillus Calmette-Guérin
BCL-6	B cell lymphoma 6
BLIMP1	B Lymphocyte-induced maturation protein
BP	Base pair
BTLA	B- and T-lymphocyte attenuator
BTN3A1	Butyrophilin 3A1
CAR	Chimeric antigen receptor
CBL-B	Casitas B-lineage lymphoma B
CCL	CC-chemokine ligand
CCR	CC-chemokine receptor
CDR	Complementarity determining regions
CDX	Cluster of Differentiation x
CLL	Chronic lymphocytic leukaemia
CLP	Common lymphoid progenitor
CMV	Cytomegalovirus
CPG	Cytosine-guanin dinucleotide
CRTH2	Chemoattractant receptor-homologous molecule expressed on TH2 cells
CTL	Cytotoxic T lymphocyte
CTLA4	Cytotoxic T lymphocyte antigen 4
CXCR	CXC-chemokine receptor
D	Diversity
DC	Dendritic cell
DN	Double negative
DNA	Deoxyribonucleic acid
DNAM1	DNAX accessory molecule-1
DNTPS	Deoxynucleotide triphosphates
DOT	Delta One T cell
DP	Double positive
EBV	Epstein-Barr virus
EGR	Early Growth Response
EOMES	Eomesodermin
FOX	Forkead box
GATA3	GATA-binding protein 3
GBV-C	Hepatitis G virus
GITR	Glucocorticoid-induced TNF-receptor related protein
GRAIL	Gene related to anergy in lymphocytes

HCV	Hepatitis C virus
HIV	Human immunodeficiency virus
HMBPP	Hydroxy-3-methyl-but-2-enyl pyrophosphate
HSC	Haematopoietic stem cell
HSCT	Hematopoietic stem cell transplantation
HSV	Herpes Simplex virus
HTS	High-throughput DNA sequencing
HVEM	Herpesvirus entry mediator
ICOS	Inducible T cell co-stimulator
ID3	Inhibitor of DNA binding 3
IFN-Γ	Interferon γ
IG	Immunoglobulin
IGSF	Immunoglobulin superfamily
IL	Interleukin
INOS	Inducible nitric oxide synthase
IPP	Isopentenyl pyrophosphate
IRF4	Interferon-regulatory factor 4
ITAMS	Immunoreceptor tyrosine-based activation motifs
ITCH	Itchy homologue E3 ubiquitin protein ligase
J	Joining
KGF	Keratinocyte growth factor
LAG3	Lymphocyte activation gene 3
LPS	Lipopolysaccharide
LTA	Lymphotoxin-α
MAF	Musculoaponeurotic fibrosarcoma oncogene
MAIT	Mucosal-associated invariant T
MBD2	Methyl-CpG-binding domain protein 2
MDSCS	Myeloid derived suppressor cells
MHC	Major histocompatibility complex
MPP	Multipotent progenitor
MR1	MHC-related protein 1
Mtb	*M. tuberculosis*
NCR	Natural cytotoxicity receptor
NEDD4	Neuronal precursor cell-expressed developmentally downregulated 4
NK	Natural Killer cell
NKG2D	C-type lectin-like NK receptor group 2 member D
NKR	NK receptor
NKT	Natural killer T
PAG	Phosphoantigen
PAMP	Pathogen associated molecular pattern
PBL	Peripheral blood lymphocyte
PBMC	Peripheral blood mononuclear cell
PCR	Polymerase chain reaction
PD1	Programmed cell death 1
PLZF	Promyelocytic leukaemia zinc-finger

PPR	Pattern recognition receptor
PTEN	Protein phosphatase and tensin homolog
PTA	Pre-TCRα
ROR	Retinoic acid receptor-related orphan receptor
ROS	Reactive oxygen species
RUNX3	Runt-related transcription factor 3
SAP	SLAM-associated protein
SFKS	Src-family kinases
SLAM	Signalling lymphocytic activation molecule
SMAD	Small mothers against decapentaplegic homologue
STAT	Signal transducer and activator of transcription
TCR	T cell receptor
TdT	Terminal deoxynucleotide transferase
TFH	T follicular helper
TGFB	Transforming growth factor β
TH	T helper
THPOK	Th-inducing POZ/Kruppel-like factor
TIL	Tissue infiltrating lymphocyte
TIM3	T cell immunoglobulin domain and mucin domain protein 3
TLR	Toll-like receptor
TNF	Tumour necrosis factor
TNFR	Tumour necrosis factor receptor
TRAIL	TNF-related apoptosis-inducting ligand
TRAILR	TNF-related apoptosis-inducting ligand receptors
ULBP	UL16 binding protein
UMI	Unique molecular identifier
V	Variability
WNV	West Nile virus

1 Introduction

There are three main lineages of lymphocytes in jawed vertebrates that use genetically recombined receptors to survey their environment and mediate host defence against disease: B cells, αβ T cells and γδ T cells. Although γδ T cell have been described for the first time in the mid-1980s, this cell type is still the least characterized among the main lymphocyte lineages. γδ T cells operate at the interface between the innate and adaptive immune systems. They share the expression of a somatically recombined T cell receptor (TCR) with conventional T cells but their reactivity and dynamics of response align with innate immunity. Despite various well described functions in immunity to infection and cancer, the molecular requirements for γδ T cell development in the thymus, or their activation upon antigen recognition in the periphery, remain poorly defined[1].

1.1 Immune System and Lymphocytes

1.1.1 Innate and Adaptive Immunity

The immune system is classically divided into two main effector arms: innate immunity, which provides the first line of defence; and adaptive immunity which specifically recognizes and selectively eliminates foreign microorganisms or transformed cells[2] (Table 1).

Innate immunity mostly consists of components that are already present before the onset of infection and are thus not specific to a given pathogen. In fact, the first host-protecting barriers that a pathogen encounters and need to transpose are physiological and anatomic ones, such as the skin or the mucosal membranes. If a pathogen overcomes these physical barriers, the innate immune system contains a large set of cells capable of discriminating between dangerous or beneficial microbes and will act within minutes after pathogenic exposure, creating a protecting inflammatory response and subsequently regulating an effective adaptive immune response[3].

The innate immune system includes hematopoietic cells such as macrophages, dendritic cells (DC), mast cells, neutrophils, basophils, eosinophils and natural killer (NK) cells. These cells are activated during an inflammatory response and quickly differentiate into short-lived effector cells, ready to clear off the infection[3]. Some of the main effector functions of innate immunity includes phagocytosis exerted by some of these cells, like neutrophils and tissue macrophages; proinflammatory cytokines released by macrophages, such as IL-6, IL-12 and TNF, which are endowed with antimicrobial activity[4]; activation of the complement cascade to identify bacteria and promote their clearance[5]; release of reactive oxygen species (ROS) by neutrophils, which are very cytotoxic for bacteria[6]; elimination of infected cells by NK cells, that are rapidly stimulated by innate cytokines, and release of cytolytic molecules such as granzymes and perforin, which are crucial for the clearance of virus-infected and also tumour cells[7,8].

Table 1.1 Innate and adaptive immunity (adapted from [2])

Attribute	*Innate immunity*	*Adaptive immunity*
Receptors	Not rearranged	Rearranged
Distribution	Population, non-clonal	Clonal
Recognition	Conserved molecular pattern	Antigen specific structure
Self and non-self discrimination	"Perfect" selected over evolutionary time	"Imperfect": selected in individual somatic cells
Action time	Immediate	Delayed
Response	Co-stimulatory molecules Cytokines Chemokines Phagocytosis Cytotoxicity	Clonal expansion Effector cytokines Cytotoxicity

On the other hand, adaptive immunity mediates reactions that are specific to antigenic challenges, thanks to their ability of recognize antigen and selectively eliminate cells bearing that antigen. Therefore, adaptive cellular immune responses are characterized by antigenic specificity, diversity and immunological memory.

The two major mediators of adaptive immunity are T and B lymphocytes, which develop in primary lymphoid organs (thymus and bone marrow, respectively) and then traffic to secondary lymphoid organs (such as lymph nodes and spleen) and tissues, where they can be exposed to antigens. It is important to highlight that the innate and adaptive immune systems are not independent, but rather tightly linked and interdependent: cells of the innate immune system are able to activate and recruit T and B lymphocytes, which in turn can amplify innate immune responses[9].

Moreover, the compartmentalization into innate and adaptive immunity is not really clear-cut (Figure 1.1). Straddling at the interface between innate and adaptive immunity there are some cell types[10], namely B-1 cells, NKT cells and γδ T cells, which are the focus of this thesis.

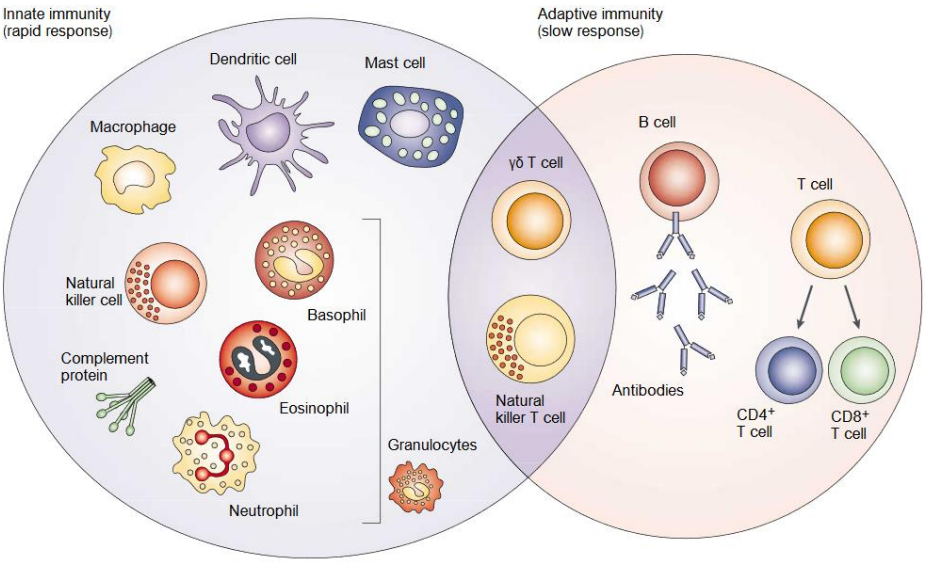

Figure 1.1 The innate immune response is the first line of defence against infection. It consists of soluble factors, such as complement proteins, and diverse cellular components including granulocytes (basophils, eosinophils and neutrophils), mast cells, macrophages, dendritic cells and natural killer cells. The adaptive immune response is slower to develop but manifests as increased antigenic specificity and memory. It consists of B cells, and CD4⁺ and CD8⁺ T lymphocytes. Natural killer T cells and γδ T cells are cytotoxic lymphocytes that straddle the interface of innate and adaptive immunity[10].

1.1.2 Hematopoietic stem cell (HSC) differentiation into T cells

Blood cells originate from common precursors named haematopoietic stem cells (HSC) (Figure 1.2), a subset of pluripotent progenitors with the ability to differentiate into many different cell types and to self-renew, thus maintaining their homeostasis by cell division. Human haematopoiesis starts with the production of primitive erythroid cells containing embryonic haemoglobin in the embryonic yolk sac during the first weeks of development. After this stage and around the third month of gestation, HSCs migrate from the yolk sac to the foetal liver and spleen, and appear and start to differentiate in the bone marrow[11]. HSCs are defined by the expression of CD49f and other markers, but their heterogeneity has not been investigated. Subsequent steps in haematopoiesis towards the T cell commitment are the differentiation in multipotent progenitors (MPPs), identified by the loss of CD49f expression, and in common lymphoid progenitor (CLP) with the acquisition of CD10 and CD45RA expression[12]. A finely tuned system of transcription factors regulates this process. The commitment of a HSC to the CLP pathway is regulated by different transcription factors, such as c-Myb, PU.1, GATA-2 and Ikaros[13]. The following event in T cell development, upon export of CLPs from the bone marrow to the thymus, is the commitment to the T cell lineage, which involves additional transcription factors such as GATA-3 and Notch1[14]. The crucial event that later locks the commitment of a cell to the T cell lineage is the rearrangement of the gene loci encoding the T cell receptor (TCR).

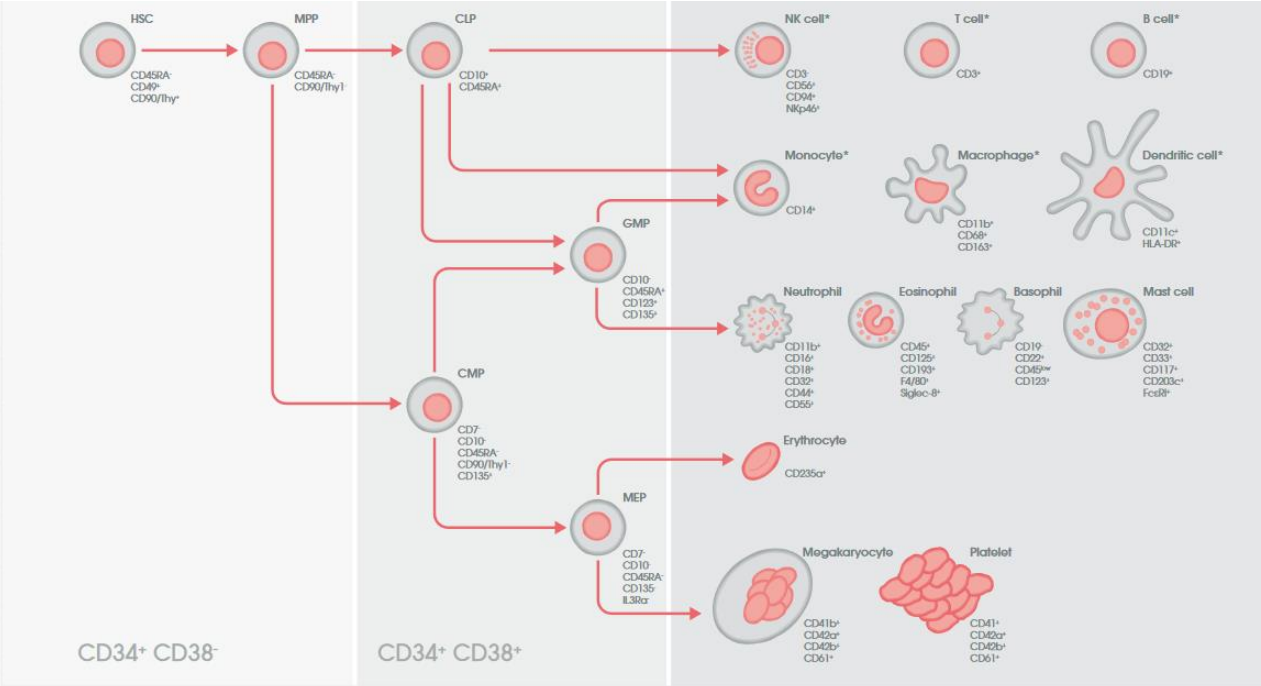

Figure 1.2 Human immune cell populations. Origin and some of the most distinctive markers for the human hematopoietic cells of innate and adoptive immunity (from Abcam: https://www.abcam.com/primary-antibodies/immune-cell-markers-poster)

Once the hematopoietic program is completed, the T cell compartment is formed but is not completely functionally differentiated. T cells play several important roles in immune responses by directly secreting soluble mediators or through cell contact-dependent mechanisms. Distinct T cell subsets, or differentiation states, can be identified based on cell surface markers expressed and/or effector molecules produced by a particular T cell population (Table 1.2). Although effector T cells were originally considered to be terminally differentiated, a growing body of evidence has challenged this view and suggested that the phenotype of effector T cells is not completely fixed but is more flexible or plastic. T cells can have 'mixed' phenotypes and can interconvert from one subset phenotype to another, although instructive signalling can lead to long-term fixation of cytokine memory. T cell plasticity can be important for adaptation of immune responses in different microenvironments and might be particularly relevant for host defence against pathogens that colonize different tissues[15,16].

Table 1.2 Summary of current understanding of the surface markers, transcriptional regulators, effector molecules and functions of the different T cell subsets that participate in immune responses. Adapted from [17]

Subgroup	Cell Type	Surface phenotype	Transcription factors	Effector factors	Function
Naïve	$CD4^+$ αβ T cell	αβ TCR, CD3, CD4, CD45RA, CCR7, CD62Lhi, IL-7R (CD127)	THPOK		Patrol through lymph nodes scanning peptide–MHC class II molecule complexes on APCs for the presence of their cognate antigen. Following activation by APCs, naive $CD4^+$ T cells differentiate into effector or regulatory T cells; activated naive T cells also give rise to memory T cells.
	$CD8^+$ αβ T cell	αβ TCR, CD3, CD8, CD45RA, CCR7,	RUNX3		Patrol through lymph nodes scanning peptide–MHC class I molecule complexes for the presence of their cognate antigen. Following activation

		CD62Lhi, IL-7R (CD127)			by APCs, they differentiate into CTLs and memory T cells.
	Cytotoxic T cell	αβ TCR, CD3, CD8	EOMES, T-bet, BLIMP-1	Perforin, granzyme, IFN-γ	Cytotoxicity through effector molecules
	Exhausted T cell	CD3, CD8, PD1, TIM3, 1B11, LAG3	BLIMP1		Generated in response to chronic antigen-mediated TCR stimulation. These cells express inhibitory receptor and lack effector cytokine production
	Anergic T cell	αβ TCR, CD3, BTLA		GRAIL, CBL-B, ITCH, NEDD4	These cells are generated following TCR activation in the absence of co-stimulatory signals. This leads them to become unresponsive to subsequent stimulatory signals.
Regulatory	Tr1 cell	αβ TCR, CD3, CD4	Not known	IL-10	IL-10 mediated immunosuppression. These cells are generated from naive T cells in the presence of TGFβ and IL-27
	Natural Treg cell	αβ TCR, CD3, CD4, CD25, CTLA4, GITR	FOXP3, STAT5, FOXO1, FOXO3	IL-10, TGFβ, IL-35	Mediate immunosuppression and tolerogenic responses through contact-dependent and -independent mechanisms. These cells are generated in the thymus
	Inducible Treg cell	αβ TCR, CD3, CD4, CD25, CTLA4, GITR	FOXP3, FOXO1, FOXO3, STAT5, SMAD2, SMAD3, SMAD4	IL-10, TGFβ	Promote immunosuppression and tolerance by contact-dependent and independent mechanisms. These cells are generated from naive T cells in the periphery
	NKT cell	NK1.1, SLAMF1, SLAMF6, TGFβR, Vα24, Jα18	PLZF	IL-4, IFN-γ, IL-17A	Pro- and anti-inflammatory functions. Can modulate the immune responses in several different settings, including cancer, autoimmunity, allergy, infection and GVHD. CD1-restricted TCR.
	MAIT cell	Invariant Vα7.2, Jα19			Their TCR is MR1 restricted but have similarities to NKT cells
	CD8αα cell	αβ or γδ TCR, CD3, CD8αα, B220		IL-10, TGFβ	Gut intraepithelial lymphocytes. They can develop intra- or extra-thymically. γδ TCR$^+$ cells express KGF, whereas αβ TCR$^+$ cells do not. Most αβ TCRs are enriched for self-reactivity. They can have regulatory functions through the production of IL-10 and TGFβ.
	γδ T cell	γδ TCR, CD3, NKRs		IFN-γ, IL-17A, IL-17F, IL-22,	Enriched at epithelial surfaces, can have pro- and anti-inflammatory functions. Have characteristics of both innate and adaptive immunity
Memory	Central memory T cell	CCR7hi, CD44, CD62Lhi, TCR, CD3, IL-7R (CD127), IL-15R	BCL-6, BCL-6B, MBD2, BMκ1	IL-2, CD40L, low levels IL-4, IFN-γ, IL-17A	Preferentially reside in secondary lymphoid organs, mounting recall responses to antigens. Even though these cells lack immediate effector functions, they rapidly proliferate and differentiate into effector T cells following antigen stimulation.
	Effector memory T cell	CD62Llow, CD44, TCR, CD3, IL-7R (CD127), IL-15R, CCR7low	BLIMP1	Rapid and high production of inflammatory cytokines	Preferentially found in peripheral tissues. They provide immediate protection upon antigen challenge through, for example, the rapid production of effector cytokines.

Helper	TH1 cell	αβ TCR, CD3, CD4, IL-12R, IFN-γR, CXCR3	T-bet, STAT4, STAT1	IFN-γ, IL-2, LTα	Promote protective immunity against intracellular pathogens. By secreting IFN-γ, they induce activation of macrophages and upregulation of iNOS, leading to the killing of intracellular pathogens such as Leishmania major, Listeria monocytogenes and Mycobacterium spp. Their development is regulated by IL-12.
	TH2 cell	αβ TCR, CD3, CD4, IL-4R, IL-33R, CCR4, IL-17RB, CRTH2	GATA3, STAT6, DEC2, MAF, IRF4	IL-4, IL-5, IL-13, IL-10	Promote humoral immune responses and host defence against extracellular parasites. However, they can also potentiate allergic responses and asthma. Their development and maintenance are regulated by IL-4, IL-25 and IL-33.
	TH9 cell	αβ TCR, CD3, CD4	PU.1	IL-9, IL-10	Involved in host defence against extracellular parasites, primarily nematodes. Despite their production of anti-inflammatory IL-10, they promote allergic inflammation. Their role in other inflammatory diseases still remains unclear as this subset has only recently been characterized
	TH17 cell	αβ TCR, CD3, CD4, IL-23R, CCR6, IL-1R, CD161	RORγt, STAT3, RORα	IL-17A, IL-17F, IL-21, IL-22, IL-26, CCL20	Promote protective immunity against extracellular bacteria and fungi, mainly at mucosal surfaces. Also promote autoimmune and inflammatory diseases. Generated in the presence of TGFβ and IL-6 and/or IL-21 and are maintained by IL-23 and IL-1.
	TH22 cell	αβ TCR, CD3, CD4, CCR10	AHR	IL-22	Identified in inflammatory skin diseases. Their role in host defence remains unclear as this subset has only recently been characterized. Their identity as an independent TH cell subset needs to be confirmed.
	TFH cell	αβ TCR, CD3, CD4, CXCR5, SLAM, OX40L, CD40L, ICOS, IL-21R, PD1	BCL-6, STAT3	IL-21	These cells are involved in promotion of germinal centre responses and provide help for B cell class switching.

1.1.3 The γδ T cell lineage

γδ T cells have been discovered more than three decades ago[18] but are still not well defined in terms of their mechanisms of activation and target cell recognition. Despite the relatively small abundance of γδ T cells in the human blood, this lymphocyte population plays an important role at the interface between the innate and the adaptive immune systems. These cells share T cell receptor (TCR) rearrangements and memory functions[19] with their αβ T cell counterparts, but differ in their response kinetics and mechanisms of target cell recognition. Thus, γδ T cell activation is typically independent of antigen presentation by major histocompatibility complex (MHC) molecules. Furthermore, γδ T cells bear a plethora of NK cell receptors (NKRs) on their surface, which allow for very fast responses against infected or transformed

cells[20], thus contributing to an earlier line of defence that precedes antigen-specific αβ T cell responses[21]. Unlike αβ T cells, there is little evidence of thymic negative selection of self-reactive γδ T cells, but they seemingly expand in the periphery in response to microbial or stress-induced antigens.

1.2 The γδ TCR

What characterizes a γδ T cell is the surface expression of a TCR composed by the variable γ and a δ chains. The γδ TCR is a disulphide-linked membrane-anchored heterodimeric protein and member of the immunoglobulin superfamily (Figure 1.3)[22]. Each chain is composed of two extracellular domains: a variable (V) region and a constant (C) region, both of Immunoglobulin superfamily (IgSF) domain. The constant region is proximal to the cell membrane, followed by a transmembrane region and a short cytoplasmic tail, while the variable region binds to the antigenic determinant on the target cell. The variable domain of both chains has three hypervariable or complementarity determining regions (CDRs)[22]. The rearrangement of V, D, and J region sequence elements during lymphocyte maturation creates an enormous degree of diversity in an area referred to as the complementarity determining region 3 (CDR3) loop that is therefore the main CDR responsible for recognizing antigen[23]. Variations in the used V, D, and J elements used, precise points of recombination, and random nucleotide addition all lead to extensive length and sequence heterogeneity. TCR delta CDR3s are the most variable in size and are significantly longer than L and gamma chains, respectively. In contrast, TCR alpha and beta chain distributions are highly constrained, with nearly identical average CDR3 lengths, and their length distributions are not altered by thymic selection. Perhaps most significantly, these CDR3 length profiles suggest that γδ TCRs are more similar to Igs than to αβ TCRs in their putative ligand binding region[24], suggesting that they may have fundamentally different recognition properties.

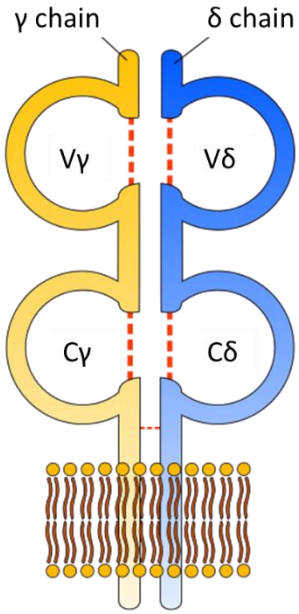

Figure 1.3 Schematic representation of the γδTCR

1.2.1 Genomic organization of the TCR γ and δ Loci

In humans, γδ T cells have a small repertoire of V gene segments to select from when undergoing chain rearrangement in comparison with those available for Vα (43–45)[25], Vβ (40–48)[26], Ig light (IgVκ 34–38, IgVλ 29–33)[27,28], or Ig heavy (38–46)[29] chain rearrangement. All the genetic information including the V, D, J segments and the C regions required to express functional γδ TCRs are encoded in the TRG and in the TRD loci. The human TRG locus is located on chromosome 7[30] at band 7p15-p14[31], is reverse-oriented and spans 160 kb. It consists of 19-22 genes: 12-15 TRGV belonging to 6 subgroups, upstream of a duplicated J-C cluster, which comprises, for the first part, 3 TRGJ (TRGJP1, TRGJP and TRGJ1) and the TRGC1 gene, and for the second part, 2 TRGJ (TRGJP2 and TRGJ2) and the TRGC2 gene (Figure 1.4). Two haplotypes with 12 or 14 TRGV genes correspond to allelic polymorphism by insertion or deletion of the TRGV4 and TRGV5 genes. A rare haplotype with 15 TRGV genes that includes the TRGV3P gene has been detected by Southern hybridization analysis but has not been sequenced[32]. Among the TRGV genes 4-7 are functional (Vγ2, Vγ3,

Vγ3P, Vγ4, Vγ5, Vγ8 and Vγ9), 3 are in ORF (Vγ1, Vγ10 and Vγ11) and 5 are pseudogenes (Vγ5P, Vγ6, Vγ7, VγA and VγP)[33] (Table 1.3).

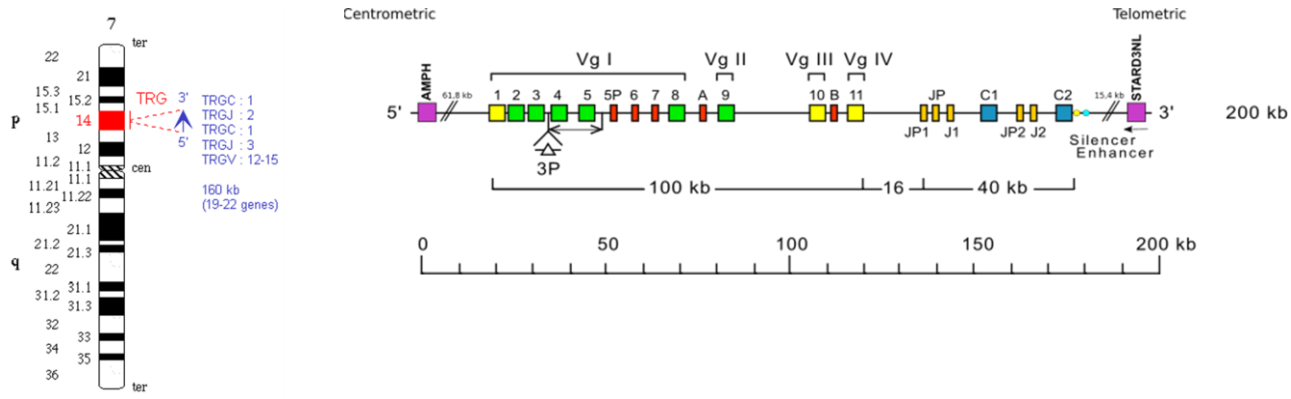

Figure 1.4 Location of the TRG gene (left) and genomic organization of the TRG locus (right).

On the other hand, the human TRD locus is forward-oriented, it spans 60 kb and is embedded in the TRA locus between the TRAV and TRAJ genes on chromosome 14[34] on the long arm at band 14q11.2[30] (Fig 1.2A). It comprises a cluster of 10 genes: 1 TRDV, 3 TRDD (D1, D2, D3 and D4) and 4 TRDJ (J1, J2, J3 and J4), the unique TRDC gene and 1 TRDV in inverted orientation at the 3' of the TRDC gene. 1 TRDV gene is located at 360 kb of TRDC, among the TRAV gene (Figure 1.5). 5 genes described as TRAV/DV have been found rearranged to either TRDD or to TRAJ and can therefore be used for the synthesis of δ and α chains. Except for the TRAV29/DV5 that can be functional or not according to the haplotype, all the described TRDV and TRAV/DV, TRDD, TRDJ and TRDC are functional (Table 1.3). Nevertheless, only three main Vδ gene segments, Vδ1, Vδ2 and Vδ3, are most frequently used in rearrangement of the δ chain; less commonly used are the five V segments that have both Vδ and Vα designation (Vδ4/TRAV14, Vδ5/TRAV29, Vδ6/TRAV23, Vδ7/TRAV36 and Vδ8/TRAV38)[35].

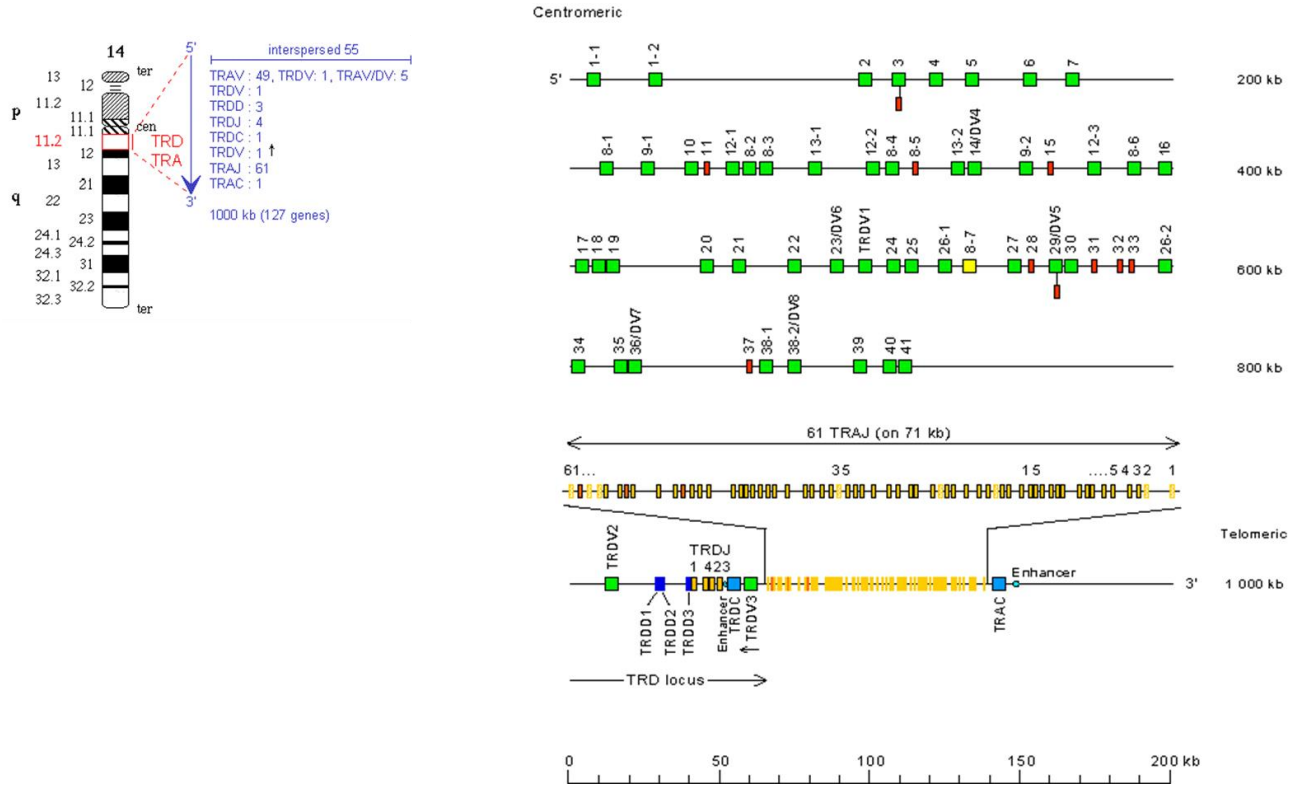

Figure 1.5 Location of the TRD gene (left) and genomic organization of the TRD locus (right).

*Table 1.3 TRG and TRD variable segment groups and functionality. ORF = Open Reading Frame; F = Functional; * = Allelic polymorphism by insertion/deletion, with no reported functionality; F** = Allelic polymorphism by insertion/deletion, reported to be functional in some haplotypes; P = Pseudogene.*

TRGV		
Subgroup	**Gene name**	**Functional**
1	TRGV1	ORF
	TRGV2	F
	TRGV3	F
	TRGV3P	*
	TRGV4	F**
	TRGV5	F**
	TRGV5P	P
	TRGV6	P
	TRGV7	P
	TRGV8	F
2	TRGV9	F
3	TRGV10	ORF
4	TRGV11	ORF
A	TRGVA	P
B	TRGVB	P

TRGD	
Gene name	**Functional**
TRDV1	F
TRDV 2	F
TRDV 3	F
TRAV14/DV4	F
TRAV23/DV6	F
TRAV29/DV5	F
TRAV36/DV7	F
TRAV38.2/DV8	F

1.2.2 V(D)J rearrangements

The somatic assembly of the TCR generates a diverse T cell repertoire and is an essential component of thymocyte development that instructs numerous cell lineage and cell fate decisions. TCR genes are assembled through V(D)J recombination, a site specific recombination process directed by the lymphoid-specific recombinase RAG (composed of RAG1 and RAG2) and ubiquitously expressed DNA repair proteins[36]. RAG proteins create double-strand breaks at recombination signal sequences (RSSs) that flank TCR variable (V), diversity (D) and joining (J) gene segments, and these breaks are subsequently resolved by nonhomologous end joining. A successfully recombined γ chain is composed by the rearrangement of a TRGV and TRGJ segment whereas a δ chain results from the TRDV, TRDD and TRDJ rearrangement.

The TRG V-J rearrangements create a combinatorial diversity of 20-30 recombinations. However, most of the γδ T cells from the peripheral blood express predominantly γδ T cell receptors with a V9-JP-C1 γ chain. The TRD V(D)J rearrangements (D-J then V to D-J rearrangements) create a combinatorial diversity of 36-224 recombinations. Two or three TRDD may be used in a V-D-D-J and V-D-D-D-J rearrangements leading to 192 or 224 potential recombinations, respectively. One important additional mechanism contributing to the T cell receptor γ and δ chain diversity is the N (for nucleotides) diversity, which results from the deletion and/or the addition of nucleotides at random position by the terminal deoxynucleotidyl transferase and creates regions not encoded in the germline DNA at the V(D)J junction. There are up to four N diversity regions in the V(D)J junctions in the δ chains comprising 3 TRDD. Altogether these mechanisms lead to a combinatorial diversity of 10^4 γ and 10^8 δ chains[33]. A second type of nucleotide insertion, termed P (palindromic), occurs adjacent to nontruncated V, D or J segments[37] and it is constituted by a very short inverted repeat of the adjacent full-length gene segment. These insertions are quite infrequent since occur in <10% of endogenous junctions, but have been demonstrated to happen when the terminal deoxynucleotidyl transferase activity is absent[38] and as consequence of resolution of a hairpin precursor during the V(D)J segment rearrangement[39]. Taking this into account, it is noteworthy that rearranged TCR delta genes can be very diverse at the V(D)J junctional region, since they can include D-D recombination which potentially increase the number of possible sequence combinations, and introduce additional sites for variable, template-independent N nucleotide insertion[40]

Although the thymus can generate all the possible combinations of TRG and TRD genes, the major γδ T cell population in peripheral blood (PB) expresses a TCR composed by Vγ9 recombined with JP and paired with Vδ2[41]. In fact, this specifically rearranged Vγ9Vδ2$^+$ T cell subset is mostly produced during foetal life but still constitutes the major γδ T cell subset in adults. Antigen-driven stimulation in the periphery underlies a strong and specific expansion of this subset after birth and during the lifespan of each individual. This topic will be further discussed in the next paragraph.

1.2.3 Foetal and post-natal γδ T cell development

The human γδ T cell repertoire global architecture undergoes several drastic changes from foetal to post-natal life. Indeed, the γδ PBMCs from healthy individuals are mostly composed of Vγ9Vδ2$^+$ lymphocytes, typically comprising 1–10% of total peripheral blood T cells and starting to expand during childhood[42]. These cells have the ability to respond to small pyrophosphate antigens (pAg) in a TCR-dependent manner,

a process relying on target cell expression of the butyrophilin (BTN) family member BTN3A1[43–45]. However, the expression pattern of γ and δ chains and their rearrangement change as ontogeny proceeds. More in detail, Vδ gene expression in the post-natal thymus can be distinguished from that occurring in foetal thymus, most clearly by the developmental change in Vδ2 expression. Vδ2 is the most conspicuously expressed δ gene segment in the foetal thymus and, as reported so far, may be even the earliest Vδ gene to be expressed. Hence, a high abundance of Vδ2-encoded γδ TCRs in the foetal thymus may at least in part be determined at the level of differentially regulated Vδ gene expression, but further experimental evidences are needed. Strikingly, the thymic expression of Vδ2 is drastically reduced soon after birth and this is consistent with the rarity of Vδ2 encoded TCRs in the post-natal thymus[46]. On the other hand, there is no Vγ gene predominantly expressed throughout foetal thymic ontogeny and, in particular, Vγ9 is not the predominant Vγ gene in the foetal thymus, despite the propensity of its product to pair with Vδ2. Expression of Vγ9 also declines dramatically in the post-natal thymus[46,47]. Other events changing the repertoire architecture take place as ontogeny proceeds. Indeed, the nucleolytic activity, meaning the N trimming of the sequences at the V(D)J joins, and the addition of N-nucleotides increase and this change is especially evident in post-natal Dδ3 and Jδ sequences, maybe reflecting true changes in enzymatic activity. For some reason, the increased nucleolytic activity does not seem to act on the Vδ gene segments: the 3' breakpoint of both Vδ1 and Vδ5 segments are strikingly limited and similar at all foetal and post-natal time points. In addition to the increase in N nucleotide diversification due to nucleolytic activity, there are also changes in gene segment utilization. The earliest Vδ-Dδ recombinations involve only Dδ3. At 17 weeks, Vδ5 joins show usage of Dδ1 and Dδ2 elements whereas these are only rarely apparent in Vδ1 joins at the same time. These data further support a model for regulated utilization of different gene segments in different sets of cells, with several populations of cells being present in the thymus at any one time. A model for regulated utilization of different gene segment is also suggested by the distinct shift to Jδ1 usage in post-natal thymus. Summarizing, as ontogeny proceed, junctional diversity increases, through at least three mechanisms: regulated utilization of more gene segments, increased N nucleotide insertions with more nucleolytic activity and increased variability in gene segment breakpoints[46].

Another big change happening straight after birth is a consistent shift in Vδ chain expression from Vδ2 to Vδ1. This change is then reflected in the difference between peripheral blood and thymus γδ cell distribution and, as consequence, it is particularly apparent at the level of Vγ9 cells, which in the peripheral blood is mostly expressed in the absence of Vδ1, while in the thymus it appears to be equally distributed on $V\delta1^-$ and $V\delta1^+$ cells. In addition, most of the adult $V\gamma9V\delta2^+$ cells express a receptor of very restricted molecular composition consisting of a Vγ9-JP-Cγ1 chain paired with a δ chain carrying the Vδ2 segment. In sharp contrast, thymic Vγ9 is rarely rearranged to the JP segment, being mostly joined to J2 and occasionally to JP1, J1 and JP2 and express the Cγ2 isotype. On the other hand, Vδ1 gene products pair with various Vγ with no clear biased for any Vγ; and are preferentially joined to Cγ2[47]. Therefore, compared to thymic repertoires, the peripheral γδ TCR repertoire appears therefore to be non-random at four levels: V gene usage, V-J combinations, pairing of Vδ chains to the Cγ1 or Cγ2 isotype and pairing of Vγ and Vδ[46,47].

As mentioned before, $V\gamma9V\delta2^+$ T cells dominate the γδ T cell repertoire[48] by mid-gestation (20–30 weeks - Figure 1.6) and $V\delta1^+$ T cell generation increases later in gestation, until this population comprises the majority of the γδ repertoire in cord blood and in paediatric thymus[48–50]. This change in chain expression is not reflected in the composition of adult γδ repertoires from healthy subjects, in which the $V\gamma9V\delta2^+$ subset persist as the most abundant. Microbial exposure is responsible for the dramatic postnatal numerical expansion of $V\gamma9V\delta2^+$ T cells, which ultimately dominate the circulating γδ T cell repertoire during childhood[19,51]. Consistent with this, $V\gamma9V\delta2^+$ T cells mature in phenotype early after birth concomitant with

their numerical expansion; moreover, several infections stimulate Vγ9Vδ2$^+$ expansion, and tellingly, identical twins have different Vγ9Vδ2$^+$ profiles[51].

In addition, another event influencing the Vγ9Vδ2$^+$ T cell architecture takes place during the prenatal life. As summarized in Figure 1.6, Vγ9Vδ2$^+$ T cell development is shaped by both prenatal and postnatal events, which impact Vγ9Vδ2$^+$ TCR repertoire and phosphoantigen (pAg) reactivity. Importantly, the human Vγ9Vδ2$^+$ TCR repertoire is composed of highly public Vγ9 chains, resulting in a semi-invariant repertoire largely preconfigured from birth for pAg reactivity[52]. Alongside public Vγ9 sequences, the Vδ2$^+$ repertoire is very diverse and private, and changes between neonatal and adult Vδ2$^+$ TCR repertoires suggest several selection events throughout life. Vδ2-Jδ3 TCRs are prevalent in cord blood and these may be positively selected in foetal development for recognition of host pAgs, or alternatively, these rearrangements may be preferentially generated in early gestation. Vδ2-Jδ1 chains with longer CDR3 and hydrophobic amino acids at position 5 ultimately dominate the Vδ2$^+$ repertoire in adults, and these may be selected from rare rearrangements in cord blood following microbial pAg exposure, or further Vγ9Vδ2$^+$ T cell generation may occur in the postnatal thymus. Nevertheless, these selection events produce a repertoire that exploits the somatically recombined Vγ9Vδ2$^+$ TCR as a surrogate pattern recognition receptor to sense pAgs.

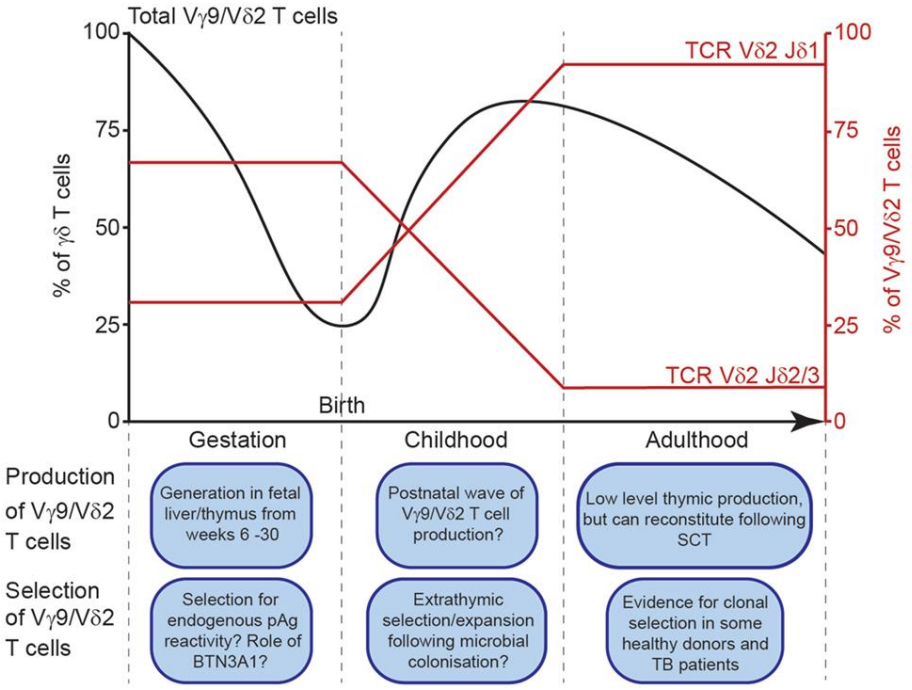

Figure 1.6 Schematic depiction of Vγ9Vδ2$^+$ T cell generation and selection throughout life. Vγ9Vδ2$^+$ T cells as a percentage of total peripheral blood γδ T cells throughout life (black line, left axis). Jδ usage among Vγ9Vδ2$^+$ T cells (red lines, right axis) throughout life[41].

1.2.4 The Vγ9Vδ2$^+$ TCR Repertoire in Healthy Adults: features for antigen responsiveness

Early studies identified Vγ9Vδ2$^+$ TCR features required for pAg responsiveness. Interestingly, adult Vδ2 CDR3s are highly diverse, composed of Vδ2 mainly joined to only one D segment (usually Dδ3), and typically used J segment Jδ1[53,54]. Additionally, a hydrophobic amino acid, typically Val/Leu/Ile at position 97 of the Vδ2 framework generated by N-nucleotide addition, was required for pAg recognition[54,55]. Conversely, Vγ9 gene segments are relatively restricted in CDR3γ sequence and length, and exclusively utilized JγP and

constant region Cγ1[47,53,56]. Several public clonotypes, generated by germline recombination with no N-nucleotide addition and minimal N trimming, have also been identified and conserved irrespectively of age, sex and race[56–58]. This could be the result of a strong postnatal peripheral selection and amplification of specific clonotypes following microbial exposure[59] or can be the product of a convergent recombination. Indeed, the most prevalent public clonotype[56] can be generated by near-germline recombination of Vγ9 and JγP gene segments with minimal nucleotide trimming and no N-nucleotide addition, incorporation of one or more palindromic (P)-nucleotides, addition of one or several non-templated (N)-nucleotides by terminal deoxynucleotide transferase (TdT), resulting in the same amino acid sequence, highlighting the presence of public sequences arisen *via* many independent recombination events in each donor from high frequency precursor sequences[60].

1.2.5 How to study the TCR repertoire

The generation of an adaptive immune receptor repertoire can be considered a strategy that uses individual cell clones within the multicellular organism to mimic the ability of microbial populations to rapidly undergo multiple rounds of reproduction, diversification and evolutionary selection, providing a successful counter-strategy partially overcoming the competitive disadvantage of organism whose generation times are measured in years rather than minutes[61]. This clonal diversity is extremely useful to the host but has constituted a major barrier to the comprehensive study of the adaptive immune receptors until quite recently, with the introduction of high-throughput DNA sequencing (HTS) methods.

1.2.5.1 Sequencing strategies

Pioneering work studying complex Ig/TCR loci and V(D)J gene rearrangements involved traditional molecular techniques like cloning, probe hybridization and Sanger sequencing [62–64]. Some important general features of the loci and the first characterization of the receptor repertoires have emerged from these pioneer studies, but the low throughput workflow limited the ability to fully assess the repertoire diversity. This issue was solved only recently with the advent of HTS technologies, that allowed the generation of massive amounts of data on the receptor diversity in human subjects, leading to new challenges in data analysis, sharing and archiving. Most of the current data in the literature and in public archives was generated using the Roche (454), Illumina and Ion Torrent instruments[61]. Common to the different platforms is the initial workflow: the starting materials are converted into double stranded DNA molecules which are then bounded with barcoded adapters for the ligation into linear DNA molecules. An important technical decision prior to starting is the choice of template (genomic DNA or cDNA synthesized from either total RNA or mRNA). This will lead to a different outcome: using gDNA for HTS will allow the sampling and the analysis of productive and unproductive V(D)J segment rearrangements for specific applications; using RNA as template will give a greater likelihood of capturing a more complete representation of clonal distribution and frequency[65,66]. After the library generation, the dsDNA molecules are bounded with adapters. The adapters themselves work as bridge between the resultant library with either micro beads or a flow cell, for the amplification through emulsion polymerase chain reaction (PCR) or bridge PCR. Moreover, because of the close proximity of rearranged V(D)J segments, the PCR amplification can be designed to include the full V(D)J region using various gene-specific primer strategies, therefore allowing the amplification of the critical CDR3 sequence and providing sufficient information to examine many of the

receptor features including the analysis of receptor diversity, detection clonal expansions, or tracking of particular clones and clonotypes[61]. By definition, a clonotype is a unique nucleotide sequence that arises during the gene rearrangement process for that receptor[67]. Therefore, each γδ T cell has two clonotypes, one for the γ chain and one for the δ chain. After the PCR amplification, the reaction product must be sequenced, and this step will be different among the distinct platforms: Roche 454 employs a pyrosequencing strategy whereas Illumina and Ion Torrent use a sequencing-by-synthesis strategy (Figure 1.7).

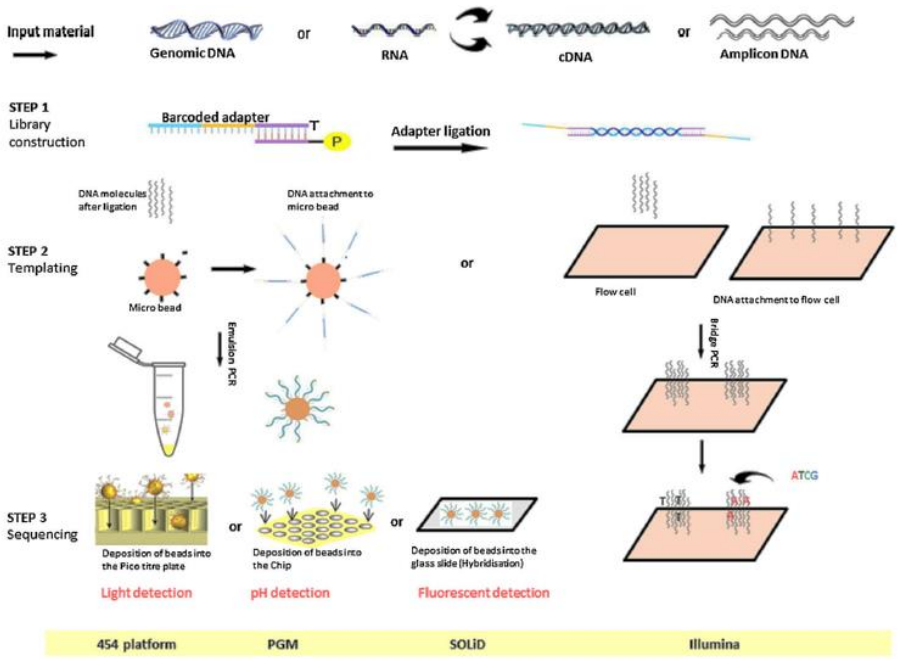

Figure 1.7 Graphic representation of the library construction, templating and sequencing process of HTS platforms. Different types of starting materials are converted into double stranded DNA molecules which are then bounded with barcoded adapters for ligation into linear DNA molecules. Adapters enable the bounding of the resultant library with either microbeads or a flow cell, for amplification through emulsion PCR or bridge PCR. The ensuing clonal amplicons are then deposited on the picotiter plate, chip or glass slide for sequencing depending upon the sequencing platforms. Adapted from[68]

In more details, pyrosequencing is a method of DNA sequencing that relies on the detection of pyrophosphate release and the generation of light upon nucleotide incorporation; during the sequencing-by-synthesis, a fluorescently labelled and reversible terminator is imaged as each dNTP is added, and then cleaved to allow incorporation of the next base. Since all four reversible terminator dNTPs are present during each sequencing cycle, natural competition minimizes incorporation bias. The result is true base-by-base sequencing that enables accurate data for a broad range of applications. The method virtually eliminates errors and missed calls associated with strings of repeated nucleotides (homopolymers). Therefore, the main difference in the sequencing step is that Roche (454) and Ion Torrent platforms use reaction mixtures containing only one of the deoxynucleotide triphosphates (dNTPs) per sequencing cycle, whereas Illumina uses a mix of all four dNTPs with nucleotide-specific fluorophores in each sequencing cycle[61]. While the Ion torrent and Roche platforms produce longer reads (table 1.4), they are more vulnerable than the Illumina platform to sequencing errors in homopolymer regions. Possibly owing partly to this and also due to continual length improvements (the current longest supported runs yield paired-end sequences of 300 bases on the Illumina MiSeq), Illumina instruments have become the dominant platform for Ig repertoire sequencing[61,68].

Table 1.4 Comparison of the three-leading benchtop HTS platforms

Company	Platform	Sequencing chemistry	Read length/ Output	Advantages	Disadvantages
Roche	454	Pyrosequencing	400-500bp/35Mb	Long read length Fast run time	Expensive Low throughput Homopolymer errors
Illumina	MiSeq	Sequencing by synthesis	2*300bp/15Gb	Least number of errors High throughput Low cost Fully automated workflow	Long run time Short reads
Life Technologies	Ion proton	Sequencing by synthesis	200bp/10Gb	Short run time Highly scalable Low cost	High error rate

1.2.5.2 Bioinformatics pipelines for the pre- and pro-processing analysis of adaptive immune repertoires

The bioinformatics and other data analysis approaches applied to the generated HTS data are critical for deriving biologically meaningful results. Some features in processing raw HTS data from adaptive receptor repertoire sequencing experiments are common to all studies and can be grouped as pre-processing workflow (Figure 1.8). For HTS data generated from paired-end DNA sequencing, such as on the Illumina MiSeq instrument, early steps involve merging of read-pairs followed by demultiplexing of barcodes to determine sample identity and extraction of unique molecular identifiers (UMIs). Many pipelines will include primer and library adapter trimming to remove sequence data derived from the experimental protocol and, as last step, quality filtering. Merged and trimmed reads are then aligned to the V, D and J germline segments, enabling analysis of the degree of exonuclease shortening of segment ends and the addition of non-templated nucleotides (N) in the segment junctions that occur during the V(D)J recombination[61]. The most popular choices for the alignment to the germline segments are IMGT/V-QUEST[69], IgBLAST[70] and MiXCR[71].

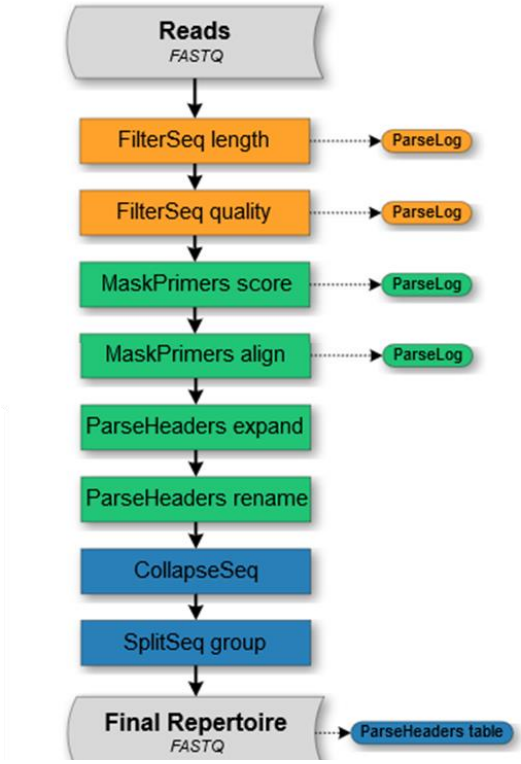

Figure 1.8 Bioinformatics pipeline for the pre-processing analysis of the adaptive immune repertoires

1.2.5.3 Software used for TCR repertoire analysis

If the pre-processing analysis until the alignment to the germline sequences can be considered universal for the adaptive immune repertoire analysis, most of the useful information can be obtained through the post-processing analysis, a more personal and subjective way of analysing adaptive immune repertoires. In this section I will briefly describe the software employed to obtain the data present in this PhD thesis, from the alignment to the germline sequences to the post-analysis of the T cell receptor repertoires.

- MiXCR[71] is a universal framework that processes big immunome data from raw sequences to quantitated clonotypes. MiXCR handles paired- and single-end reads, considers sequence quality, corrects PCR errors and identifies germline segments and hypermutation employing a built-in library of reference germline V, D, J and C gene sequences for human and mouse based on corresponding loci from GenBank[72]. Since it also captures all CDRs and framework regions of immune genes, MiXCR can also assembles identical reads into clonotypes.
- IMGT[69] is a web portal that provides the high-quality results of germline alignment and junctional analysis for the antigen receptor repertoire sequences generated from HTS. The results are based on the use of standardized gene and allele nomenclature, standardized description and delimitation of labels (especially for the CDRs and FRs regions), and extensive and accurate analysis of the junctional regions. It analyses up to 150,000 nucleotide sequences per batch and performs statistical analysis on the results of up to 450,000 sequences[69].
- VDJ tool[73] is a complementary software suite that solves a wide range of T cell receptor (TCR) repertoires post-analysis tasks, providing a detailed tabular output and graphics. VDJtools analysis routines can be grouped into 6 modules:
    1. Basic statistics and segment usage module include general statistics (clonotype and read count, number and frequency of non-coding clonotypes, convergent recombination of CDR3 amino acid sequences, insert size statistics, etc), spectratyping (distribution of clonotype frequency by CDR3 length), V and J segment usage profiles and their pairing frequency in rearranged receptor junction sequences.
    2. Repertoire overlap module includes routines for computing sets of overlapping clonotypes and their characteristics, and scatter plots of clonotype frequencies.
    3. Diversity analysis includes routines for visualizing clonotype frequency distribution, computing repertoire diversity estimates and rarefaction plots.
    4. The fourth set of routines can be used to create clonotype abundance profiles and track clonotypes in time course of vaccination, myeloablation and blood cell transplant.
    5. Sample clustering is implemented based on computed repertoire similarity measures and could be used to distinguish various biological conditions, cell subsets and tissues.
    6. Auxiliary routines provide means for clonotype table filtering (e.g. by segment usage or non-coding CDR3 sequence) as well as annotation with custom or pre-built pathogen-specific clonotype database.
- tCR[74] is an R package for the post-analysis of TCR repertoires that integrates widely used methods for individual repertoires analyses and TCR repertoires comparison. Its features consist of: gene usage comparison, customisable search for clonotypes shared among repertoires, spectratyping, random TCR repertoire generation, various repertoire diversity measures and other commonly used approaches to the repertoire analysis. The tCR statistics include counts and percentages of TCR nucleotide and amino acid clonotypes, V and J gene usage, clonal count skewness and distribution of CDR3 sequence lengths
- Vegan[75] is an R package that provides tools for descriptive community ecology. It has most basic functions of diversity analysis, community ordination and dissimilarity analysis. This software was employed to estimate the Shannon index diversity. The measure was originally proposed by Claude Shannon to quantify the entropy (uncertainty or information content) in strings of text. The idea is that the more different letters there are, and the more equal their proportional abundances in the string of interest, the more difficult it is to correctly predict which letter will be the next one in the

string. The Shannon entropy quantifies the uncertainty (entropy or degree of surprise) associated with this prediction.

- Treemap[76] is a R package useful for space-filling visualization of hierarchical structures

1.3 γδ T cell signalling

γδ T cell immune functions depends on their ability to become activated, differentiate, kill the infected or transformed cells and switch off their activity. These processes are finely tuned by different classes of surface receptors that transform extracellular stimuli into downstream intracellular signals. In particular, these surface receptors influencing γδ T cell physiology could be clustered in five subtypes types: the T cell receptor (TCR) complex, costimulatory receptors, cytokine receptors, NK receptors, and inhibitory receptors[20].

1.3.1 The γδ TCR complex

The γδ TCR itself has no intrinsic signalling capacity and it is organized in a multimeric complex to exert its function after antigen recognition. More in detail, the γδ TCR complex is composed by a clonotypic γδ TCR heterodimer, by the CD3δε and/or CD3γε dimer and by the ζζ dimer, following the final TCRγδCD3ε_2γδζ_2 stoichiometry[77]. The TCR-dependent intracellular cascade starts when the Src-family kinases (SFKs) Lck and Fyn phosphorylate the immunoreceptor tyrosine-based activation motifs (ITAMs) in the CD3 cytoplasmic domains[78]. SFKs have been shown to be indispensable in γδ T cells activation[79] but how their recruitment takes place is still unknown, since CD4 or CD8, the mediators of SFK recruiting upon αβTCR ligation[78] , are not expressed in most γδ T cells. Secondly in the signalling cascade is the phosphorylation and activation of Zap70, event that in turns facilitates phosphorylation of the scaffolding proteins SLP-76 and LAT. The so formed supramolecular complex (signalosome) allows the recruitment of PLCγ1, resulting in the propagation of downstream signalling events[80].

In the case of Vγ9Vδ2$^+$ T cells, whose TCR specificity is described in 1.5.5, their ligand is able to trigger *bona fide* Vγ9Vδ2$^+$ TCR signalling through an induced rapid and persistent PKC-dependent phosphorylation of ERK1/2, p38 MAPK, and JNK. These events result in NF-κB and AP-1 activation as well as in the release of MIP-1α, MIP-1β, IFN-γ, and TNF-α[81]. Moreover, antigen stimulation and CD3-crosslinking produced identical phosphorylation of the signalling proteins Zap70, PI3K, LAT, ERK1/2, and p38 MAPK[82,83]; and induced highly sustained calcium signalling in Vγ9Vδ2$^+$ T cells [84].

1.3.2 Costimulatory Receptors

The best described costimulatory receptor, CD28, has historically yielded paradoxical results on γδ T cells[85]. Although CD28 is constitutively expressed on around 60% of freshly isolated γδ T and on around 10% of activated cells, its stimulation promotes survival and proliferation via IL-2 production[86], but in contrast to αβ T cells, TNF-α production in Vγ9Vδ2$^+$ T lymphocytes is independent of CD28 co-stimulation and highly dependent on TCR-induced p38 kinase[87]. Another important player in the co-stimulation to the γδ TCR is CD27, a protein of the tumour necrosis factor receptor (TNFR) superfamily; in fact, engaging CD27 with its natural ligand CD70 enhanced Vγ9Vδ2$^+$ T cell expansion *in vitro*, whereas both anti-CD27 or anti-CD70

antibodies blocked this effect. CD27 signalling cascade, indeed, induces calcium fluxes and upregulation of *Cyclin D2* and *Bcl2a1* gene expression, promoting cell cycle and anti-apoptosis respectively[88]. Upon activation, γδ T cells can also express another TNFR superfamily member, CD30[89]; its expression potentiates calcium fluxes induced by TCR activation and enhances pro-inflammatory cytokine production[90]. Interestingly, activated Vγ9Vδ2$^+$ T cells also express high levels of 4-1BBL (CD137L), which acts as a ligand for 4-1BB on T and NK-cells and participates in Vγ9Vδ2$^+$ T cell activation due to its known reverse signalling ability[91,92]

1.3.3 Cytokine Receptors

Interleukins are key determinants of T cell survival, proliferation, and differentiation. IL-7, IL-15, and IL-2 are essential for lymphocyte development and homeostasis; upon inflammation, other cytokines, namely, IL-1β, IL-12, IL-18, IL-21, and IL-23, take a central role in determining T cell functions. Among those, IL-7 together with an agonist-mediated TCR stimulation seems to support the expansion of human IL-17-producing γδ T cells[93], a subset of γδ T cells that is commonly implicated in inflammation[94]. Other cytokines, such as IL-15 and IL-2, are involved in human γδ thymocyte differentiation into functional effector cells, promoting cytotoxicity and IFN-γ production and their potent antitumor functions. Indeed, our group has shown that while *ex vivo*-isolated γδ thymocytes produce negligible IFN-γ and lacked cytolytic activity against leukaemia cells, stimulation with IL-2 or IL-15, but not IL-4 or IL-7, promoted thymocyte differentiation via the MAPK/ERK signalling pathway towards inducing *de novo* expression of the transcription factors T-bet and eomesodermin, as well as the cytolytic enzyme perforin, required for the cytotoxic type 1 program. Unexpectedly, TCR activation was dispensable for these stages of functional differentiation[50]. These data supported previous findings showing that, IL-15, in contrast to IL-2, activates tumour-specific γδ T cells through IL-2Rβ and IL-2Rγ, but not IL-2Rα. These enhanced *in vitro* tumour-specific and proliferative responses of γδ T cells seen with IL-15 suggest a rational adjuvant immunotherapeutic use of γδ T cells in cancer patients[95]. However, additional reports on peripheral Vγ9Vδ2$^+$ T cell cultures showed that IL-15 or IL-2 stimulation, despite efficient ERK and AKT activation, were not sufficient to induce effector responses; these required phosphoantigen-dependent TCR activation and downstream calcium mobilization[96,97]. Importantly, IL-2 and IL-15 play key roles in the peripheral expansion of Vγ9Vδ2$^+$ T cells in response to microbial phosphoantigens or synthetic drugs like bisphosphonates[96,98].

Effector γδ T cell differentiation is also greatly impacted by inflammatory cytokines, particularly IL-12 and IL-18 that typically promote IFN-γ production; and IL-1β and IL-23 that mostly drive IL-17 production. Type 1 differentiation is also predominant in human γδ T cells, and can be further enhanced by IL-18[99,100] or IL-21[101]. The induction of a type 17 program in human γδ T cells requires persistent stimulation with IL-23 for neonatal Vγ9Vδ2$^+$ T cells[102]; and IL-23 and IL-1β in the presence of TGF-β for adult Vγ9Vδ2$^+$ T cells[103,104]. Finally, IL-21 was recently suggested to endow human Vγ9Vδ2$^+$ T cells with B-cell helper activity associated with a T follicular helper cell-like phenotype[105,106], which may impact on the generation of high affinity antibodies against microbial infections.

1.3.4 Natural Killer Receptors

γδ T cells also express of a wide set of germline-encoded receptors that were initially described and thought to be restricted to NK cells, and hence are collectively known as NK receptors (NKRs), including natural cytotoxicity receptors (NCRs). This is an important key characteristic that allows them the recognition of transformed cells.

The most characterized NKR in γδ T cells is the C-type lectin-like NK receptor group 2 member D (NKG2D). NKG2D binds extracellularly to multiple ligands that belong to the MICA/ MICB and ULBP families in humans and that are induced upon cellular stress, such as DNA damage, and thus resulting in immune activation immune silencing [107,108]. Beside these described functions, a primary stimulatory versus a costimulatory role for NKG2D in γδ T cells was matter of debate[85,109]. The costimulatory function of NKG2D in human Vγ9Vδ2$^+$ T cells was supported by additive effects on TCR-mediated activation, with an upregulation of cytokine production upon MICA-NKG2D interactions[110] and an increase in intracellular calcium mobilization and cytotoxic activity[84]. The primary stimulatory function was supported by the NKG2D-mediated activation of γδ T cells in the absence of TCR engagement. Indeed, NKG2D ligation can upregulate CD69 expression in Vγ9Vδ2$^+$ T cells to similar extent as TCR stimulation[111]. Moreover, NKG2D but not TCR blockade can inhibit Vγ9Vδ2$^+$ T cell cytotoxicity against various haematological tumours[112]. Another NKR implicated in tumour cell recognition by Vγ9Vδ2$^+$ T cells is DNAX accessory molecule-1 (DNAM-1), an Ig-like family glycoprotein. It has been showed indeed that antibody-mediated DNAM-1 blockade impaired Vγ9Vδ2$^+$ T cell cytotoxicity and IFN-γ production against hepatocellular carcinoma lines expressing Nectin-like-5[113].

In addition to the physiologically expressed NCRs, Vδ1$^+$ T cells from blood can stably express NKp30 and NKp44, which had been previously regarded as NK-specific markers, but only after cytokine- and TCR-mediated induction[114] (see section 1.6.1).

1.3.5 Inhibitory Receptors

After an efficient activation and deployment of effector functions, it is necessary to negatively regulate the immune response in order to return to a homeostatic level. Although γδ T cells rarely express CTLA-4, they can upregulate PD-1 upon activation, while they constitutively express BTLA. Therefore, these two receptors may be the key to control the negative phase of γδ T cell responses[20].

Programmed death-1 (PD-1), known to be critical for the negative regulation of the immune response, is absent or low expressed on circulating Vγ9Vδ2$^+$ T cells but can be rapidly induced upon activation[115] and can act in two ways: through the phosphorylation of its cytoplasmic tail, recruiting negative regulators that block Lck activity downstream of the TCR complex[116]; and augmenting the activity of the protein phosphatase and tensin homolog (PTEN), thus impairing survival, proliferation, and IL-2 release[117]. The expression of the ligand PD-L1 on tumour cells is an important tumour escape mechanism, inhibiting Vγ9Vδ2$^+$ T cell cytotoxicity and IFN-γ production. However, zoledronate treatment and consequent Vγ9Vδ2$^+$ TCR activation seemed to overcome the inhibitory effect of PD-1/PD-L1 interactions[115].

B- and T-lymphocyte attenuator (BTLA) is member of the CD28 family and structurally related to PD-1 and CTLA-4. The binding to its ligand (herpesvirus entry mediator (HVEM)), induces attenuation of cellular

activation and growth[118]. Indeed, BTLA engagement with HVEM reduced TCR-mediated signalling and inhibited Vγ9Vδ2$^+$ T cell proliferation, also in response to lymphoma cells. Conversely, BTLA-HVEM blockade using monoclonal antibodies enhanced Vγ9Vδ2$^+$ TCR signalling and may thus have therapeutic potential for the positive manipulation of γδ T cells [119].

1.4 γδ T cell development and homeostasis

While αβ T cells undergo positive and negative selection in the thymus depending on their TCR avidity for thymically expressed self-antigens [120], there is little evidence supporting the hypothesis of human γδ T cells being or not positively and/or negatively selected in the thymus. Indeed, post-natal human γδ T cells seem to only complete their maturation program in the periphery, especially upon infection challenge that their triggers clonal expansion[50,121–124]. Thus, the goal of post-natal thymic development seems to be the generation of a highly diverse, naïve and immature human γδ T cell repertoire. As such, the main event for developing γδ T cells is the generation of a functional TCR through the rearrangement of the variable (V), diversity (D) and joining (J) segments and subsequent pairing of the rearranged γ and δ chains. These events alone could lead to the establishment of a large number of diverse antigen receptors, but the addition and/or subtraction of non-templated (N) and palindromic (P) nucleotides at the gene segment junctions contribute substantially to increasing diversity, providing nearly limitless potential to the γδ TCR repertoire[125] .

1.4.1 γδ cell lineage commitment and thymic development

αβ and γδ T cells derive from a common bipotent progenitor and it is believed that the choice between the two lineages is the first decision made by progenitors after they commit to the T cell lineage[126,127]. Double negative (DN) CD4$^-$CD8$^-$ thymocytes rearrange three out of four TCR loci: *Tcrb*, *Tcrg* and *Tcrd*[18]. The cells at this stage are arrested in proliferation and require TCR expression to re-enter cell cycle. If a cell succeeds in an in-frame *Tcrb* rearrangement, it expresses TCRβ in a complex with the germline-encoded pre-TCRα (pTα) chain. Expression of the pre-TCR complex leads to a burst of proliferation, upregulation of the CD4 and CD8 coreceptor, silencing of *Tcrg* and initiation of *Tcra* rearrangement, which results in the excision of the *Tcrd* locus. If *Tcra* is productively rearranged, CD4$^+$CD8$^+$ double positive (DP) thymocytes express TCRαβ at the cell surface and can further differentiate. The progression through the DP stage is the hallmark of αβ lineage commitment. Progenitors that productively rearrange *Tcrg* and *Tcrd* loci express the γδ TCR at the cell surface. These cells likewise undergo a burst of proliferation but most them avoid progression through the DP stage and egress the periphery with a DN phenotype.

Early explanations of the divergent development of these cells arose from an observation that γδ T cells appeared in the mouse thymus prior to αβ T cells, hence suggesting that the progenitor was poised to preferentially give rise to a γδ T cell[18]. This timing dependent or stochastic model was directly opposed by the discovery of a γ gene silencer that resulted in normal αβ T cell frequencies in γδ T cell transgenic mice[128]. As the absence of this silencer led to reduced αβ T cell frequencies, a second instructional model was proposed whereby the uninhibited expression of γδ TCR or pre-TCR (pTα/TCRβ) would directly result in development along the γδ or αβ lineage[128,129]. Subsequent studies investigating this theory at a single cell

level showed that DN3 progenitors expressing pre-TCR or γδ TCR retained the potential to progress towards either lineage, hence discounting the original instructional model[126,130]. These findings among others lend direct support to a quantitative signal strength model, whereby the amount of signal accumulated downstream of the TCR would drive the differentiation of progenitors along either lineage[127,131–133]. More specifically, the model suggests that a strong γδ TCR signal would result in higher activation of the ERK-MAPK pathway, leading to a higher induction of the Early Growth Response (EGR1, EGR3) transcription factors and their target Inhibitor of DNA binding 3 (Id3)[134–136]. Id proteins are direct inhibitors of E2A, a helix-loop-helix protein, which serves an important role in thymocyte development as a checkpoint regulator[137]. As proposed by the signal strength hypothesis, the higher accumulation of Id3 results in stronger inhibition of E2A, and thus expression of γδ T cell hallmark genes. Conversely, weaker signals through the Notch receptors and pre-TCR would result in more modest accumulation of Id3, and hence weaker inhibition of E2A leading to further development along the αβ lineage[127]. Although it has been proposed that in some instances the simple expression of the γδ TCR is sufficient to initiate the differentiation signals[138,139], more recent evidences point the possibility of an active role for the γδ TCR – ligand interaction during the development of at least some subsets with known ligands in mouse[130,140].
It can therefore be concluded that differences in signal strength dictate αβ versus γδ lineage choice through modulation of lineage specific transcription factors. It is then also likely that within these distinct lineages, the graded signals downstream of each TCR results in differential regulation of transcription factors essential for the functional maturation of effector subtypes[141].

Finally, γδ T cell differentiation program is not completed in the thymus and it does not require TCR/co-receptor activation in the periphery. Indeed, it has been demonstrated that after the commitment of a precursor cell to the γδ T cell lineage, human γδ thymocytes are functionally immature[142]. Given that circulating γδ peripheral blood lymphocytes (PBLs) display type 1 effector properties[88,143] and express memory markers[144], human γδ T cells must thus complete their differentiation in the periphery where they become strongly biased toward IFN-γ production (type 1 effectors). Interestingly, IL-2 or IL-15 and not IL-7 signals are sufficient to drive the differentiation of human γδ thymocytes into effector cells producing IFN-γ/TNF-α and therefore endowed with potent cytotoxicity against tumour targets. In addition, and unexpectedly, TCR activation was not required *in vitro* for the functional differentiation of human γδ thymocytes[142]. This might mimic a second step in γδ T cell functional differentiation that could be provided by activated and IL-2 producer T cells (either γδ T cells themselves or their αβ counterparts) or IL-15 by myeloid and epithelial cells in the periphery.

1.4.2 Peripheral γδ T cell homeostasis and response to challenges

After the egress from the thymus, post-natal human γδ T cells are functionally immature and seem to complete their maturation program only in the periphery[50], especially upon infection challenge that triggers clonal expansion[121–124,145]. As result, the pool of adult γδ T cells in peripheral blood always contains variable degrees of highly proliferated oligoclonal sequences, with individual clones occasionally reaching frequencies over 20% of all TRG and TRD sequences. Notably, clonotypic expansions leading to the establishment of adult repertoires were relatively stable over time[122,124]. In contrast, neonatal γδ TCR repertoires are more diverse and less focused on a few proliferated Vγ9^{+} and Vγ9^{-}[122].

More in detail, in the case of Vδ1$^+$ cells, the clonal expansion was accompanied by phenotypic differentiation and a distinct functional biology. Neonatal and unfocused TCR repertoires are enriched with apparently naïve Vδ1$^+$ populations characterized by a CD27^{hi}CCR7$^+$CD28$^+$IL-7Rα$^+$CD62L$^+$ and with characteristics of naïve cells, such as responsiveness to IL-7, secondary lymphoid homing receptors, slow proliferation after TCR stimulation and low cytotoxic marker expression. Conversely, the adult TCR repertoires showing clonally expanded cells display a CD27$^{lo/neg}$CCR7^{neg}CD62L^{lo}CD28^{neg}IL-7Rα^{neg} phenotype and a functional effector status. This was indeed characterized by fast activation and proliferation in response to TCR/ CD3 stimulation, upregulation of cytotoxic markers, cytokine responsiveness and homing receptor expression[124].

Additionally, beside the aforementioned semi-invariant characteristic of the adult Vγ9$^+$ repertoire in Vγ9Vδ2$^+$, adult TRG Vγ9Vδ2$^-$ repertoires have a consistent fraction of overlapping sequences, whereas a huge diversity among proliferated TRD repertoires was observed, with rarely any identical TRD sequence shared by adults. Thus, it is tempting to conclude that the TRG repertoire is public and the TRD repertoire is private[122,124]. The presence of shared and public TRG sequences raises the question of whether γδ T cells bearing these sequences have been selected by a specific cognate antigen. Supporting this hypothesis, proliferation of Vδ1$^+$ T cells, but not of Vδ2$^+$ T cells, is often correlated to viral infection, as shown after infection with CMV following kidney transplantation and in allo-HSCT patients[146–149]. Indeed, patients experiencing reactivation of CMV systematically displayed strong clonal proliferation of heterogeneous Vδ1$^+$, Vδ3$^+$ and unconventional Vδ2$^+$ clones that precisely correlated with viral activity[122]. Clonal expansion of the γδ T cells expressing some specific CDR3γ sequences was also observed in pulmonary tuberculosis patients with *M. tuberculosis* (*Mtb*) infection. The number of unique CDR3δ sequences was significantly increased, suggesting increased CDR3 diversity in the TRD repertoire of this cohort[145]. Taking these considerations into account, it is possible to state that each γδ T cell repertoire could reflect an individual history of immunological exposure.

Not only pathogenic factors, but also host factors participate in shaping the γδ TCR repertoire. Indeed, in the case of regeneration of TRG and TRD repertoires after allo-HSCT, the global architecture of the repertoires after transplantation were qualitatively comparable to the hosts' before transplantation. However, the new clonotypes very different from the ones from the hosts' repertoires before transplantation, which suggested that they were generated *de novo* in the host thymus from donor stem cells[122]. Another example is given by the recent analysis of the intrahepatic γδ T cell pool. These cells are enriched for clonally expanded effector T cells, whereas naïve γδ T cells are largely excluded. Moreover, whereas a distinct proportion of circulating T cell clonotypes was present in both the liver tissue and peripheral blood, a functionally and clonotypically distinct population of liver-resident γδ T cells was also evident, suggesting that factors triggering γδ T cell clonal selection and differentiation, such as infection, can drive enrichment of γδ T cells into liver tissue, allowing the development of functionally distinct tissue-restricted memory populations specialised in local hepatic immune surveillance[123].

1.5 γδ T cells in immune surveillance

The involvement of γδ T cells in different pathophysiologic processes is reflected in their wide array of effector functions. They can kill infected, activated and transformed cells, through pathways involving the engagement of death-inducing receptors, such as FAS and TNF-related apoptosis-inducting ligand receptors (TRAILR); they can also release cytotoxic effector molecules, such as perforin and granzymes, which are usually responsible for the clearance of tumour cells[150]. γδ T cells are known to kill a vast repertoire of tumour cell lines and primary samples *in vitro*, such as leukaemia, lymphoma, melanoma, neuroblastoma

and several types of carcinoma[151]. In addition to their cytotoxic functions, γδ T cells are also able to produce a large array of immunomodulatory cytokines involved in protective immunity against virus and intracellular pathogens (TNF and IFN-γ), extracellular bacteria and fungi (IL-17) and extracellular parasites (IL-4, IL-5, and IL-13); importantly, such cytokine responses can also have deleterious effects, such as tumour-induced inflammation, autoimmunity, allergy or asthma[151–154]. Additionally γδ T cells have the ability to downmodulate innate and adaptive immune effector cells through the production of TGF-β and IL-10[155]; and can also promote tissue healing and epithelial cell regeneration[156]. Human γδ T cells can also affect the outcome of immune responses in a more indirect way, acting as APC for αβ cells and also regulating humoral immunity[157].

1.5.1 The role of γδ T cells in tumours

Intra-tumour γδ T cells emerged as the most favourable cancer-wide prognostic population in a recent study based on transcriptional signatures[158]. Both main subsets of γδ T cells can contribute to this phenomenon. Indeed, both Vδ1$^+$ and Vγ9Vδ2$^+$ T cells have potent antitumor activity, inhibiting cancer cell proliferation, angiogenesis, lymphangiogenesis, and increasing cancer cell apoptosis[159,160,161]. However, a functional subset of γδ T cells, characterized by their production of IL-17, can promote the accumulation and expansion of immunosuppressive cells and expedite the development of a variety of cancer types[162]. Indeed, it has been reported that Vγ9Vδ2$^+$ T cells can be polarized into γδ T17 cells (producing only IL-17), γδ T1/17 cells (producing both IFN-γ and IL-17), γδ T1 cells (producing both IFN-γ and TNF-α) and γδ T2 cells (producing increased IL-4) with distinct cytokines being required for their polarization initiation and maintenance[103,163,164]. Because of their plasticity, γδ T cells can therefore be viewed both as being a “friend” or a “foe” of cancer progression[165].

γδ T cells can exert a direct antitumoral role in several ways. First, after migrating to the tumour local environment, γδ T cells can lyse cancer cells through the perforin-granzyme pathway in a TCR and NKG2D dependent manner, both *in vitro* against several patient-derived cancer cells and neck squamous carcinoma[166,167] and *in vivo* as shown in renal carcinoma[168]. Second, γδ T cells can eliminate cancer cells through TRAIL and FasL[169,170]. Third, γδ T cells can kill cancer cells via antibody-dependent cellular cytotoxicity (ADCC). ADCC occurs when CD16 (FcγR III) present on γδ T cells binds to the Fc region of IgGs, which constitutes another means of γδ T cell target recognition. CD16 can also be up-regulated on γδ T cells, depending on the precise biological situation. Binding to its target may trigger either cytotoxicity or other effector functions (e.g., IFN-γ secretion)[171,172]. Lastly, γδ T cells are an important early sources of IFN-γ and TNF-α[173,174], inhibiting cancer growth through several mechanisms, such as enhancing of antitumor immunity, and inhibiting cancer angiogenesis[175]. However, γδ T cells can also exert their antitumor effect in indirect ways by interacting with B cells, DCs, αβ T cells, and NK cells. After co-culture of Vγ9Vδ2$^+$ T cells with IPP and IL-21, Vγ9Vδ2$^+$ T cells polarized toward a lymphocyte subset displaying features of follicular B-helper T (Tfh) cells secreting IL-4, IL-10, and CXCL13, and help B cells to produce antibody *in vitro*[105,106]. γδ T cells can also act as antigen presenting cells (APCs) for αβ T cell priming, upregulating CD36, a scavenger receptor involved in the uptake of apoptotic cells by immature DCs and macrophages[176,177]. γδ T cells trigger DC maturation and, in return, DCs induce the activation and proliferation of γδ T cells, enhancing their cytotoxic and immunoregulatory functions[178]. Finally, γδ T cells induce robust NK cell-mediated antitumor cytotoxicity through CD137 engagement, enhancing NK cell cytotoxicity to NK-resistant cancers[91].

On the other hand, γδ T cells have been reported to support cancer progression by promoting angiogenesis in gallbladder cancer, ovarian cancer, as well as others cancer types[179,180]. Indeed, γδ T17 cells can be a major source of IL-17, which induces the production of vascular endothelial growth factor, as well as other angiogenesis related factors. Moreover, given that IL-17 is one of the main chemo-attractant driving forces for the recruitment of myeloid derived suppressor cells (MDSCs)[162,181,182], it facilitates cancer progression in several types of cancers, including: breast cancer, colorectal cancer (CRC), and hepatic carcinoma. Innate γδ T17 cells could therefore convert cancer-elicited inflammation into immunosuppression through MDSCs. Finally, γδ T17 cells can affect neutrophils in breast cancer through the secretion of IL-1β and that stimulate their expansion and polarization. These tumour-induced neutrophils acquire the ability to suppress cytotoxic T lymphocytes carrying the $CD8^+$ antigen, which in turn facilitates the establishment of metastases[183], and also peripheral $V\gamma9V\delta2^+$ T cells[184,185].

Additional findings highlighted that human breast tumour infiltrating $V\delta1^+$ γδ T cells could inhibit DC maturation and their APC functions, resulting in an impaired naïve αβ T cell activation and differentiation into effector T cells[186]. Furthermore, in pancreatic ductal adenocarcinoma, it has been shown that γδ T cells express high levels of PD-L1 and support pancreatic oncogenesis by restraining αβ T cell activation[187]. The broader relevance of these findings remains to be established.

1.5.2 Ligands recognized in tumours

Early research on the molecular mechanisms of γδ T cell recognition in the 1990s led to the realization of its unusual independence of peptide processing and MHC-restricted presentation, in marked contrast with αβ T lymphocytes[188–190]. One of the first lines of evidence came from non-peptidic prenyl pyrophosphates (a pAg) recognized by $V\gamma9V\delta2^+$ TCRs[191,192]. Among these compounds, isopentenyl pyrophosphate (IPP) and dimethylallyl pyrophosphate are natural intermediates of the mevalonate pathway of isoprenoid and steroid synthesis in eukaryotic cells. Importantly, the dysregulation of the mevalonate pathway in some tumour cells allows for the accumulation of these pAgs, thus promoting $V\gamma9V\delta2^+$ TCR-mediated recognition[169]. Furthermore, treatment with zoledronate or pamidronate (which are approved drugs) was shown to be very effective at inducing the accumulation of intracellular pAgs like IPP, and thus potentiate TCR-dependent $V\gamma9V\delta2^+$ T cell cytotoxicity against tumour cell targets, including cancer stem cells[169].

Besides sensing PAgs, γδ T cells seemingly recognize transformed cells through proteins that are expressed at the cell surface in a stress-induced manner. Some examples are typically endogenous proteins, such heat shock protein 60[193–196] or FI-ATPase[197], that can be ectopically expressed on the cell membrane upon transformation and recognized by $V\gamma9V\delta2^+$ TCRs to promote tumour cell lysis. More recently, endothelial protein C receptor (EPCR), which acts on the coagulation cascade, was shown to be exposed on the cell surface during transformation and recognized by a $V\delta2^-$ ($V\gamma4V\delta5$) TCR[198]. Similarly, Annexin A2, expressed on tumour cells in response to increasing quantities of reactive oxygen species, engaged directly with a $V\gamma8V\delta3$ TCR[199]. The identification of these rather different ligands highlights the complexity of tumour cell recognition *via* γδ TCRs (Figure 1.10). This notwithstanding, it is clear that γδ T cells also rely on "NK-like" mechanisms for tumour cell recognition, using receptors originally thought to be specific to NK cells.

Consensual in the scientific community is the role of NKG2D, which is widely expressed not only in NK cells but also in most γδ T cells[200,201]. In human γδ T cells, both $V\delta1^+$ and $V\delta2^+$ subsets, NKG2D was shown to be responsible for recognition of tumour cells expressing MHC class I chain-related (MIC) A/B[110,201–204] or UL16

binding protein (ULBP) 1/2/3/4 ligands[112,169,205–208]. In fact, human carcinoma samples from lung, breast, kidney, ovary, and prostate cancers expressing MICA or MICB presented higher levels of infiltrating Vδ1$^+$ T cells, which in turn were able to target and kill autologous and heterologous tumour cells. Our group's work revealed that ULBP1 was particularly important for leukaemia and lymphoma cell recognition by pAg-activated Vγ9Vδ2$^+$ T cells[112]. Notwithstanding, one should note the relevance of a synergistic TCR engagement for an efficient cytotoxic response[206,207]. In fact, some works suggested that MIC or ULBP recognition by γδ T cells is not only restricted to NKG2D but also involves the γδ TCR[201,209]. A similar recognition pattern was also observed against human MutS homolog 2 (hMSH2) ectopically expressed in epithelial tumour cell lines. Both γδ TCR and NKG2D were able to interact with hMSH2 and contribute to Vδ2$^+$ γδ T cell-mediated cytotoxicity and IFN-γ production[196,210].

Besides NKG2D, DNAM-1 was also shown to be widely expressed in Vδ1$^+$, Vδ2$^+$, and Vδ1$^-$Vδ2$^-$ γδ T cell subsets and masking DNAM-1 on γδ T cells significantly inhibited tumour cell killing[211,212]. DNAM-1-dependent γδ T cell recognition was reported for hepatocellular carcinoma[113], acute[211] and chronic[212] myeloid leukaemia, and multiple myeloma[213] cell lines. More specifically, Vγ9Vδ2$^+$ T cells were shown to use DNAM-1 to interact with Nectin-2 and PVR that are widely expressed in the tumour cell targets[113,211]. Curiously, PVR engagement potentiated γδ T cell cytotoxicity, whereas Nectin-2 blocking did not affect it[113]. Tumour targets that expressed both DNAM-1 and NKG2D ligands were able to engage both receptors on γδ T cells, having a synergistic effect on their cytolytic activity[113,212,213]. Moreover, therapeutic strategies that enhanced the expression of NKG2D or DNAM-1 ligands, such as MICA/B and ULBP1/2, or Nectin-2 and PVR, respectively, potentiated γδ T cell recognition of colon cancer, glioblastoma, multiple myeloma, and lymphoma cells[214–217].

1.5.3 Recognition of infected cells by human γδ T cells

Multiple lines of evidence since the late 1980s have shown that γδ T cells display strong activities against bacteria, viruses and parasites. Indeed, γδ T cells play an important role in the response to *M. tuberculosis* (*Mtb*), since γδ T cells and mainly Vγ9Vδ2$^+$ from healthy human donors, selectively expanded *in vitro* in the presence of *Mtb*[218–220]. It was also observed that DCs infected with Bacillus Calmette-Guérin (BCG) rapidly induced the activation and proliferation of Vγ9Vδ2$^+$[221]. Purified blood γδ T cells proliferated vigorously in response to *Mtb* and in the presence of PBMCs. Also, γδ T cells could not proliferate on their own in the absence of CD4 T cells or exogenous IL-2 but could upregulate CD25 (IL-2R), suggesting that interaction with Th1-type CD4 T cells were necessary for efficient activation of peripheral blood γδ T cells by *Mtb*[222]. However, patients with pulmonary tuberculosis had reduced numbers of *Mtb*-reactive Vγ9Vδ2$^+$ cells in their blood and lungs. This was due to an increased apoptosis and could be explained by a rapid induction of Fas and FasL in γδ T cells upon presence of *Mtb* antigens. Blocking the Fas-FasL interaction resulted in a 75-80% reduction of apoptosis[223]. Vγ9Vδ2$^+$ T cells are also involved in immunity to *Yersinia enterocolitica*. They undergo through a marked proliferation step when in contact with Yersinia-infected lymphoblastoid cell lines or fixed intact Yersinia but not heat-inactivated Yersinia. Moreover, Vγ9Vδ2$^+$ T cells killed infected mismatched cells more efficiently than autologous targets[224]. The role of Vγ9Vδ2$^+$ cells was also studied in an *ex vivo* co-culture model of human PBMC responses to *Escherichia coli*: Vγ9Vδ2$^+$ cells underwent rapid TCR-dependent proliferation and functional transition from cytotoxic, inflammatory cytokine immunity, to cell expansion with diminished cytokine but increased costimulatory molecule expression, and capacity for professional phagocytosis with a myeloid-like APC response in response to *Escherichia coli* infectious

stimuli[225]. A protective role for Vγ9Vδ2$^+$ T cells during Salmonella infection was also hypothesized. γδ T cells fraction is indeed increased in Salmonella infected patients and also in other bacterial infections. Moreover, when PBLs from normal individuals were cultured with live Salmonella, γδ T cells were preferentially activated and expanded. Most of them expressed a Vγ9Vδ2$^+$ TCR[226]. Finally, *in vitro* Vγ9Vδ2$^+$ T cell expansion was also induced by coculture with *Listeria monocytogenes* infected cells[227]. 70-fold and 110-fold increase in absolute numbers of Vγ9Vδ2$^+$ cells were registered by day 5 and day 15 of infection in patients affected by listeriosis. These expansions were long-lasting, persisting up to four months after infection[228,229].

γδ T cells also participate in the immune response to several viral infections, becoming activated and homing to the sites of viral replication. Significant long-term expansions of Vδ2$^-$ but not Vδ2$^+$ γδ T cells were observed during CMV reactivation early after allo-HSCT[149] and after renal transplantation[146], suggesting a direct involvement of γδ T cells in anti-CMV immune responses. Additionally, significantly higher numbers of Vδ2$^-$ γδ T cells were detected in CMV-seropositive healthy persons compared to seronegative donors whereas the absolute numbers of Vδ2$^+$ cells were not significantly different: γδ T cell expansion is indeed concomitant with the resolution of CMV infection and disease, regardless of the CMV serologic status of donor and recipient before transplantation[230]. Interestingly, Vδ2$^-$ γδ T cells were found as naive cells in CMV$^-$ patients but exhibited the cytotoxic effector/memory phenotype in CMV$^+$ patients. This complete remodelling of the Vδ2$^-$ γδ T cell population by CMV predicts their ability to exhibit an adaptive anti-CMV immune response and, consistent with this, the secondary response to CMV has been found to be associated with a faster γδ T cell expansion and a better resolution of infection than the primary response[121]. At a repertoire analysis level, patients experiencing reactivation of CMV systematically displayed strong clonal proliferation of heterogeneous Vδ1$^+$, Vδ3$^+$ and unconventional Vδ2$^+$ clones that precisely correlated with viral activity[122,146].

γδ T cells have also a role in HIV infection. Studies have shown that the absolute numbers of γδ T cells increase during HIV infection and that activated Vδ1$^+$ T cells are present in the peripheral blood and lung of HIV-seropositive patients[231]. This increase in the Vδ1$^+$ T cell compartment resulted from an inversion of the normal ratio of Vδ2$^+$ T cells to Vδ1$^+$ T cells observed in healthy individuals. The depletion of Vγ9Vδ2$^+$ T cells is the earliest known TCR-specific cell depletion associated with HIV-infection and may contribute to the establishment of viral persistence in AIDS by reducing the level of type 1 cytokines[232]. Vγ9Vδ2$^+$ T cells from HIV$^+$ individuals had lower expression of granzyme B and reduced cytotoxicity against a B cell lymphoma cell line, with an increased FasR expression, which could represent a mechanism for depletion of these cells during disease[233].

Expansion and activation of γδ T cells were observed in Hepatitis C virus (HCV) patients[234,235], with a polyclonal activation of the Vδ1$^+$ subset during the chronic phase of infection[236], and in other flavivirus infections such as hepatitis G virus (GBVC)[237]. Liver-derived γδ T cell lines from patients with chronic HCV exhibited high levels of cytotoxic activity against different targets, including primary hepatocytes, and produced IFN- γ, TNF-α and IL-8 after anti-CD3 activation *in vitro*. Many studies described a protective role of γδ T cells and specifically Vγ9δV2 in the immune-surveillance against herpesviruses: Herpes Simplex virus (HSV)-specific γδ T cells isolated from infected persons have strong cytotoxicity with lytic activity[238]; and γδ T cells are expanded also during the acute phase of Epstein-Barr virus (EBV)-induced infectious mononucleosis, expressing activation molecules and persisting during the convalescent phase[239]. γδ T cells have been found to be increased in terms of frequency in human T cell lymphotropic virus type I (HTLV-I)[240,241] ,HBV[242] and Ebola infections[243] while are decreased in frequency with weaker cytotoxic ability in RSV[243–245] and measles[246] infections.

γδ T cells function also in the immune response to parasites. Not long after the γδ TCR was discovered, a number of studies were published describing the existence of elevated levels (up to threefold increased and for 3-4 weeks after treatment) of γδ T cells in human patients during or after an episode of *P. falciparum* malaria[247,248]. γδ T cells exert a protective effect in immunity to malaria infection, since they were shown to inhibit replication of blood-stage *P. falciparum in vitro* in a dose-dependent fashion[249]. Moreover, upon infection γδ T cells produce pro-inflammatory cytokines, such as IFN-γ, IL-1β, TNF-α and TNF-β[250]. It was observed that γδ T cells from nonimmune donors produce high levels of TNF-α and IFN-γ within 18 hours of contact with mycoplasma-free *P. falciparum*-infected erythrocytes *in vitro*, pointing out to possible implications in the pathogenesis of cerebral malaria and severe anemia[251]. When γδ T cells become activated during *P. falciparum* infection, they are likely to recognize phosphoantigens derived from the parasite; is also possible that phosphoantigens present in erythrocytes and released after burst, are recognized by γδ T cells[251–253]. However, it has been demonstrated *in vitro* that the replication of intraerythrocytic stages of the parasite is not affected by coculture with human γδ T cells, and that parasite inhibition required contact between γδ T cells and merozoites. Since the same cells were able to inhibit replication of blood-stage *P. falciparum in vitro*, it was proposed that these cells recognize extracellular merozoites in transit to new host erythrocytes[249].

1.5.4 Recognition of ligands of infectious origin

As for the recognition of transformed cells, the mechanisms of activation and infected cell recognition through the TCR are mostly unknown except for the well described reactivity of Vγ9Vδ2$^+$ TCR. In addition, γδ can exert their effector functions *via* a broad panel of NKRs.

Vγ9Vδ2$^+$ T cells can be specifically and potently activated by PAgs like (E)-4-hydroxy-3-methyl-but-2-enyl pyrophosphate, an intermediate of the 2-C-methyl-D-erythritol 4-phosphate pathway employed by eubacteria and apicomplexan protozoa but not by eukaryotes[35,243,254,255]. This likely underlies the striking expansions of Vγ9Vδ2$^+$ T cells in individuals infected with *M. tuberculosis*[220,256] or *P. falciparum*[257]. Besides pAgs, several other molecules of microbial origin have been proposed as γδ T cell antigens accounting for the specific recognition of infected cells. These candidates include the bacterial superantigens SEA (and to a lesser extent SEE)[258]; OXYS and DXS2, two mycobacterial proteins found to activate γδ T cells from BCG-infected human subjects but not from healthy donors[259,260]; and HSV-1 glycoprotein I, specifically recognized by a Vγ1.2Vδ8$^+$ TCR independently from antigen processing and MHC presentation[261].

Subsequent reports demonstrated that γδ T cells also recognize stress antigens of cellular origin, either in antibody-like or antigen-presentation-like fashion. γδ T cells can indeed directly recognize stress proteins like hMSH2, a nuclear protein ectopically expressed on the cell surface of different epithelial tumour cells and induced by EBV transformation[210,262]; and Annexin A2 whose expression was induced by CMV infection and recognized specifically by a Vγ8Vδ3$^+$ T cell clone[199]. On the other hand, γδ T cells can recognize nonpolymorphic MHC-like (class Ib) proteins presenting lipids, such as CD1 proteins, in a similar way to other unconventional T cells like NKT or MAIT cells[263–265]. In particular, a subpopulation of Vδ1$^+$ T cells has been clearly shown to bind CD1d loaded with the self-lipid sulfatide[265] but any concrete link to the recognition of infected (or transformed) cells remains to be established. Of note, another CD1-like protein, EPCR, was shown to bind directly (independently of lipid cargo) the TCR of a Vγ4Vδ5$^+$ T cell clone (expanded from a CMV$^+$ individual), thus allowing it to recognize endothelial cells infected with CMV[198].

In addition to the TCR (Figure 1.9), γδ T cells can also use NKG2D to recognize cells infected with various viruses and intracellular bacteria[110,266]. More specifically, the stress-inducible molecule, MICA, was induced on the surface of dendritic and epithelial cells by *M. tuberculosis* infection *in vitro* and *in vivo*; and its binding to NKG2D, substantially enhanced the TCR-dependent Vγ9Vδ2$^+$ T cell response to PAgs[201]. Furthermore, in the case of *Brucella*, ULBP1 was the main NKG2D ligand upregulated on infected macrophages, and its engagement promoted Vγ9Vδ2$^+$ T cell cytotoxicity and cytokine production, which contributed to the inhibition of bacterium development[266].

A few other receptors have implicated in γδ T cell recognition of infected cells. Thus, another NKR, NKG2C, constitutively expressed on Vδ1$^+$ T cells, induced a cytolytic response against HIV-infected CD4$^+$ T cells expressing its ligand, HLA-E[267]. On the other hand, NKp30 can also play an important role in HIV-1 infection upon its induced expression in Vδ1$^+$ T cells; NKp30 ligation triggered the production of CCL3, CCL4, and CCL5 chemokines that suppressed the replication of a CCR5 tropic strain of HIV-1[268]. Finally, in the case of avian influenza (H5N1), γδ T cells were reported to use sialic acid receptors for the recognition of viral hemagglutinin[269].

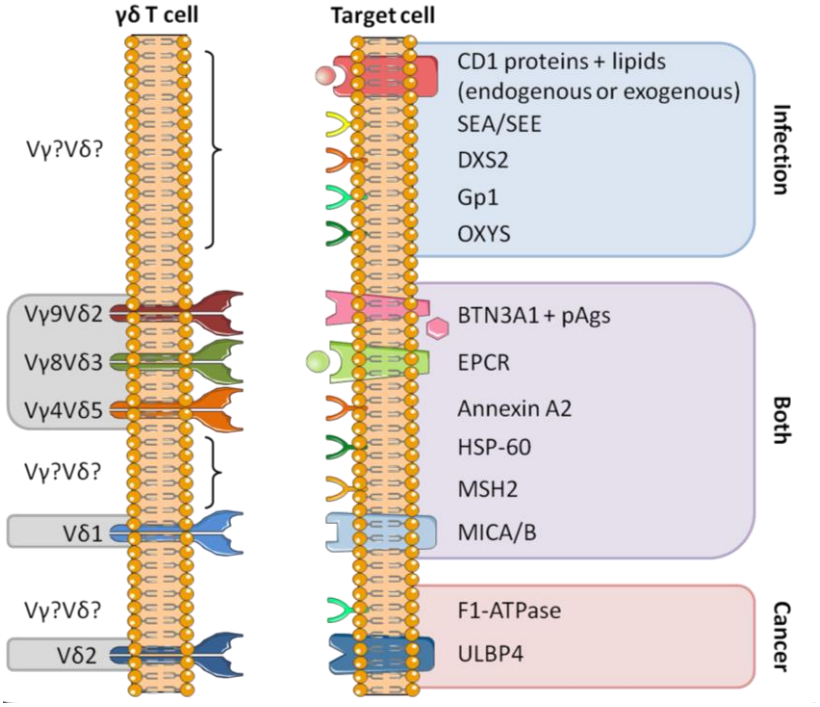

Figure 1.9 TCR-mediated reactivity against transformed and infected targets. Based on ref [270]

1.5.5 Focus on Vγ9Vδ2$^+$ TCR ligand

The vast majority of human blood γδ T cells respond to so called "phosphoantigens" (pAg)[219,271,272]. Their TCR share a characteristic rearrangement and Vδ2-containing chains bearing one of the hydrophobic amino acids: Leucine (L), Isoleucine (I), Valine (V), or Glycine (G) at position 97[47,54,55,273].

PAg are products of isoprenoid synthesis, which specifically activate Vγ9Vδ2$^+$ T cells. The building blocks of isoprenoid synthesis are isopentenyl pyrophosphate (IPP) and its isomer dimethylallyl pyrophosphate. Both are weak pAg[188,274] and 1000- to 10000-fold less potent than the strongest naturally occurring pAg (*E*)-4-

Hydroxy-3-methyl-but-2-enyl pyrophosphate (HMBPP)[43,255,274]. HMBPP is the immediate precursor in the synthesis of IPP by the non-mevalonate pathway also known as DOXP, MEP, or Rohmer pathway. The non-mevalonate-pathway is restricted to eubacteria, cyanobacteria, plants, and apicomplexan protozoa [43,255]. HMBPP is the driving force of a massive Vγ9Vδ2$^+$ T cell expansion in infections with HMBPP producing parasites or bacteria, which can lead to an increase of Vγ9Vδ2$^+$ T cells from 1 to 5% of blood T cells to more than 50% [43,275]. In mammals and most other animals, IPP is synthesized via the mevalonate pathway whose manipulation can render human cells into Vγ9Vδ2$^+$ T cell activators. Cells pulsed with aminobisphosphonates (e.g., zoledronate or pamidronate) become potent activators of primary Vγ9Vδ2$^+$ T cells[276,277] and of Vγ9Vδ2$^+$ TCR transductants[278] most likely in consequence of IPP accumulation after inhibition of the IPP metabolizing farnesyl diphosphate synthase (FPPS)[276,279]. As example, some tumours such as the human B cell lymphoma Daudi [53,190] spontaneously activate Vγ9Vδ2$^+$ T cells. This activation depends on intracellular accumulation of IPP and can be abolished by statins, which inhibit the HMG-CoA reductase and consequently also IPP synthesis[279].

Therefore, altogether the Vγ9Vδ2$^+$ TCR acts as a kind of pattern recognition receptor, which senses microbial infections as well as metabolic changes found in transformed, infected, or drug treated host cells[253]. This reactivity can also be harnessed clinically since remission of certain tumour entities after Vγ9Vδ2$^+$ T cell activation was observed in clinical trials.

PAg acts not as soluble molecules but need to be “presented”. A key recent breakthrough was the discovery of butyrophilin-related proteins, especially BTN3A1, as major molecular determinants of Vγ9Vδ2$^+$ TCR-mediated recognition of pAgs, even if the underlying mechanism has gathered some controversy. A model supporting extracellular PAg presentation to the Vγ9Vδ2$^+$ T cell (in a MHC-like manner) was first proposed, with biophysical and structural data in support[280]. However, following reports demonstrated that pAgs interact directly with the intracellular B30.2 domain of BTN3A1 through a positively charged surface pocket; and that charge reversal of pocket residues abrogates PAg binding and Vγ9Vδ2$^+$ T cell activation, with no detectable association with the extracellular domain of BTN3A1[45,281]. More recently, it has been shown that changes in the juxtamembrane domain of BTN3A1, which is located close to the start of the B30.2 domain, induced marked alterations in Vγ9Vδ2$^+$ T cell reactivity, thus highlighting the importance of the intracellular domain for the correct Vγ9Vδ2$^+$ T cell function and activation[282]. Because of its location between the intracellular and the extracellular domains, the B30.2 domain seems critical in translating the pAg-induced conformational change of BTN3A1 from the inside to the outside of the target cells[283,284].

1.6 γδ T cells in immunotherapy

Recently, γδ T cell transcriptional signatures were associated with highly favourable prognosis in a broad spectrum of malignancies[158]. However, the data based on the quantification of γδ TIL numbers in tumour biopsies have been less clear, for instance in renal cell carcinomas[147,285–287] or in nasopharyngeal carcinomas[288]. Moreover, Vδ1$^+$ γδ TIL infiltration into necrotizing melanoma tissue correlates with survival[289], but in prostate and breast tumours, , Vδ1$^+$ γδ TILs appear to be rather immunosuppressive and favour the growth of the tumour through IL-10 release[186,290].

Despite their pleiotropic roles in the tumour environment, γδ T cells remain an attractive candidate for adoptive cell therapies. Due to their relative abundance in peripheral blood and known (and selective)

reactivity to phosphoantigens, all clinical trials have so far focused on the Vγ9Vδ2$^+$ T cell subset. In addition, the availability of FDA-approved drugs, such as zoledronate and pamidronate, that allow their activation and expansion *in vivo*, facilitates their possible therapeutic application. In more detail, aminobisphosponates, such as pamidronate, ibandronate, alendronate and zoledronate, can indeed activate and selectively expand Vγ9Vδ2$^+$ cells *in vitro* from healthy donor derived PBMCs and induce the secretion of IFN-γ[291]. Pamidronate infusions in patients lead also to the increase of circulating Vγ9Vδ2$^+$ T cells to variable extent[292]. Indeed, the combination of the potent anti-tumour functions of Vγ9Vδ2$^+$ cells and the potential to expand γδ T cells directly *in vivo*[292] or *in vitro*[293] before reinfusion using aminobisphosphonates alone or in combination with cytokine(s) offers a comparatively cheaper and more straightforward delivery alternative. The expansion and activation of Vγ9Vδ2$^+$ cells *in vitro* resulted in promising pre-clinical results for these cells as ACT against TB [294] and has already been tested in various cancer clinical trials[295] that documented its safety and some albeit sub-optimal efficacy[296–298].

Data from a comprehensive review of the ongoing clinical trials, including 157 patients[295], revealed that around 49% of them received infusion of γδ T cell-enriched populations, while the other 51% had received drugs to expand and activate endogenous γδ T cells. It also emerged that patients with solid tumours were most often treated with adoptive T cell transfer as compared with γδ T cell-expanding drugs, whereas patients affected by haematological malignancies were more often treated with drugs[299] than with γδ T cells expanded *ex vivo*[300]. Despite the fact that the initial evaluation of γδ T cell-based immunotherapy shows some promise, there is large room for improvement. Overall, conventional response rates are poor, with only 10.8% objective responses documented. However, 39.2% achieved disease stabilization, a successful outcome of immunotherapy, indicating that clinical benefits can be achieved by a high proportion of patients subjected to γδ T cell-based immunotherapy[295].

1.6.1 Delta 1 T (DOT) cells and other Vδ1$^+$ T cell-based products for immunotherapy

In contrast to Vδ2$^+$ T cells, the Vδ1$^+$ T cell subset is not as susceptible to AICD, and tumour-reactive Vδ1$^+$ T cells can persist in the circulation for many years[301,302]. Moreover, the cytotoxic function of Vδ1$^+$ T cells has been described for lymphoid and myeloid malignancies, neuroblastoma, and cancers of the lungs, colon, and pancreas[161]. However, no clinical trial has yet focused on this γδ T cell subset, mostly due to the lack of clinical-grade protocols allowing their successful expansion. Importantly, our laboratory has recently developed a clinical-grade process to effectively expand Vδ1$^+$ T cells while also inducing NCR (and augmenting NKG2D) expression; and established the proof-of-concept in a leukaemia xenograft models[114].

The first demonstration that NCRs, including NKp30 and NKp46 that are widely considered to be two of the most specific NK markers, could be expressed in a considerable Vδ1$^+$ PBL subset dates back to 2011[303]. Indeed, the NCR induction is coupled to TCR-mediated proliferation of Vδ1$^+$ cells, while also requiring γ_c cytokine signals, thereby endowing Vδ1$^+$ T cells with more potent cytolytic activity against hematologic tumours. This could have been achieved *in vitro* with a combination of IL-2 or IL-15 with PHA or OKT3, consistently with previous reports demonstrating that the *in vitro* acquisition of NK receptors by liver or umbilical cord T cells depends on IL-15[304,305].

These findings were at the basis for the development, in our laboratory, of a new protocol designed to selectively expand Vδ1$^+$ T cells[114].The major novelties of the protocol consisted in its direct clinical adaptability, since it involves the use of reagents and materials currently available in pharmaceutical grade, and the uncoupling of the expansion from the differentiation stages. This new two-step treatment allowed

the highest expansion of Vδ1$^+$ T cells ever recorded *in vitro* (on 96-well plates): >60,000-fold increase in 21 days, compared to <25,000-fold obtained by Siegers and colleagues[306]. The method is indeed robust enough, including in larger cell bags, to enrich >60% and expand up to 2,000-fold Vδ1$^+$ T cells from PBMCs from chronic lymphocytic leukaemia (CLL) patients, differentiating them into NCR-expressing and highly cytotoxic DOT cells. Moreover, DOT cells were tested in a xenograft model of CLL, and induced a reduction in tumour size and prevented tumour dissemination, providing a first preclinical proof-of-concept for the use of DOT cells in CLL treatment[114].

2 Aims of the thesis

While Vδ1$^+$ γδ T cells are the second most abundant subset in the human PB, they are the predominant γδ T cell subset in the post-natal thymus and in peripheral tissues such as the intestine or the liver. This γδ T subset plays an important role during viral infections, especially CMV, and are associated to a favourable prognosis in some cancer settings. Moreover, in contrast to the main γδ subset in the blood (Vγ9Vδ2$^+$ T cells), Vδ1$^+$ T cells are less susceptible to AICD, can persist in the body for extended periods of time and have never been tested in clinical trials. Given their unique features, we decided to focus on Vδ1$^+$ γδ T cells and to pursue three main areas of investigation and to provide further characterization with new insights on their anti-tumour functions and ligand recognition. In this context, the aims of the thesis were: 1) to perform the repertoire analysis and characterization of the thymic output of the Vδ1$^+$ γδ T cell compartment; 2) to characterize the Vδ1$^+$ cells after expansion with the DOT cell protocol and, consequently, test the Vδ1$^+$ based product to obtain the pre-clinical proof of concept for the treatment of AML; 3) to identify new ligands for Vδ1$^+$ γδ T cells.

Thanks to recent technical advances in the comprehensive analysis of TCR repertoires using next-generation sequencing (NGS) approaches, it has become more accessible to understand the dynamics of T cell development and homeostasis, and T cell expansion in response to infections or tumours. Indeed, to characterize the human Vδ1$^+$ thymocytes TCR repertoire, we obtained cells from thymic specimens routinely collected during paediatric corrective cardiac surgery. We isolated highly pure Vδ1$^+$ thymocytes and provided a detailed description of transcribed (mRNA) V(D)J recombination products. Since cord blood and peripheral blood Vδ1$^+$ TCR sequencing data are already available to the scientific community, the results from this part of the project will contribute to the establishment of a compelling picture of the Vδ1$^+$ repertoire in humans, providing useful information for an earlier step in Vδ1$^+$ thymocyte ontogeny.

Next, we generated DOT cells, the clinical grade product mainly composed of expanded Vδ1$^+$ with higher or *de novo* expression of NCRs. We provided a new level of analysis, comparing the *TRG* and *TRD* repertoires from DOT cells with the *ex vivo* Vδ1$^+$ cells collected from the same donors and, next, we tested DOT cell anti-tumour functions against several AML tumour cell lines and AML primary samples. We dissected the role of a TCR mediated mechanism in DOT cell targeting of tumour cells using blocking antibodies and generating Vδ1$^+$ cell clones. Finally, converging the properties and potential of DOT cells with the unmet immunotherapy needs of AML, we used *in vivo* models to purpose DOT cells for AML treatment and to obtain the preclinical proof-of-concept for DOT cell application in AML treatment.

Finally, we aimed at providing new insights in the TCR mediated recognition of tumour targets supporting the strong evidences in the literature for the antitumor activity of Vδ1 $^+$ T cells. We used the *ex vivo* and DOT repertoire data to select Vδ1$^+$ clones (generated using a modified version of the DOT-cell expansion protocol) accordingly to their frequency in the *ex vivo* and in the DOT repertoires of the analysed donors. We also tested clone cytotoxicity and TCR dependence in targeting AML cells. Next, we generated cell reporters by TCR molecular cloning and into the J.RT3 cell lines. Since J.RT3 cells lack β chain and TCR expression on the membrane, we used their T cell machinery to assess TCR-transduced J.RT3 cells activation after co-incubation with several tumour targets measuring CD69 expression and upregulation and CD3/Vδ1 downregulation. If successful, the identification of new ligands from transformed cells will provide key insights on the Vδ1$^+$ T cell recognition and may have a strong impact on the current Vδ1$^+$ T cell-based therapies being developed, including DOT cells.

3 Materials and methods

3.1 High-throughput analysis of the human thymic Vδ1 $^{+}$ TCR repertoire

3.1.1 Sample collection and preparation

Thymic specimens were routinely collected during paediatric corrective cardiac surgery, after obtaining written informed consent. The study was approved by the Ethics Board of the Faculdade de Medicina da Universidade de Lisboa. Buffy coats from healthy volunteers were obtained under the agreement (15.12.2003) between Instituto de Medicina Molecular – João Lobo Antunes and Instituto Português do Sangue e da Transplantação approved by the local ethical committee (Centro de Ética do Centro Hospitalar Lisboa Norte - Hospital de Santa Maria). Thymic samples (from 5 days old to 15 months old children) were processed by tissue dispersion and Histopaque-1077 (Sigma-Aldrich) density gradient. Peripheral blood was collected from buffy coat cells, diluted with 1 volume of PBS (Invitrogen Life Technologies), and separated on a Histopaque-1077 density gradient. γδ T cells were first isolated by magnetic cell sorting (MACS) using a negative selection strategy (αβ depletion kit by Miltenyi Biotech); and then stained with anti-TCRVδ1 (clone TS8.2), anti-TCRVδ2 (clone B6), anti-CD3 (clone HIT3a) and anti-TCRαβ (clone IP26) mAbs; and FACS-sorted (CD3 $^{+}$ TCRVδ1^{+}) to >98% purity in FACS Aria III (BD Biosciences). Flow cytometry acquired data was analysed with FlowJo X software (Tree Star).

3.1.2 TRG and TRD amplicon generation, library preparation and NGS

FACS-sorted cells were subjected to RNA extraction using the RNAeasy mini kit (Qiagen). Next, 12µl mRNA of each sample was reverse transcribed with the Superscript III enzyme kit (Invitrogen) according to the manufacturers protocol. Next, CDR3 TRG and TRD sequencing amplicons were generated as described previously[122] using 7 µl cDNA template. In detail, primers were designed for all functional variable (V) and constant (C) gene segments of the human TRG and TRD locus having following sequences (5' – 3') h*TRD*V1: TCAAGAAAGCAGCGAAATCC; h*TRD*V2: ATTGCAAAGAACCTGGCTGT; h*TRD*V3: CGGTTTTCTGTGAAACACATTC; h*TRD*V5/29: ACAAAAGTGCCAAGCACCTC; h*TRD*C1: GACAAAAACGGATGGTTTGG; h*TRG*V (2,3,4,5,8): ACCTACACCAGGAGGGGAAG; h*TRG*V9: TCGAGAGAGACCTGGTGAAGT; h*TRG*C (1,2): GGGGAAACATCTGCATCAAG. Moreover, Illumina adaptor sequences (GTCTCGTGGGCTCGGAGATGTGTATAAGAGACAG and TCGTCGGCAGCGTCAGATGTGTATAAGAGACAG) were added as overhangs All forward primers for either TRG or TRD were combined in equal concentrations. PCR conditions are as following 1× PCR buffer (without $MgCl_2$; Invitrogen), 1.5 mM $MgCl_2$, 10 mM dNTPs, 0.5 µM forward primer mix, 0.5 µM reverse primer and 0.04 units recombinant Taq polymerase (Invitrogen). Cycling conditions were 3 min at 95 °C; 30s at 95 °C, 30s at 63 °C and 30s 72 at °C, for 5 cycles; 30s at 95 °C and 35s 72 at °C, for 20–25 cycles; and 4 min at 72 °C. PCR samples were run for gel electrophoresis on a 1%-Agarose-Gel, PCR amplicons (350 bps for TRG and 250 bps) were excised and gel-purified according to the QIAquick gel extraction kit (Qiagen). The multiplex-based CDR3 amplicon generation strategy has been previously validated by the 5'RACE-based CDR3 amplicon generation methods[122].

For Illumina Miseq analysis, PCR amplicons were further subjected to an index PCR. In that case, individual 10 µl purified PCR amplicons were combined with 10 µl Advantage II PCR buffer (Clontech), 5 µl 10mM dNTP (Clontech), 5 µl N50X and 5 µl N70X index primer (Nextera Index Kit, Illumina), 1 µl Advantage II

polymerase (Clontech) and 30 µl dH_2O for eight additional PCR cycles. PCR products were purified using the Agencourt AMPure XP PCR purification kit (Beckman Coulter) and eluted in 100 µl dH2O. After quantifying DNA concentrations with the QuantIT PicoGreen Assay (Invitrogen) PCR amplicons were pooled in equal concentration to generate the library pool and diluted to 4 nM. According to the Illumina Denature and Dilute Library guidelines the library was diluted to 10 pM, while 20% PhIX was added as a control. The library was subjected to Illumina MiSeq analysis (paired-end sequencing) using following parameters: Amplicon chemistry; dual index; read 1: 250bps; read 2: 250bps; FASTQ only; use adaptor trimming.

3.1.3 NGS data analysis

3.1.3.1 Processing and annotation of obtained TRG and TRD sequences

Data Processing and Analysis TRG and TRD FASTQ sequences were subjected to quality controls through FASTQC (http://www.bioinformatics.babraham.ac.uk/projects/fastqc). Paired-end TRG sequences were joined at their overlapping ends using FASTQ-join of the command-line tool ea-utils with default parameters, while TRD sequences were fully covered from both ends and were processed directly. All TRG and TRD sequences obtained were annotated using IMGT/HighV-Quest.

3.1.3.2 Post-analysis of TCR repertoire

The post analysis of the TCR repertoire was performed using in-house *UNIX* (steps 1-4) and *R* scripts (steps 5-12; R version 3.2.2)

1. *Convert data from the IMGT output format to vdjtools output format*

The IMGT output contains germline alignment and junctional analysis data. Results are based on the use of standardized gene and allele nomenclature, standardized description and delimitation of labels (especially for the CDRs and FRs regions), but its tabular output must be converted to the VTDtools format before using VDJtools software

> java -Xmx16G -jar /home/bdilorenzo/vdjtools-1.1.1/vdjtools.jar Convert -S ImgtHighVquest /home/bdilorenzo/Desktop/Thy2018/Thy1/Gamma **/3_Nt-sequences.txt /home/bdilorenzo/Desktop/**Thy2018/Thy1/Gamma **/Analysis/conv**

Load VDJtools (**java -Xmx16G –jar /home/bdilorenzo/vdjtools-1.1.1/vdjtools.jar**), convert the IMGT tabular output (**Convert -S ImgtHighVquest /home/bdilorenzo/Desktop/** Thy2018/Thy1/Gamma **/3_Nt-sequences.txt**) and save the new output in (**/home/bdilorenzo/Desktop/** Thy2018/Thy1/Gamma **/Gamma/Analysis/conv**)

2. *Calculate Basic Statistics*

VDJtools can compute basics statistics (such as number of reads, number of clonotypes, mean and geometric mean of clonotype frequency, mean CDR3 length, CDR3 convergence and number of N nucleotides) as well as diversity measurement (such as the Shannon-Wiener diversity index after collapsing the clonotypes, mean value and standard deviation of the diversity estimate) from HTS raw data (step 3).

> java -Xmx16G -jar /home/bdilorenzo/vdjtools-1.1.1/vdjtools.jar CalcBasicStats /home/bdilorenzo/Desktop/ Thy2018/Thy1/Gamma **/Analysis/conv.3_Nt-sequences.txt /home/bdilorenzo/Desktop/** Thy2018/Thy1/Gamma **/Analysis/Calcbasicstats**

Load VDJtools (**java -Xmx16G –jar /home/bdilorenzo/vdjtools-1.1.1/vdjtools.jar**), calculate basic statistics from the newly generated tabular output (**CalcBasicStats /home/bdilorenzo/Desktop/** Thy2018/Thy1/Gamma **/Analysis/conv.3_Nt-sequences.txt**), and save the generated stats as a new table (**/home/bdilorenzo/Desktop/** Thy2018/Thy1/Gamma **/Analysis/Calcbasicstats**)

3. Calculate Diversity

> java -Xmx16G -jar /home/bdilorenzo/vdjtools-1.1.1/vdjtools.jar CalcDiversityStats /home/bdilorenzo/Desktop/ Thy2018/Thy1/Gamma **/Analysis/conv.3_Nt-sequences.txt /home/bdilorenzo/Desktop/** Thy2018/Thy1/Gamma **/Analysis/CalcDiversitystats**

Load VDJtool (**java -Xmx16G –jar /home/bdilorenzo/vdjtools-1.1.1/vdjtools.jar**), calculate intra-sample diversity from the newly generated tabular output (**CalcDiversityStats /home/bdilorenzo/Desktop/** Thy2018/Thy1/Gamma **/Analysis/conv.3_Nt-sequences.txt**), and save the generated stats as a new table (**/home/bdilorenzo/Desktop/** Thy2018/Thy1/Gamma **/Analysis/ CalcDiversitystats**)

4. V-J segment usage analysis and representation

This function can generate a tabular output and a graphical representation of the V and J segment usage

> java -Xmx16G -jar /home/bdilorenzo/vdjtools-1.1.1/vdjtools.jar PlotFancyVJusage /home/bdilorenzo/Desktop/ Thy2018/Thy1/Gamma **/Analysis/conv.3_Nt-sequences.filt.txt /home/bdilorenzo/Desktop/** Thy2018/Thy1/Gamma **/Analysis/fancyspectra**

Load VDJtool (**java -Xmx16G –jar /home/bdilorenzo/vdjtools-1.1.1/vdjtools.jar**), and using the **PlotFancyVJusage** function, load the previously converted table (**/home/bdilorenzo/Desktop/** Thy2018/Thy1/Gamma **/Analysis/conv.3_Nt-sequences.filt.txt**) and use it to generate the tabular and the graphical output in the selected folder (**/home/bdilorenzo/Desktop/** Thy2018/Thy1/Gamma **/Analysis/fancyspectra**).

The generated tabular output is a matrix with rows corresponding to different J segments and columns corresponding to different V segments. Each cell contains the frequency of a given V-J junction. The graphical output for the V-J junction is a *circos* plot (Figure 3.1): arcs correspond to different V and J segments, scaled to their frequency in sample and ribbons represent V-J pairings and their size is scaled to the pairing frequency.

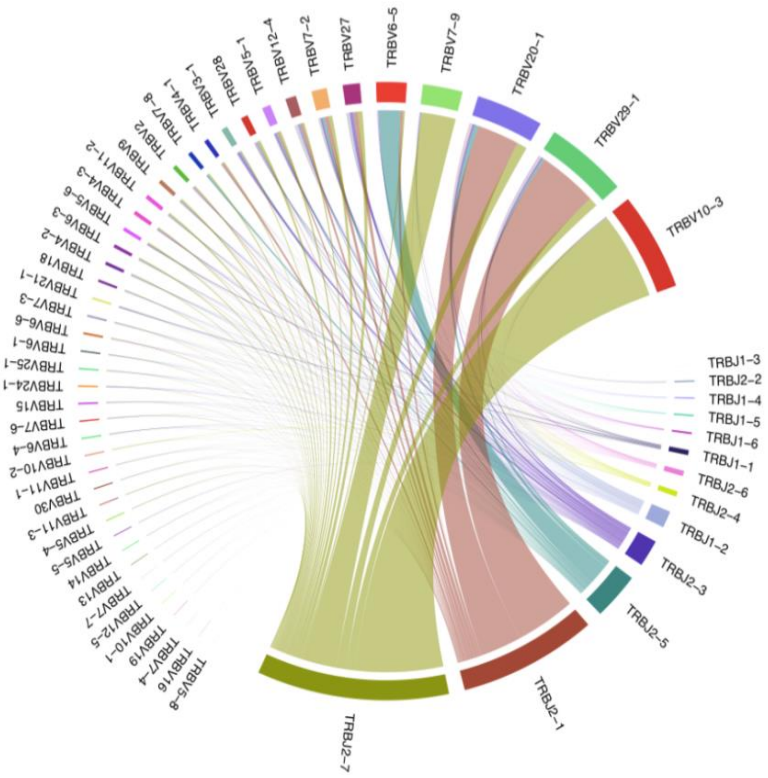

Figure 3.1 Example of V-J junction circos plot for a single sample. Arcs correspond to different V and J segments, scaled to their frequency in sample. Ribbons represent V-J pairings and their size is scaled to the pairing frequency (weighted in present case).

5. *Load the main and accessory packages needed for the NGS chain representation*

> library("tcR")

Platform for the advanced analysis of T cell receptor and Immunoglobulin repertoires data and visualization of the analysis results (see paragraph 1.2.5.3; https://cran.r-project.org/web/packages/tcR/index.html)[74].

> library("RColorBrewer")

The package provides palettes for drawing plots and figures shaded according to a variable (https://cran.r-project.org/web/packages/RColorBrewer/index.html).

> library("treemap")

R package useful for space-filling visualization of hierarchical structures (https://cran.r-project.org/web/packages/treemap/index.html).

> library("devEMF")

It starts the graphics device driver for producing enhanced metafile (emf+/emf) graphics, which can be imported natively as vector graphics in Microsoft Office (https://cran.r-project.org/web/packages/devEMF/index.html).

6. *Set the default colors for Treemap graphical output*

> colori_gamma = c("#DC143C", "#FFC125", "#C1FFC1", "#00C78C", "#00BFFF", "#00688B", "#9F79EE", "#030303")

> colori_delta = c("#00CED1", "#FF7F50", "#848484", "#006400", "#EE00EE", "#432c66")

These strings generate two variables containing color codes in the h*exadecimal format and will be used to standardize the Treemap graphical output of the repertoire representation*

7. Load dataset

```
> thy18_1gamma <- read.delim("/home/bdilorenzo/Desktop/Thy2018/Thy1/Gamma/Analysis/conv.3_Nt-sequences.txt")
```

8. Change V chain nomenclature

To standardize the TRG- and TRD- V gene nomenclature, the chain names were changed as follow.

TRGV:

```
> thy18_1gamma$v <- sub("TRGV1","TRGV01", thy18_1gamma$v)
> thy18_1gamma$v <- sub("TRGV2","TRGV02", thy18_1gamma$v)
> thy18_1gamma$v <- sub("TRGV3","TRGV03", thy18_1gamma$v)
> thy18_1gamma$v <- sub("TRGV4","TRGV04", thy18_1gamma$v)
> thy18_1gamma$v <- sub("TRGV5P","TRGV05", thy18_1gamma$v)
> thy18_1gamma$v <- sub("TRGV5","TRGV05", thy18_1gamma$v)
> thy18_1gamma$v <- sub("TRGV8","TRGV08", thy18_1gamma$v)
> thy18_1gamma$v <- sub("TRGV9","TRGV09", thy18_1gamma$v)
```

TRDV:

```
> thy18_1delta$v <- sub("TRDV1","TRDV01", thy18_1delta$v)
> thy18_1delta$v <- sub("TRDV2","TRDV02", thy18_1delta$v)
> thy18_1delta$v <- sub("TRDV3","TRDV03", thy18_1delta$v)
> thy18_1delta$v <- sub("TRAV29/DV5","TRDV05(TRAV29)", thy18_1delta$v)
> thy18_1delta$v <- sub("TRAV14/DV4","TRDV04(TRAV14)", thy18_1delta$v)
> thy18_1delta$v <- sub("TRAV38.2/DV8","TRDV08(TRAV38.2)", thy18_1delta$v)
```

9. Remove TRGV01

Since this gene is found to be in ORF but does not appear to be functional, we removed TRGV01 sequences from the datasets. However, TRGV01 sequences were really rare or absent: **thy18_1gamma** dataset contains only one TRGV01 sequence.

```
> thy18_1gamma <- thy18_1gamma[-c(50406),]
```

10. Change column and row names

The word *Chain* was set as name for the column including the TR(G or D)V information and the clonotype IDs (the first column of the VDJtool converted tabular output) were set as row names

> names(thy18_1gamma)[5]<-paste("Chain")

> ID = rownames(thy18_1gamma)

> thy18_1gamma$ID <- ID

11. Treemap representation of the repertoire

> emf("/home/bdilorenzo/Desktop/New output/2018thy1gamma.emf", bg = "transparent", fg = "black", family = "Helvetica", emfPlus=FALSE)

First, the emf device needs to be loaded in order to generate images that can be easily exported and adjusted in the Microsoft environment. In this step, file name, background color (**Bg**), font color (**fg**) and style (**family**) together with emf advanced options are set.

> treemap::treemap(thy18_1gamma, index = "ID", vSize = "count", vColor = "Chain", type= "categorical", title = "Thymus 1 - 2018 (Gamma)", border.col = "white", fontsize.labels = 0 , border.lwds = 1, palette = colori_gamma)

When the emf device is set, all the subsequently generated output will be automatically written in the emf file. To generate a Treemap graphical representation, we selected the treemap function from the treemap package (treemap::treemap). This function requires a dataset (**thy18_1**) that includes a column with specified value names (index = "ID"), a column containing the value size (vSize = "count"), a column for which the data will be clustered (vColor = "Chain") and the type of treemap (type= "categorical"). In this type of treemap, the colors are given by groups; other options are index (meaning a color per clonotype), value (to assign a specific color to all the values), comp (colors indicate change of the size with respect to another numeric column in the dataset), dens (color are assigned in a density map fashion), depth (in which colors are given by aggregation levels) or manual. Graph title, axes font and size, graph border can also be set. In this string a command from the **RColorBrewer** package (palette) was included in order to set two color palettes and to standardize color usage for chain clustering among different samples.

> dev.off()

Finally, to avoid subsequent overwriting on the same emf file, we closed the emf device.

12. CDR3 lengths graphical representation

> cdr3thy18_1gamma <- parse.vdjtools("/home/bdilorenzo/Desktop/Thy2018/Thy1/Gamma/Analysis/conv.3_Nt-sequences.txt")

We used the tcR R suite for the graphical representation of CDR3 length. First of all, the VDJtool tabular output needs to be converted in the **tcR** format. To do so, we employed the parse.vdjtools function.

> emf("/home/bdilorenzo/Desktop/New output/cdr2018thy1gamma.emf", bg = "transparent", fg = "black",family = "Helvetica", emfPlus=FALSE)

> plot(vis.count.len(cdr3thy18_1gamma,.name = "Thymus 1 - 2018 (Gamma)"))

> dev.off()

As for the treemap representation, we started opening an emf file device to facilitate following graph adjustments in Microsoft environment. Once the device is set, the **tcR** function **vis.count.len** integrated

with the R **plot** function will automatically select the column containing the CDR3 length information in the parsed table (cdr3thy18_1gamma) and will plot these information in a histogram of counts (Figure 3.2).

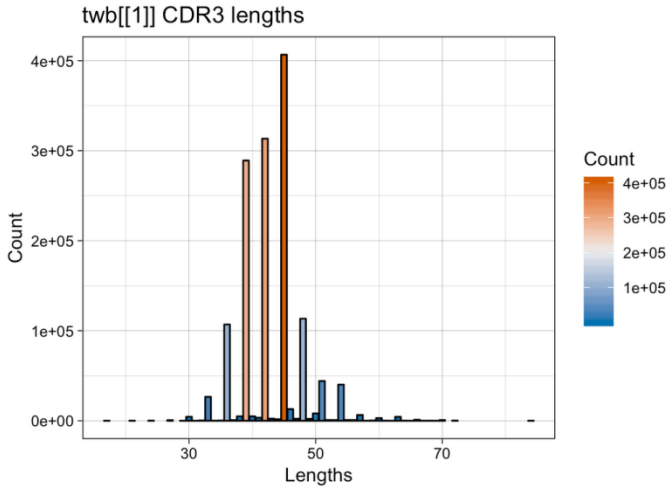

Figure 3.2 Example of CDR3 nucleotide sequences length distribution plot. Colors are assigned in a heat map fashion accordingly to length frequency: lower frequencies in blue and higher in red.

3.1.4 Statistical analysis

Statistical analysis was performed using GraphPad Prism software. All data are expressed as mean +/- SEM and comparisons of two groups were made using Student's t-test

3.1.5 Data availability

FASTQ files of thymic TRG and TRD sequences are available and deposited with links to BioProject accession number PRJNA495594; the complete list of samples is displayed in Table 3.1. Blood-derived Vδ1^{+} TRG and TRD sequences used as control are described in Table 3.2 and available in the BioProject #PRJNA491919 under the following accession number: SRR7878381, SRR7878385, SRR7878376, SRR7878367, SRR7878393, SRR7878388. (https://www.ncbi.nlm.nih.gov/bioproject/).

Table 3.1 Sample SRA accession numbers included in the BioProject #PRJNA495594

Accession	Title	Biosample_accession	Filename
SRR7993359	Rna-Seq of hyman V1^{+} thymocytes, gamma chain. Donor1	SAMN10228156	DG_S31_L001_R1_001.fastq.gz
SRR7993360	Rna-Seq of hyman V1^{+} thymocytes, gamma chain. Donor2	SAMN10228157	AG_S28_L001_R1_001.fastq.gz
SRR7993357	Rna-Seq of hyman V1^{+} thymocytes, gamma chain. Donor3	SAMN10228158	EG_S32_L001_R1_001.fastq.gz
SRR7993358	Rna-Seq of hyman V1^{+} thymocytes, gamma chain. Donor4	SAMN10228159	CG_S30_L001_R1_001.fastq.gz
SRR7993355	Rna-Seq of hyman V1^{+} thymocytes, gamma chain. Donor5	SAMN10228160	FG_S10_L001_R1_001.fastq.gz
SRR7993356	Rna-Seq of hyman V1^{+} thymocytes, gamma chain. Donor6	SAMN10228161	GG_S11_L001_R1 _001.fastq.gz
SRR7993353	Rna-Seq of hyman V1^{+} thymocytes, gamma chain. Donor7	SAMN10228162	HG_S12_L001_R1_001.fastq.gz
SRR7993354	Rna-Seq of hyman V1^{+} thymocytes, gamma chain. Donor8	SAMN10228163	IG_S13_L001_R1_001.fastq.gz
SRR7993361	Rna-Seq of hyman V1^{+} thymocytes, delta chain. Donor1	SAMN10228164	DD_S36_L001_R1_001.fastq.gz

SRR7993362	Rna-Seq of hyman $V1^+$ thymocytes, delta chain. Donor2	SAMN10228165	AD_S33_L001_R1_001.fastq.gz
SRR7993351	Rna-Seq of hyman $V1^+$ thymocytes, delta chain. Donor3	SAMN10228166	ED_S37_L001_R1_001.fastq.gz
SRR7993352	Rna-Seq of hyman $V1^+$ thymocytes, delta chain. Donor4	SAMN10228167	CD_S35_L001_R1_001.fastq.gz
SRR7993349	Rna-Seq of hyman $V1^+$ thymocytes, delta chain. Donor5	SAMN10228168	FD_S22_L001_R1_001.fastq.gz
SRR7993350	Rna-Seq of hyman $V1^+$ thymocytes, delta chain. Donor6	SAMN10228169	GD_S23_L001_R1_001.fastq.gz
SRR7993347	Rna-Seq of hyman $V1^+$ thymocytes, delta chain. Donor7	SAMN10228170	HD_S24_L001_R1_001.fastq.gz
SRR7993348	Rna-Seq of hyman $V1^+$ thymocytes, delta chain. Donor8	SAMN10228171	ID_S25_L001_R1_001.fastq.gz

3.2 Broad cytotoxic targeting of acute myeloid leukemia by highly polyclonal Delta One T cells

3.2.1 Ethics statement

Primary AML cells were obtained from the peripheral blood of patients at first presentation, after informed consent and institutional review board approval. Buffy coats from healthy volunteers were obtained under the agreement (15.12.2003) between Instituto de Medicina Molecular – João Lobo Antunes and Instituto Português do Sangue e da Transplantação approved by the local ethical committee (Centro de Ética do Centro Hospitalar Lisboa Norte - Hospital de Santa Maria)

3.2.2 Mice

NSG, NSGS, NRGS mice were obtained from the Jackson Laboratories. Age and sex-matched animals were randomly distributed among the different groups. All animal procedures were performed in accordance to national guidelines from the Direção Geral de Veterinária and approved by the Ethics Committee.

3.2.3 DOT cell production

Delta One T (DOT) cells were obtained using the previously patented and described protocol[114]. Peripheral blood was collected fresh blood of healthy volunteers (see 3.3.1), diluted with 1 volume of PBS (Invitrogen Life Technologies), and separated on a Histopaque-1077 density gradient. γδ T cells were first isolated by magnetic cell sorting (MACS) using a negative selection strategy (non-γδ depletion kit by Miltenyi Biotech). (MACS)-sorted γδ T cells were resuspended in serum-free culture medium (OpTmizer-CTS) supplemented with 5% FBS and 2 mmol/L L-glutamine (Thermo Fischer Scientific). Cells were transferred to a closed gas-permeable cell culture plastic bag (Saint-Gobain), at a maximum concentration of 1*10^6 cells/mL. Animal-free human cytokines (100 ng/mL rIL4, 70 ng/mL rIFNg, 7 ng/mL rIL21, and 15 ng/mL rIL1b; all from Peprotech) and a soluble antibody (70ng/mL anti-CD3 mAb, clone OKT-3; BioXcell) were added to the medium. Cells were incubated at 37 C° and 5% CO2. Every 5 to 6 days, old medium was removed and replaced with fresh medium supplemented with a cytokine cocktail specific per time point (Figure 4.3).

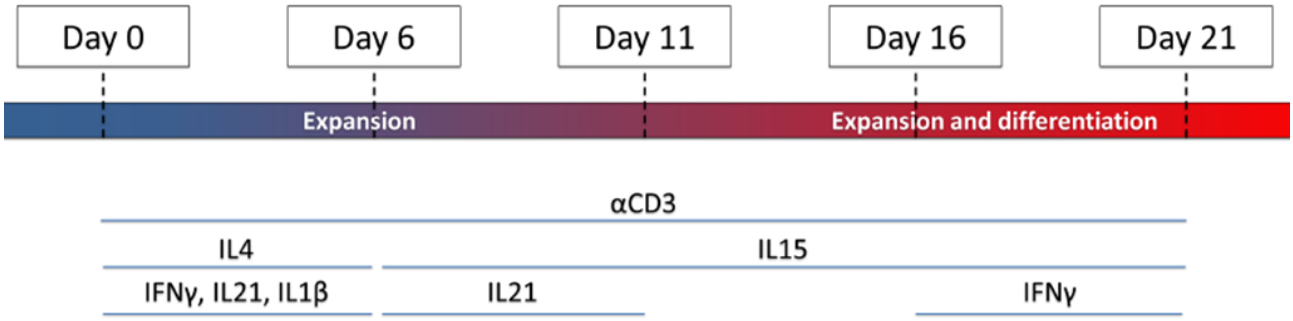

Figure 3.3 Schematic representation of the DOT cell expansion protocol

3.2.4 Vδ1$^+$ clone generation

For DOT cell clone generation, we design a modified version of the DOT cell expansion protocol described in 2.2.3. PBMCs were enriched for γδ T cells using by magnetic cell sorting (MACS) using a negative selection strategy (non-γδ depletion kit by Miltenyi Biotech). (MACS)-sorted γδ T cells were then stained with anti-TCRVδ1 (clone TS8.2), anti-TCRVδ2 (clone B6), anti-CD3 (clone HIT3a), enriched for CD3$^+$ TCRVδ1$^+$TCRVδ2- cells and sorted as single cells into 96 wells/plate using a FACS-AriaIII machine (BD). CD3$^+$ TCRVδ1$^+$TCRVδ2- single cells were cultured for 21 days using the DOT cell protocol in the presence of (weekly-renewed) 5*10^4 irradiated autologous PBMCs (feeders). For more details, refer to paragraph 3.3.2.

3.2.5 DOT cell expansion with TCR or cytokine stimulation

We tested two additional experimental protocols (Figure 3.4 B and C) dissecting the impact of TCR or cytokine stimulation after expansion. B) αβ depleted PBMCs were cultured for 21 days in the presence of IL2 (100ng/ml) and αCD3 (OKT3 - 1µg/ml) or C) in the presence of the standard expansion medium but using IL2 (100ng/ml) instead of αCD3.

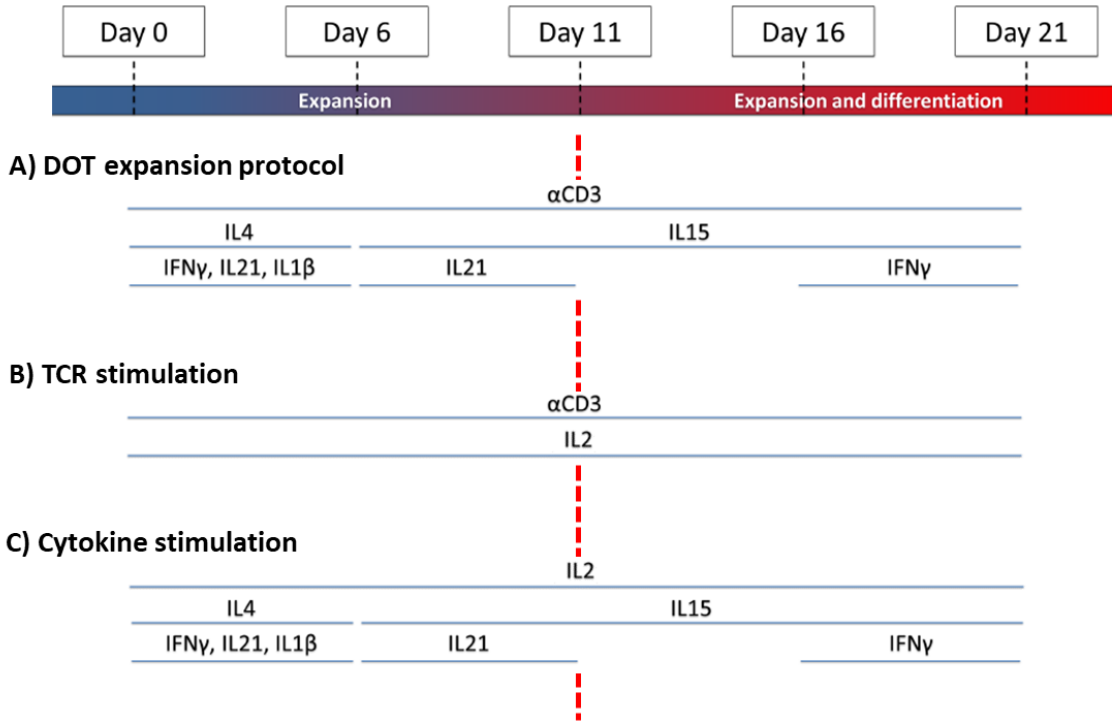

Figure 3.4 Schematic representation of the DOT, TCR and cytokine expansion protocols

3.2.6 Expansion of naïve Vδ1$^+$CD27$^+$ and differentiated Vδ1$^+$CD27-

Peripheral blood was collected from buffy coat cells, diluted with 1 volume of PBS (Invitrogen Life Technologies), and separated on a Histopaque-1077 density gradient. γδ T cells were first isolated by magnetic cell sorting (MACS) using a negative selection strategy (non-γδ depletion kit by Miltenyi Biotech). (MACS)-sorted γδ T cells were stained with anti-TCRVδ1 (clone TS8.2), anti-TCRVδ2 (clone 123R3), anti-CD3

(clone HIT3a), anti-CD27 (clone O323), anti-TCRαβ (clone IP26) and sorted on FACS-Aria III (BD) as $CD3^{+}$αβ-$TCRV\delta1^{+}TCRV\delta2$-$CD27^{+}$ or $CD3^{+}$ αβ-$TCRV\delta1^{+}TCRV\delta2$-CD27-. Cells were then plated into 96 wells/plate at a maximum concentration of 20000/well.

3.2.7 TCR repertoire analysis

For TRGV and TRDV repertoire analysis, $V\delta1^{+}$ T cells were FACS-sorted either from the initial blood sample (*ex vivo*); or from the final (3-week culture) DOT cell products (3.2.3, 3.2.5 and 3.2.6). Next-generation sequencing and data analysis were performed as described in 3.1.2 and 3.1.3, respectively.

3.2.8 Data availability

FASTQ files are available and deposited with links to BioProject accession number PRJNA491919. (https://www.ncbi.nlm.nih.gov/bioproject/). A complete list of deposited samples is displayed in Table 3.2

Table 3.2 Sample SRA accession numbers included in the BioProject #PRJNA491919

Accession	Title	BioSample	SRA.filename
SRR7878382	RNA-Seq of human Vdelta1 T cells from peripheral blood. Donor 1, gamma chain	SAMN10092784	D1-Gamma-PortugalPBH_S37_L001_R2_001.fastq.gz, D1-Gamma-PortugalPBH_S37_L001_R1_001.fastq.gz
SRR7878381	RNA-Seq of human Vdelta1 T cells from peripheral blood. Donor 2, gamma chain	SAMN10092785	D2-Gamma-PortugalPBH_S38_L001_R2_001.fastq.gz, D2-Gamma-PortugalPBH_S38_L001_R1_001.fastq.gz
SRR7878380	RNA-Seq of human Vdelta1 T cells from peripheral blood. Donor 3, gamma chain	SAMN10092786	D3-Gamma-PortugalPBH_S39_L001_R2_001.fastq.gz, D3-Gamma-PortugalPBH_S39_L001_R1_001.fastq.gz
SRR7878379	RNA-Seq of human Vdelta1 T cells from peripheral blood. Donor 4, gamma chain	SAMN10092787	D4-Gamma-PortugalPBH_S40_L001_R1_001.fastq.gz, D4-Gamma-PortugalPBH_S40_L001_R2_001.fastq.gz
SRR7878383	RNA-Seq of human Vdelta1 T cells from peripheral blood. Donor 4, delta chain	SAMN10092787	F11-Delta-PortugalPB_S71_L001_R2_001.fastq.gz, F11-Delta-PortugalPB_S71_L001_R1_001.fastq.gz
SRR7878386	RNA-Seq of human Vdelta1 T cells from peripheral blood. Donor 1, delta chain	SAMN10092788	F8-Delta-PortugalPBH_S68_L001_R2_001.fastq.gz, F8-Delta-PortugalPBH_S68_L001_R1_001.fastq.gz
SRR7878385	RNA-Seq of human Vdelta1 T cells from peripheral blood. Donor 2, delta chain	SAMN10092789	F9-Delta-PortugalPBH_S69_L001_R1_001.fastq.gz, F9-Delta-PortugalPBH_S69_L001_R2_001.fastq.gz
SRR7878384	RNA-Seq of human Vdelta1 T cells from peripheral blood. Donor 3, delta chain	SAMN10092790	F10-Delta-PortugalPB_S70_L001_R2_001.fastq.gz, F10-Delta-PortugalPB_S70_L001_R1_001.fastq.gz
SRR7878378	RNA-Seq of DOT cells. Cultured cells from Donor 1, gamma chain	SAMN10092792	D5-Gamma-PortugalB_S41_L001_R1_001.fastq.gz, D5-Gamma-PortugalB_S41_L001_R2_001.fastq.gz
SRR7878377	RNA-Seq of DOT cells. Cultured cells from Donor 2, gamma chain	SAMN10092793	D6-Gamma-PortugalB_S42_L001_R1_001.fastq.gz, D6-Gamma-PortugalB_S42_L001_R2_001.fastq.gz
SRR7878370	RNA-Seq of DOT cells. Cultured cells from Donor 3, gamma chain	SAMN10092794	D7-Gamma-PortugalB_S43_L001_R1_001.fastq.gz, D7-Gamma-PortugalB_S43_L001_R2_001.fastq.gz
SRR7878369	RNA-Seq of DOT cells. Cultured cells from Donor 4, gamma chain	SAMN10092795	D8-Gamma-PortugalB_S44_L001_R1_001.fastq.gz, D8-Gamma-PortugalB_S44_L001_R2_001.fastq.gz
SRR7878372	RNA-Seq of DOT cells. Cultured cells from Donor 1, delta chain	SAMN10092796	F12-Delta-PortugalBu_S72_L001_R1_001.fastq.gz, F12-Delta-PortugalBu_S72_L001_R2_001.fastq.gz
SRR7878371	RNA-Seq of DOT cells. Cultured cells from Donor 2, delta chain	SAMN10092797	G1-Delta-PortugalB_S73_L001_R2_001.fastq.gz, G1-Delta-PortugalB_S73_L001_R1_001.fastq.gz
SRR7878374	RNA-Seq of DOT cells. Cultured	SAMN10092798	G2-Delta-PortugalB_S74_L001_R2_001.fastq.gz, G2-

	cells from Donor 3, delta chain		Delta-PortugalB_S74_L001_R1_001.fastq.gz
SRR7878373	RNA-Seq of DOT cells. Cultured cells from Donor 4, delta chain	SAMN10092799	G3-Delta-PortugalB_S75_L001_R2_001.fastq.gz, G3-Delta-PortugalB_S75_L001_R1_001.fastq.gz
SRR7878376	RNA-Seq of human Vdelta1 T cells from peripheral blood. Donor 5, gamma chain	SAMN10092800	TRG6_S6_L001_R2_001.fastq.gz, TRG6_S6_L001_R1_001.fastq.gz
SRR7878375	RNA-Seq of human naive Vdelta1 T cells from peripheral blood. Donor 5, gamma chain	SAMN10092801	TRG1_S1_L001_R2_001.fastq.gz, TRG1_S1_L001_R1_001.fastq.gz
SRR7878368	RNA-Seq of human differentiated Vdelta1 T cells from peripheral blood. Donor 5, gamma chain	SAMN10092802	TRG3_S3_L001_R1_001.fastq.gz, TRG3_S3_L001_R2_001.fastq.gz
SRR7878367	RNA-Seq of human Vdelta1 T cells from peripheral blood. Donor 6, gamma chain	SAMN10092803	TRG7_S7_L001_R1_001.fastq.gz, TRG7_S7_L001_R2_001.fastq.gz
SRR7878391	RNA-Seq of human naive Vdelta1 T cells from peripheral blood. Donor 6, gamma chain	SAMN10092804	TRG4_S4_L001_R2_001.fastq.gz, TRG4_S4_L001_R1_001.fastq.gz
SRR7878392	RNA-Seq of human differentiated Vdelta1 T cells from peripheral blood. Donor 6, gamma chain	SAMN10092805	TRG2_S2_L001_R2_001.fastq.gz, TRG2_S2_L001_R1_001.fastq.gz
SRR7878393	RNA-Seq of human Vdelta1 T cells from peripheral blood. Donor 5, delta chain	SAMN10092806	TRD6_S19_L001_R2_001.fastq.gz, TRD6_S19_L001_R1_001.fastq.gz
SRR7878394	RNA-Seq of human naive Vdelta1 T cells from peripheral blood. Donor 5, delta chain	SAMN10092807	TRD1_S14_L001_R2_001.fastq.gz, TRD1_S14_L001_R1_001.fastq.gz
SRR7878387	RNA-Seq of human differentiated Vdelta1 T cells from peripheral blood. Donor 5, delta chain	SAMN10092808	TRD3_S16_L001_R2_001.fastq.gz, TRD3_S16_L001_R1_001.fastq.gz
SRR7878388	RNA-Seq of human Vdelta1 T cells from peripheral blood. Donor 6, delta chain	SAMN10092809	TRD7_S20_L001_R1_001.fastq.gz, TRD7_S20_L001_R2_001.fastq.gz
SRR7878389	RNA-Seq of human naive Vdelta1 T cells from peripheral blood. Donor 6, delta chain	SAMN10092810	TRD4_S17_L001_R1_001.fastq.gz, TRD4_S17_L001_R2_001.fastq.gz
SRR7878390	RNA-Seq of human differentiated Vdelta1 T cells from peripheral blood. Donor 6, delta chain	SAMN10092811	TRD2_S15_L001_R2_001.fastq.gz, TRD2_S15_L001_R1_001.fastq.gz

3.2.9 *In vitro* cell targeting using DOT cells

3.2.9.1 AML cell lines and primary samples

AML cell lines (Table 3.3) were obtained from and authenticated by the German Resource Center for Biologic Material (DSMZ). For *in vitro* targeting, AML cell lines or primary samples were co-incubated with previously CFSE-stained (1:1000 in PBS with no FBS) DOT cells or Vδ1^{+} clones at optimized effector: target ratios for 3 hours. A pre-treatment to block the TCR on the clone was performed using an anti- Vδ1 antibody (clone TCS-1). After the co-incubation, cells were washed and stained with Annexin-V; flow cytometry data were acquired on a LSR Fortessa (BD) and data was analyzed with FlowJo X software (Tree Star). High-complexity barcode construction, lentiviral-barcode production, barcoding of AML cell lines and *in vivo* chemotherapy Drugs-resistance studies were performed as described[307].

3.2.9.2 Healthy controls

Peripheral blood was collected from buffy coat cell, diluted with 1 volume of PBS (Invitrogen Life Technologies), and separated on a Histopaque-1077 density gradient. αβ positive selection (Miltenyi) was performed on total PBMCs and the αβ- fraction was labeled using anti-CD33 (clone P67.6), anti-123 (clone 6H6), anti-CD56 (clone HCD56), anti-CD19 (clone HIB19) and sorted on Aria III (BD) for single positive $CD33^+$, $CD123^+$, $CD56^+$, $CD19^+$ cells. The day after, DOT cells from three different donors were stained with CFSE and the $\alpha\beta^+$ fraction was stained with anti-CD3 (clone OKT3). DOT cells and the target populations were co-incubated at optimized effector : target ratios for 3 hours (5 : 1, E : T). After the co-incubation, cells were washed and stained with Annexin-V; flow cytometry data were acquired on a LSR Fortessa (BD) and data was analyzed with FlowJo X software (Tree Star).

3.2.10 AML cell targeting *in vivo*

For in vivo targeting, three xenograft hAML models were established as represented in Figure 3.4. Tumour burden was assessed by staining with anti-human CD45 (clone HI30) and CD33 (clone P67.6) antibodies. Flow cytometry acquisition was performed on a LSR Fortessa (BD) and data was analyzed with FlowJo X software (Tree Star).

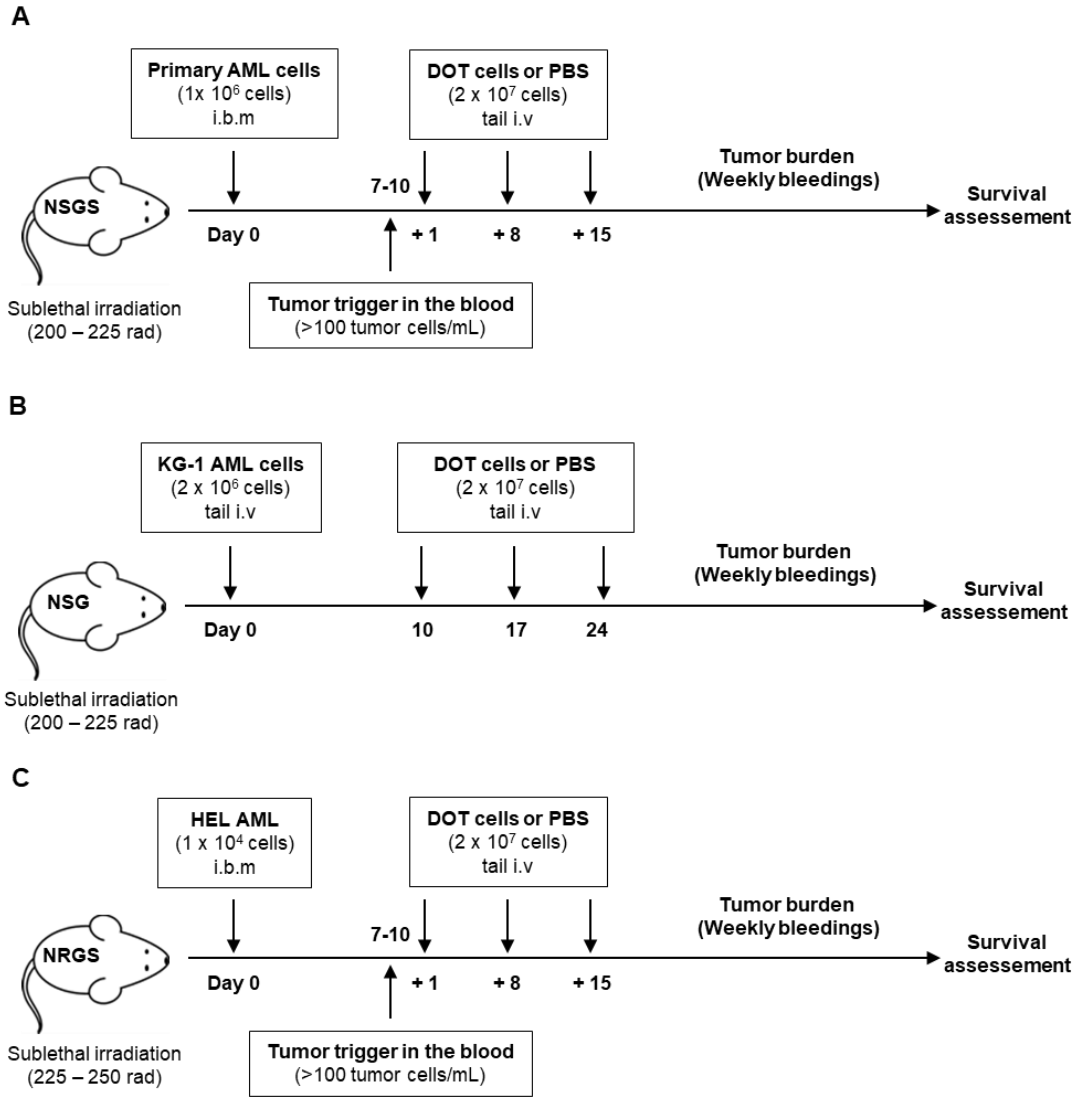

Figure 3.5 Xenograft models for in vivo AML targeting by DOT cells. (A) Irradiated (200-225 rad) 8-12 week old NOD-SCIDγc-/--SGM3 (NSGS) mice were anaesthetized and subsequently transplanted in the right tibia (intra-bone marrow - i.b.m.) with 1 x 106 primary human AML cells. (B) Irradiated (200-225 rad) NSG 8-12 week old NOD-SCIDγc-/- (NSG) mice were injected intravenously (i.v.) with 2 x 106 human KG-1 cells. (C) Irradiated (225-250 rad) 8-12 weeks old NOD.Rag1-γc-/--SGM3 (NRGS) mice were anaesthetized and subsequently transplanted in the right tibia (i.b.m.) with 1x104 human HEL cells. In (A) and (C), tumor engraftment was assessed through detection *of at least 100 tumor cells (tumor trigger) in the blood, 1-week after tumor cells injection. Treatments started as soon as 100 tumor cells were detected in the mouse blood (tumor trigger). In (B), treatments with either PBS or DOT cells started 10 days after intravenous injection of tumor cells. Animals were treated with three intravenous injections of PBS or 2 x 107 DOT cells, separated by 5 days

3.2.11 Statistical analysis

Statistical analyses were performed using GraphPad Prism software. All data are expressed as mean $^{+}$/- SEM. Comparisons of two groups was done by Student's t-test; and more than two groups by ANOVA test with Dunnet's post-test. Animal survival comparisons were performed using Log-rank (Mantel-Cox) test.

Table 3.3 Description of the AML cell lines employed in this study

Cell line	Cell type	Diagnosis	Karyotype/Genotype	Immunological markers	DSMZ ACC-No.
THP-1	Monocyte	Acute monocytic leukemia	Near-tetraploid carries t(9;11) associated with AML M5, leading to KMT2A-MLLT3 fusion transcripts (MLL-MLLT3; MLL-AF9)	CD3-, CD4$^+$, CD13$^+$, CD15$^+$, CD19-, CD34-, cyCD68$^+$, HLA-DR$^+$	ACC 16
HEL	Erythroblast	Erythroleukemia	Hypotriploid with 2.3% polyploidy carries also masked 5q- and 20q- consistent with AML M6/MDS and carried JAK2 V617F mutation	CD3-, CD13$^+$, CD14-, CD19-, CD33$^+$, CD41a$^+$, CD71$^+$, CD235a$^+$	ACC 11
AML-193	Monocyte	Acute monocytic leukemia	Hyperdiploid with 4% polyploidy	CD3-, CD4$^+$, CD13-, CD15$^+$, CD19-, CD33$^+$, CD34-, HLA-DR-	ACC 549
MV4-11	Macrophage	Acute monocytic leukemia	Hyperdiploid carry a t(4;11) and carries an FLT3 internal tandem duplication	CD3-, CD4$^+$, CD5-, CD8-, CD10-, CD14-, CD15$^+$, CD19-, CD33$^+$, CD34-	ACC 102
HL-60	Promyeloblast	Acute myeloid leukemia	Flat-moded hypotetraploid with hypodiploid sideline and 1.5% polyploidy, c-myc amplicons present in der(1) and in both markers	CD3-, CD4$^+$, CD13$^+$, CD14-, CD15$^+$, CD19-, CD33$^+$, CD34-, HLA-DR-	ACC 3
U-937	Histiocyte	Histiocytic lymphoma	Flat-moded hypotriploid carries t(10;11) (seen in AML M5) and t(1;5) resembles variant of t(2;5)	CD3-, CD4$^+$, CD14-, CD15$^+$, CD19-, CD33$^+$, CD34-, CD54$^+$	ACC 5
OCI-AML3	Myeloblast	Acute myeloid leukemia	Hyperdiploid carry an NPM1 gene mutation (type A) and the DNMT3A R882C mutation	CD3-, CD4$^+$, CD13$^+$, CD14-, CD15$^+$, CD19-, cyCD68$^+$, HLA-DR-	ACC 582
Kasumi-1	Myeloblast	Acute myeloid leukemia	Hypodiploid carry the t(8;21) leading to RUNX1-RUNX1T1 (AML1-ETO) fusion transcript and carry the KIT mutation N822	CD3-, CD4$^+$, CD13$^+$, CD14-, CD15$^+$, CD19-, CD33$^+$, CD34$^+$, CD38$^+$, CD71$^+$, HLA-DR$^+$	ACC 220
KG-1	Macrophage	Acute myeloid leukemia	Hypodiploid with 4.5% polyploidy and express fusion gene FGFR1OP2-FGFR1 (OP2-FGFR1)	CD3-, CD13$^+$, CD14-, CD15$^+$, CD19-, CD33$^+$, CD34$^+$, HLA-DR$^+$	ACC 14

3.3 A NGS-based approach for the identification of new ligands for Vδ1$^+$ T cell

3.3.1 Donor selection and DOT cell (bulk) expansion

Fresh blood samples were collected from a cohort of 9 volunteers, diluted with 1 volume of PBS (Invitrogen Life Technologies), and separated on a Histopaque-1077 density gradient. 0.5*10^6 PBMCs/donor were then stained with anti-TCRVδ1 (clone TS8.2), anti-TCRVδ2 (clone 123R3), anti-CD3 (clone HIT3a) for the flow cytometry data acquisition on LSR Fortessa (BD); the remaining samples were stored at 4° overnight. On the next day, four donors with the highest Vδ1$^+$ cell fraction were selected, and their PBMC samples were subjected to DOT cell expansion protocol as described in 3.2.3 and summarized in figure 3.3.

Note:

1. Donor 5 was substituted by Donor 4 in a following expansion because the expansion protocol did not work as described and a rare NK subset was expanded at the expenses of the Vδ1$^+$ one;
2. Samples obtained from these four donors are the same described in 3.2.3;
3. At the end of expansion, bulk DOT cells were frozen as viable cells and as dry pellet for HTS sequencing after snap-freezing in liquid nitrogen (see 3.2.6)

3.3.2 Vδ1$^+$ clone generation

A limiting dilution and a single-cell sorting protocols were designed and tested to generate Vδ1$^+$ clones

3.3.2.1 Limiting dilution protocol to generate Vδ1$^+$ clone

Limiting dilution has been the golden standard protocol in T cell clone generation and, in order to generate Vδ1$^+$ clone, 5000 FACS-sorted CD3$^+$ TCRVδ1$^+$TCRVδ2- in decuplicate were plated in 96 wells/plate and diluted 1:2 until the final concentration of 0.038 cell/well was reached (17 dilutions). Irradiated autologous feeders were subsequently added. Accordingly to the previously described formula based on a Poisson distribution ($m = -\ln F_0$)[308], a clone is successfully established at whichever dilution of the cell suspension that gives 37% negative cultures.

3.3.2.2 Single-cell sorting protocol to generate Vδ1$^+$ clone

A second, faster and easier, protocol for Vδ1$^+$ clone generation was established using a modified version of the DOT cell expansion protocol described in 3.2.3. PBMCs were MACS-sorted for γδ TCR using a negative selection strategy (non-γδ depletion kit by Miltenyi Biotech). Positive fraction was collected and frozen in aliquots as viable cells. MACS-sorted γδ T cells were then stained with anti-TCRVδ1 (clone TS8.2), anti-TCRVδ2 (clone B6), anti-CD3 (clone HIT3a), FACS-enriched for CD3$^+$ TCRVδ1$^+$TCRVδ2- cells and sorted as single cells into 96 wells/plate using a FACS AriaIII machine (BD). 300 CD3$^+$TCRVδ1$^+$TCRVδ2- single cells per

donor (for a total of 1200 single cells) were cultured for 21 days using the DOT cell protocol in the presence of $5*10^4$ irradiated autologous blood γδ depleted PBMCs. This feeder population was weekly renewed.

3.3.3 DOT bulk and Vδ1$^+$ clone phenotypic and functional characterization

Starting from the expansion day 11, DOT cells from bulk expansions were weekly counted and phenotyped using the antibody mixes listed in table 3.4. Vδ1$^+$ clones obtained from the single cell seeding protocol were stained with an antibody cocktail containing anti-TCRVδ1 (clone TS8.2), anti-TCRVδ2 (clone B6), anti-CD3 (clone UCHT13), anti-NKp30 (clone P30-15) and anti-NKp44 (clone P44) or anti-TCRVδ1 (clone TS8.2), anti-TCRVδ2 (clone B6), anti-CD3 (clone UCHT13) and anti-Vγ9 (clone B3).

Table 3.4 Antibody cocktails for DOT cell phenotype analysis

Mix 1		**Mix 2**		**Mix 3**		**Mix 4**		**Mix 5**	
Marker	*Clone*	*Marker*	*Clone*	*Marker*	*Clone*	*Marker*	*Clone*	*Marker*	*Clone*
CD20	2H7	CD8	HIT8a	CD69	FN50	Vδ1	TS8.2	CD27	LG7F9
CD19	HIB19	TCRγδ	B1	Vδ1	REA173	NKp30	P30-15	Vδ1	REA173
CD14	HCD14	CD3	HIT3a	CD3	HIT3a	NKG2D	1D11	CD62L	DREG-56
CD56	HCD56	TCRαβ	BW242/412	Vδ2	123R3	NKp44	P44-8	CD45RA	HI100
CD3	UCHT13	CD4	OKT4	CD25	BC96	CD3	WM15	CD3	WM15
CD16	3G8								

AML cell lines (Table 3.3) were obtained from and authenticated by the German Resource Center for Biologic Material (DSMZ). For DOT and clone functional characterization, AML cell lines were co-incubated with previously CFSE-stained (1:1000 in PBS with no FBS) DOT cells or Vδ1$^+$ clones at optimized effector: target (5 : 1) ratio for 3 hours. A pre-treatment to block the TCR on the clone was performed using an anti-Vδ1 antibody (clone TCS-1). After the co-incubation, cells were washed and stained with Annexin-V; flow cytometry data were acquired on a LSR Fortessa (BD) and data was analyzed with FlowJo X software (Tree Star).

3.3.4 RNA extraction, cDNA synthesis and sequencing

RNA extraction was performed using the RNAeasy micro kit (Qiagen). Next, 12µl mRNA of each sample were reverse transcribed with the RevertAid H Minus First Strand cDNA Synthesis Kit (Thermo Scientific) using oligo-dT primers and following manufacturer's guidelines. cDNA samples were then amplified by PCR (40 and 45 cycles for γ and δ amplification, respectively) using the following forward (5'-3'; TRDV1: CTGTCAACTTCAAGAAAGCAGCGAAATC; TRGV2F: ATACCGAGAAAAGGACATCTATG; TRGV9F: CGGCACTGTCAGAAAGGAATC; TRGV9F: CGGCACTGTCAGAAAGGAATC) and reverse primers (5'-3'; TRGCB: CAAGAAGACAAAGGTATGTTCCAG; TRDCB: GTAGAATTCCTTCACCAGACAAG). PCR products were sent to Genewiz for Sanger sequencing. Finally, CDR3 regions were mapped using IMGT/V-QUEST

3.3.5 Clone selection

From the starting 1200 $CD3^{+}TCRV\delta1^{+}TCRV\delta2$- single cells, clones were selected accordingly to their doubling time, number of cells in culture, phenotype, functional and TCR-mediated killing of the AML Kg1 cell line, presence in the *ex vivo* blood sample and in the DOT expanded bulk of the same and other donors.

3.3.6 TCR cloning

TCRs from selected clones were subjected to molecular cloning to generate a J.RT3 cell line reporter with the TCR of interest[198,199].

3.3.6.1 RNA extraction and cDNA synthesis

RNA extraction was performed on $0.5*10^6$ cells (when possible) using the RNAeasy micro kit (Qiagen). Next, 12µl mRNA of each sample was reverse transcribed with the RevertAid H Minus First Strand cDNA Synthesis Kit (Thermo Scientific) using oligo-dT primers and following manufacturer's guidelines.

3.3.6.2 Chain amplification and purification from gel

TCR cDNAs were isolated using a Phusion High-Fidelity DNA Polymerase (New England Biolabs). The following primers were designed (5'-3'): forward gamma 8 AAAAAGATCTTGAGAGGGTCTT; forward gamma 9 AAAAAAGATCTGACACCGCTTTACAACGA; reverse gamma (GD04) AAAAAGTCGACGTGAGGTTCTCTGTGT; forward delta1 AAAAAGATCTCTTCAGGCACCACAACT; Reverse delta AAAAAGTCGACAGCGTATCACTTGTAGGAGTAA. BglII (AGATCT) and SalI (GTCGAC) restriction sites were added. The PCR mix/sample for chain isolation was composed of: 10µL HF Buffer; 1µL dNTP mix (10mM); 2x1µL primers (forward and reverse - 10µM); 3µL cDNA product; 33.5µL water (to 50µL). PCR was designed to have 40 amplification cycles as follow: 98°C 5'; (98°C 10''; 57°C 30''; 72°C 45'')*40; 72°C 10'. PCR products were then verified on 1.5% agarose gel. Bands with amplicons having the expected size (1000-1300bp) were excised and purified using the MinElute Gel Extraction Kit (Qiagen) following manifacturer's instructions. Purified PCR products were then measured using a Nanodrop 2000 (Thermo Fischer).

3.3.6.3 Ligation into plasmid and bacterial transformation

Ligation of purified PCR products was done in the pCR-Blunt vector and using TOP10 competent cells (Zero Blunt™ PCR Cloning Kit - Thermo Fischer) following manufacturer's instruction. The ligation step was modified increasing the reaction time (ON at 16°C) and using the following reaction mix: 1µL pCR blunt plasmid (25ng); 70ng (1000bp) to 85ng (1200bp) of PCR product (1-5µL); 1µL 10X ligation buffer; 1µL T4 DNA ligase; water to 10µL final volume. Transformation reactions were plated at two different concentration (10µL/plate and 100µL/plate) in Agar plates with Kanamycin (50µg/ml) for bacterial selection.

3.3.6.4 Plasmid purification and colony selection

We used two procedures to verify plasmids:

1) **Analysis by restriction digest:** 10 colonies/plate were selected (up to 24 colonies analysed at the same time), grown ON in 2mL LB medium $^{+}$ Kanamycin (50µg/ml) and plasmid were purified the day after using the GeneJET Plasmid Miniprep Kit (Thermo Fisher) following manufacturer's instructions. Purified plasmids were digested using A) EcoRI and B) BglI $^{+}$ SalI following manufacturer's instruction (restriction enzymes were all purchased from New England BioLabs). EcoRI makes two visible fragments in the δ cDNA but only one in the γ cDNA. BglII $^{+}$ SalI return one fragment of 1100 - 1200bp. Positive colonies were sent to sequencing and saved as glycerol stock.

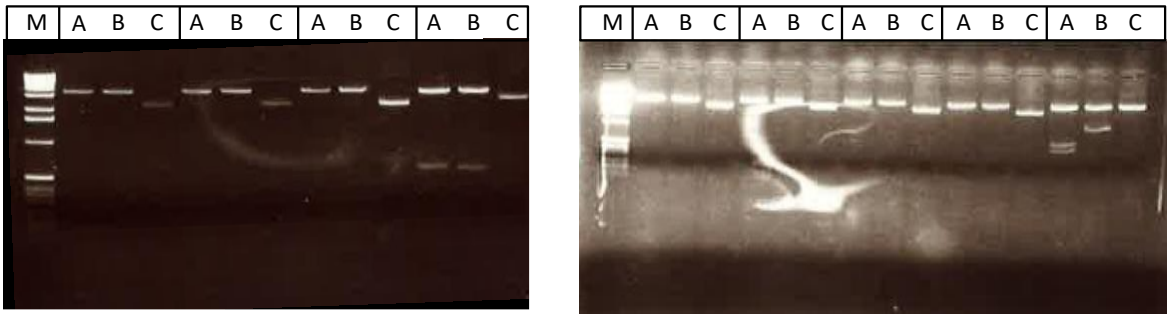

Figure 3.6 Example of analysis by restriction digest. A positive digest for γ chain is shown on the left picture (forth group) and for δ chain on the right (fifth group)

2) **Analysis by PCR**: 10 to 20 colonies/plate (up to 96 colonies analysed at the same time) were picked and resuspended in 30µL in 96 wells/plates. 15µL of bacterial suspension were used for the PCR reaction and 15µL were saved at RT until the reaction was completed. PCR reaction and primers are described in 3.3.6.2. The first step in the PCR reaction, with the temperature increasing to 98°C, is enough to lyse bacterial cells in suspension. After the PCR reaction, the products were analyzed on an 1.5% agarose gel. Bacteria which gave a successful amplification were grown ON, in 2mL LB medium $^{+}$ Kanamycin (50µg/ml) and plasmid were purified the day after using the GeneJET Plasmid Miniprep Kit (Thermo Fisher), sent to sequencing and saved as glycerol stock.

3.3.6.5 Plasmid sequencing and sequence analysis

Positive colonies were sent to Genewiz (Bordeaux) or to Stab Vida (Lisbon) for sequencing. Once retrieved the results (in form of paired ends), sequences were merged to obtain the full-length cDNA insert. Merged sequences were subjected to 4 validation steps:

1) CDR3 region was analysed and compared to the sequencing data obtained for the clone selection (3.3.5); primer regions were also identified in order to delimitate the insert size inside the plasmid vector;
2) ORFs were analysed on https://www.ncbi.nlm.nih.gov/orffinder/ and translated into amino acid sequence using the same webtool; only the inserts that had no stop codon and that were comparable in size to other described TCRs were selected;

3) Prediction of transmembrane helices in the insert was evaluated (http://www.cbs.dtu.dk/services/TMHMM/);
4) The insert sequence was aligned using ClustalW to other TCRs of reference (Table 3.5 and 3.6).

Table 3.5 γ chains of reference used for the sequence alignment

>LESγ4	MQWALAVLLAFLSPASQKSSNLEGRTKSVIRQTGSSAEITCDLAEGSTGYIHWYLHEGKAPQRLLYYDSYTSSVVLESGISPGKYDT YGSTRKNLRMILRNLIENDSGVYYCATWDGFYYKKLFGSGTTLVVTDKQLDADVSPKPTIFLPSIAETKLQKAGTYLCLLEKFFPDIIKI HWQEKKSNTIMGSQEGNTMKTNDTYMKFSWLTVPEESLDKEHRCIVRHENNKNGIDQEIIFPPIKTDVTTVDPKDSYSKDANDVI TMDPKDNWSKDANDTLLLQLTNTSAYYMYLLLLLKSVVYFAIITCCLLGRTAFCCNGEKS
>γ8Nantes	MLLALALLLAFLPPASQKSSNLEGRTKSVTRPTGSSAVITCDLPVENAVYTHWYLHQEGKAPQRLLYYDSYNSRVVLESGISREKYH TYASTGKSLKFILENLIERDSGVYYCATWDSSKLFGSGTTLVVTDKQLDADVSPKPTIFLPSIAETKLQKAGTYLCLLEKFFPDIIKIHW QEKKSNTILGSQEGNTMKTNDTYMKFSWLTVPEESLDKEHRCIVRHENNKNGIDQEIIFPPIKTDVTTVDPKYNYSKDANDVITMD PKDNWSKDANDTLLLQLTNTSAYYTYLLLLLKSVVYFAIITCCLLRRTAFCCNGEKS
>PINγ4	MLLALALLLAFLPPASQKSSNLEGRTKSVTRPTGSSAVITCDLPVENAVYTHWYLHQEGKAPQRLLYYDSYNSRVVLESGISREKYH TYASTGKSLKFILENLIERDSGVYYCATWDNYKKLFGSGTTLVVTDKQLDADVSPKPTIFLPSIAETKLQKAGTYLCLLEKF FPDIIKIHWQEKKSNTILGSQEGNTMKTNDTYMKFSWLTVPEESLDKEHRCIVRHENNKN GIDQEIIFPPIKTDVTTVDPKYNYSKDANDVITMDPKDNWSKDANDTLLLQLTNTSAYYTYLLLLLKSVVYFAIITCCLLRRTAFCCNG EKS
>CHAMγ	MQWALAVLLAFLSPASQKSSNLEGRTKSVIRQTGSSAEITCDLAEGSTGYIHWYLHQEGKAPQRLLYYDSYTSSVVLESGISPGKYD TYGSTRKNLRMILRNLIENDSGVYYCATWEGYKKLFGSGTTLVVTDKQLDADVSPKPTIFLPSIAETKLQKAGTYLCLLEKFFPDVIKI HWQEKKSNTILGSQEGNTMKTNDTYMKFSWLTVPEKSLDKEHRCIVRHENNKN GVDQEIIFPPIKTDVITMDPKDNCSKDANDTLLLQLTNTSAYYMYLLLLLKSVVYFAIITCCLLRRTAFCCNGEKS
>MAUγ9	MLSLLHTSTLAVLGALCVCGAGHLEQPQISSTKTLSKTARLECVVSGITISATSVYWYRERPGEVIQFLVSISYDGTVRKESGIPSGKFE VDRIPETSTSTLTIHNVEKQDIATYYCALWEVQSVEKLFGSGTTLVVTDKQLDADVSPKPTIFLPSIAETKLQKAGTYLCLLEKFFPDIIK IHWQEKKSNTILGSQEGNTMKTNDTYMKFSWLTVPEESLDKEHRCIVRHENNKNGIDQEIIFPPIKTDVTTVDPKYNYSKDANDVI TMDPKDNWSKDANDTLLLQLTNTSAYYTYLLLLLKSVVYFAIITCCLLRRTAFCCNGEKS
>γ9clone26	MLSLLHTSTLAVLGALCVYGAGHLEQPQISSTKTLSKTARLECVVSGITISATSVYWYRERPGEVIQFLVSISYDGTVRKESGIPSGKFE VDRIPETSTSTLTIHNVEKQDIATYYCALWEGNHYYKKLFGSGTTLVVTDKQLDADVSPKPTIFLPSIAETKLQKAGTYLCLLEKFFPDI IKIHWQEKKSNTILGSQEGNTMKTNDTYMKFSWLTVPEESLDKEHRCIVRHENNKNGIDQEIIFPPIKTDVTTVDPKYNYSKDAND VITMDPKDNWSKDANDTLLLQLTNTSAYYTYLLLLLKSVVYFAIITCCLLRRTAFCCNGEKS
>γ9Nantes	MLSLLHASTLAVLGALCVYGAGHLEQPQISSTKTLSKTARLECVVSGITISATSVYWYRERPGEVIQFLVSISYDGTVRKESGIPSGKFE VDRIPETSTSTLTIHNVEKQDIATYYCALWEAQQELGKKIKVFGPGTKLIITDKQLDADVSPKPTIFLPSIAETKLQKAGTYLCLLEKFFP DVIKIHWEEKKSNTILGSQEGNTMKTNDTYMKFSWLTVPEKSLDKEHRCIVRHENNKNGVDQEIIFPPIKTDVITMDPKDNCSKD ANDTLLLQLTNTSAYYMYLLLLLKSVVYFAIITCCLLRRTAFCCNGEKS

Table 3.6 δ chains of reference used for the sequence alignment

>MAUδ	MGQKVTQAQSSVSMPVRKAVTLNCLYETSWWSYYIFWYKQLPSKEMIFLIRQGSDEQNAKSGRYSVNFKKAAKSVALTISALQ LEDSAKYFCALGDLTGVPITDKLIFGKGTRVTVEPRSQPHTKPSVFVMKNGTNVACLVKEFYPKDIRINLVSSKKITEFDPAIVISPS GKYNAVKLGKYEDSNSVTCSVQHDNKTVHSTDFEVKTDSTDHVKPKETENTKQPSKSCHKPKAIVHTE KVNMMSLTGSLHHILDAQKMVWNHR
>CHAMδ	MLFSSLLCVFVAFSYSGSSVAQKVTQAQSSVSMPVRKAVTLNCLYETSWWSYYIFWYKQLPSKEMIFLIRQGSDEQNAKSGRYS VNFKKAAKSVALTISALQLEDSAKYFCALGAPPLLLYWGITDKLIFGKGTRVTVEPRSQPHTKPSVFVMKNGTNVACLVKEFYPKD IRINLVSSKKITEFDPAIVISPSGKYNAVKLGKYEDSNSVTCSVQHDNKTVHSTDFEVKTDSTDHVKPKETENTKQPSKSCHKPKAI VHTE KVNMMSLTVLGLRMLFAKTVAVNFLLTAKLFFL
>PINδ	MLFSSLLCVFVAFSYSGSSVAQKVTQAQSSVSMPVRKAVTLNCLYETSWWSYYIFWYKQLPSKEMIFLIRQGSDEQNAKSGRYS VNFKKAAKSVALTISALQLEDSAKYFCALGDYLGDKYPSYDLLGDTTDKLIFGKGTRVTVEPRSQPHTKPSVFVMKNGTNVACLV KEFYPKDIRINLVSSKKITEFDPAIVISPSGKYNAVKLGKYEDSNSVTCSVQHDNKTVHSTDFEVKTDSTDHVKPKETENTKQPSKS CHKPKAIVHTE KVNMMSLTVLGLRMLFAKTVAVNFLLTAKLFFL
>δ1David	MLFSSLLCVFVAFSYSGSSVAQKVTQAQSSVSMPVRKAVTLNCLYETSWWSYYIFWYKQLPSKEMIFLIRQGSDEQNAKSGRYS VNFKKAAKSVALTISALQLEDSAKYFCALGELGDDKLIFGKGTRVTVEPRSQPHTKPSVFVMKNGTNVACLVKEFYPKDIRINLVS SKKITEFDPAIVISPSGKYNAVKLGKYEDSNSVTCSVQHDNKTVHSTDFEVKTDSTDHVKPKETENTKQPSKSCHKPKAIVHTE KVNMMSLTVLGLRMLFAKTVAVNFLLTAKLFFL
>LESδ5	MAMLLGASVLILWLQPDWVNSQQKNDDQQVKQNSPSLSVQEGRISILNCDYTNSMFDYFLWYKKYPAEGPTFLISISSIKDKN EDGRFTVFLNKSAKHLSLHIVPSQPGDSAVYFCAASSPIRGYTGSDKLIFGKGTRVTVEPRSQPHTKPSVFVMKNGTNVACLVKE FYPKDIRINLVSSKKITEFDPAIVISPSGKYNAVKLGKYEDSNSVTCSVQHDNKTVHSTDFEVKTDSTDHVKPKETENTKQPSKSCH KPKAIVHTEKVNMMSLTVLGLRMLFAKTVAVNFLLTAKLFFL
>δ3Nantes	MILTVGFSFLFFYRGTLCDKVTQSSPDQTVASGSEVVLLCTYDTVYSNPDLFWYRIRPDYSFQFVFYGDNSRSEGADFTQGRFSV KHILTQKAFHLVISPVRTEDSATYYCAFTGLGDTSHADKLIFGKGTRVTVEPRSQPHTKPSVFVMKNGTNVACLVKEFYPKDIRIN

	LVSSKKITEFDPAIVISPSGKYNAVKLGKYEDSNSVTCSVQHDNKTVHSTDFEVKTDSTDHVKPKETENTKQPSKSCHKPKAIVHT EKVNMMSLTVLGLRMLFAKTVAVNFLLTAKLFFL
>δ3clone26	MILTVGFSFLFFYRGTLCDKVTQSSPDQTVASGSEVVLLCTYDTVYSNPDLFWYRIRPDYSFQFVFYGDNSTSEGADFTHGRFSV KHILTQKAFHLVISPVRTEDSATYYCAFIGRYGYTDKLIFGKGTRVTVEPRSQPHTKPSVFVMKNGTNVACLVKEFYPKDIRINLVS SKKITEFDPAIVISPSGKYNAVKLGKYEDSNSVTCSVQHDNKTVHSTDFEVKTDSTDHVKPKETENTKQPSKSCHKPKAIVHTEKV NMMSLTVLGLRMLFAKTVAVNFLLTAKLFFL
>δ2Nantes	CAPPAGYQLHRGGGRSRTSGSPGEAMQRISSLIHLSLFWAGVMSAIELVPEHQTVPVSIGVPATLRCSMKGEAIGNYYINWYRK TQGNTMTFIYREKDIYGPGFKDNFQGDIDIAKNLAVLKILAPSERDEGSYYCACDTLGMGGEYTDKLIFGKGTRVTVEPRSQPHT KPSVFVMKNGTNVACLVKEFYPKDIRINLVSSKKITEFDPAIVISPSGKYNAVKLGKYEDSNSVTCSVQHDNKTVHSTDFEVKTDS TDHVKPKETENTKQPSKSCHKPKAIVHTEKVNMMSLTVLGLRMLFAKTVAVNFLLTAKLFFL

3.3.6.6 Ligation and second bacterial transformation

Colonies bearing validated cDNA sequences were grown ON in 2mL LB medium + Kanamycin (50 µg/ml) and plasmid were purified the day after using the GeneJET Plasmid Miniprep Kit (Thermo Fisher). Purified plasmids were digested using BglI + SalI following manufacturer's instruction for 3 hours and the digestion products were ligated ON at 16°C into a TEEW vector provided by our collaborators in Bordeaux. The ligation mix was composed as follow: 1µL vector; 1µL insert; 1µL T4 buffer; 7µL RNAse free water. 1µL T4 ligase (New England BioLabs) was added at the end. Endura competent cells were transformed the day after using the heat shock protocol used in 3.3.6.3. Transformation reactions were plated at two different concentration (10µL/plate and 100µL/plate) in Agar plates with Ampicillin (100µg/mL) for bacterial selection.

3.3.6.7 Plasmid purification and verification

10 colonies/plate were selected (up to 24 colonies analysed at the same time), grown ON in 2mL LB medium + Ampicillin (100µg/mL) and plasmid were purified the day after using the GeneJET Plasmid Miniprep Kit (Thermo Fisher) following manufacturer's instructions. Purified plasmids were digested using A) BamHI + SalI and B) XhoI + SalI following manufacturer's instruction (restriction enzymes were all purchased from New England BioLabs). BamHI + SalI digestion gives no bands whereas XhoI + SalI digestion will result in a fragment between 1000 – 1200bp.

3.3.6.8 Lentiviral production

$2*10^6$ HEK293T cells (obtained from a laboratory in IMM) were plated in Petri dishes the day before transfection in DMEM 10%FBS, 1%PenStrep and 1%NEEA. The day after, the transfection mix was added to the plate containing (per plate): 500µL OPTIMEM medium, 15µL X-tremeGENE™ 9 DNA Transfection Reagent (Sigma-Aldrich), 17µg pCL-Eco and 4.25µg pCMV-VSV-G plasmids and 21.25µg of plasmid containing the cDNA for the TCR of interest (pCL-Eco and pCMV-VSV-G plasmids were produced transforming TOP10 competent cells with plasmid aliquots provided by a lab member). The transfection mix was then added to the plates. Culture medium was changed on the next day. Three daily medium harvests were planned to start from the second day after transformation. Briefly, medium was collected, centrifuged and filter using low protein binding filters to eliminate medium contaminants such as cells and debris; next, medium was centrifuged at 75600g for 2 hours at 4°C. After centrifugation, supernatant was eliminated, and pellet resuspended in fresh medium, aliquoted, frozen in nitrogen and stored at -80°C.

3.3.6.9 Reporter generation

Cell line J.RT3 was used as background to generate TCR reporters. This is a mutant line derived from the E6-1 clone of Jurkat (ATCC TIB 152) that lacks the β chain of the T cell antigen receptor. The cells do not express either CD3 or the αβ TCR on the surface. $1*10^6$ J.RT3 cells were plated into 6 wells/plate at the concentration of $0.4*10^6$ cells/ml and transduced using increasing volumes (24µL, 48µL or 96µL) of viral suspension (3.3.6.8). The day after, cells were washed twice and moved to T25 flasks. One week after transduction, efficiency of transduction was assessed in terms of CD3 and γδ TCR expression by flow cytometry using anti-TCRVδ1 (clone TS8.2) and anti-CD3 (clone HIT3a). Data were acquired on a LSR Fortessa 2 (BD).

3.3.7 Reactivity assay

To assess reporter activity in terms of TCR mediated recognition of target cells, $0.05*10^6$ J.RT3-TCR$^+$ cells were stained with DDAose (1:1000) and co-incubated with target cell lines, primary samples or PBMCs (Table 3.7) at 1:1 ratio during 4 hours. At the end of the co-culture, activation was evaluated by CD69 activation (MFI). Cells were stained with anti-TCRVδ1 (clone TS8.2), anti-CD3 (clone HIT3a) and anti-CD69 (clone FN50). The protocol was successively modified to include reporter incubation with 2µg/mL anti-CD3 (clone HIT3a) for 10'. Additional experimental controls were added: target cell incubation with Fc Receptor Binding Inhibitor Polyclonal Antibody (anti-CD16, anti-CD32, anti-CD64 - Thermo Fischer) or anti IgG2a (clone eBM2a) on the target cells and pre-incubating the reporters with other anti-CD3 clones (OKT3 and UCHT1).

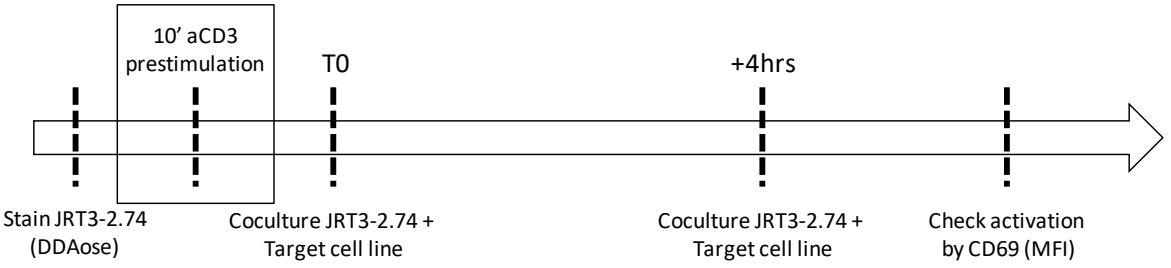

Table 3.7 Cell lines and cells used for the reactivity assay

Cell line	*Disease*
GDM-1	Myelomonoblastic leukemia
KG-1a	Acute myelogenous leukemia
HEL	Erythroleukemia
AML-193	Acute monocytic leukemia
MV4-11	Biphenotypic B myelomonocytic leukemia
HL-60	Acute promyelocytic leukemia
U-937	Histiocytic lymphoma
OCI-AML3	Acute myeloid leukemia (AML FAB M4)
Peer	T cell acute lymphoblastic leukemia (T-ALL)

Thp-1	Acute monocytic leukemia
KG-1	Acute myelogenous leukemia
Dohh2	B cell lymphoma
Molt-4	Acute lymphoblastic leukemia
Nalm-6	Acute lymphoblastic leukemia (ALL)
Jurkat	Acute T cell leukemia
Mec-1	Chronic B cell leukemia
Mec-2	Chronic B cell leukemia
Ramos	Burkitt's lymphoma (American)
Hpb-all	T cell leukemia ALL
Daudi	Burkitt's lymphoma
Rs4-11	Acute lymphoblastic leukemia (ALL L2)
Rch-acv	Common acute lymphoblastic leukemia (cALL)
Reh	Acute lymphocytic leukemia (non-T; non-B)
697	Acute lymphoblastic leukemia (cALL)
Raji	Burkitt's lymphoma
Pc-3	Prostatic adenocarcinoma
Hct-116	Colorectal carcinoma
Mda-mb-231	Mammary gland adenocarcinoma
He-la	Cervical carcinoma
Primary AML samples	See 3.2.9
PBMCs	See 3.2.9

3.3.8 Statistical analysis

Performed using GraphPad Prism software. All data expressed as mean +/- SEM. Comparisons of two groups by Student’s t-test.

4 Results

4.1 High-throughput analysis of the human thymic Vδ1 $^{+}$ TCR repertoire

In press in ***Scientific Data*** (Di Lorenzo et al.)

4.1.1 Introduction

γδ T cells constitute a small (~5-10%) but unique subpopulation of T cells. Because of their features, including antigen recognition through a somatically rearranged T cell receptor (TCR) as well as through several NK cell receptors[270], cytokine production and immunoregulation[19], they can act as a bridge between innate and adaptive immunity, rapidly responding to infected or transformed cells in a major histocompatibility complex (MHC)-independent manner[270].

It is well established that αβ T cells undergo positive and negative selection in the thymus depending on their TCR avidity for thymically expressed self-antigens[120] and this further results in expression of one single β-chain due to allelic exclusion during thymic development[309]. However, there is little evidence supporting the hypothesis of human γδ T cells being positively and/or negatively selected in the thymus. Indeed, post-natal human γδ T cells seem to only complete their maturation program in the periphery, especially upon infection challenge that triggers clonal expansion[50,121–124]. Thus, the goal of post-natal thymic development seems to be the generation of a highly diverse, naïve and immature human γδ T cell repertoire. As such, the main event for developing γδ T cells is the generation of a functional TCR through the rearrangement of the variable (V), diversity (D) and joining (J) segments and subsequent pairing of the rearranged γ and δ chains. These events alone could lead to the establishment of a large number of diverse antigen receptors, but the addition and/or subtraction of non-templated (N) and palindromic (P) nucleotides at the gene segment junctions contribute substantially to increasing diversity, providing nearly limitless potential to the TCRγδ repertoire[125].

There are several subsets of human γδ T cells, identified by the combination of specific TCRγ- and δ-chains generated after successful V(D)J rearrangement of the TRG and TRD loci. 14 TRGV genes, of which only 6 are functional (Vγ2, Vγ3, Vγ4, Vγ5, Vγ8 and Vγ9), can rearrange with 5 TRGJ (JP1, JP, J1, JP2 and J2) genes, whereas 7 TRDV genes (Vδ1, Vδ2, Vδ3 and Vα14/ Vδ4, Vα23/ Vδ6, Vα29/ Vδ5, Vα36/Vδ7, Vα38-2/ Vδ8) can rearrange with three TRDD (D1, D2 and D3) and with four TRDJ genes (J1, J4, J2 and J3)[33]. Although the thymus can generate all the possible combinations of TRG and TRD genes, the major γδ T cell population in peripheral blood (PB) expresses a TCR composed by Vγ9 recombined with JP and paired with Vδ2[41]. In fact, this specifically rearranged Vγ9Vδ2 T cell subset is mostly produced during foetal life but still constitutes the major γδ T cell subset in adults. Antigen-driven stimulation in the periphery underlies a strong and specific expansion of this subset after birth and during the lifespan of each individual[52]. Indeed, Vγ9Vδ2 T cells can rapidly recognize, in a TCR-dependent manner, cellular dysregulation resulting from infection or malignant transformation. The key partner of the Vγ9Vδ2 TCR is Butyrophilin subfamily 3 member A1 (BTN3A1), a receptor of the Ig superfamily that changes its extracellular conformation upon increase of intracellular phosphoantigens (pAgs), an event that typically occurs as consequence of cellular stress[41,270].

Vδ1$^+$ γδ T cells are the second most abundant subset in the human PB, but they are actually the predominant γδ T cell subset in the post-natal thymus and in peripheral tissues (such as the intestine or the liver), where Vδ1 is mainly paired to Vγ8 or Vγ9 chains. These γδ T cells play an important role during viral infections, especially CMV[121,122], and tumour progression[310]. Indeed, a subpopulation of Vδ1$^+$ T cells recognizes nonpolymorphic MHC-like (class Ib) proteins presenting lipids, such as CD1 proteins, in a similar way to other unconventional T cells like NKT or MAIT cells[264,265,270,311].

In fact, we have recently developed a clinical-grade method for expansion and differentiation of Vδ1$^+$ T cells aiming towards the development of a novel, Vδ1$^+$ T cell-based cancer immunotherapy[114].

Thanks to recent technical advances in the comprehensive analysis of TCR repertoires using next-generation sequencing (NGS) approaches, it has become more accessible to understand the dynamics of T cell development and homeostasis[123,312], and T cell expansion in response to infections[122,313] or tumours[314]. In this contest, the purpose of this study is to characterize the Vδ1$^+$ TCR repertoire in the thymus of young children, namely by providing a detailed description of transcribed (mRNA) V(D)J recombination products in highly (FACS-)purified thymic Vδ1$^+$ T cells.

Moreover, PB and cord blood Vδ1$^+$ T cells were described to display private *TRD* repertoires, in contraposition to the respective *TRG* repertoire that showed a fraction of common (shared among individuals) sequences[122,124]. Here, we show that is also the case for purified Vδ1$^+$ thymocytes, albeit these shared TRG clonotypes consist of TRGJ1 gene segments. This raises the interesting question whether the public TRG clonotypes of Vδ1$^+$ T cells are selected (upon ligand encounter) in the thymus; or simply the output of a favoured TCR rearrangement. This, in fact, is an open question also on the Vγ9-JPVδ2 rearrangement that is prevalent in foetal life[41].

4.1.2 Results

In order to study the clonality of the Vδ1$^+$ thymocyte population, we collected thymic samples from 8 patients that underwent corrective cardiac surgery (*n*=8), from 5 days old up to 15 months of age[315]. To ensure the most reliable results and the lowest interferences coming from contaminating cells, we first depleted the thymic samples for αβ T cells and then we sorted CD3$^+$ TCRVδ1$^+$ TCRVδ2$^-$ thymocytes by FACS. Using this purification strategy, we were able to obtain Vδ1$^+$ thymocyte samples that were between 98% and 99.6% pure (Figure 4.1A-C). Next, we performed NGS experiments on sorted cells as summarized in Figure 4.1D. Number of reads and number of unique clonotypes (productive and non-productive) obtained after sequencing of the *TRG* and *TRD* repertoires are listed in Table 4.1. Since no clustering for age or sex was observed in the datasets of *TRG* and *TRD* repertoires (Figure 4.1E-F), the herein described analyses were made with no subset for these two parameters. Surprisingly, despite the high purities, the NGS analysis revealed that among the retrieved sequences, only around 75% of them were Vδ1 sequences, whereas the remaining fraction was almost entirely constituted of Vδ2 (and much fewer Vδ3) sequences (Figure 1G-H). For consistency, examples of alignment are supplied as Supplementary Material. Of note, only the chains that were predicted to be functional were considered for the analysis. Importantly, the presence of non-Vδ1 sequences in the pure Vδ1$^+$ thymocyte samples was not observed in the PB Vδ1$^+$ T cell samples used as controls[316], where most of the sequences were indeed Vδ1. Thus, the Vδ2 (and Vδ3) sequence pool accounted for around 20% of the whole repertoire of sorted CD3$^+$ TCRVδ1$^+$ TCRVδ2$^-$ thymocytes, whereas it constituted a negligible fraction of the PB samples (Figure 4.1H). Importantly, this was true for in every donor analysed (*n*=8 for thymus, *n*=3 for PB controls), as highlighted by the minimal standard errors (Figure 4.1H). Moreover, the analysis of V-J rearrangement in the *TRG* repertoires showed that V segments, including the Vγ9 sequences, rearranged preferentially with the TRGJ1 segment (Figure 1I-J); whereas they did not include the VγJPVδ2 segment, thus excluding foetal-derived Vγ9Vδ2 T cells.

Table 4.1Number of reads and number of unique, productive and non-productive clonotypes for the TRG and TRD repertoires

TRG					***TRD***				
Sample	**Reads (#)**	**Unique clonotypes (#)**	**Productive clonotypes (#)**	**Non-productive clonotypes (#)**	**Sample**	**Reads (#)**	**Unique clonotypes (#)**	**Productive clonotypes (#)**	**Non-productive clonotypes (#)**
Thy01	124241	76328	67507	8821	*Thy01*	131535	100266	91681	8585
Thy02	96287	56506	50685	5821	*Thy02*	121295	87858	80976	6882
Thy03	64503	33011	28952	4059	*Thy03*	74996	45926	43040	2886
Thy04	79888	45902	40174	5728	*Thy04*	65350	39273	35977	3296
Thy05	93350	73592	61880	11712	*Thy05*	183095	158166	142893	15273
Thy06	120272	87512	74731	12781	*Thy06*	210602	164881	150875	14006
Thy07	67874	53047	46856	6191	*Thy07*	107236	94185	85930	8255
Thy08	74645	44767	38204	6563	*Thy08*	118791	70505	63701	6804
PB01	46645	561	561	0	*PB01*	58483	744	673	71
PB02	74560	30475	22417	8058	*PB02*	158279	39499	32136	7363
PB03	95516	28347	21738	6609	*PB03*	126199	41244	34534	6710

A

Sample	Age	Sex	Purity	# cells for NGS (*10^6)
Thy01	14 m	F	99.5%	0.55
Thy02	15 m	M	99.0%	0.39
Thy03	5 m	F	98.6%	0.45
Thy04	-	-	98.0%	0.35
Thy05	6 m	M	99.6%	0.3
Thy06	1 m	F	99.5%	0.3
Thy07	5 d	M	98.9%	0.02
Thy08	23 d	F	99.2%	0.4
PB 1	33 y	F	98.9%	0.5
PB 2	32 y	M	99.5%	0.05
PB 3	35 y	M	99.1%	0.05

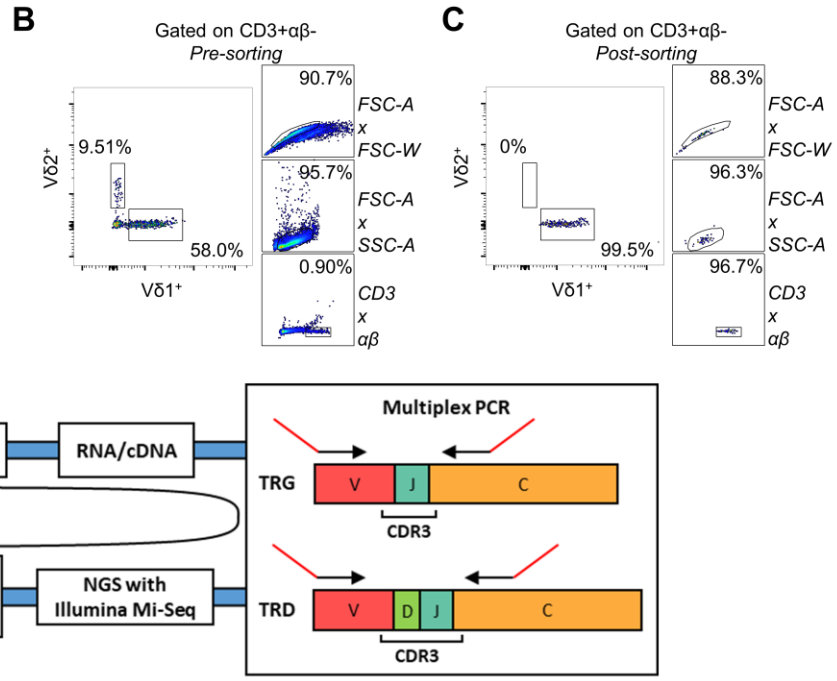

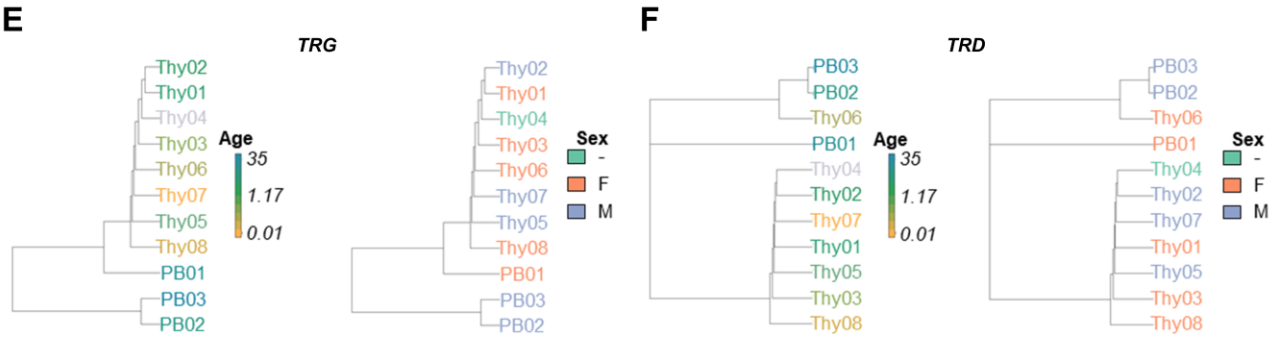

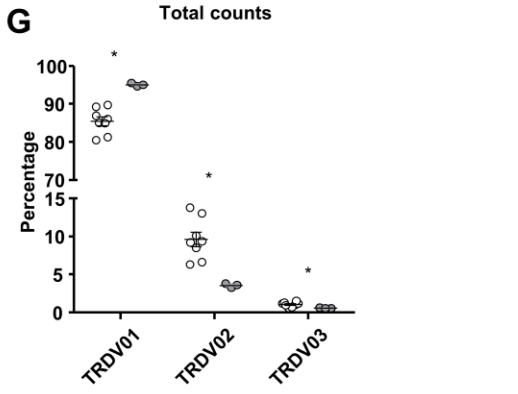

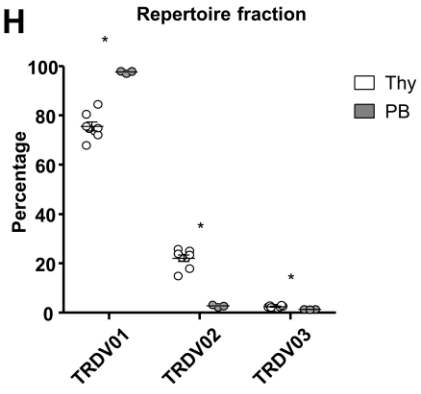

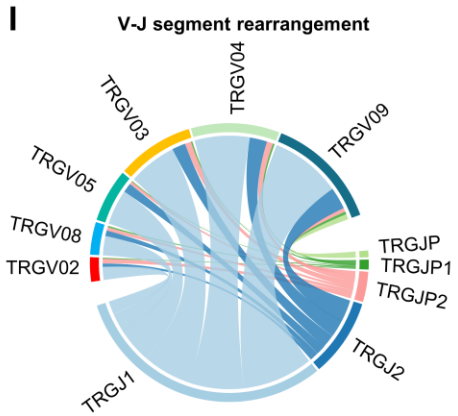

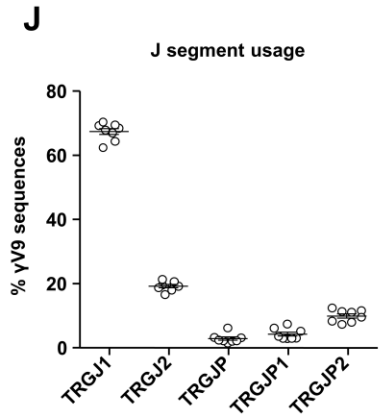

*Figure 4.1 Isolated naïve Vδ1⁺ thymocyte repertoires include a considerable fraction of Vδ2 TCR sequences. FACS-sorted CD3⁺ TCRVδ1⁺ TCRVδ2- thymocytes were analysed at the mRNA level by next-generation sequencing of CDR3 regions of TRG and TRD. (a) Name, age (d = days, m = months), sex, purity and number of sorted cells of the analysed samples (n=8). (b-c) Pre- and post-sorting gating strategy. CD3⁺ TCRαβ- TCRVδ1⁺ TCRVδ2- cells were sorted to >98% final purity. After selection of Singlets (FSC-A x FSC-W) and exclusion of debris/dead cells (FSC-A x SSC-A), Vδ1⁺ cells were sorted from the CD3⁺αβ- population. (d) Amplicons were generated from sorted Vδ1⁺ thymocyte by mRNA/cDNA based multiplex PCR technology. Multiplex primer sets amplify CDR3 regions by targeting Vγ or Vδ and constant gene segments, with the addition of Illumina sequencing adapters as overhangs (red). Sequences were obtained by Illumina MiSeq sequencing and next annotated by IMGT as described in the methods section before downstream bioinformatics analysis. (e-f) Hierarchical clustering of thymic and PB TRG and TRD samples using F pairwise similarity metric. Samples were clustered by age (months and days were normalized per year in order to have the same unit of measure - left) and sex (right). (g) Total NGS counts and (h) relative fraction within repertoire of the thymic TRDV01, TRDV02 and TRDV03 sequences compared to those found in the PB of an unrelated cohort of healthy donors (n=3). Graphical representation of V-J rearrangement in the TRG repertoire (i) and in the Vγ9 sequences (j) indicates a preferential usage of the J1 segment. Indicated are mean ± SEM; Mann-Whitney test was used to compare groups (*p<0.05)*.

We next employed a Treemap type of graph for the clonotype graphical representations (Figure 4.2A-C). In these graphs, clonotypes are grouped and colour-coded by chain (TRGV-02, -03, -04, -05, -08 and -09 for the *TRG* datasets; TRDV-01, -02, -03, -04, -05 and -08 for the *TRD* datasets). Other layers of information are included in these graphs. Indeed, each square represents a unique clonotype and its area is proportional the clonotype relative fraction in the dataset. Clonotypes are then ordered by frequency from the most (top left corner) to the least (bottom right corner) abundant. This analysis clearly revealed the presence of many different sequences with very low frequencies in the thymic samples, and no skewing towards a specific clonal pattern in either *TRG* or *TRD* repertoires (Figure 2A-B), whereas repertoires from PB are defined as oligoclonal in the sense that the top 20 clonotypes (by frequency) usually account for more than 70% of the whole repertoire (Figure 4.2C). Consistent with this, we found no significant biases in terms of CDR3 length distributions in the thymic samples (Figure 4.2C-D), whereas the distribution plot for the PB control shows clear signs of immunological memory with the loss of the typical gaussian-shaped distribution characteristic of naïve repertoires and the acquisition of spikes of more frequent sequences with CDR3 segment of the same length. Interestingly, the clonotype graphical representation also highlighted that the non-Vδ1 sequences were the most frequent and abundant clonotypes within the repertoire of the purified Vδ1⁺ thymocyte samples (Figure 4.2B) and were almost absent in the PB control (Fig. 4.2C). Also, no differences where observed in the CDR3 distributions of Vδ1 and Vδ2, except (and as expected) for the CDR3 length median value.

Looking more deeply into the clonal diversity of the *TRG* and *TRD* repertoires, we found thymic samples clustering together and separately from the PB controls, with the thymic *TRG* and *TRD* datasets being considerably more diverse than the PB counterparts (Figure04. 2H-I). Despite the presence of thousands of low abundant sequences, it was interesting to observe that a considerable number of *TRG* clonotypes was shared between donors, up to $6.9*10^3$ shared sequences between Thy01 and Thy02 samples (Figure 4.2J). This phenomenon was clearly restricted to the γ-chain, since the highest number of shared *TRD* clonotypes observed was just 116 between Thy05 and Thy06 samples (Figure 4.2K). Thus, whereas common *TRG* sequences are found across thymic Vδ1⁺ samples, their *TRD* repertoires are essentially private.

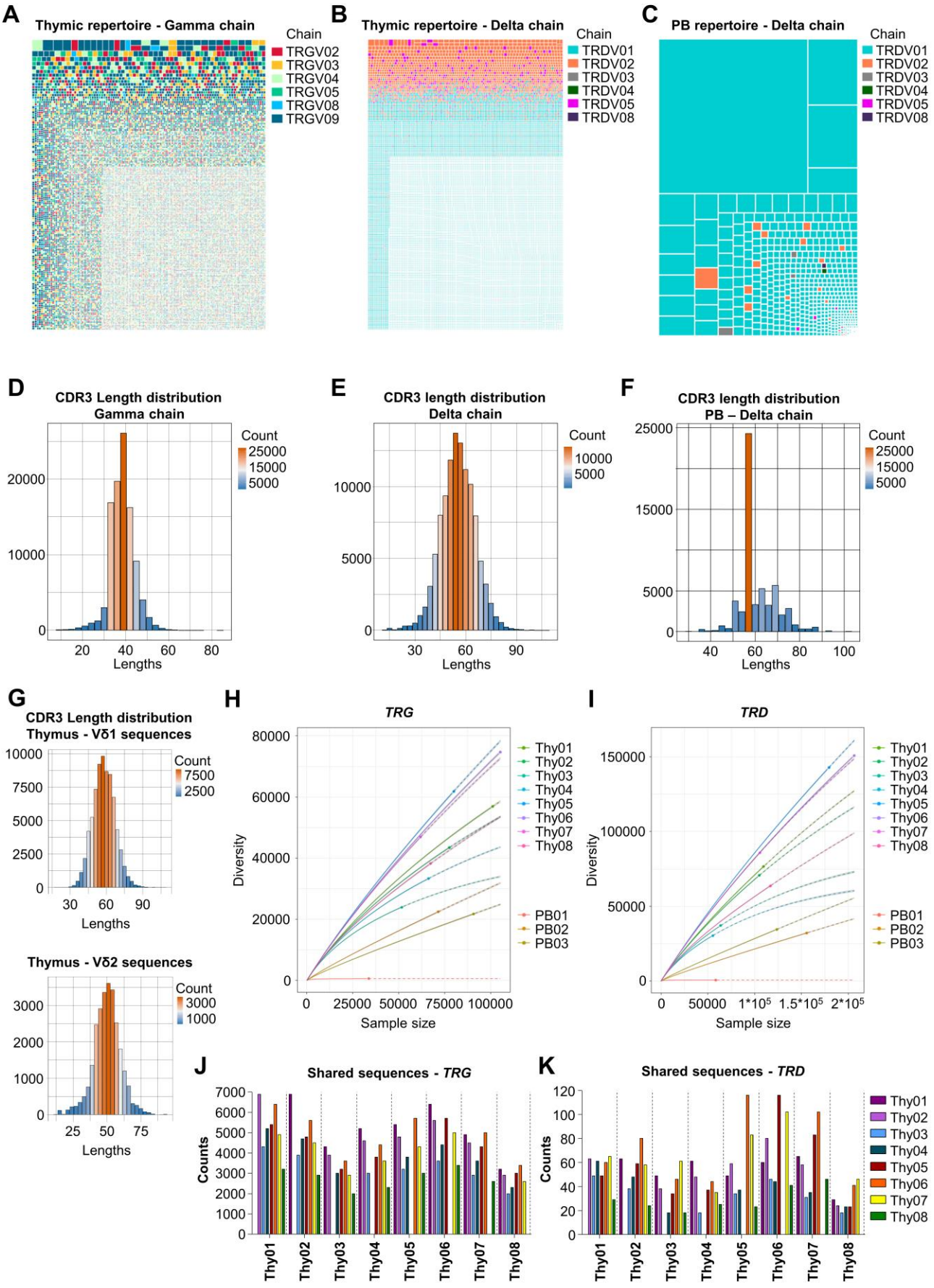
A
Thymic repertoire - Gamma chain
Chain
TRGV02
TRGV03
TRGV04
TRGV05
TRGV08
TRGV09
B
Thymic repertoire - Delta chain
Chain
TRDV01
TRDV02
TRDV03
TRDV04
TRDV05
TRDV08
C
PB repertoire - Delta chain
Chain
TRDV01
TRDV02
TRDV03
TRDV04
TRDV05
TRDV08
D
CDR3 Length distribution
Gamma chain
Count
25000
15000
5000
20000
10000
0
20
40
60
80
Lengths
E
CDR3 length distribution
Delta chain
Count
10000
5000
10000
5000
0
30
60
90
Lengths
F
CDR3 length distribution
PB – Delta chain
Count
25000
15000
5000
25000
15000
5000
0
40
60
80
100
Lengths
G
CDR3 Length distribution
Thymus - Vδ1 sequences
Count
7500
2500
10000
7500
5000
2500
0
30
60
90
Lengths
Thymus - Vδ2 sequences
Count
3000
1000
3000
2000
1000
0
25
50
75
Lengths
H
TRG
80000
60000
40000
20000
0
Diversity
0
25000
50000
75000
100000
Sample size
Thy01
Thy02
Thy03
Thy04
Thy05
Thy06
Thy07
Thy08
PB01
PB02
PB03
I
TRD
150000
100000
50000
0
Diversity
0
50000
1*10^5
1.5*10^5
2*10^5
Sample size
Thy01
Thy02
Thy03
Thy04
Thy05
Thy06
Thy07
Thy08
PB01
PB02
PB03
J
Shared sequences - TRG
7000
6000
5000
4000
3000
2000
1000
0
Counts
Thy01
Thy02
Thy03
Thy04
Thy05
Thy06
Thy07
Thy08
K
Shared sequences - TRD
120
100
80
60
40
20
0
Counts
Thy01
Thy02
Thy03
Thy04
Thy05
Thy06
Thy07
Thy08

Figure 4.2 Thymic TCRγ repertoire contains a fraction of public sequences whereas TCRδ is private. (a-b) Graphical representation of the thymic TRG (left) and TRD (right) repertoires. In these Treemap graphs, each square represents a clonotype bearing a unique nucleotide sequence, its area being proportional to relative abundance in the repertoire; and the colours group the clonotypes by TCR chains. (c) Graphical representation of a PB TRD control repertoire. (d-e) Thymic and PB (f) CDR3 length (number of nucleotides) distributions for each TCR chain. (g) Example of CDR3 length distribution of thymic Vδ1 (top) and Vδ2 (bottom) sequences. (h-i) Rarefaction analysis of repertoires from thymic and PB samples. The number of unique clonotypes in a sample are plotted against its size. Solid and dashed lines are diversity estimates computed by interpolating and extrapolating using a multinomial model respectively. (j-k) Number of shared TRGV and TRDV sequences across donors (Thy1-8).

4.1.3 Concluding remarks

In this study we applied NGS to highly (FACS-)purified Vδ1$^+$ T cells, which allowed us to reveal unsuspected aspects of the rearranged and expressed (at the mRNA level) TRG and TRD repertoires of this cell population. The most striking and surprising observation was the presence of a big fraction (~20%) of Vδ2 sequences in the thymic TRD repertoire of all 8 donors. While a small fraction of Vδ2 sequences, like the one found in the PB Vδ1$^+$ T cell pool, could be due to contamination during the FACS sorting of CD3$^+$ Vδ1$^+$ Vδ2- cells, this cannot explain the large fraction of Vδ2 sequences in the thymic Vδ1$^+$ samples. In fact, the most abundant and frequent thymic clonotypes in all the 8 donors were Vδ2, which globally accounted for around one fifth of the TRD repertoire. Of note, these Vδ2 sequences are predicted to be functional and do not include the common rearrangement with the VγJP segment, thus excluding a foetal origin.

At this point we can only speculate that the high amount of Vδ2 sequences could be linked to biallelic expression of δ-chains[309,317]. Although it has been reported that γδ T cells might be capable to express two functional TCR with different γ-chains[318], we rather assume that the second allele might be silence post-transcriptionally. However, to address these open questions systematically it would require a rather challenging protein or mRNA analysis at the single-cell level (or derived clones). Thus, the hypothesis that there would necessarily be a Vδ2$^+$ single chain or heterodimer retained intracellularly, in order to allow the Vδ1$^+$ TCR to be uniquely expressed on the cell surface deserves future investigation.

From a more global standpoint, and as already described for total (unsorted) γδ thymocytes[312] and their αβ counterparts[319], the thymic Vδ1$^+$ TCR (purified) repertoire was also unbiased and unfocused, with no skewing towards some clonotypes. The absence of biases in the CDR3 length distributions, with median distribution values around 40nt for TCRγ and 60nt for TCRδ, is also representative of repertoires that have not yet encountered antigen. These characteristics are thus signatures of the naïve repertoires present in the thymus or in the cord blood[124], in stark contrast with peripheral blood repertoires, that become focused toward specific clones due to antigen-mediated selection in the periphery[122,124,312].

Peripheral blood and cord blood Vδ1$^+$ T cells were described to display private TRD repertoires, in contraposition to their γ-chains that showed a fraction of common (shared among individuals) sequences[122,124]. We now show that this is also the case for purified Vδ1$^+$ thymocytes, which raises the interesting question whether the public TRG clonotypes are selected (upon ligand encounter) in the thymus; or simply the output of a favoured TCR rearrangement. This, in fact, is an open question also on the Vγ9-JPVδ2 rearrangement that is prevalent in foetal life[41].

In sum, this report constitutes a resource providing new data and qualifying previous conclusions on the TCR repertoire of human thymic γδ T cells. Critically, the unexpected presence of a large fraction of Vδ2 sequences in Vδ1$^+$ thymocytes strongly advocates for the use of highly purified cell populations, ideally complemented by single-cell validation experiments, to avoid misinterpretations of NGS data in future studies.

4.2 Broad cytotoxic targeting of acute myeloid leukaemia by highly polyclonal Delta One T cells

Published online on April 2019 in ***Cancer Immunology Research*** (Di Lorenzo et al. 2019), doi: 10.1158/2326-6066.CIR-18-0647

4.2.1 Introduction

Acute myeloid leukaemia (AML) is the most common and one of the most lethal form of acute leukaemias in adults. In Europe, the annual rate of AML incidence is 3.7 in 100,000, with 18,000 new cases estimated per year[320]. The standard treatment for the majority of newly diagnosed AML is still the same of four decades ago, although several and significant research efforts have been made[321,322]. Outside the setting of a clinical trial, the provided treatment is a combination of standard-dose cytarabine with an anthracycline (daunorubicin or idarubicin) despite the approval of new options[323]. However, with the current treatments and the improvements in the supportive care, the 5-year overall survival is in the range of 40-50% in younger patients and in the range of 10-20% in older than 60 years old patients. The major clinical problem with AML is relapse, since only ~10% of patients survive upon tumour recurrence (following an initial complete response to treatment) and ultimately face problems derived from the treatment such as the selection of chemoresistant clones that drive refractory relapses[322,324]. Indeed, most patients with AML die from progressive disease after relapse, which is associated with clonal evolution at the cytogenetic level[325,326]. More in details, two major clonal evolution patterns might occur during AML relapse: 1) the founding clone in the primary tumour gained mutations and evolved into the relapse clone, or 2) a subclone of the founding clone survived initial therapy, gained additional mutations, and expanded at relapse (Figure 4.3)[327]. Some mutations gained at relapse may alter the growth properties of AML cells, or confer resistance to additional chemotherapy. Regardless of the mechanism, each tumour displayed clear evidence of clonal evolution at relapse, and a higher frequency of transversions that were probably induced by DNA damage from chemotherapy. Although chemotherapy is required to induce initial remissions in AML patients, there could also be the possibility that it contributes to relapse by generating new mutations in the founding clone or one of its subclones, which then can undergo selection and clonal expansion[327].

Several new agents are currently under development, but there is still a clear need for newer therapies aiming not only at the complete remission but also at the increasing of the progression-free survival and minimal residual disease after treatment[328]. Promising alternatives to chemotherapy are novel targeted therapies[322,329] and upcoming immunotherapies[324], especially chimeric antigen receptor (CAR) T cell transfer, fuelled by notable recent success in B-cell malignancies[330] . By contrast, we are focusing on *ex vivo* differentiated Delta One T (DOT) cells that rely on physiological receptors, namely TCR and NCR such as NKp30 and NKp44, to distinguish transformed from healthy cells[114,270,303]. Importantly, DOT cells are derived from peripheral blood Vδ1$^+$ γδ T cells, whose *in vivo* expansion correlated with enhanced long-term disease-free survival of leukaemia patients that received allogeneic hematopoietic stem cell transplantation[302].

While the clinical manipulation of Vδ1$^+$ γδ T cells has been hindered by their relatively low abundance (<0.5%) among peripheral blood lymphocytes, we recently devised the first clinical-grade protocol to expand and differentiate large numbers of DOT cells endowed with potent anti-tumour cytotoxicity[114,303]. Thus, our 3-week protocol achieves > 1,000-fold expansions of Vδ1$^+$ γδ T cells, for which the synergistic

action of TCR and IL4 stimulation is critical (during its 1st stage), whereas the 2nd stage focuses on the IL15-dependent differentiation of potent anti-tumour DOT cell effectors endowed with NCR expression[114]. Converging the properties and potential of DOT cells with the unmet immunotherapy needs of AML, in this study we aimed to purpose DOT cells specifically for AML treatment.

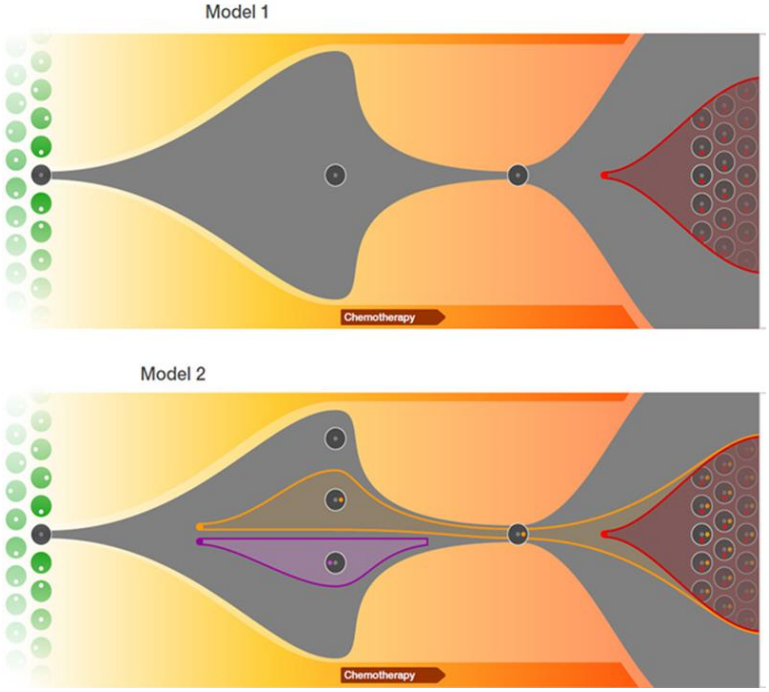

Figure 4.3 Graphical representation of two clonal evolution patterns. The upper graph shows the dominant clone in the primary tumour evolving into the relapse clone by gaining relapse-specific mutations; the bottom model shows a minor clone carrying the vast majority of the primary tumour mutations survived and expanded at relapse. Adapted from[327].

4.2.2 DOT cell repertoire diversity characterization

On our path to the development of a novel Vδ1⁺ γδ T cell-based adoptive cell therapy for cancer[114,303], we started this study by further characterizing the DOT cell product. Strikingly, we found DOT cells to be extremely polyclonal and thus devoid of dominant clones, in stark contrast to ex vivo Vδ1⁺ T cells from all donors analysed (Figure 4.4A-D).

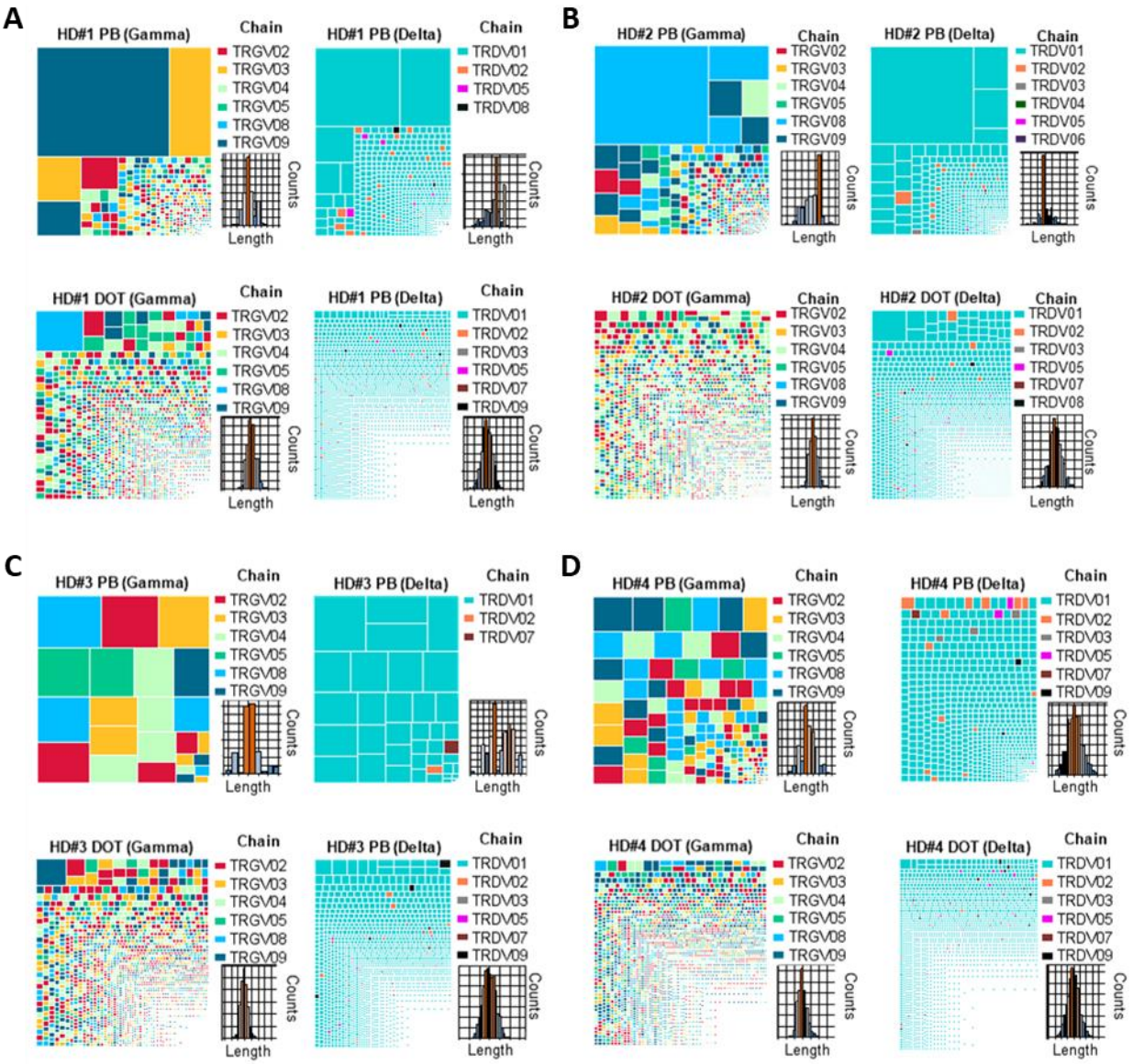

Figure 4.4 PB and DOT TCRγ and TCRδ repertoires of fresh PB samples (upper panels) and of DOT cell (bottom) derived from the same donors. Repertoires from four different healthy donors were analysed (A-D). Graphical representation of the TRG (left) and TRD (right) repertoires. Each square represents a clonotype bearing a unique nucleotide sequence, its area being proportional to relative abundance in the repertoire; and the colours group the clonotypes by TCR chains. In the bottom right corner, CDR3 length (number of nucleotides) distributions for each TCR chain.

This was also clearly illustrated by the contribution of the top 20 expanded clones to the overall Vδ1⁺ TCR repertoire: whereas they represented >60% in the peripheral blood, they accounted for less than 10% in the DOT cell products (Figure 4.5).

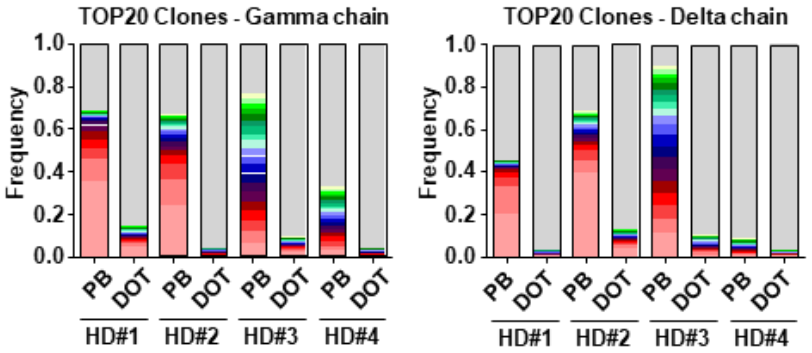

Figure 4.5 Contribution of the top 20 clones to the overall Vδ1⁺ TRG (left) and TRD (right) repertoires of each sample (HD #1-4, healthy donors 1 to 4). Frequency of the top 20 clones is represented as coloured stacked bars.

We next aimed to better understand the basis for the remarkable diversification of the DOT cell repertoire testing different conditions, as described in 3.2.5 and 3.2.6. First, we analysed two stimulation cocktails: cytokine with no αCD3 stimulation (Ck) and αCD3 ⁺ IL2 stimulation with no additional cytokines (TCR) at day 11 (expansion mid time point), and at the end of the culture (day 21). Surprisingly, there were no significant differences in the repertoire diversification using the two differently supplemented media at the two time-points that were examined (Figure 4.6 and Figure 4.7).

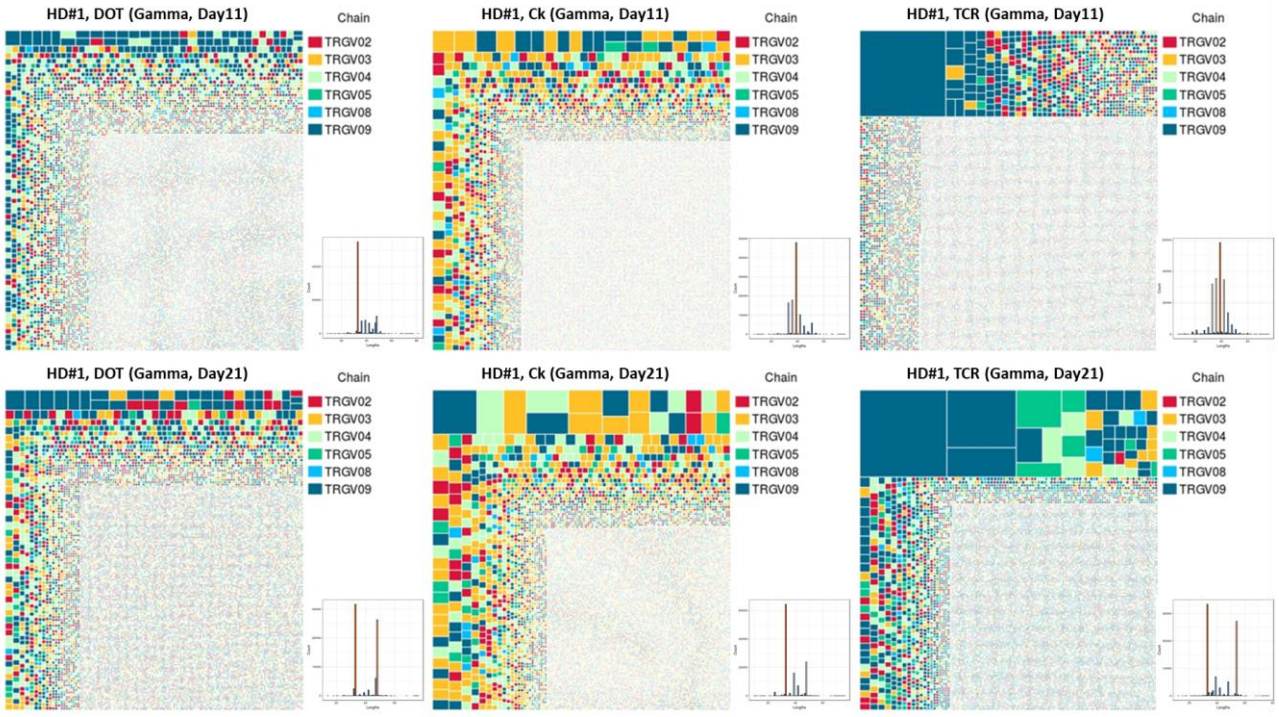

Figure 4.6 TRGV repertoire comparison of DOT medium with no αCD3 (Ck) and αCD3 ⁺ IL2 (TCR) supplemented media. Graphical representation of TRGV repertoire and CDR3 length distribution after expanding cells with the standard DOT expansion protocol (IL4, IFN-γ, IL21, IL1β and αCD3 - left), with no αCD3 stimulation (IL4, IFN-γ, IL21, IL1β and IL2 – Ck, center) and with αCD3 stimulation (IL2 and αCD3) at two time points (day 11 and day 21 – graphs on the top and on the bottom, respectively). Each square represents a clonotype bearing a unique nucleotide sequence, its area being proportional to relative abundance in the repertoire; and the colours group the clonotypes by TCR chains. In the bottom right corner, CDR3 length (number of nucleotides) distributions for each TCR chain

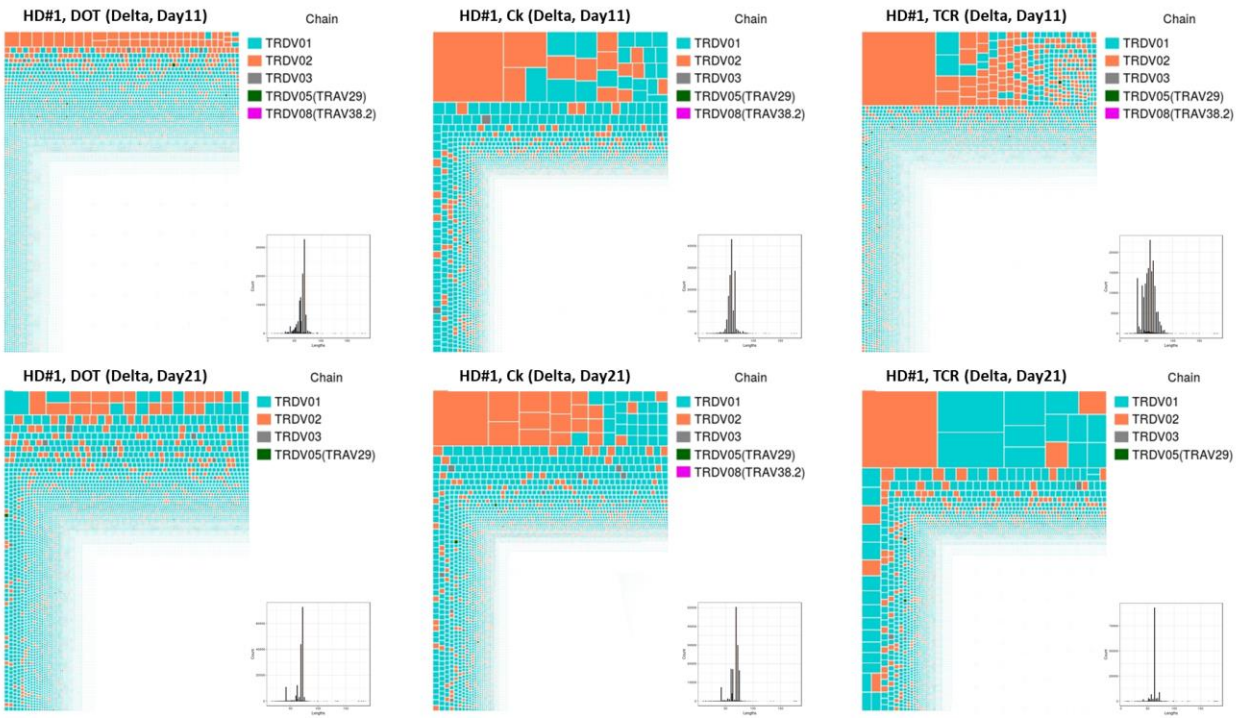

Figure 4.7 TRGD repertoire comparison of DOT medium with no αCD3 (Ck) and αCD3 + IL2 (TCR) supplemented media.. Graphical representation of TRGD repertoire and CDR3 length distribution after expanding cells with the standard DOT expansion protocol (IL4, IFN-γ, IL21, IL1β and αCD3 - left), with no αCD3 stimulation (IL4, IFN-γ, IL21, IL1β and IL2 – Ck, center) and with αCD3 stimulation (IL2 and αCD3) at two time points (day 11 and day 21 – graphs on the top and on the bottom, respectively). Each square represents a clonotype bearing a unique nucleotide sequence, its area being proportional to relative abundance in the repertoire; and the colours group the clonotypes by TCR chains. In the bottom right corner, CDR3 length (number of nucleotides) distributions for each TCR chain.

To further investigating the basis for DOT cell repertoire diversification, we next compared the TCR clonality of DOT cells produced from pre-sorted differentiated CD27- versus naïve CD27+ subsets, sorted as displayed in Figure 4.8.

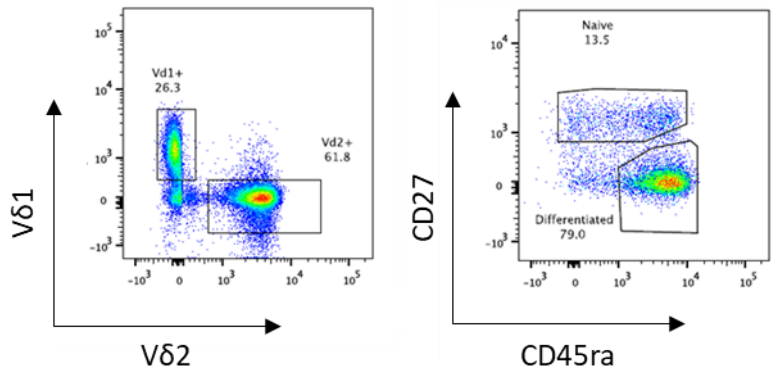

Figure 4.8 FACS sorting gating strategy for CD27- versus CD27+ subsets. Events displayed in the left panel are gated on Singlet/live/CD3+. CD27+ and CD27- cells from the Vδ1+ population were sorted in parallel.

After 21 days in culture, sorted Vδ1+CD27- and Vδ1+CD27+ consistently displayed distinct proliferation capacities under the DOT cell protocol (Figure 4.9 A) and showed intrasample diversity, as indicated by the Shannon diversity index measurements (Figure 4.9 B), and repertoire graphical representation similar to PB and DOT samples, respectively (Figure 4.10 and Figure 4.11). Moreover, DOT cells obtained from HD#1-4 were highly enriched (87% to 98%) for CD27+ cells (Figure 4.9 C).

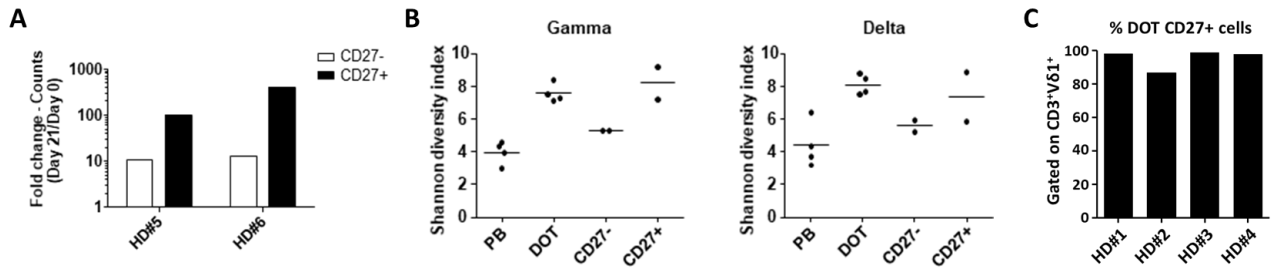

Figure 4.9 Vδ1⁺CD27- and Vδ1⁺CD27⁺ diversification analysis under the DOT cell protocol. (A) Fold expansion of pre-sorted CD27- versus CD27⁺ Vδ1⁺ T cells after 21 days with the DOT cell protocol (HD#5-6, healthy donors 5 and 6). (B) Shannon indices for intra-sample variability of Vδ1⁺CD27- and Vδ1⁺CD27⁺ TRGV and TRDV repertoires and from Figure 6.2. (C) Percentage of CD27⁺ cells after 21 days DOT cell expansion protocol inside the CD3⁺Vδ1⁺ population.

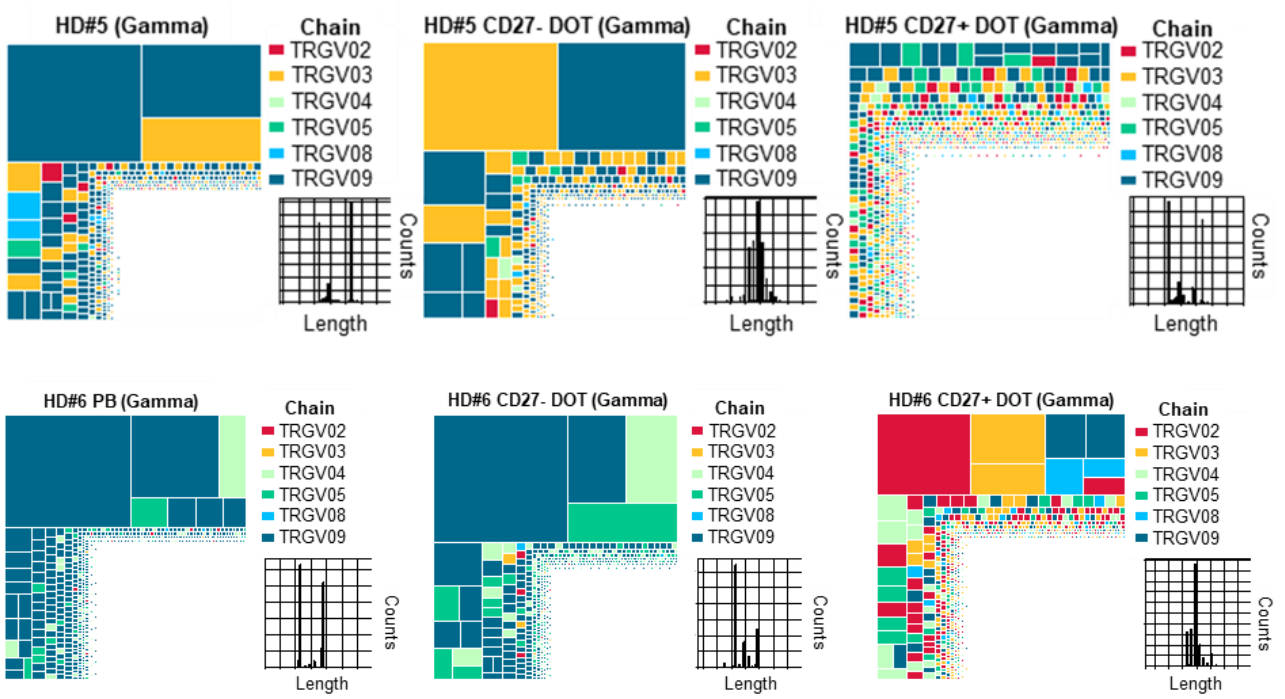

Figure 4.10 Vδ1⁺ CD27- and Vδ1⁺ CD27⁺ TRGV repertoires. Graphical representation of TRGV repertoire and CDR3 length distribution of ex vivo Vδ1⁺ cells (left panels) and using the standard DOT cell protocol to expand pre-sorted Vδ1⁺CD27- (middle panels) or Vδ1⁺CD27⁺ lymphocytes (right panels). Top graphs display results for HD#5 and bottom graphs for HD#6. Each square represents a clonotype bearing a unique nucleotide sequence, its area being proportional to relative abundance in the repertoire; and the colours group the clonotypes by TCR chains. In the bottom right corner, CDR3 length (number of nucleotides) distributions for each TCR chain

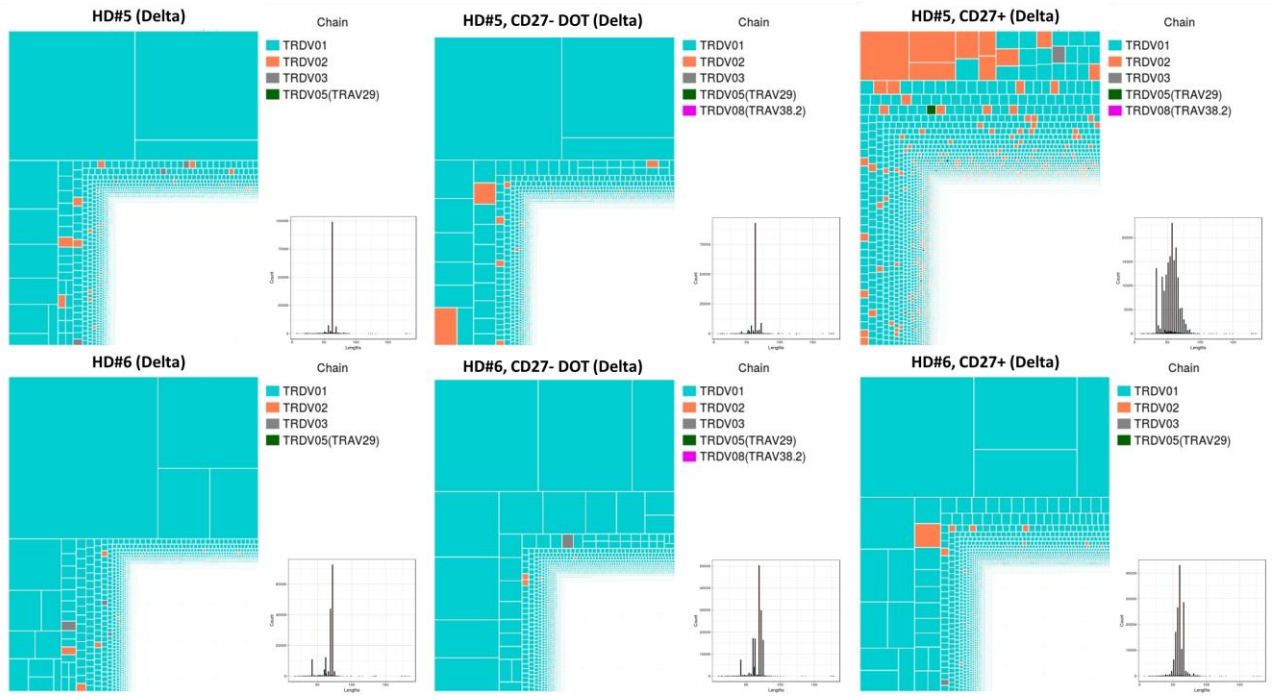

Figure 4.11 Vδ1⁺ CD27- and Vδ1⁺ CD27⁺ TRDV repertoires. Graphical representation of TRDV repertoire and CDR3 length distribution of ex vivo Vδ1⁺ cells (left panels) and using the standard DOT cell protocol to expand Vδ1⁺CD27- (middle panels) or Vδ1⁺CD27⁺ lymphocytes (right panels). Top graphs display results for HD#5 and bottom graphs for HD#6. Each square represents a clonotype bearing a unique nucleotide sequence, its area being proportional to relative abundance in the repertoire; and the colours group the clonotypes by TCR chains. In the bottom right corner, CDR3 length (number of nucleotides) distributions for each TCR chain.

4.2.3 DOT cell recognition of AML cells

To evaluate DOT cell anti-AML activity, we tested bulk DOT cell products (from multiple donors) against various AML cell lines (Table 3.3) as well as primary samples obtained from patients at diagnosis). DOT cells from HD#1-4 were co-incubated at 10:1 (E:T) ratio for three hours with several AML cell line targets (Figure 4.12, left panel), AML primary samples (Figure 4.12, middle) and normal leukocyte populations (Figure 4.12, right panel). Plots represent the percentage of Annexin V⁺ target cells after co-incubation. Critically, DOT cells promptly induced Annexin V⁺ expression in AML primary cell lines and primary samples but did not target any normal leukocyte population (neither myeloid nor lymphoid) from the peripheral blood of healthy volunteers. Of note, DOT cell cytotoxicity clearly associated with increased degranulation and expression of perforin and granzyme B upon tumour cell recognition (Figure 4.13)

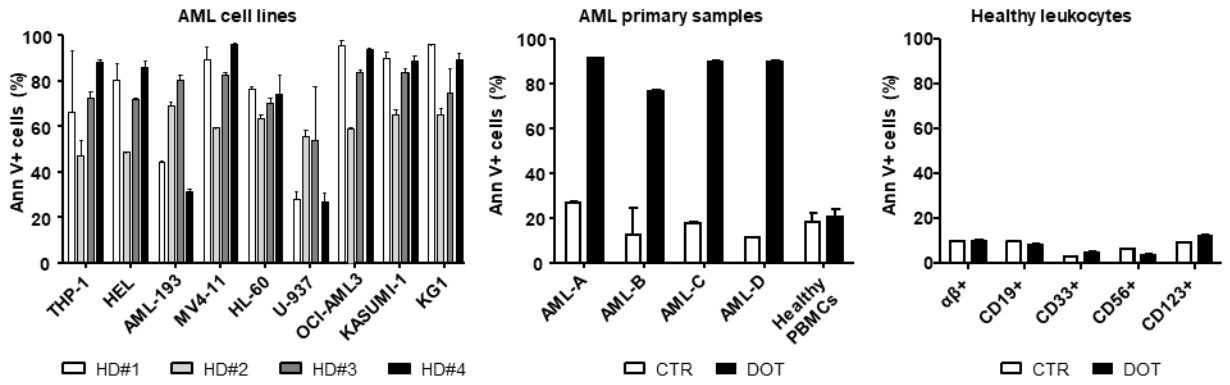

Figure 4.12 DOT cells target multiple AML cell types but not healthy leukocytes. In vitro killing assays with DOT cells produced from 4 healthy donors, co-incubated for 3 hours at 10:1 (E:T) ratio with the indicated AML cell lines (left), primary AML samples (middle) or normal leukocyte populations FACS-sorted from the peripheral blood (right). CTR refers to tumour cells alone, without adding DOT cells. Experiments were performed with technical triplicates

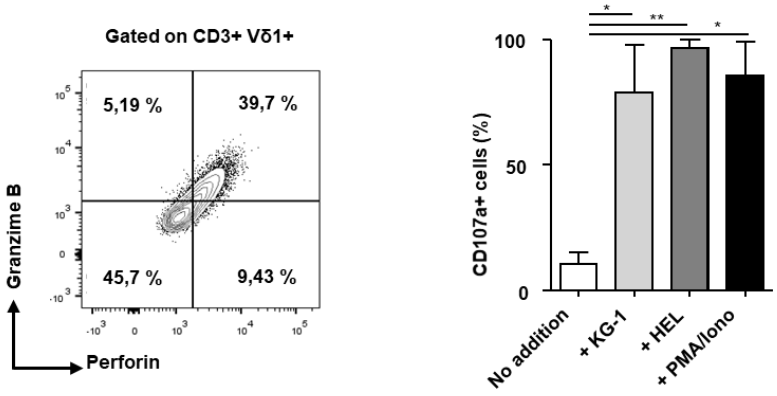

*Figure 4.13 DOT cell cytotoxicity via degranulation upon AML cell recognition. (Left) DOT cell expression of Granzyme B and Perforin as assessed by intracellular flow cytometry. (Right) Percentage of CD107a⁺ DOT cells after co-incubation with AML tumour targets; or upon PMA/ionomycin stimulation (positive control); or no addition (negative control). Results are from two healthy donors, tested in triplicates. Indicated are mean ⁺ SEM; *, p < 0.05, **, p < 0.01.*

To further assess the functional relevance of DOT cell polyclonality, we generated clones from single-cell sorted Vδ1⁺ T cells, expanded using an adapted DOT cell protocol including the addition of feeder cells to support expansion from single-cells (Methods 3.3.2). $CD3^{+}TCRV\delta1^{+}TCRV\delta2$- single cells were FACS-sorted into 96 wells/plates; and cultured for 21 days using the DOT cell protocol in the presence of (weekly-renewed) 10^4 irradiated autologous PBMCs (feeders). Cloning efficiency was between 21% and 28% (Figure 4.14 left), with average doubling times of 1.43, 1.62, 1.79 and 1.52 (Figure 4.14 middle). Absolute DOT cell numbers in established clones are represented by individual dots Figure 4.14, right panel.

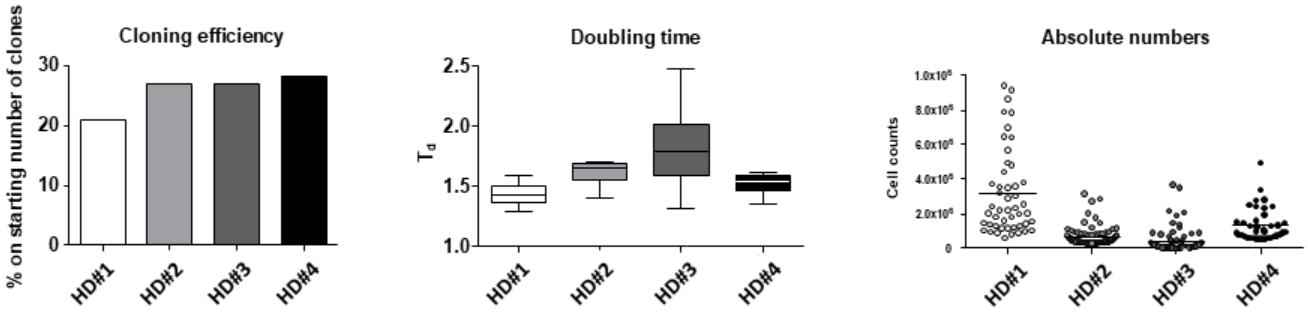

Figure 4.14 Vδ1⁺ T cells clone generation. Left, cloning efficiency measured as percentage of successfully established clones on the starting number of plated cells. Middle, doubling time of the established clones showed as box and whisker plot. Right, absolute DOT cell numbers in the established clones (represented by individual dots).

We next tested clone cytotoxicity against the AML cell line KG-1 (Figure 4.15); cells were co-incubated for three hours at 10:1 (E:T) ratio and then analysed by Annexin V staining (percentage of positive events among pre-labelled KG-1 cells). Each bar represents an individual clone and the red dashed line represent the percentage of Annexin V⁺ KG-1 cells with no clone addition.

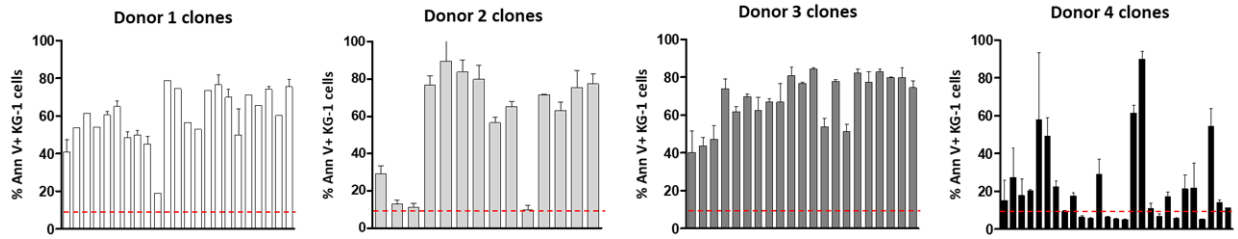

Figure 4.15 In vitro killing of AML KG-1 cells by DOT cell clones generated from single Vδ1⁺ T cells sorted from healthy donors Cells were co-incubated for 3 hours at 10:1 (E:T) ratio and then analysed by Annexin V staining (percentage of positive events among pre-labelled KG-1 cells). Each bar represents an individual clone and the red dashed line represent the percentage of Annexin V⁺ KG-1 cells with no clone addition; experiments were performed in two technical replicates.

To functionally test if the TCR is involved, we performed the killing assay in the presence of an anti-Vδ1⁺ TCR specific blocking monoclonal antibody (or isotype control) and observed a partial reduction (from 10% to 80%, most frequently around 30%) in KG-1 cell targeting across a number of clones from different donors (Figure 4.16).

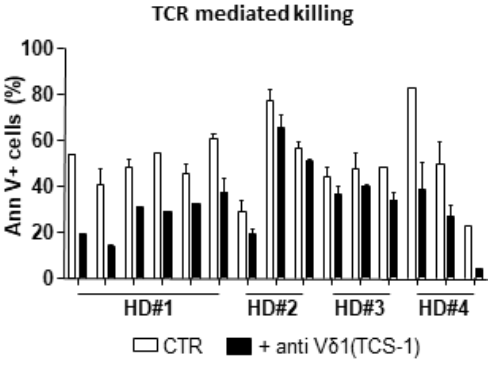

Figure 4.16 Effect of δ chain blockade using monoclonal antibody. Cells were co-incubated for 3 hours at 10:1 (E:T) ratio and then analysed by Annexin V staining (percentage of positive events among pre-labelled KG-1 cells). Each bar represents an individual clone. An anti-Vδ1⁺ TCR specific monoclonal antibody (TCS-1) or isotype control (CTR) was added to the cultures. Clones herein displayed were selected for the highest blocking effect. Experiments were performed in technical duplicates.

Since the TCR blockade induced only a partial reduction, we analysed the expression of two NCRs (NKp30 and NKp44) in DOT cells and observed that NKp30 was the most expressed. We next performed a CRISPR/Cas9 knockout of the putative NKp30 ligand (B7-H6) on the AML cell line HEL and we tested DOT cell capability of inducing apoptosis in the newly target cell line. The absence of B7-H6 reduced the killing of nearly 40% (Figure 4.17)

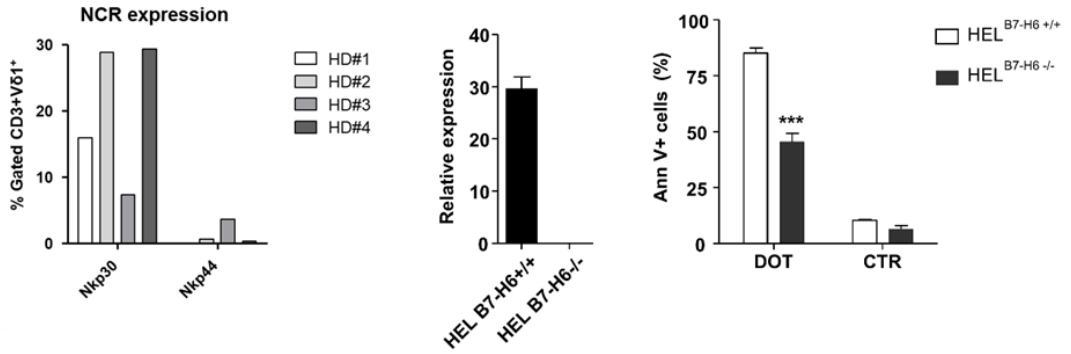

*Figure 4.17 DOT cells employ NKp30 to kill AML cells.NKp30 Real-time PCR assessing B7-H6 mRNA in parental (B7-H6$^{+/+}$) and CRISPR/Cas9-manipulated (B7-H6$^{-/-}$) AML HEL cell lines (middle). On the right, In vitro killing of B7-H6$^{+/+}$ or B7-H6$^{-/-}$ AMLHEL cells by bulk DOT cells produced from 3 healthy donors (tested in technical duplicates). Cells were coincubated for 3 hours at 10:1 (E:T) ratio and then analysed by Annexin V staining (shown are percentages of positive events among prelabelled HEL cells). Indicated are mean + SEM (***, P<0.001).*

To test DOT cells against AML *in vivo*, we established three independent xenograft models of AML (Figure 4.18). DOT cells were transferred to NSG mice pre-injected with KG-1 AML cells (A-B); HEL-bearing NRGS hosts; or NSGS mice bearing primary AML cells. Tumour burden was assessed in the blood and liver one week after the last DOT cell transfer or through weekly bleedings. Strikingly, both in AML cell line models (Figure 4.18A-C) and patient-derived xenografts (Figure 4.18D-E), DOT cell treatment markedly reduced tumour burden and increased host survival, without any noticeable toxicity.

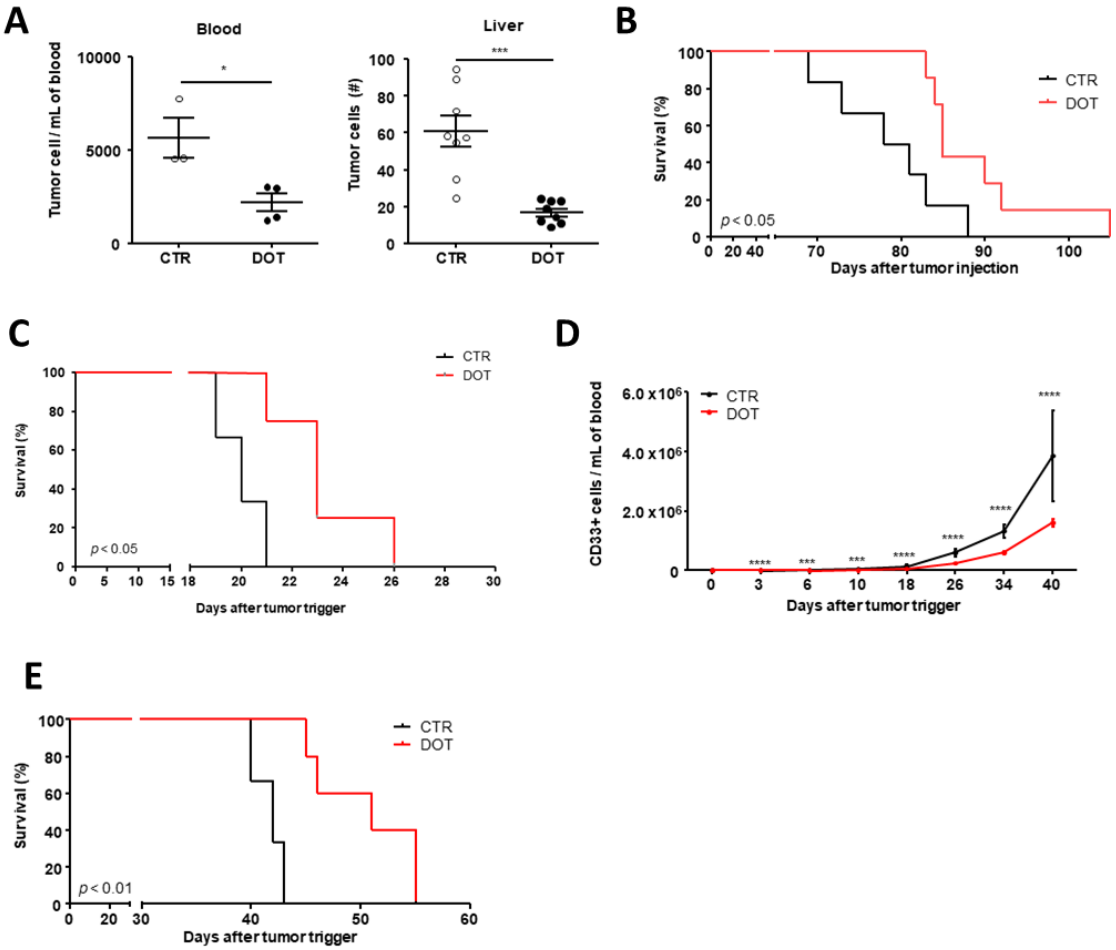

Figure 4.18 In vivo AML targeting by DOT cells. DOT cells were transferred to NSG mice (n = 6 CTR, 7 DOT treated mice) pre-injected with KG-1 AML cells (A-B); HEL-bearing NRGS hosts (n = 5 CTR, 4 DOT treated mice; p < 0.05); or NSGS mice (n = 5 CTR, 5 DOT treated mice) bearing primary AML cells (D-E). Tumour burden was assessed in the blood and liver one week after the last DOT cell transfer (A); or through weekly bleedings (D). Animals were sacrificed when advanced disease symptoms (such as back leg paralysis) were observed. Survival curves are presented in panels B (p < 0.05), C (p < 0.05) and E (p < 0.01).

Given that the major therapeutic problem in AML is chemoresistance, we subjected AML cells to high doses of cytarabine plus doxorubicin for 72h, which led to >99% tumour cell elimination; and then allowed the survivor cells to re-grow before re-treating them with chemotherapy or DOT cells. Whereas the cytotoxic efficacy of chemotherapy was drastically reduced, that of DOT cells was not impacted (Figure 4.19 A). We also questioned the ability of DOT cells to re-target AML cells "relapsing" after a first DOT cell treatment that also eliminated >99% tumor cells in 72h (Figure 4.19 B). Interestingly, DOT cells killed DOT-pre-treated AML cells as efficiently as non-treated controls (Figure 4.19 C). To track the AML clonal dynamics upon therapeutic (DOT cells or chemotherapy) pressure, we tagged single AML cells with cellular barcodes. Whereas chemotherapy selectively targeted approximately half of all barcoded AML single-cell lineages, DOT cells mostly preserved the clonal architecture of the AML population (Figure 4.19 D-E).

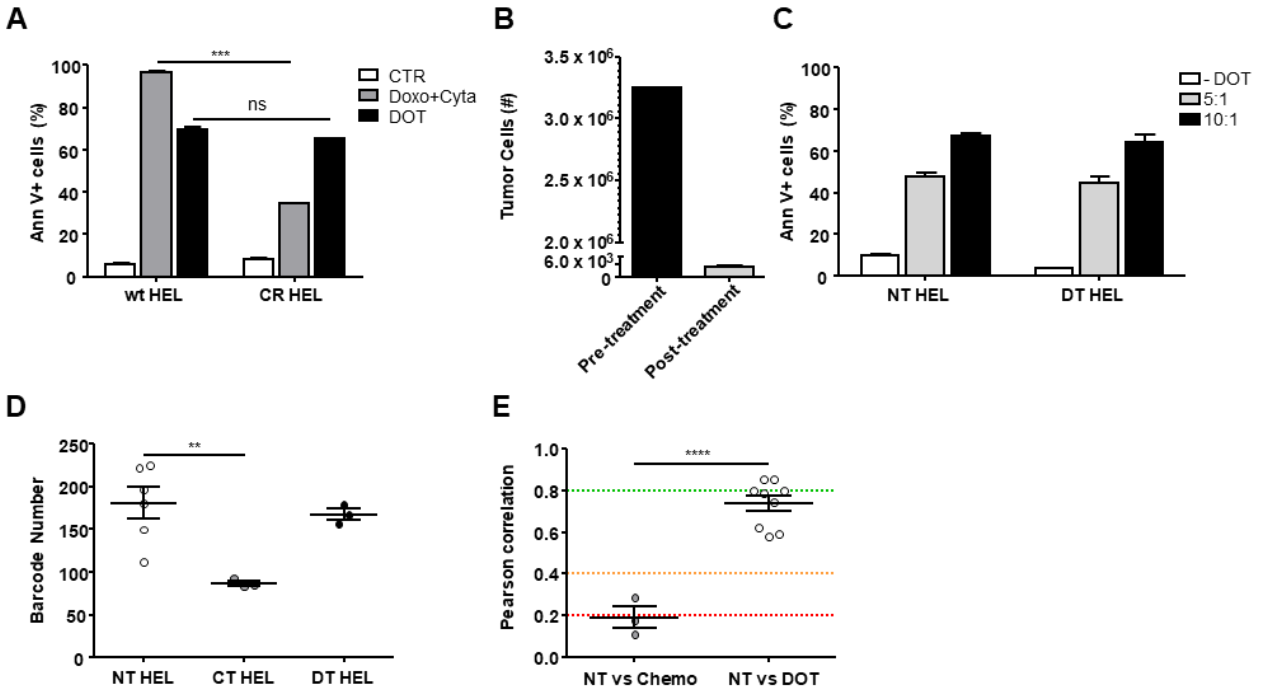

*Figure 4.19 DOT cells efficiently (re-)target chemotherapy-resistant AML Comparison of the in vitro anti-AML activity of DOT cells and standard chemotherapy. (A) DOT cells and standard AML chemotherapy (Doxorubicin plus Cytarabine) treatments were tested against chemotherapy-naïve (wild type, wt) or chemo-relapsed (CR, re-grown after >99% HEL cell elimination) AML cells. Shown are the percentages of Annexin V⁺ HEL cells after 3 hours of treatment. (B) Number of AML HEL cells before and after 72 hours of treatment with DOT cells (at 5:1 E:T ratio). Surviving cells (<1%) were re-sorted and allowed to re-grow, thus generating the DOT-treated (DT) samples of (C-E). (C) DOT cells were co-incubated for 3 hours with non-treated (NT) or previously DOT-treated (DT) AML HEL cells at 5:1 or 10:1 (E:T) ratios. Shown are the percentages of Annexin V⁺ HEL cells. (D) Number of barcoded AML single-cell lineages in non-treated (NT), chemotherapy-treated (CT) or DOT-treated (DT) AML HEL cells. (E) Pearson correlation for distribution of barcoded AML single-cell lineages between different treatments. Indicated are mean SEM; *, p < 0.05, **, p < 0.01, ***, p < 0.001, ****, p < 0.0001.*

4.2.4 Conclusions

Recent reports on the analysis of γδ TCR repertoires described the clonal expansion and focusing of the adult peripheral blood Vδ1$^+$ T cell repertoire[124], likely driven by common pathogens such as CMV[122,123] or *Mycobacterium tuberculosis*[145]. Therefore, we wondered what the impact of the DOT cell expansion/differentiation process on the TCR repertoire was, in order to first assess if the protocol was selective for specific clonotypes or if it was solely expanding the pool of circulating PB Vδ1$^+$ T cells and thus maintaining the global clonotype architecture. We stated that after performing NGS of the CDR3 regions in TRGV and TRDV genes (before and after the 3-week cultures) our starting hypotheses were not confirmed. Indeed, we observed a dramatic increase in the repertoire diversity with loss of the oligoclonality typical of the PB Vδ1 repertoires, as highlighted as well by the contribution of the top 20 most frequent clones to the repertoire distribution (Figures 4.4 and 4.5) and by the increase in the intrasample diversity upon DOT cell protocol (Figure 4.9). Moreover, signs of previous immunological history, evaluated by CDR3 length distribution, were lost (Figure 4.4).

We next aimed to better understand the basis for the remarkable diversification of the DOT cell repertoire, questioning if the cytokine combination could somehow have an impact. We found that different stimulations, namely a combination of IL2, IL4, IL15, IFN-γ, IL21 and IL1β or of αCD3 $^+$ IL2 (Figure 4.6), did not contribute to increase the repertoire diversification. In addition, we observed that the diversification was already established at the middle-term time point of DOT protocol (day 11). We successively hypothesized that the protocol could have been selective for Vδ1$^+$ subtypes. Indeed, given the previous association of CD27 downregulation with pre-expanded/differentiated Vδ1$^+$ T cells[124], we compared the TCR clonality of DOT cells produced from pre-sorted CD27- versus CD27$^+$ subsets, which consistently displayed distinct proliferation capacities under the DOT cell protocol (Figure 4.9). We found that the generation of highly diverse DOT cells was restricted to CD27$^+$ precursors (Figure 4.10). These data suggest that the DOT cell protocol preferentially expands naïve-like CD27$^+$Vδ1$^+$ T cells with an extremely diverse TCR repertoire, at the expense of pre-expanded and terminally differentiated CD27-Vδ1$^+$ T cells, as highlighted as well by the high abundance of CD27$^+$Vδ1$^+$ T cells at the end of the cultures (Figure 4.9 C).

At this stage we hypothesized that DOT cell polyclonality could associate with breadth of recognition of AML cells. We first generated Vδ1$^+$T cell clones starting from single cell seeding; indeed, this approach was more productive (in terms of cloning efficiency and time/resource consumption) than the standard limiting dilution approach. Strikingly, we found the vast majority of clones (from different donors) to be highly efficient at inducing apoptosis of KG-1 cells upon short (3-hour) co-incubation *in vitro* (Figure 4.15). These results showed that DOT cell products are composed of multiple clones with intrinsic capacity to target AML cells. Moreover, TCR blockade induced only a partial and variable reduction in the killing capacity of Vδ1$^+$ T cell clones, from 10% to 80% decrease, with most frequently a reduction of 30%. The remaining reactivity is likely mediated by natural cytotoxicity receptors[114,270,303], as highlighted by the B7-H6 knockout on the AML target cells. Indeed, at this stage, we hypothesized that most of the reactivity was mediated by natural cytotoxicity receptors, particularly NKp30. In fact, DOT cell cytotoxicity was significantly decreased upon CRISPR/Cas9-mediated knockout (at the population level) of the best-established tumour-associated NKp30 ligand, B7-H6, in target AML cells (Figure 4.17).

We also tested DOT cell capability of killing several AML cell lines and AML primary samples. In all cases, DOT cells readily (within 3 hours) killed AML cells *in vitro* (Figure 4.12), in similar fashion to what was reported for CAR-T cells[331–333]. Critically, DOT cells did not target any normal leukocyte population (neither myeloid nor lymphoid) from the peripheral blood of healthy volunteers (Figure 4.12 – right panel), including CD33$^+$ and CD123$^+$ myeloid progenitor cells whose off-target depletion by the respective CAR-T cells is known to be responsible for the unwanted myeloablation[324,332].

To assess DOT cell tumoricidal function *in* vivo, we established three xenograft mouse models to test DOT cell targeting of AML primary samples and of AML cell lines, namely KG-1 and HEL. In the tested models, DOT cell treatment markedly reduced tumour burden and increased host survival, without any noticeable toxicity. However, the survival benefits herein obtained were smaller than the ones reported for CAR-T cells treatment of AML xenografts[331–333], although these models were biased to AML cell lines uniformly expressing the target antigens. Furthermore, and critically, xenografts cannot evaluate the toxicity of a strategy predicted to induce myeloablation in patients. Overall, we believe that the combined safety and efficacy profiles of DOT cells make them very attractive candidates for adoptive cell therapy of AML in the near future.

Finally, considering that the major therapeutic problem in AML at the present time is chemoresistance, which drives deadly relapses, we next asked whether DOT cells could target chemoresistant AML cells. Surprisingly, we demonstrated that DOT cells have the superior capacity of targeting chemoresistant AML cells, previously treated with high doses of cytarabine plus doxorubicin for 72h, which led to >99% AML cell elimination.

In light of this and taking into account the highly polyclonal and multireactive DOT cell repertoire, we also questioned the ability of DOT cells to re-target AML cells “relapsing” after a first DOT cell treatment that also eliminated >99% tumour cells in 72h (Figure 4.19B). Interestingly, DOT cells killed DOT-pre-treated AML cells as efficiently as non-treated controls (Figure 4.19C), suggesting that DOT cell treatment did not select for a specific subset of DOT-resistant AML cells. To track the AML clonal dynamics upon therapeutic (DOT cells or chemotherapy) pressure, we tagged single AML cells with cellular barcodes. Whereas chemotherapy selectively targeted approximately half of all barcoded AML single-cell lineages, DOT cells mostly preserved the clonal architecture of the AML population (Figure 4.19D-E).

These data collectively suggest that the breadth of AML targeting based on many cytotoxic DOT cell clones avoids the selection of resistant lineages and allows efficient re-treatment. Given the urgency of preventing the emergence of deadly refractory relapses, namely after standard chemotherapy, our work provides strong pre-clinical proof-of-concept for clinical application of DOT cells in AML treatment.

4.3 An NGS-based approach for the identification of new ligands for the Vδ1$^+$ TCR

This chapter describes unpublished data obtained in the context of this PhD thesis.

4.3.1 Introduction

More than three decades after the discovery of γδ T cells[18], the research community is still missing a compelling picture on their mechanisms of antigen recognition, especially since γδ T cell activation is typically independent of peptide presentation by MHC molecules. Indeed, early research on the molecular mechanisms of γδ T cell recognition in the 1990s led to the realization of its unusual independence of peptide processing and MHC-restricted presentation, in marked contrast with αβ T lymphocytes[188–190]. One of such lines of evidence came from non-peptidic prenyl pyrophosphates (a pAg) recognized by Vγ9Vδ2$^+$ TCRs[191,192]. Among these compounds, isopentenyl pyrophosphate (IPP) and dimethylallyl pyrophosphate are natural intermediates of the mevalonate pathway of isoprenoid and steroid synthesis in eukaryotic cells. Importantly, the dysregulation of the mevalonate pathway in some tumour cells allows for the accumulation of these pAgs, thus promoting Vγ9Vδ2$^+$ TCR-mediated recognition[169]. Furthermore, treatment with zoledronate or pamidronate (which are approved drugs) was shown to be very effective at inducing the accumulation of intracellular pAgs like IPP, and thus potentiate TCR-dependent Vγ9Vδ2$^+$ T cell cytotoxicity against tumour cell targets, including cancer stem cells[169].

Vγ9Vδ2$^+$ T cells can be specifically and potently activated by PAgs like (E)-4-hydroxy-3-methyl-but-2-enyl pyrophosphate, an intermediate of the 2-C-methyl-D-erythritol 4-phosphate pathway employed by eubacteria and apicomplexan protozoa but not by eukaryotes[35,243,254,255]. This likely underlies the striking expansions of Vγ9Vδ2$^+$ T cells in individuals infected with *M. tuberculosis*[220,256] or *P. falciparum*[257]. Besides pAgs, several other molecules of microbial origin have been proposed as γδ T cell antigens accounting for the specific recognition of infected cells. These candidates include the bacterial superantigens SEA (and to a lesser extent SEE)[258]; OXYS and DXS2, two mycobacterial proteins found to activate γδ T cells from BCG-infected human subjects but not from healthy donors[259,260]; and HSV-1 glycoprotein I, specifically recognized by a Vγ1.2Vδ8$^+$ TCR independently from antigen processing and MHC presentation[261].

Subsequent reports demonstrated that γδ T cells also recognize stress antigens of cellular origin, either in antibody-like or antigen-presentation-like fashion. γδ T cells can indeed directly recognize stress proteins like hMSH2, a nuclear protein ectopically expressed on the cell surface of different epithelial tumour cells and induced by EBV transformation[210,262]; and Annexin A2 whose expression was induced by CMV infection and recognized specifically by a Vγ8Vδ3$^+$ T cell clone[199]. On the other hand, γδ T cells can recognize nonpolymorphic MHC-like (class Ib) proteins presenting lipids, such as CD1 proteins, in a similar way to other unconventional T cells like NKT or MAIT cells[263–265]. In particular, a subpopulation of Vδ1$^+$ T cells has been clearly shown to bind CD1d loaded with the self-lipid sulfatide[265] but any concrete link to the recognition of infected (or transformed) cells remains to be established. Of note, another CD1-like protein, EPCR, was shown to bind directly (independently of lipid cargo) the TCR of a Vγ4Vδ5$^+$ T cell clone (expanded from a CMV$^+$ individual), thus allowing it to recognize endothelial cells infected with CMV[198].

γδ T cells can seemingly also recognize transformed cells through proteins that are expressed at the cell surface in a stress-induced manner. Some examples are typically endogenous proteins, such heat shock protein 60[193–196] or FI-ATPase[197], that can be ectopically expressed on the cell membrane upon

transformation and recognized by Vγ9Vδ2^{+} TCRs to promote tumour cell lysis. More recently, endothelial protein C receptor (EPCR), which acts on the coagulation cascade, was shown to be exposed on the cell surface during transformation and recognized by a Vδ2^{-} (Vγ4Vδ5) TCR[198]. Similarly, Annexin A2, expressed on tumour cells in response to increasing quantities of reactive oxygen species, engaged directly with a Vγ8Vδ3 TCR[199]. The identification of these rather different ligands highlights the complexity of tumour cell recognition *via* γδ TCRs (Figure 1.9).

Building on the previous chapters and the major focus of thesis on the by Vδ1^{+} subset of human by γδ T cells, the aim of the study described in this chapter was to identify new tumour ligands for Vδ1^{+} TCRs. We chose AML target cells to converge with our interest in providing a new Vδ1^{+} T-cell (DOT)-based therapeutic option for AML treatment (see Results 4.2).

4.3.2 Donor selection and DOT cell generation

In our attempt to discover new ligands for Vδ1⁺ T cells, we started by identifying good donors for Vδ1⁺ T cells according to the absolute number and relative frequencies of this cell subset among circulating CD3⁺ cells (Table 4.2). We processed the blood samples by density gradient centrifugation; a fraction of PBMCs was then counted and stained. After the analysis, we initially selected HD#1, HD#2, HD#3 and HD#5 for Vδ1⁺ T cell expansion using our patented DOT protocol. However, HD#5 was substituted by HD#4 at a later time as it was not possible to obtain a reproducible DOT cell expansion from HD#5 blood sample.

Table 4.2 CD3⁺, Vδ1⁺ and Vδ2⁺ frequencies and counts.

Donor	*CD3⁺*	*Vδ1⁺ subset Freq in CD3*	*Vδ2⁺ subset Freq in CD3*	*Counts (*10⁶)*	*Vδ1⁺ (*10⁶)*
#1	66.3	0.43	3.74	100	0.43
#2	57.6	3.36	1.61	34.44	0.664692
#3	64.8	0.83	4.51	34.32	0.185328
#4	57.5	0.55	3.12	23.8	0.07616
#5	57.4	1.42	2.04	18.2	0.14924
#6	68.8	0.65	1.43	19.4	0.0873
#7	62.3	0.44	14.3	13.1	0.03537
#8	56.3	0.2	2.91	24.2	0.02662
#9	70.6	0.2	1.05	27.3	0.03822

We next cultured αβ depleted cell for 21 days as previously described (Materials and methods 3.3), collecting an aliquot of cell suspension at day 11, day 16 and day 21, in order to evaluate cell expansion (Figure 4.20) and to perform phenotypic analysis of the cultures over time (Figure 4.21). Total cells in culture increased from a starting value approximately included between 10-30*10⁶ cells to a final cell number of 150-200*10⁶, with the exception of HD#1 that showed the highest number of cells at day 21 (Figure 4.21, left). More in details, among these growing cell populations, Vδ1⁺ cells were increasing in number, as highlighted by their fold increase (Vδ1⁺ cells count at given time point/ Vδ1⁺ cell counts at day 0; Figure 4.20, right). The phenotypic analysis of cultured cells over time revealed that 90-95% of the cells in culture after 11 days was constituted by CD3⁺ cells (Figure 4.21A). Of these, approximately 70% to 98% (accordingly to the donor) were γδ⁺ T cells (Figure 4.21B) composed by 65% to 75% of Vδ1⁺ cells (Figure 4.21C). Of note, at the end of expansion, DOT cells were highly positive for NKG2D, had a low to mild expression of NKp30 and very low or absent NKp44 expression (Figure 4.21D).

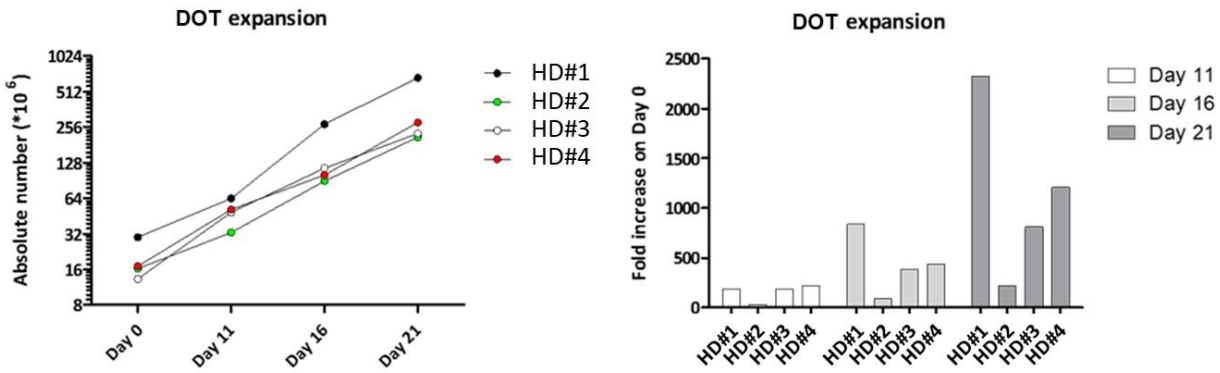

Figure 4.20 DOT cell expansions and Vδ1⁺ cell fold increase. αβ depleted cells were cultured for 21 days, collecting an aliquot of cell suspension at day 11, day 16 and day 21. Total cell counts are displayed on the left and Vδ1⁺ fold increase on the right (Vδ1⁺ cells count at given time point/ Vδ1⁺ cell counts at day 0)

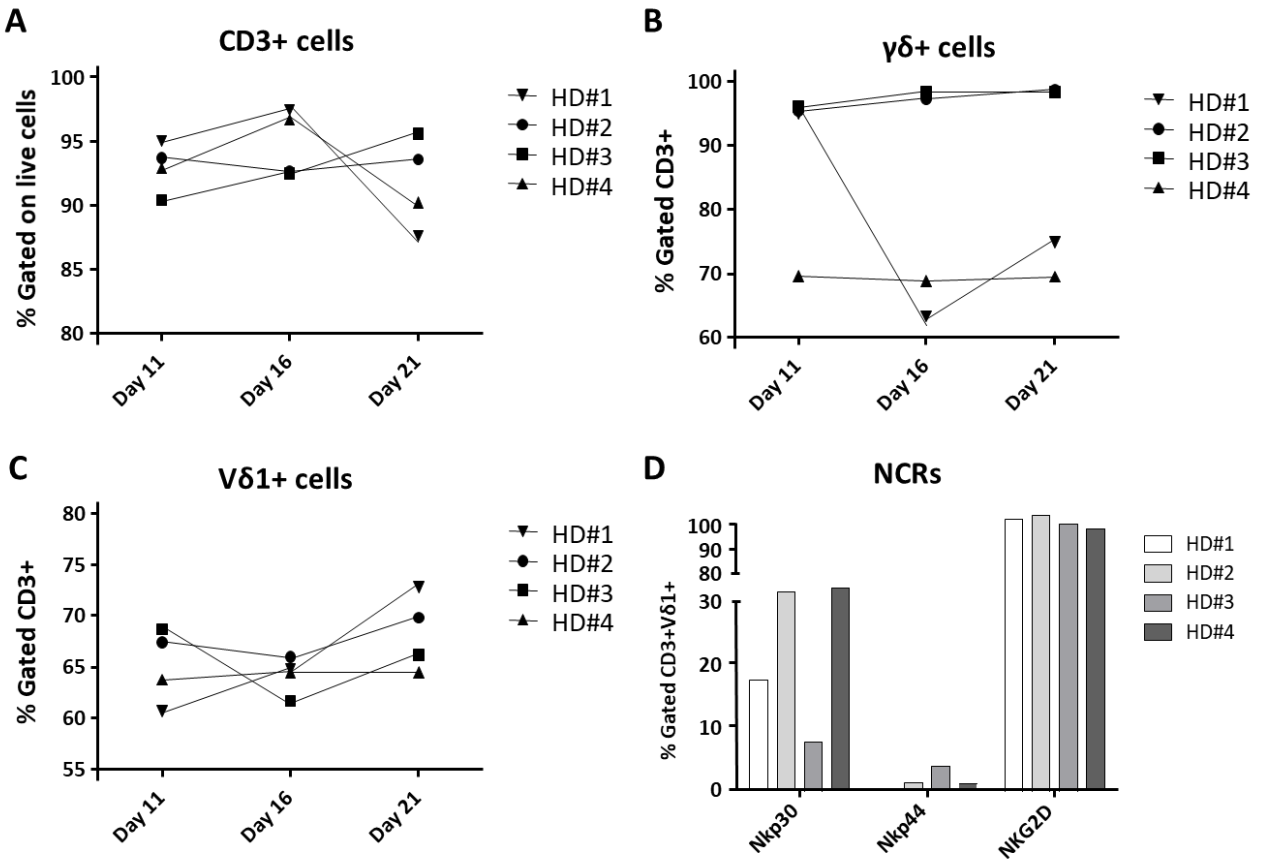

Figure 4.21 Phenotypic analyses of DOT cell cultures over time. (A) 90-95% of cells in culture after 11 days was constituted by CD3⁺ cells. Of these, approximately 70% to 98% were γδ⁺ T cells (B), composed by 65% to 75% of Vδ1⁺ cells (C). (D) Of note, at the end of expansion, DOT cells were highly positive for NKG2D, had a low to mild expression of NKp30 and very low or absent NKp44 expression.

At the end of expansion, DOT cells from multiple donors (HD#1-4) were tested against various AML cell lines (Table 3.3) to evaluate DOT tumour cell killing capacity. We co-incubated DOT cells at 10:1 (E:T) ratio for three hours with several target cell lines and we next measured the percentage of Annexin V⁺ target cells after co-incubation (Figure 4.22).

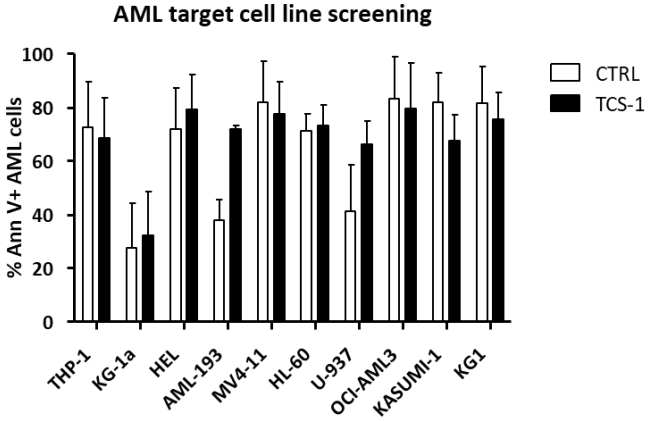

Figure 4.22 DOT cells target multiple AML cell types. In vitro killing assays with DOT cells produced from 4 healthy donors, co-incubated for 3 hours at 10:1 (E:T) ratio with the indicated AML cell lines in the presence of Ig control or anti-Vδ1 (TCS-1) antibody. Experiments were performed with technical triplicates

4.3.3 TCR repertoire analyses of *ex vivo* PB and DOT samples

After generating DOT cells from donors #1-4, we analysed DOT cell TCR repertoires and compared the results with the respective repertoires at the beginning of the expansion (*ex vivo*). DOT cell polyclonality and the relative contribution of the top 20 expanded clones to the overall Vδ1$^+$ TCR repertoire were described in Figure 4.4 and Figure 4.5 respectively. Additionally, DOT cell diversification was demonstrated also by the increased DOT cell intrasample variety in both γ and δ chains assessed in terms of Shannon-Weaver diversity index (Table 4.3).

Table 4.3 PB and DOT Shannon-Weaver diversity index. The index, indicator for intrasample diversity, was at least doubled in DOT samples compared to the respective ex vivo PB samples. Additionally, δ chains showed a higher intrasample variability than γ chains.

Shannon-Weaver diversity index		Peripheral blood	DOT
Gamma chain	HD#1	3.018141	6.961294
	HD#2	3.84359	7.207013
	HD#3	2.86877	7.487087
	HD#4	4.480681	8.286124
Delta chain	HD#1	3.890377	8.491646
	HD#2	3.724056	7.526714
	HD#3	3.207685	7.66618
	HD#4	6.381638	8.776023

We next analysed DOT TRG repertoires focusing on their clonotype composition; the number of detectable γ chain clonotypes in DOT samples (represented by coloured histogram bars) drastically increased when compared to the clonotype counts before expansion – grey bars (Figure 4.23), going from as few as some tens to several hundred in the case of HD#3 and HD#4.

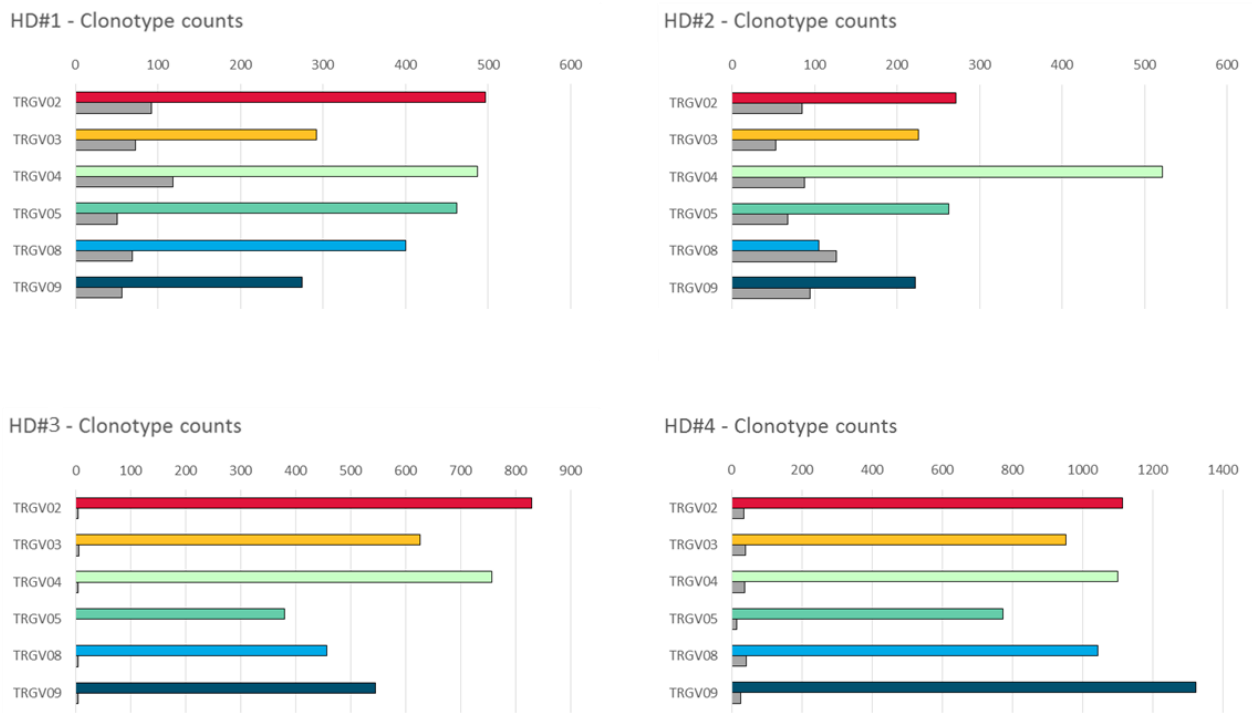

Figure 4.23 Clonotype count analyses. Detectable γ chain clonotypes in DOT samples are represented with coloured histogram bars. Clonotype counts of the ex vivo samples from all donors are showed in grey.

We next asked if the experimental procedure was somehow favouring the selection of specific clonotypes from the PB samples. We chose the clonotypes that were shared among DOT and PB samples of the same donor (Table 4.4) and measured their fold increase. This was estimated correlating the ratio of a clonotype relative abundance in the DOT repertoire over its abundance in the *ex vivo* repertoire sample with its ranking (by frequency) in DOT (Figure 4.24A and C) or PB repertoire samples (Figure 4.24B and D). We failed to reveal any trend between the relative increase of each shared clonotype with the initial (PB) or final (DOT) frequencies in the repertoire. Additionally, since the ID rank is a measure of clonotype abundance, we correlated the ID rank of a clonotype in the PB with the respective ID after expansion, observing that this measurement in the PB sample was not predictive of high clonotype frequency in the DOT-cell repertoire (Figure 4.25A-D).

Table 4.4 Clonotypes shared in the donor repertoires before (PB) and after (DOT) expansion

Gamma	***PB***	***DOT***	***Common***	***Delta***	***PB***	***DOT***	***Common***
HD#1	488	2706	57	***HD#1***	775	7376	11
HD#2	561	1734	63	***HD#2***	602	4791	20
HD#3	29	3844	4	***HD#3***	50	4591	0
HD#4	222	6868	28	***HD#4***	807	9592	7

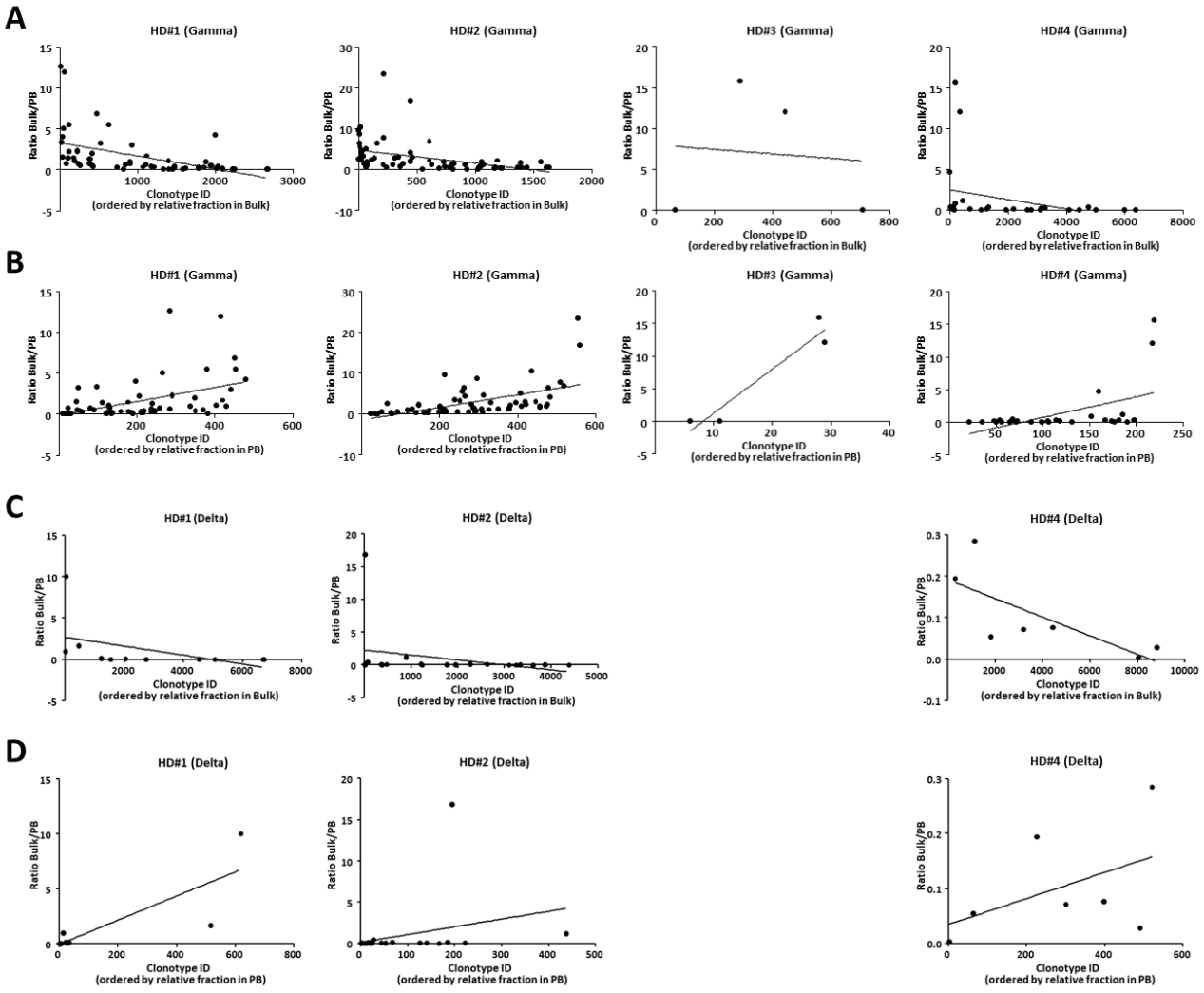

Figure 4.24 Correlation of clonotype frequencies before (PB) and after (DOT) cell expansion. The graphs show the correlation between the ratio of a clonotype relative abundance in the DOT-cell repertoire over its abundance in the ex vivo repertoire sample with its ranking (by frequency) in DOT (A and C) or PB repertoire samples (B and D). No trend for the relative increase of each shared clonotype with the initial (PB) or final (DOT) frequencies in the repertoire emerged.

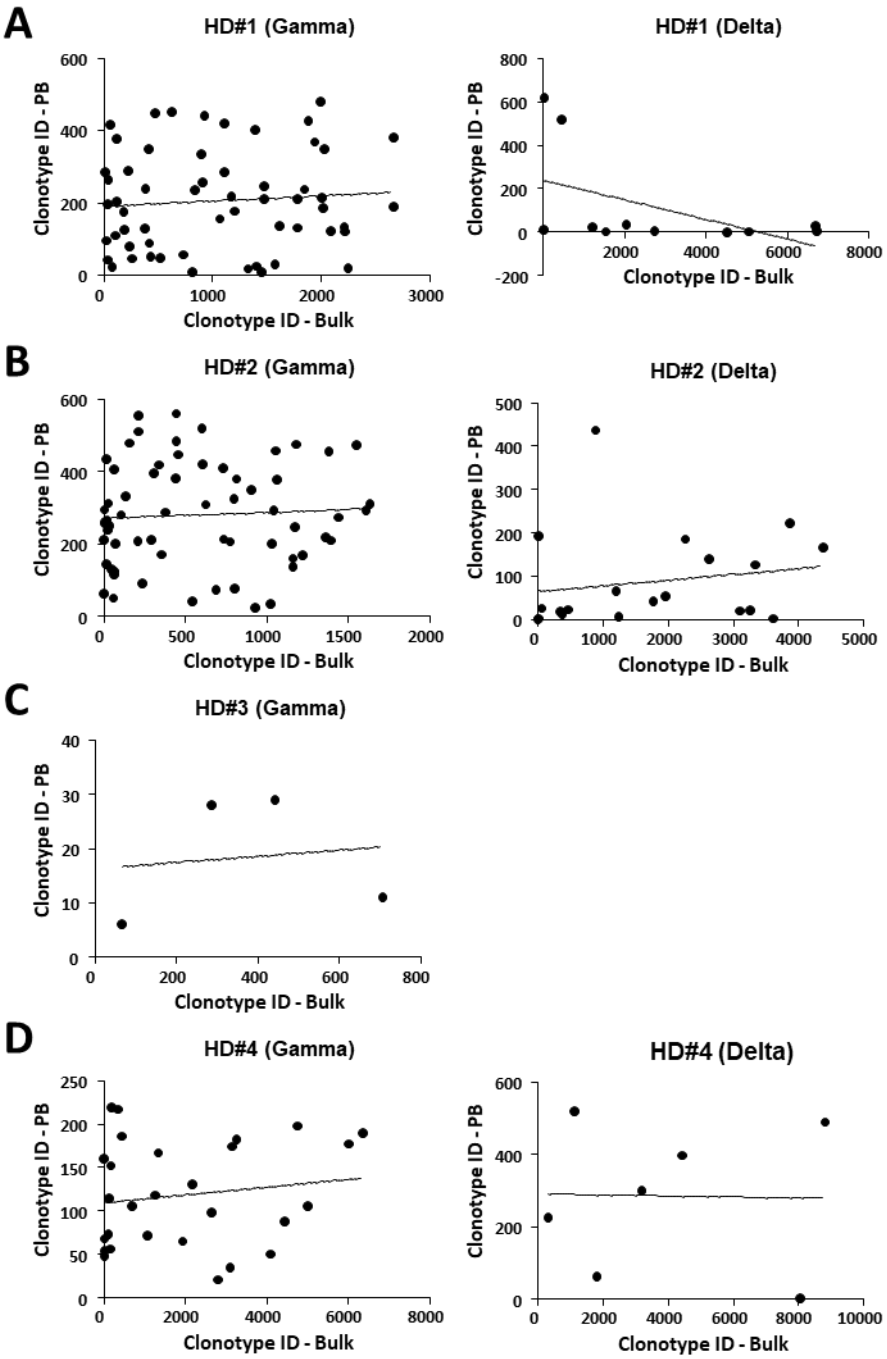

Figure 4.25 ID rank correlation before and after DOT-cell expansion. Correlation of the ID rank of a clonotype in the PB with the respective ID after DOT-cell expansion.

4.3.4 Generation and characterization of Vδ1⁺ T-cell clones

To isolate single TCRs and proceed with ligand identification, we generated clones of Vδ1⁺ T cells, using an adapted DOT cell protocol that included the addition of feeder cells to support the expansion (Methods 3.3.2). To obtain Vδ1⁺ T cell clones, we tested two different approaches: a limiting dilution method, that resulted in a dilution of approximately 1:1.22 to 2.44 to generate a Vδ1⁺ T cell clone; and single cell seeding approach. For this second method, $CD3^+$ $TCRV\delta1^+$ $TCRV\delta2^-$ single cells were FACS-sorted into 96

wells/plates; and cultured for 21 days using the DOT cell protocol in the presence of (weekly-renewed) 10^4 irradiated autologous PBMCs (feeders). The efficiency of cloning was between 21% and 28% (Figure 4.26A), with average doubling times of 1.43, 1.62, 1.79 and 1.52 (Figure 4.26B). Absolute DOT cell numbers in established clones (represented by individual dots) were also estimated (Figure 4.26C and Table 6.4).

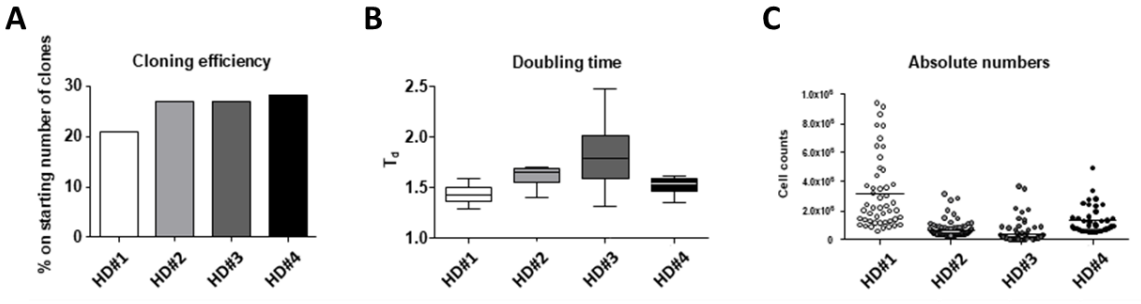

Figure 4.26 Vδ1⁺ T cells clone generation. (A) Cloning efficiency, (B) average doubling time and (C) absolute DOT cell numbers in established clones (represented by individual dots).

We next checked for $CD3^+$ and $V\delta1^+$ percentages in each clone to avoid any possible contamination from other cell sources (*i.e.* FACS impurity or feeder layer), alongside with Vγ9 (Table 4.5), NKp30 and NKp44 expression (Figure 4.27). We also tested clone cytotoxicity against the AML KG-1 cell line and evaluated the potential dependence on a TCR-mediated mechanism by blocking the TCRδ chain with the TCS-1 monoclonal antibody (clone TCS-1); cells were co-incubated for three hours at 5:1 (E:T) ratio and then analysed by Annexin V staining (percentage of positive events among pre-labelled KG-1 cells) in the presence of IgG control or α-$V\delta1^+$ antibodies. We extracted RNA from the clones and sent cDNA samples for Sanger sequencing to our collaborators in David Vermijlen's laboratory (Brussels, Belgium). Table 6.4 summarises information about counts, amount of RNA and relative amount of RNA/cell, Vγ9 expression, killing of the target cell line (percentage of Annexin V^+ KG-1 cells after co-incubation) and decrease in killing after Vδ1 blockade.

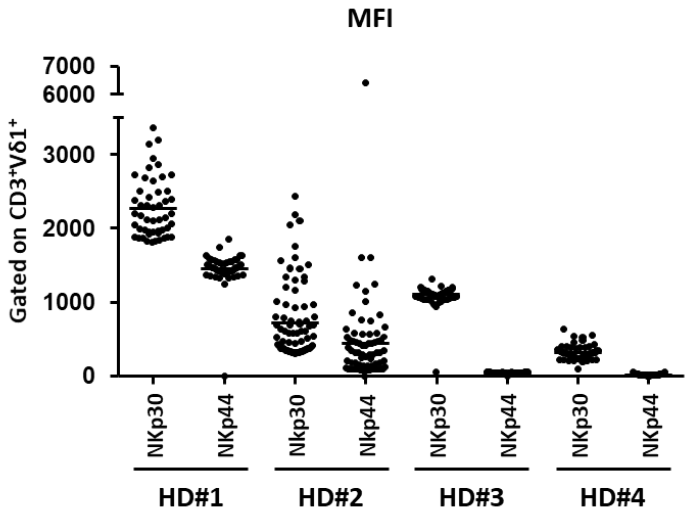

Figure 4.27 NKp30 and NKp44 MFI in the generated clones Each dot represents an individual clone (HD #1-4, healthy donors 1 to 4)

Table 4.5 Summary of clone analysis. Counts, amount of RNA and relative amount of RNA/cell, Vγ9 expression, killing of the target cell line (percentage of Annexin V⁺ KG-1 cells after co-incubation) and decrease in killing after Vδ1 blockade of each clone.

HD#1	Counts (*10⁶)	Rna (ng)	µg/cell number	Vγ9	Killing (%)	Killing reduction (%)
3	1.083	730.8	0.674792244	na	73.5	17.42
4	0.291	219.8	0.75532646	na	60.3	5.47
5	0.558	436.8	0.782795699	na	56.6	19.53
6	0.711	357	0.502109705	na	53.8	64.68
11	0.81	1100.4	1.358518519	na	75.5	3.38
12	1.179	693	0.58778626	na	40.85	67.04
13	0.987	1149.4	1.164539007	na	76.55	15.15
17	0.111	72.8	0.655855856	na	61.3	57.26
18	0.801	753.2	0.940324594	na	49.9	34.47
26	0.381	316.4	0.830446194	na	52.9	19.09
28	0.279	135.8	0.486738351	na	71.1	12.24
29	0.144	198.8	1.380555556	na	65	38.15
30	0.18	135.8	0.754444444	na	46.85	16.18
31	0.132	56	0.424242424	na	69.95	15.08
34	0.183	172.2	0.940983607	na	74.15	6.54
35	0.174	86.8	0.498850575	na	19.1	24.61
36	0.204	105	0.514705882	na	48.5	35.46
37	0.618	516.6	0.83592233	na	54.1	46.39
39	0.147	82.6	0.561904762	na	45.15	28.02
42	0.192	141.4	0.736458333	na	50	14.9
48	0.453	326.2	0.7200883	na	57.45	-11.75
49	0.246	116.2	0.472357724	na	78.9	20.41
63	0.162	142.8	0.881481481	na	60.5	39.01

HD#2	Counts (*10^6)	RNA (ng)	ug/cell number	Vγ9	Killing (%)	Killing reduction (%)
11	0.11760929	na	na	+	46.30	36.18
14	0.139321045	na	na	+	21.40	24.18
17	0.220650579	270	1.22	-	82.90	0.66
18	0.35708714	na	na	+	24.90	-104.02
20	0.110717391	na	na	+	21.50	-129.53
31	0.18295283	256	1.40	-	84.05	2.44
32	0.190964115	89.8	0.47	+	44.80	-101.23
37	0.09358933	174.4	1.86	-	83.85	11.39
48	0.08861165	53.6	0.60	-	86.55	-1.62
49	0.106937975	142.4	1.33	-	79.85	8.89
53	0.104817647	na	na	+	21.45	-24.94
62	0.117906826	na	na	+	75.90	-13.57
64	0.142833333	na	na	+	21.70	-61.98
74	0.10369479	na	na	+	23.30	-46.57
81	0.080387511	na	na	-	70.00	5.64
91	0.395836283	334	0.84	-	81.85	-0.37
100	0.131037998	na	na	+	23.40	4.70
102	0.092798507	na	na	-	87.10	-3.73
105	0.108090206	na	na	+	17.95	-25.07

116	0.340205036	498	1.46	-	83.05	0.06

HD#3	*Counts (*10^6)*	*RNA (ng)*	*µg/cell number*	*Vγ9*	*Killing (%)*	*Killing reduction (%)*
10	0.311142633	57.2	0.18	+	34.50	13.33
17	0.536067	276	0.51	-	20.10	38.31
40	0.178407379	na	na	-	21.15	27.19
68	0.348763002	69.6	0.20	-	27.60	11.23
74	0.17063633	na	na	+	29.75	31.94
76	0.260866202	256	0.98	+	49.65	-6.85

HD#4	*Counts (*10^6)*	*RNA (ng)*	*ug/cell number*	*Vγ9*	*Killing (%)*	*Killing reduction (%)*
1	0.300586207	na	na	+	10.85	1.34
2	0.354	na	na	+	7.62	10.64
10	0.112694361	na	na	-	59.40	25.67
15	0.073943609	na	na	-	23.60	52.97
17	0.123	na	na	+	9.06	21.70
45	0.242	na	na	-	8.71	31.11
51	0.423	na	na	+	7.39	17.20
52	0.621554054	220.4	0.35	-	28.80	24.83
53	0.185626697	na	na	-	66.30	15.01
56	0.072	na	na	-	28.65	20.07
57	0.304	na	na	-	6.90	2.32
58	0.074427589	na	na	-	52.00	43.46
59	0.167	na	na	+	7.29	33.36
60	0.18856383	na	na	+	20.20	74.88
61	0.316957286	108.8	0.34	+	87.95	8.70
65	0.092357719	na	na	-	27.80	35.79
69	0.124	na	na	-	21.95	54.40
72	0.139	na	na	-	14.80	29.02
79	0.115	na	na	-	14.55	35.50
84	0.077	na	na	-	18.20	18.68
85	0.073933898	na	na	-	30.45	54.68
88	0.162845708	na	na	+	19.50	-140.00
92	0.349	231.2	0.66	-	52.80	11.08
99	0.1	na	na	-	8.77	16.83
100	0.094	na	na	-	64.35	3.03
102	0.121	na	na	+	7.27	23.33
103	0.199650754	na	na	+	46.80	-65.60
105	0.074396907	na	na	-	26.60	61.67
107	0.069642466	na	na	-	23.65	32.56
113	0.157	na	na	+	6.47	4.95
114	0.072	na	na	+	12.20	34.43

We further investigated if Vδ1⁺ clone growth ability (Figure 4.28A), NKp30 or NKp44 expression correlated with clone ability to kill the KG-1 cell line in the absence (left) or in the presence (middle) of the α-Vδ1⁺ TCS-1 antibody (Figure 4.28B-C). In the panels on the right, clone counts (A) or NKp30/NKp44 MFI data (B-C) are plotted with the percentage of killing decrease. None of the analysed parameters correlated with the induction of apoptosis in KG-1 AML cells.

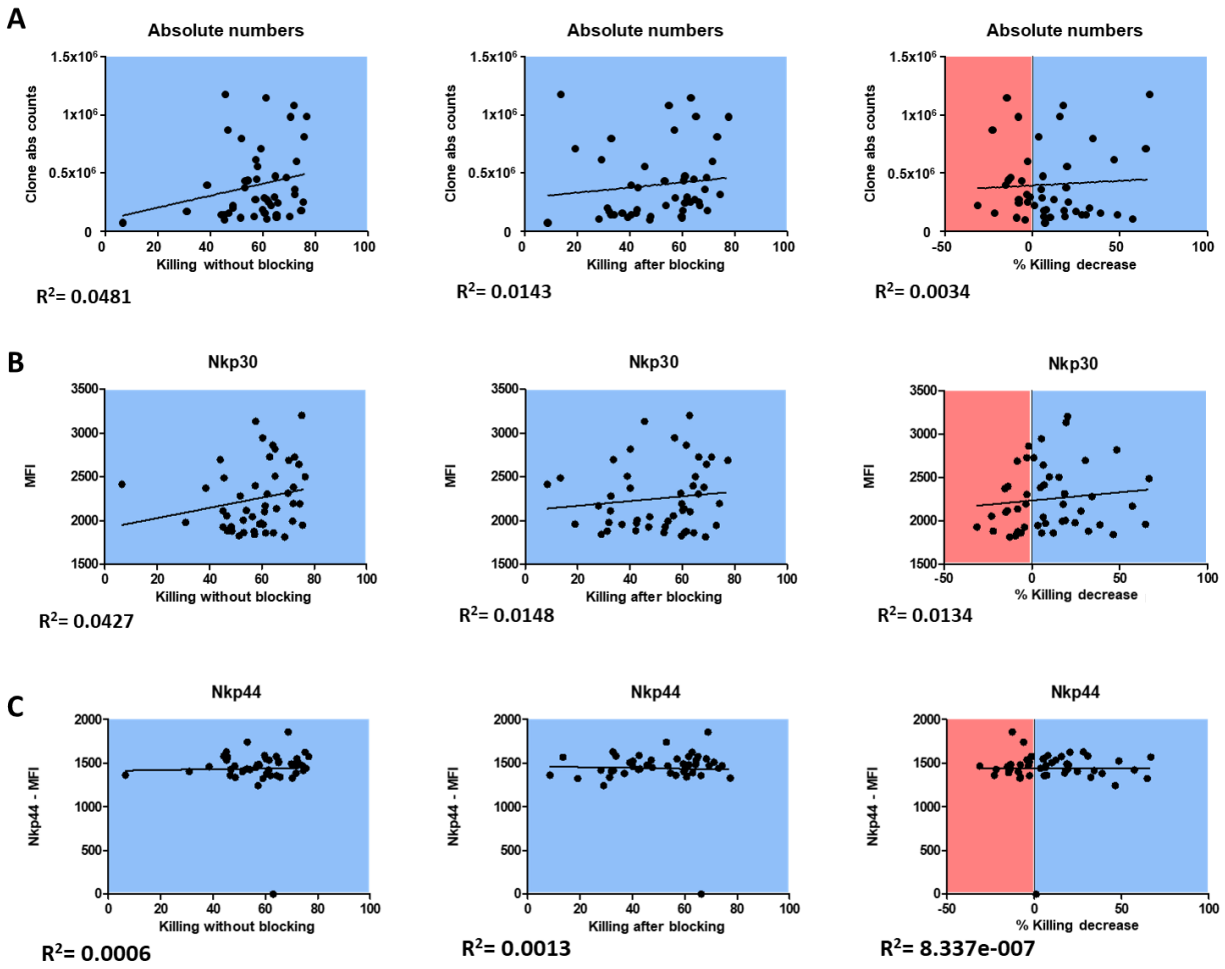

Figure 4.28 Clone counts and NKR expression correlation with killing capacity. Correlation of (A) Vδ1⁺ clone growth ability,(B) NKp30 or (C)Kp30 expression with clone ability to induce apoptosis in the KG-1 cell line in the absence (left) or in the presence (middle) of the α-Vδ1⁺ TCS-1 antibody. In the panels on the right, clone counts (A) or NKR expression data (B-C) are correlated with the percentage of killing decrease.

4.3.5 Analysis of clones: TCR sequences and selection for subsequent studies

We assigned each clone an identifier (ID) composed by a first digit, representative for the donor of origin, followed by a two- or three-digit number.

After the phenotypic and functional characterization, we analysed the clones by Sanger sequencing focusing on the CDR3 region of both γ and δ chains. Once retrieved the results, we looked for sequence counts and frequency in the samples before (*ex vivo*) and after (DOT) expansion within the donor from which they have been isolated and, additionally, from the other donors. Table 4.6 and Table 4.7 contain the nucleotide and aminoacidic junctional region sequences, γ and δ chains absolute counts and relative frequency, respectively. Several clone-derived γ chains were shared among different donors either as

nucleotide clonotype, meaning bearing the same nucleotide sequence, or at the aminoacidic level. Additionally, Table 4.8 includes the available information about aminoacidic clonotypes (same aminoacidic but different nucleotide sequences) of the clones described in Table 4.6. Finally, we aligned the junctional regions of γ chains to genomes of reference available on IMGT to retrieve information about γ chain usage (Table 4.9).

Combining the sequencing information with the data from the HTS analyses of *ex vivo* and DOT samples, we selected eight clones in order to proceed with the molecular cloning of their TCR into the JRT3.3 cell line used as reporter. We selected clones 1.06, 1.11, 1.36, 1.37, 2.11, 2.18, 3.17 and 3.74 accordingly to their dependence on a TCR-mediated mechanism to induce apoptosis in the target KG-1 cell line, to the presence of their γ and δ chains in the *ex vivo* and DOT repertoires of the donor of origin and to their presence in other donor samples (Table 4.10). Additionally, clone 3.74 γ chain is an aminoacidic clonotype of clones 1.06 and 1.36.

In more detail, the γ chain derived from clone 1.11 and 1.37 accounted for 35.08% of HD#1 *ex vivo* repertoire. Although these two clones bore the same γ chain clonotype, they expressed two different δ chains: contrarily to 1.11 δ chain that was not detected in either PB or DOT repertoires, 1.37 δ chain accounted for 11.85% of HD#1 TRD repertoire and was found in the DOT repertoire of the same donor. Moreover, blocking 1.37 δ chain with an α-Vδ1 antibody (TCS1) reduced the clone ability of inducing apoptosis in the KG-1 target cells of 46.39% (Table 6.4), but had almost no effect on clone 1.11 (3.38% reduction). Clone 2.11 γ chain was present in low frequency in the *ex vivo* repertoire of the same donor and in the DOT repertoire of HD#1 (0.28% and 0.047% respectively). Clone 3.74 γ chain was highly conserved among *ex vivo* and DOT repertoires of all donors with the exception of DOT sample generated from HD#3. γ chains derived from clones 1.06 and 1.36 were shared among DOT repertoires of HD#2-4. Clone 3.17 γ chain was found as aminoacidic clonotype in the *ex vivo* repertoire of HD#1 and was detected in all the DOT repertoires. Finally, the δ chain derived from clone 2.18 constituted the 37.84% of HD#2 *ex vivo* repertoire, 4.16% of HD#2 DOT repertoire and was found in HD#1 DOT repertoire (0.014%).

Table 4.6 Analysis of clone-derived TCRγ chains. The table displays the CDR3 regions at nucleotide and aminoacidic level, chain absolute counts and relative frequency among all donors (= only one sequenced chain; ** = no sequencing results; *** = aa clonotype)*

Clone ID	nt junction sequence	aa junction sequence	Clonotype counts in PB	Clonotype fraction in PB	% clonotype in PB	Shared in PB samples	Clonotype fraction	% clonotype	Clonotype counts in DOT	Clonotype fraction	% clonotype in DOT	Shared in DOT samples	Clonotype fraction	% clonotype
1.03	tgtgcacctggttcaagaaactyttt	CATWFKKLF												
1.04	tgtgcacctggaggaggaccaaagtggctttt	CATWDGTKVVF												
1.05	tgtgcacctggaggaggccccggaattataagaaactcttt	CATWDGPNYYKKLF												
1.06	tgtgccttgtggaggtgtggtattataagaaactcttt	CALWEVRYYKKLF				HD#3***	2,58E-05	2,58E-03				HD#2***	4,97E-04	0,049745619
												HD#2***	9,04E-05	0,009044658
												HD#3***	5,37E-04	0,053735311
												HD#3***	1,70E-04	0,016969046
												HD#3	5,66E-05	0,005656349
												HD#3***	5,66E-05	0,005656349
												HD#4***	9,40E-04	0,094038786
												HD#4***	7,14E-04	0,071393745
												HD#4	2,05E-04	0,02089573
												HD#4***	1,92E-04	0,019154419
												HD#4***	6,97E-05	0,006965243
1.11	tgtgccttgtggaggttaccaggaaaactcttt	CALWEVTRKLF	17532	0,350822428	35,08224277							HD#2	2,71E-04	2,71E-02
1.12	tgtgcacctggaggaggcaggcggagaataagaagaactcttt	CATWDRPENKKLF												
1.13	tgtgccttgtggaggtgcggtattataagaaactcttt	CALWEVRYYKKLF	*refer to clone 1.06*						*refer to clone 1.06*					
1.17*														
1.18*														
1.26	tgtgcacctggaggtgcacaatttatataagaaactcttt	CATWDAQFYKKLF												
1.28**														
1.29*														
1.30	tgtgcacctggaggaggacagttatataagaaactcttt	CATWDDSYYKKLF												
1.31	tgtgcacctggaggaggcctgaggttgaggaaactcttt	CATWDRPGFEKLF												
1.34	tgtgcacctggaggaggcctataagaaactcttt	CATWDGPYKKLF	14	2,80E-04	2,80E-02							HD#2***	0,00110797	0,11079706
												HD#2	2,26E-04	0,022611645
												HD#3	3,96E-04	0,03959444
												HD#3***	3,11E-04	0,031109917
												HD#3***	1,27E-04	0,012726784
												HD#3***	1,13E-04	0,011312697
												HD#3***	5,66E-05	0,005656349
												HD#4***	6,79E-04	0,067911123
												HD#4	4,01E-04	0,04005015
												HD#4***	2,26E-04	0,022637041
												HD#4***	1,92E-04	0,019154419
												HD#4***	1,22E-04	0,012189176
												HD#4***	8,71E-05	0,008706554
1.35	tgtgcacctggaggatggagattataagaaactcttt	CATWDGNYKKLF										HD#2***	0,00115319	0,115319389
												HD#2	2,04E-04	0,02035048
												HD#3***	1,56E-04	0,015554958
												HD#3***	1,27E-04	0,012726784
												HD#3***	1,27E-04	0,012726784
												HD#3***	1,13E-04	0,011312697
												HD#4***	5,05E-04	0,050498015
												HD#4***	1,04E-04	0,010447865
												HD#4***	1,04E-04	0,010447865
												HD#4***	1,74E-05	0,001741311

Clone ID	nt junction sequence	aa junction sequence	Clonotype counts in PB	Clonotype fraction in PB	% clonotype in PB	Shared in PB samples	Clonotype fraction	% clonotype	Clonotype counts in DOT	Clonotype fraction	% clonotype in DOT	Shared in DOT samples	Clonotype fraction	% clonotype
1.36	tgtgccttgtgggaggtgcggtattataagaaactcttt	CALWEVRYYKKLF	*refer to clone 1.06*						*refer to clone 1.06*					
1.37	tgtgccttgtgggaggttaccaggaaactcttt	CALWEVTRKLF	*refer to clone 1.11*						*refer to clone 1.11*					
1.39	tgtgccacctgggccgggaataagaaactcttt	CATWAGNKKLF												
1.42*														
1.48	tgtgccacctgggacaggccgcggtattataagaaactcttt	CATWDRPRYYKKLF										HD#2***	4,75E-04	4,75E-02
												HD#2***	2,26E-04	2,26E-02
												HD#2***	1,58E-04	1,58E-02
												HD#2***	6,78E-05	6,78E-03
												HD#3***	1,27E-04	1,27E-02
												HD#3***	8,48E-05	8,48E-03
												HD#4***	1,04E-04	1,04E-02
												HD#4	6,97E-05	6,97E-03
												HD#4***	5,22E-05	5,22E-03
												HD#4***	3,48E-05	3,48E-03
1.49	tgtgccacctgggacaggccgcggtattataagaaactcttt	CATWDRPRYYKKLF	*refer to clone 1.48*						*refer to clone 1.48*					
1.63	tgtgccttgtgggaggaggggtataagaaactcttt	CALWEEGYKKLF												
2.11	tgtgccacctgggataggaggaggcattcgaattattataagaaactcttt	CATWDRRRHSNYYKKLF	131	0,002808447	0,280844678							HD#1	4,70E-04	4,70E-02
2.14**														
2.17	tgtgccacgtgggacgggcttttgaaggtattt	CATWDGLLKVF												
2.18	tgtgccacctggattaccgggcgtagtagtgattggatcaagacgttt	CATWITGRSSDWIKTF	11003	0,235888091	23,58880909							HD#1	0,04486519	4,486518744
												HD#3	7,07E-05	0,007070436
2.20**														
2.31	tgtgccacctggattaccgggcgtagtagtgattggatcaagacgttt	CATWITGRSSDWIKTF	*refer to clone 2.18*						*refer to clone 2.18*					
2.32**														
2.37	tgtgccacctgggataggaggaggcattcgaattattataagaaactcttt	CATWDRRRHSNYYKKLF	*refer to clone 2.11*						*refer to clone 2.11*					
2.48	tgtgccacctgggacaggccagagaaactcttt	CATWDRPEKLF	118	0,002529746	0,252974595	HD#1***	6,40E-04	6,40E-02	7	1,58E-04	1,58E-02	HD#1	7,60E-04	7,60E-02
												HD#1***	3,80E-04	3,80E-02
												HD#1***	1,27E-04	1,27E-02
												HD#3***	5,94E-04	5,94E-02
												HD#4***	1,22E-04	1,22E-02
												HD#4***	1,22E-04	1,22E-02
2.49	tgtgccacgtgggacgggcttttgaaggtattt	CATWDGLLKVF												
2.53*														
2.62**														
2.64**														
2.74**														
2.81	tgtgccacctgggataggaggaggcattcgaattattataagaaactcttt	CATWDRRRHSNYYKKLF	*refer to clone 2.11*						*refer to clone 2.11*					
2.91	tgtgccacctggattaccgggcgtagtagtgattggatcaagacgttt	CATWITGRSSDWIKTF	*refer to clone 2.18*						*refer to clone 2.18*					
2.100**														
2.102	tgtgccacctggattaccgggcgtagtagtgattggatcaagacgttt	CATWITGRSSDWIKTF	*refer to clone 2.18*						*refer to clone 2.18*					
2.105**														
2.116*														

Clone ID	nt junction sequence	aa junction sequence	Clonotype counts in PB	Clonotype fraction in PB	% clonotype in PB	Shared in PB samples	Clonotype fraction	% clonotype	Clonotype counts in DOT	Clonotype fraction	% clonotype in DOT	Shared in DOT samples	Clonotype fraction	% clonotype
3.10	tgtgccttgtgggaggtgaggggactgactagtgagaaactcttt	CALWEVRGLTSEKLF												
3.17	tgtgccacctgggataggcgttattataagaaactcttt	CATWDRRYYKKLF				HD#1***	5,00E-04	5,00E-02	8	1,13E-04	1,13E-02	HD#1***	7,78E-04	7,78E-02
												HD#1***	6,33E-04	6,33E-02
												HD#1	2,17E-04	2,17E-02
												HD#2***	3,39E-04	3,39E-02
												HD#2***	2,26E-04	2,26E-02
												HD#2	1,58E-04	1,58E-02
												HD#2***	6,78E-05	6,78E-03
												HD#4***	4,18E-04	4,18E-02
												HD#4***	2,44E-04	2,44E-02
												HD#4	1,57E-04	1,57E-02
												HD#4***	1,39E-04	1,39E-02
												HD#4***	1,04E-04	1,04E-02
												HD#4***	8,71E-05	8,71E-03
												HD#4***	5,22E-05	5,22E-03
3.40	tgtgccacctgggatgggcctaaatataagaaactcttt	CATWDGPKYKKLF										HD#1***	5,43E-04	5,43E-02
												HD#1***	2,17E-04	2,17E-02
												HD#2***	1,13E-04	1,13E-02
												HD#2***	6,78E-05	6,78E-03
3.68	tgtgccacctgggacttgtataagaaactcttt	CATWDLYKKLF				HD#1***	2,00E-04	2,00E-02				HD#2***	2,71E-04	2,71E-02
												HD#4***	1,74E-04	1,74E-02
												HD#4***	5,22E-05	5,22E-03
3.74	tgtgccttgtgggaggtgcgatattataagaaactcttt	CALWEVRYYKKLF				HD#1***	6,20E-04	6,20E-02				HD#1***	0,00117543	0,117542813
												HD#1	1,81E-04	0,01808351
												HD#1***	7,23E-05	0,007233404
												HD#1***	7,23E-05	0,007233404
												HD#2***	4,97E-04	0,049745619
												HD#2	9,04E-05	0,009044658
												HD#4***	9,40E-04	0,094030786
												HD#4	7,14E-04	0,071393745
												HD#4***	2,09E-04	0,02089573
												HD#4***	1,92E-04	0,019154419
												HD#4***	6,97E-05	0,006965243
3.76	tgtgccttgtgggggtgctggtcggtgggaaactcttt	CALWGVLVGGKLF												
4.01	tgtgccttgtgggaggtgaattattataagaaactcttt	CALWEVNYYKKLF				HD#3	2,58E-05	2,58E-03	73	0,001271157	0,127115693	HD#1	9,40E-04	9,40E-02
												HD#1***	4,70E-04	4,70E-02
												HD#2	6,56E-04	6,56E-02
												HD#2***	1,81E-04	1,81E-02
												HD#3	4,10E-04	4,10E-02
4.02**														
4.10	tgtgccacctgggtaaccccgaattattataagaaactcttt	CATWVTPNYYKKLF												
4.15	tgtgccacctgggacaggccgaggtattataagaaactcttt	CATWDRPRYYKKLF										HD#1***	2,35E-04	2,35E-02
												HD#1***	9,04E-05	9,04E-03
												HD#2	4,75E-04	4,75E-02
												HD#2***	2,26E-04	2,26E-02
												HD#2***	1,58E-04	1,58E-02
												HD#2***	6,78E-05	6,78E-03
												HD#3	1,27E-04	1,27E-02
												HD#3***	8,48E-05	8,48E-03

Clone ID	nt junction sequence	aa junction sequence	Clonotype counts in PB	Clonotype fraction in PB	% clonotype in PB	Shared in PB samples	Clonotype fraction	% clonotype	Clonotype counts in DOT	Clonotype fraction	% clonotype in DOT	Shared in DOT samples	Clonotype fraction	% clonotype
4.17**														
4.45**														
4.51**														
4.52*														
4.53*														
4.56*														
4.57**														
4.59*	tgtgccacctgggacaaaacggggtataagaaactcttt	CATWDKTGYKKLF												
4.58	tgtgccacctgggatggatatagtagtgattggatcaagacgttt	CATWDGYSSDWIKTF				HD#2***	6,43E-05	6,43E-03				HD#1***	6,87E-04	6,87E-02
												HD#1***	5,61E-04	5,61E-02
												HD#1***	5,06E-04	5,06E-02
												HD#2***	2,26E-04	2,26E-02
												HD#2***	1,58E-04	1,58E-02
												HD#3***	2,83E-04	2,83E-02
												HD#3***	2,55E-04	2,55E-02
												HD#3***	1,84E-04	1,84E-02
4.60	tgtgccacctgggataagaattwttataagaaactcttt	CATWDKNXYKKLF												
4.61	tgtgccttgtgggagccctattataagaaactcttt	CALWEPYYKKLF										HD#1***	0,00126585	0,126584568
												HD#1***	1,09E-04	1,09E-02
												HD#2	2,26E-05	2,26E-03
												HD#3	9,90E-05	9,90E-03
												HD#3***	8,48E-05	8,48E-03
												HD#3***	2,83E-05	2,83E-03
4.65*	tgtgccttgtgggaggccctgttgggcaaaaaaatcaaggtattt	CALWEALLGKKIKVF												
4.69	tgtgccacctgggatttttataagaaactcttt	CATWDFYKKLF				HD#1	8,00E-05	8,00E-03	7	1,22E-04	1,22E-02	HD#2	2,04E-04	2,04E-02
												HD#3***	2,69E-04	2,69E-02
4.72	tgtgccttgtgggagccctattataagaaactcttt	CALWEPYYKKLF												
4.79*	tgtgccacctgggataggaagcgccattattataagaaactcttt	CATWDRKRHYYKKLF												
4.84**														
4.85**														
4.88	tgtgccttgtgggaggtgcggctcccttattataagaaactcttt	CALWEVRLPYYKKLF												
4.92*														
4.99	tgtgccacctgggacaggcttctagggtattataagaaactcttt	CATWDRLLGYYKKLF												
4.100	tgtgccacctgggacgggcctatttataagaaactcttt	CATWDGPIYKKLF										HD#1***	3,44E-04	3,44E-02
4.102*														
4103	tgtgccttgtggccatggaattattataagaaactcttt	CALWPWNYYKKLF												
4105	tgtgccacctgggatgggccgggagggaaactcttt	CATWDGPGGKLF				HD#1***	4,60E-04	4,60E-02						
4.107*														
4.113**														
4.114	tgtgccacctgggtttattataagaaactcttt	CATWVYYKKLF				HD#1	2,80E-04	2,80E-02	21	3,66E-04	3,66E-02	HD#2	7,91E-04	7,91E-02
												HD#2***	4,52E-05	4,52E-03
												HD#3	3,39E-04	3,39E-02
												HD#3***	1,70E-04	1,70E-02

Table 4.7 Analysis of clone-derived TCRδ chains. The table displays the CDR3 regions at nucleotide and aminoacidic level, chain absolute counts and relative frequency among all donors (= only one sequenced chain; ** = no sequencing results; *** = aa clonotype).*

Clone ID	nt junction sequence	aa junction sequence	Clonotype counts in PB	Clonotype fraction in PB	% clonotype in PB	Shared in PB samples	Clonotype fraction	% clonotype	Clonotype counts in DOT	Clonotype fraction	% clonotype in DOT	Shared in DOT samples	Clonotype fraction	% clonotype
1.03	tgtgctcttggggaatacacttcgcacggccttcctacggctgggggtcacaatgctcgaagcaccgataaactcatcttt	CALGEYTSHGLPTAGGHNARSTDKLIF												
1.04	tgtgctcttggggaactgcctccccttggtaggtacaccgataaactcatcttt	CALGELPPLGRYTDKLIF												
1.05	tgtgctcttggggaactggccttgagttcccctctggggccgtacaccgataaactcatcttt	CALGELALSSPLGPYTDKLIF												
1.06	tgtgctcttggggggccttcctacgatcggtactgggggatacccgataaactcatcttt	CALGGPSYDRYWGIPDKLIF												
1.11	tgtgctcttggggagtctttgcgcgatactttttacaccgataaactcatcttt	CALGESLRDTFYTDKLIF												
1.12	tgtgctcttggggaactattgatccactcccacgaggaccgattgacagcacaactcttcttt	CALGELLIHSHEDRLTAQLFF												
1.13	tgtgctcttggggccatcctaggaggtggggtgggggaatcaagattcaccgataaactcatcttt	CALGAILGGGVGESRFTDKLIF												
1.17*	tgtgctcttggggaattggccccgaaggtatccactgggggatacggtctgaccgataaactcatcttt	CALGELAPKVSTGGYGLTDKLIF												
1.18*	tgtgctcttggggaactcatcccatcggggatacggcccgataaactcatcttt	CALGELIPSGIRPDKLIF												
1.26	tgtgctcttggggaacaaacaactgggggatacgttgtcaccgataaactcatcttt	CALGEQTTGGYVVTDKLIF												
1.28**														
1.29*	tgtgctcttggggaacgctcctctcttgttytggtgggggatacacggccccgggacgggggggactcgaccgataaactcatcttt	CALGERSSLVLVGDTRPRDGGDSTDKLIF												
1.30	tgtgctcttggggatctccatttggggggataagaacaccgataaactcatcttt	CALGDLHLGDKNTDKLIF												
1.31	tgtgctcttggggaggaaggccctttcctgcaggctggggggatcaccgataaactcatcttt	CALGEEGPFLQAGGITDKLIF												
1.34	tgtgctcttggggaacccgagggtacgaagtaccctacctttcctaccgtggaactcatcttt	CALGEPEGTKYPTFPTVELIF												
1.35	tgtgctcttggggaccctttttcctggtactggggggatacatgcctaccatcaccgataaactcatcttt	CALGDPFPGTGGYMPTITDKLIF												
1.36	tgtgctcttggggagaagaaaaggactgggggattactcatcttt	CALGEKKRTGGLLIF												
1.37	tgtgctcttggggacattccccgaaggtcgctacgaatcgggggagggaatttgtacaccgataaactcatcttt	CALGDIPRRSLRIGGGNLYTDKLIF	10290	0,118541559	11,85415587				10	1,75E-04	1,75E-02			
1.39	tgtgctcttggggaacggctgggggatacgcgcaccgataaactcatcttt	CALGERLGDTRTDKLIF												
1.42*	tgtgctcttgggaacggggggtctgggggattgcggtgcaccgataaactcatcttt	CALGNGGSGGLRCTDKLIF												
1.48	tgtgctcttggggaactagcgccaaccaagtactgggggataatgaccgataaactcatcttt	CALGELAPTKYWGIMTDKLIF												
1.49	tgtgctcttgggggagaggtcccggggggggaccgataaactcatcttt	CALGGEVPGGTDKLIF												
1.63	tgtgctcttggggaaaggaagagactcctcacggggatagggactacgtacaccgataaactcatcttt	CALGERKRLLTGIGTTYTDKLIF												
2.11	tgtgctcttggggaaacggatggggggatacaggcccgggattacaccgataaactcatcttt	CALGETDGGIQARDYTDKLIF	333	0,005693962	0,569396235				27	5,19E-04	5,19E-02			
2.14**														
2.17	tgtgctcttggggaactcctccctactcaacttcccttgtacgccgataaactcatcttt	CALGELLPTQLPLYADKLIF	1243	0,02125404	2,125403964	HD2	1,39E-05	1,39E-03						
2.18	tgtgctcttgaccaagggtccgggggatacctaaagagcaccgataaactcatcttt	CALDQGSGGYLKSTDKLIF	22133	0,378451858	37,84518578				2168	0,041662663	4,166266311	HD#1	1,40E-04	1,40E-02
2.20**														
2.31	tgtgctcttgaccaagggtccgggggatacctaaagagcaccgataaactcatcttt	CALDQGSGGYLKSTDKLIF	*refer to clone 2.18*						*refer to clone 2.18*					
2.32**														
2.37	tgtgctcttggggaaacggatggggggatacaggcccgggattacaccgataaactcatcttt	CALGETDGGIQARDYTDKLIF	*refer to clone 2.11*						*refer to clone 2.11*					
2.48	tgtgctcttggggaacgggcttcctcgtactgggggatagggatcaccgataaactcatcttt	CALGERASSYWGIGITDKLIF	92	0,001573107	0,157310671				6	1,15E-04	1,15E-02			
2.49	tgtgctcttggggaactcctccctactcaacttcccttgtacgccgataaactcatcttt	CALGELLPTQLPLYADKLIF	*refer to clone 2.17*						*refer to clone 2.17*					
2.53*	tgtgctcttgaccaagggtccgggggatacctaaagagcaccgataaactcatcttt	CALDQGSGGYLKSTDKLIF	*refer to clone 2.18*						*refer to clone 2.18*					
2.62**														
2.64**														
2.74**														
2.81	tgtgctcttggggaaacggatggggggatacaggcccgggattacaccgataaactcatcttt	CALGETDGGIQARDYTDKLIF	*refer to clone 2.11*						*refer to clone 2.11*					
2.91	tgtgctcttgaccaagggtccgggggatacctaaagagcaccgataaactcatcttt	CALDQGSGGYLKSTDKLIF	*refer to clone 2.18*						*refer to clone 2.18*					
2.100**														
2102	tgtgctcttgaccaagggtccgggggatacctaaagagcaccgataaactcatcttt	CALDQGSGGYLKSTDKLIF	*refer to clone 2.18*						*refer to clone 2.18*					
2.105**														
2.116*	tgtgctcttgaccaagggtccgggggatacctaaagagcaccgataaactcatcttt	CALDQGSGGYLKSTDKLIF	*refer to clone 2.18*						*refer to clone 2.18*					

Clone ID	nt junction sequence	aa junction sequence	Clonotype counts in PB	Clonotype fraction in PB	% clonotype in PB	Shared in PB samples	Clonotype fraction	% clonotype	Clonotype counts in DOT	Clonotype fraction	% clonotype in DOT	Shared in DOT samples	Clonotype fraction	% clonotype
3.10	tgtgctcttgggggatgccttcctacaggctgggaaggggggaaccgataaactcatcttt	CALGGCLPTGWEGGTDKLIF												
3.17	tgtgctcttgggggaacgggtctacatgggggctgggggataccgataaactctatcttt	CALGERVYMGLGDTDKLIF												
3.40	tgtgctcttgggggactatctactttacgggatacgccgataaactcatcttt	CALGDYLLTGYADKLIF												
3.68	tgtgctcttgggggaaaaggttccctatcccgataaactcatcttt	CALGEKVPYPDKLIF												
3.74	tgtgctcttgggggaagacctacatacccccccagagaaagaacggctcatcttt	CALGEDLHTPPEKERLIF												
3.76	tgtgctcttgggggaacccattcctacctgggggacttgggggccgtacaccgataaactcatcttt	CALGEPIPYLGDLGPYTDKLIF												
4.01	tgtgctcttgggggaaccactcctacaccaaaatttttactgggggatacctgtacaccgataaactcatctttt	CALGEPLLHQNFTGGYLYTDKLIF												
4.02**														
4.10	tgtgctcttgggggattcatytttgtcctacggtacgtgggggatacatgggagagataaactcatcttt	CALGDSX(F/S)LSYGTWGIHGRDKLIF												
4.15	tgtgctcttgggggagccttttttccccacttgggggagcctcccataaactcatcttt	CALGEPFSPLGGASHKLIF												
4.17**														
4.45**														
4.51**														
4.52*	tgtgctcttactgtttcctacatacccccactgggggattacaccgataaactcatcttt	CALTVSYIPPLGDYTDKLIF												
4.53*	tgtgctcttgggggaatccgtacctttcctacacctatacgtactgggggatagccaccgataaactcatcttt	CALGESVPSYTYTYWGIATDKLIF												
4.56*	tgtgctcttgggggaactcaattcctacccgggggtcaaacacctagacaccgataaactcatcttt	CALGELNSYPGVKHLDTDKLIF												
4.57**														
4.58	tgtgctcttgggggaacgaaaaccaatgaatctcgtactgggggatactttcgataaactcatcttt	CALGERKPMNLVLGDTFDKLIF												
4.59*														
4.60	tgtgctcttgggggaattagtcactaccgggggatacggatcgggacacgataaactcatcttt	CALGELVTTGDTDRDTDKLIF												
4.61	tgtgctcttgggggcttacaggacgggcgtctggaccgataaactcatcttt	CALGAYRTGVWTDKLIF												
4.65**														
4.69	tgtgctcttgggaccggcaacctgattcgggggacctaggtggaccgataaactcatcttt	CALGTGNLIRGPRWTDKLIF												
4.72	tgtgctcttgggggaagggtctccctaactgggggatactctttgtacaccgataaactcatcttt	CALGEGVSLTGGYSLYTDKLIF												
4.79**														
4.84**														
4.85**														
4.88	tgtgctcttgggggagtcaattccctttcaggcccctactgggggattgggggacagggttcgccgataaactcatcttt	CALGESIPFRPLLGDWGTGFADKLIF												
4.92*	tgtgctcttgggggaactagaggaatggcctctcccccctcaggctgggggatataagggcaccgataaactcatcttt	CALGELEEWPLPLRLGDIRGTDKLIF												
4.99	tgtgctcttgggggagccttcgctcaaacgcagacgcgctgggggacacaaatcgtcccacaccgataaactcatcttt	CALGEPSLKRRRAGGHKSSHTDKLIF												
4.100	tgtgctcttgggggaactacgggaaaaaaacaccgataaactcatcttt	CALGELREKNTDKLIF												
4.102*	tgtgctcttgggggaactacgggaaaaaaacaccgataaactcatcttt	CALGELREKNTDKLIF												
4.103	tgtgctcttgggggaactctctgggggggcctacaccgataaactcatcttt	CALGELSGGAYTDKLIF												
4.105	tgtgctcttgggggaactccattcctacggttccggtccacgtagcgtcggggatccgagacgtaaactcatcttt	CALGELHSYGSGPRSVGDPRRKLIF												
4.107*	tgtgctcttgggggaacccagagtactgggggggtcccacgtacaccgataaactcatcttt	CALGEPRVLGGPTYTDKLIF												
4.113**														
4.114	tgtgctcttgggggaagtccggctcctacgggtactgggggaccacccgacgggtaaactcatcttt	CALGEVRLLRVLGDHPTGKLIF												

Table 4.8 Analysis of clone-derived TCRγ chains (aminoacidic clonotypes of clones described in Table 6.6). The table displays the CDR3 regions at nucleotide and aminoacidic level, chain absolute counts and relative frequencies among all donors

Clone ID	Clonotype counts in PB (other sequences)	Clonotype fraction in PB (other sequences)	% clonotype in PB (other sequences)	nt sequence in PB (other nt sequence)	Clonotype counts in DOT (other sequences)	Clonotype fraction (other sequences)	% clonotype in DOT (other sequences)	nt sequence (other nt sequence)
1.06	31	6,20E-04	6,20E-02	TGTGCCTTGTGGGAGGTGCGTTATTATAAGAAACTCTTT	65	0,001175428	0,11754281	TGTGCCTTGTGGGAGGTGCGCTATTATAAGAAACTCTTT
					10	1,81E-04	1,81E-02	TGTGCCTTGTGGGAGGTGCGATATTATAAGAAACTCTTT
					4	7,23E-05	7,23E-03	TGTGCCTTGTGGGAGGTGCGTTATTATAAGAAACTCTTT
					4	7,23E-05	7,23E-03	TGTGCCTTGTGGGAGGTGAGGTATTATAAGAAACTCTTT
1.34	32	6,40E-04	6,40E-02	TGTGCCACCTGGGACGGGCCTTATAAGAAACTCTTT	52	9,40E-04	9,40E-02	TGTGCCACCTGGGATGGCCCATATAAGAAACTCTTT
					29	5,24E-04	5,24E-02	TGTGCCACCTGGGACGGGCCTTATAAGAAACTCTTT
					5	9,04E-05	9,04E-03	TGTGCCACCTGGGACGGGCCATATAAGAAACTCTTT
1.35	29	5,80E-04	5,80E-02	TGTGCCACCTGGGACGGAAATTATAAGAAACTCTTT	8	1,45E-04	1,45E-02	TGTGCCACCTGGGACGGGAATTATAAGAAACTCTTT
1.48					13	2,35E-04	2,35E-02	TGTGCCACCTGGGACAGGCCCCGTTATTATAAGAAACTCTTT
					5	9,04E-05	9,04E-03	TGTGCCACCTGGGACAGGCCTCGATATTATAAGAAACTCTTT
2.48					5	1,13E-04	1,13E-02	TGTGCCACCTGGGACAGGCCGGAGAAACTCTTT
					4	9,04E-05	9,04E-03	TGTGCCACCTGGGACAGGCCTGAGAAACTCTTT
3.17					64	9,05E-04	9,05E-02	TGTGCCACCTGGGACAGGCGGTATTATAAGAAACTCTTT
					60	8,48E-04	8,48E-02	TGTGCCACCTGGGACAGGCGCTATTATAAGAAACTCTTT
					50	7,07E-04	7,07E-02	TGTGCCACCTGGGACAGGCGTTATTATAAGAAACTCTTT
					35	4,95E-04	4,95E-02	TGTGCCACCTGGGACAGGCGATATTATAAGAAACTCTTT
					12	1,70E-04	1,70E-02	TGTGCCACCTGGGATAGGCGATATTATAAGAAACTCTTT
					5	7,07E-05	7,07E-03	TGTGCCACCTGGGCGCTATTATAAGAAACTCTTT
3.68					3	4,24E-05	4,24E-03	TGTGCCACCTGGGATCTTTATAAGAAACTCTTT
3.74	1	2,58E-05	2,58E-03	TGTGCCTTGTGGGAGGTGCGTTATTATAAGAAACTCTTT	38	5,37E-04	5,37E-02	TGTGCCTTGTGGGAGGTGCGTTATTATAAGAAACTCTTT
					12	1,70E-04	1,70E-02	TGTGCCTTGTGGGAGGTCCGTTATTATAAGAAACTCTTT
					4	5,66E-05	5,66E-03	TGTGCCTTGTGGGAGGTGCGGTATTATAAGAAACTCTTT
					4	5,66E-05	5,66E-03	TGTGCCTTGTGGGAGGTGAGGTATTATAAGAAACTCTTT
4.01					10	1,74E-04	1,74E-02	TGTGCCTTGTGGGAGGTTAATTATTATAAGAAACTCTTT
4.15					6	1,04E-04	1,04E-02	TGTGCCACCTGGGATAGGCCGCGGTTATTATAAGAAACTCTTT
					4	6,97E-05	6,97E-03	TGTGCCACCTGGGACAGGCCGCGGTATTATAAGAAACTCTTT
					3	5,22E-05	5,22E-03	TGTGCCACCTGGGACAGGCCGCGATATTATAAGAAACTCTTT
					2	3,48E-05	3,48E-03	TGTGCCACCTGGGACAGGCCTAGGTATTATTAAGAAACTCTTT
4.58					9	1,57E-04	1,57E-02	TGTGCCACCTGGGACGGTTATAGTAGTGATTGGATCAAGACGTTT
					3	5,22E-05	5,22E-03	TGTGCCACCTGGGACGGCTATAGTAGTGATTGGATCAAGACGTTT
					2	3,48E-05	3,48E-03	TGTGCCACCTGGGACGGGTATAGTAGTGATTGGATCAAGACGTTT
4.69					10	1,74E-04	1,74E-02	TGTGCCACCTGGGACTTTTATAAGAAACTCTTT
					2	3,48E-05	3,48E-03	TGTGCCACCTGGGATTTCTATAAGAAACTCTTT
4.114					20	3,48E-04	3,48E-02	TGTGCCACCTGGGTCTATTATAAGAAACTCTTT

Table 4.9 TCRγ chain usage per clone. TCRγ chains were aligned to genomes of reference on IMGT: TRGVx indicates the recombined γ chain in the clone of reference, 01 or 02 values are indicative for the allele and F indicates that the sequence is predicted to be functional.

Clone ID	V region and allele
1.03	TRGV8*01 F
1.04	TRGV4*02 F
1.05	TRGV2*01 F
1.06	TRGV9*01 F
1.11	TRGV9*01 F or *02 F
1.12	TRGV5*01 F
1.13	TRGV9*01 F
1.26	TRGV4*01 F
1.30	TRGV4*02 F
1.31	TRGV3*01 F
1.34	TRGV4*02 F
1.35	TRGV4*01 F
1.36	TRGV9*01 F
1.37	TRGV9*01 F
1.39	TRGV5*01 F
1.48	TRGV5*01 F
1.49	TRGV5*01 F
1.63	TRGV9*01 F

Clone ID	V region and allele
2.11	TRGV8*01 F
2.17	TRGV2*02 F
2.18	TRGV8*01 F
2.31	TRGV8*01 F
2.37	TRGV8*01 F
2.48	TRGV5*01 F
2.49	TRGV2*02 F
2.81	TRGV8*01 F
2.91	TRGV8*01 F
2.102	TRGV8*01 F

Clone ID	V region and allele
3.10	TRGV9*01 F
3.17	TRGV8*01 F
3.40	TRGV4*01 F
3.68	TRGV5*01 F
3.74	TRGV9*01 F
3.76	TRGV9*01 F

Clone ID	V region and allele
4.01	TRGV9*01 F
4.10	TRGV8*01 F
4.15	TRGV5*01 F
4.58	TRGV4*01 F
4.59*	TRGV4*01 F
4.60	TRGV3*01 F
4.61	TRGV9*01 F
4.65*	TRGV9*01 F
4.69	TRGV8*01 F
4.72	TRGV9*01 F
4.79*	TRGV8*01 F
4.88	TRGV9*01 F
4.99	TRGV3*01 F
4.100	TRGV2*02 F
4.103	TRGV9*01 F
4.105	TRGV4*01 F
4.114	TRGV8*01 F

*Table 4.10 Summary of clone selection. * and ** denote clones with same γ but different δ sequences; a = ⁺ < 1%; ⁺⁺ < 10%; ⁺⁺⁺ > 10%. b = < 0.1%; ⁺⁺ > 0.1%.*

			γ chain				***δ chain***			
Killing reduction (αTCS1)	**Clone ID**	**Chain**	**PB[a]**	**PB (other donors)[a]**	**DOT[b]**	**DOT (other donors)[b]**	**PB[a]**	**DOT[b]**	**PB (other donors)[a]**	**DOT (other donors)[b]**
> 20%	1.37*	Vγ9	⁺⁺⁺	-	-	⁺	⁺⁺	⁺	-	-
	2.11	Vγ8	⁺	-	-	⁺	⁺	⁺	-	-
	3.74	Vγ9	⁺	⁺	-	⁺⁺	-	-	-	-
	1.06**	Vγ9	-	-	-	⁺⁺	-	-	-	-
	3.17	Vγ8	-	⁺	-	⁺	-	-	-	-
	1.36**	Vγ9	-	-	-	⁺⁺	-	-	-	-
< 20%	1.11*	Vγ9	⁺⁺⁺	-	-	⁺	-	-	-	-
	2.18	Vγ8	⁺⁺⁺	-	-	⁺⁺	⁺⁺⁺	⁺⁺	-	⁺

4.3.6 Report generation and reactivity assays

After clone selection (Table 4.10), we started the molecular cloning of their TCR into the J.RT3 cell line, used as reporter for T cell activation, following the methodology established by our collaborators in Julie Déchanet-Merville's laboratory (Bordeaux, France). RNA was extracted and retrotranscribed into cDNA; the TCR regions of both γ and δ chains were amplified by PCR, separately ligated into the pCR-blunt vector and

used to transform *TOP10* competent bacterial cells. Antibiotic-resistant colonies were selected, and the insertion of the ligation products was verified by restriction analysis or by PCR. Finally, we confirmed the presence of the inserts with the right cDNA sequence and proper ORF by Sanger sequencing. Only TCRγ sequences comprised between 980bp and 1100bp and TCRδ sequences between 747bp and 900bp were selected (Table 4.11). We were not able to identify verified colonies for 1.11, 1.36 and 3.17 TCRγ chains and for 2.31 TCRδ chain. However, J.RT3 reporters for 1.11 and 1.36 were generated using their clonotypes (1.37 and 1.06, respectively).

Table 4.11 γ and δ chain insert length in the generated plasmids.

γ chain	*nt*	*aa*	*δ chain*	*nt*	*aa*
1.06γ	1053	350	*1.06δ*	885	294
1.11γ	-	-	*1.11δ*	789	262
1.36γ	-	-	*1.36δ*	870	289
1.37γ	1026	341	*1.37δ*	900	299
2.11γ	1035	344	*2.11δ*	-	-
2.18γ	-	-	*2.18δ*	-	-
3.17γ	-	-	*3.17δ*	882	293
3.74γ	984	327	*3.74δ*	747	278

To further validate the sequences contained in the generated plasmids, we predicted the presence of transmembrane helix domains using the TMHMM Server v. 2.0 (Figure 4.29).

Furthermore, we aligned the obtained TCR γ and δ chains to a set of sequences (see Table 3.5 and Table 3.6), provided by our collaborators in Bordeaux, to check for similarities in FR and CDR length and composition. γ and δ chain alignments are listed respectively in Table 4.12 and 4.13: the CDR3 regions are highlighted in magenta and comprised between FR3 and FR4 (displayed in green).

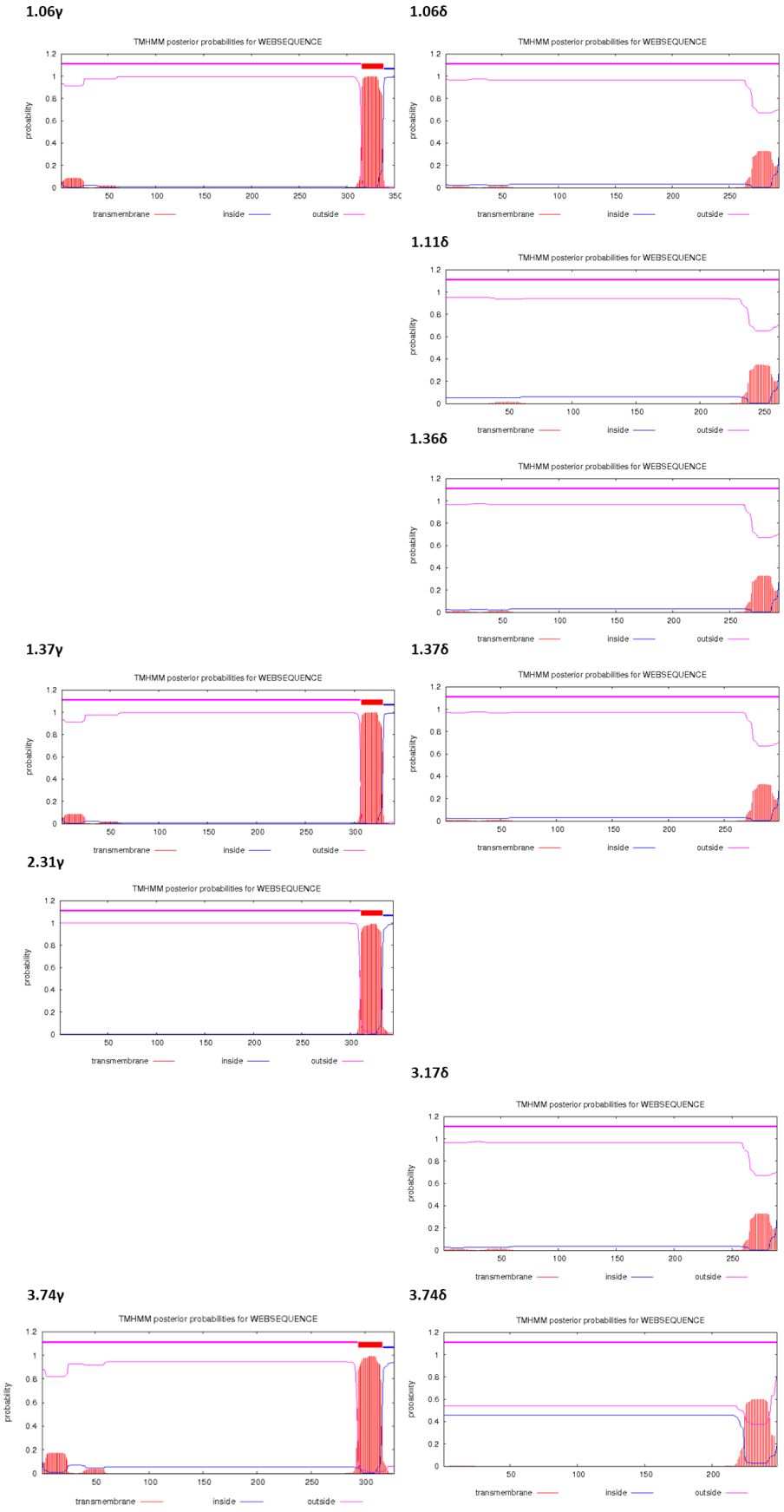

Figure 4.29 Transmembrane helix domains prediction. Plots show the posterior probabilities of inside (blue)/outside (magenta)/transmembrane (red) helix (y axis) of each amino acid (x axis) for the γ and δ chains (left and right respectively). The plots are obtained by calculating the total probability that a residue sits in helix, inside, or outside summed over all possible paths through the model. The best prediction is shown at the top of each plot (between 1 and 1.2).

Table 4.12 TCRγ chain alignment. CDR3 region (magenta) is included between FR3 and FR4 (green)

```
1.06γ          MLSLLHTSTLAVLGALCVYGAGHLEQPQISSTKTLSKTARLECVVSGITISATSVYWYRE  60
1.37γ          MLSLLHTSTLAVLGALCVYGAGHLEQPQISSTKTLSKTARLECVVSGITISATSVYWYRE  60
2.31γ          MLL-ALALLLAFLPP-ASQKSSNLEGRTKSVTRPTGSSAVITCDLPV--ENAVYTHWYLH  56
3.74γ          MLSLLHASTLAVLGALCVYGAGHLEQPQISSTKTLSKTARLECVVSGITISATSVYWYRE  60
LESγ4          MQW-ALAVLLAFLSP-ASQKSSNLEGRTKSVIRQTGSSAEITCDLAE--GSTGYIHWYLH  56
γ8Nantes       MLL-ALALLLAFLPP-ASQKSSNLEGRTKSVTRPTGSSAVITCDLPV--ENAVYTHWYLH  56
PINγ4          MLL-ALALLLAFLPP-ASQKSSNLEGRTKSVTRPTGSSAVITCDLPV--ENAVYTHWYLH  56
CHAMγ          MQW-ALAVLLAFLSP-ASQKSSNLEGRTKSVIRQTGSSAEITCDLAE--GSTGYIHWYLH  56
MAUγ9          MLSLLHTSTLAVLGALCVCGAGHLEQPQISSTKTLSKTARLECVVSGITISATSVYWYRE  60
γ9clone26      MLSLLHTSTLAVLGALCVYGAGHLEQPQISSTKTLSKTARLECVVSGITISATSVYWYRE  60
γ9Nantes       MLSLLHASTLAVLGALCVYGAGHLEQPQISSTKTLSKTARLECVVSGITISATSVYWYRE  60
               *     :  **.*   .   :.:**    *  :  ..:* : * :     .:   :** .

1.06γ          RPGEVIQF-LVSISYDGTVRKESGIPSGKFEVDRIPETSTSTLTIHNVEKQDIATYYCAL 119
1.37γ          RPGEVIQF-LVSISYDGTVRKESGIPSGKFEVDRIPETSTSTLTIHNVEKQDIATYYCAL 119
2.31γ          QEGKAPQRLLYYDSYNSRVVLESGISREKYHTYASTGK-SLKFILENLIERDSGVYYCAT 115
3.74γ          RPGEVIQF-LVSISYDGTVRKESGIPSGKFEVDRIPETSTSTLTIHNVEKQDIATYYCAL 119
LESγ4          -EGKAPQRLLYYDSYTSSVVLESGISPGKYDTYGSTRK-NLRMILRNLIENDSGVYYCAT 114
γ8Nantes       QEGKAPQRLLYYDSYNSRVVLESGISREKYHTYASTGK-SLKFILENLIERDSGVYYCAT 115
PINγ4          QEGKAPQRLLYYDSYNSRVVLESGISREKYHTYASTGK-SLKFILENLIERDSGVYYCAT 115
CHAMγ          QEGKAPQRLLYYDSYTSSVVLESGISPGKYDTYGSTRK-NLRMILRNLIENDSGVYYCAT 115
MAUγ9          RPGEVIQF-LVSISYDGTVRKESGIPSGKFEVDRIPETSTSTLTIHNVEKQDIATYYCAL 119
γ9clone26      RPGEVIQF-LVSISYDGTVRKESGIPSGKFEVDRIPETSTSTLTIHNVEKQDIATYYCAL 119
γ9Nantes       RPGEVIQF-LVSISYDGTVRKESGIPSGKFEVDRIPETSTSTLTIHNVEKQDIATYYCAL 119
                  *:. *  *   ** . *  ****   *:..     . .  : :.*: :.* ..****

1.06γ          WEV-RYY---KKLFGSGTTLVV--TDKQLDADVSPKPTIFLPSIAETKLQKAGTYLCLLE 173
1.37γ          WEV-T-----RKLFGSGTTLVV--TDKQLDADVSPKPTIFLPSIAETKLQKAGTYLCLLE 171
2.31γ          WITGRS-SDWIKTFAKGTRLIVTSPDKQLDADVSPKPTIFLPSIAETKLQKAGTYLCLLE 174
3.74γ          WEV-RYY---KKLFGSGTTLVV--TDKQLDADVSPKPTIFLPSIAETKLQKAGTYLCLLE 173
LESγ4          WDGF----YYKKLFGSGTTLVV--TDKQLDADVSPKPTIFLPSIAETKLQKAGTYLCLLE 168
γ8Nantes       WDS-------SKLFGSGTTLVV--TDKQLDADVSPKPTIFLPSIAETKLQKAGTYLCLLE 166
PINγ4          WDN------YKKLFGSGTTLVV--TDKQLDADVSPKPTIFLPSIAETKLQKAGTYLCLLE 167
CHAMγ          WEG------YKKLFGSGTTLVV--TDKQLDADVSPKPTIFLPSIAETKLQKAGTYLCLLE 167
MAUγ9          WEV-QSV---EKLFGSGTTLVV--TDKQLDADVSPKPTIFLPSIAETKLQKAGTYLCLLE 173
γ9clone26      WEGNHYY---KKLFGSGTTLVV--TDKQLDADVSPKPTIFLPSIAETKLQKAGTYLCLLE 174
γ9Nantes       WEAQQELGKKIKVFGPGTKLII--TDKQLDADVSPKPTIFLPSIAETKLQKAGTYLCLLE 177
               *          * *. ** *::   ************************************

1.06γ          KFFPDIIKIHWQEKKSNTILGSQEGNTMKTNDTYMKFSWLTVPEESLDKEHRCIVRHENN 233
1.37γ          KFFPDIIKIHWQEKKSNTILGSQEGNTMKTNDTYMKFSWLTVPEESLDKEHRCIVRHENN 231
2.31γ          KFFPDIIKIHWQEKKSNTILGSQEGNTMKTNDTYMKFSWLTVPEESLDKEHRCIVRHENN 234
3.74γ          KFFPDIIKIHWQEKKSNTILGSQEGNTMKTNDTYMKFSWLTVPEESLDKEHRCIVRHENN 233
LESγ4          KFFPDIIKIHWQEKKSNTIMGSQEGNTMKTNDTYMKFSWLTVPEESLDKEHRCIVRHENN 228
γ8Nantes       KFFPDIIKIHWQEKKSNTILGSQEGNTMKTNDTYMKFSWLTVPEESLDKEHRCIVRHENN 226
PINγ4          KFFPDIIKIHWQEKKSNTILGSQEGNTMKTNDTYMKFSWLTVPEESLDKEHRCIVRHENN 227
CHAMγ          KFFPDVIKIHWQEKKSNTILGSQEGNTMKTNDTYMKFSWLTVPEKSLDKEHRCIVRHENN 227
MAUγ9          KFFPDIIKIHWQEKKSNTILGSQEGNTMKTNDTYMKFSWLTVPEESLDKEHRCIVRHENN 233
γ9clone26      KFFPDIIKIHWQEKKSNTILGSQEGNTMKTNDTYMKFSWLTVPEESLDKEHRCIVRHENN 234
γ9Nantes       KFFPDVIKIHWEEKKSNTILGSQEGNTMKTNDTYMKFSWLTVPEKSLDKEHRCIVRHENN 237
               *****:*****:*******:************************:***************

1.06γ          KNGIDQEIIFPPIKTDVTTVDPKDSYSKDANDVTTVDPKYNYSKDANDVITMDPKDNWSK 293
1.37γ          KNGIDQEIIFPPIKTDVTTVDPKDSYSKDANDVTTVDPKYNYSKDANDVITMDPKDNWSK 291
2.31γ          KNGIDQEIIFPPIKTDVTTVDPKDSYSKDANDVTTVDPKYNYSKDANDVITMDPKDNWSK 294
3.74γ          KNGIDQEIIFPPIKTDVTT----------------VDPKYNYSKDANDVITMDPKDNWSK 277
LESγ4          KNGIDQEIIFPPIKTDVTTVDPKDSYSK----------------DANDVITMDPKDNWSK 272
γ8Nantes       KNGIDQEIIFPPIKTDVTT----------------VDPKYNYSKDANDVITMDPKDNWSK 270
PINγ4          KNGIDQEIIFPPIKTDVTT----------------VDPKYNYSKDANDVITMDPKDNWSK 271
CHAMγ          KNGVDQEIIFPPIKTDV--------------------------------ITMDPKDNCSK 255
MAUγ9          KNGIDQEIIFPPIKTDVTT----------------VDPKYNYSKDANDVITMDPKDNWSK 277
γ9clone26      KNGIDQEIIFPPIKTDVTT----------------VDPKYNYSKDANDVITMDPKDNWSK 278
γ9Nantes       KNGVDQEIIFPPIKTDVITMDPKDNCSKDAND---------------------------- 269
               ***:*************
```

```
1.06γ          DANEHVQFLLDTLLLQLTNTSAYYMYLLLLLKSVVYFAIITCCLLRRTAFCCNGEKS     350
1.37γ          DAND-------TLLLQLTNTSAYYMYLLLLLKSVVYFAIITCCLLRRTAFCCNGEKS     341
2.31γ          DAND-------TLLLQLTNTSAYYMYLLLLLKSVVYFAIITCCLLGRTAFCCNGEKS     344
3.74γ          DAND-------TLLLQLTNTSAYYMYLLLLLKSVVYFAIITCCLLGRTAFCCNGEKS     327
LESγ4          DAND-------TLLLQLTNTSAYYMYLLLLLKSVVYFAIITCCLLGRTAFCCNGEKS     322
γ8Nantes       DAND-------TLLLQLTNTSAYYTYLLLLLKSVVYFAIITCCLLRRTAFCCNGEKS     320
PINγ4          DAND-------TLLLQLTNTSAYYTYLLLLLKSVVYFAIITCCLLRRTAFCCNGEKS     321
CHAMγ          DAND-------TLLLQLTNTSAYYMYLLLLLKSVVYFAIITCCLLRRTAFCCNGEKS     305
MAUγ9          DAND-------TLLLQLTNTSAYYTYLLLLLKSVVYFAIITCCLLRRTAFCCNGEKS     327
γ9clone26      DAND-------TLLLQLTNTSAYYTYLLLLLKSVVYFAIITCCLLRRTAFCCNGEKS     328
γ9Nantes       -----------TLLLQLTNTSAYYMYLLLLLKSVVYFAIITCCLLRRTAFCCNGEKS     315
                          ************ ******************** ************
```

Table 4.13 TCRδ chain alignment. CDR3 region (magenta) is included between FR3 and FR4 (green)

```
1.06δ          --------------------------MLFSSLLCVFVAFSY--SGSS-VAQKVTQAQSSV  31
1.11δ          -------------------------MLFFQPGCGVFVAFQL--TRDQGGPRRLLQPQSSV  33
1.36δ          --------------------------MLFSSLLCVFVAFSY--SGSS-VAQKVTQAQSSV  31
1.37δ          --------------------------MLFSSLLCVFVAFSY--SGSS-VAQKVTQAQSSV  31
3.17δ          --------------------------MLFSSLLCVFVAFSY--SGSS-VAQKVTQAQSSV  31
3.74δ          ------------------------------------------------------------  0
MAUδ           ----------------------------------------------MGQKVTQAQSSV  12
CHAMδ          --------------------------MLFSSLLCVFVAFSY--SGSS-VAQKVTQAQSSV  31
PINδ           --------------------------MLFSSLLCVFVAFSY--SGSS-VAQKVTQAQSSV  31
δ1DAVID        --------------------------MLFSSLLCVFVAFSY--SGSS-VAQKVTQAQSSV  31
LESδ5          ------------------------MAMLLGASVLILWLQPDWVNSQQKNDDQQVKQNSPSL  37
δ3Nantes       -------------------------MILTV---GFSFLFFYRG----TLCDKVTQSSPDQ  28
δ3clone26      -------------------------MILTV---GFSFLFFYRG----TLCDKVTQSSPDQ  28
δ2Nantes       CAPPAGYQLHRGGGRSRTSGSPGEAMQRISSLIH--LSLFWAGVM---SAIELVPEHQTV  55


1.06δ          SMPVRKAVTLNCLYE-TSWWSYYIFWYKQLPSKEMIFLIRQGSDE---QNAKSGRYSVNF  87
1.11δ          SMPVRKAVTLNCLYE-TSWWSYYIFWYKQLPSKEMIFLIRQGSDE---QNAKSGRYSVNF  89
1.36δ          SMPVRKAVTLNCLYE-TSWWSYYIFWYKQLPSKEMIFLIRQGSDE---QNAKSGRYSVNF  87
1.37δ          SMPVRKAVTLNCLYE-TSWWSYYIFWYKQLPSKEMIFLIRQGSDE---QNAKSGRYSVNF  87
3.17δ          SMPVRKAVTLNCLYE-TSWWSYYIFWYKQLPSKEMIFLIRQGSDE---QNAKSGRYSVNF  87
3.74δ          ------------MK-PSWWSYYIFWSKQLPSKEMIFLIRQGSDE---QNAKSGRYSVNF  43
MAUδ           SMPVRKAVTLNCLYE-TSWWSYYIFWYKQLPSKEMIFLIRQGSDE---QNAKSGRYSVNF  68
CHAMδ          SMPVRKAVTLNCLYE-TSWWSYYIFWYKQLPSKEMIFLIRQGSDE---QNAKSGRYSVNF  87
PINδ           SMPVRKAVTLNCLYE-TSWWSYYIFWYKQLPSKEMIFLIRQGSDE---QNAKSGRYSVNF  87
δ1DAVID        SMPVRKAVTLNCLYE-TSWWSYYIFWYKQLPSKEMIFLIRQGSDE---QNAKSGRYSVNF  87
LESδ5          SVQEGRISILNCDYT-NSMFDYF-LWYKKYPAEGPTFLISISSIK---DKNEDGRFTVFL  92
δ3Nantes       TVASGSEVVLLCTYD-TVYSNPDLFWYRIRPDYSFQFVFYGDNSRSEGADFTQGRFSVKH  87
δ3clone26      TVASGSEVVLLCTYD-TVYSNPDLFWYRIRPDYSFQFVFYGDNSTSEGADFTHGRFSVKH  87
δ2Nantes       PVSIGVPATLRCSMKGEAIGNYYINWYRKTQGNTMTFIYREKDIY---GPGFKDNFQGDI  112
                                     .    * :        *:    .          ..:


1.06δ          KKAAKSVALTISALQLEDSAKYFCALGGPSYDR------YWGIPDKLIFGKGTRVTVEPR  141
1.11δ          KKAAKSVALTISALQLEDSAKYFCALGESLRDTF--------YTDKLIFGKGTRVTVEPR  141
1.36δ          KKAAKSVALTISALQLEDSAKYFCALGEKK----------RTGGLLIFGKGTRVTVEPR  136
1.37δ          KKAAKSVALTISALQLEDSAKYFCALGDIPRRSLRIG-GGNLYTDKLIFGKGTRVTVEPR  146
3.17δ          KKAAKSVALTISALQLEDSAKYFCALGERVYM-------GLGDTDKLIFGKGTRVTVEPR  140
3.74δ          KKAAKSVALTISALQLEDSAKYFCALGEDLHTP--------PEKERLIFGKGTRVTVEPR  95
MAUδ           KKAAKSVALTISALQLEDSAKYFCALGDLTGV---------PITDKLIFGKGTRVTVEPR  119
CHAMδ          KKAAKSVALTISALQLEDSAKYFCALGAPPLLL------YWGITDKLIFGKGTRVTVEPR  141
PINδ           KKAAKSVALTISALQLEDSAKYFCALGDYLGDKYPSYDLLGDTTDKLIFGKGTRVTVEPR  147
δ1DAVID        KKAAKSVALTISALQLEDSAKYFCALGELG-------------DDKLIFGKGTRVTVEPR  134
LESδ5          NKSAKHLSLHIVPSQPGDSAVYFCAASSPIRGYT--------GSDKLIFGKGTRVTVEPR  144
δ3Nantes       ILTQKAFHLVISPVRTEDSATYYCAFTGL-GDT--------SHADKLIFGKGTRVTVEPR  138
δ3clone26      ILTQKAFHLVISPVRTEDSATYYCAFIGR---Y--------GYTDKLIFGKGTRVTVEPR  136
δ2Nantes       DIAKNLAVLKILAPSERDEGSYYCACDT--------LGMGGEYTDKLIFGKGTRVTVEPR  164
                 : :   * *      *.. *:**                     **************
```

```
1.06δ          SQPHTKPSVFVMKNGTNVACLVKEFYPKDIRINLVSSKKITEFDPAIVISPSGKYNAVKL 201
1.11δ          SQPHTKPSVFVMKNGTNVACLVKEFYPKDIRINLVSSKKITEFDPAIVISPSGKYNAVKL 201
1.36δ          SQPHTKPSVFVMKNGTNVACLVKEFYPKDIRINLVSSKKITEFDPAIVISPSGKYNAVKL 196
1.37δ          SQPHTKPSVFVMKNGTNVACLVKEFYPKDIRINLVSSKKITEFDPAIVISPSGKYNAVKL 206
3.17δ          SQPHTKPSVFVMKNGTNVACLVKEFYPKDIRINLVSSKKITEFDPAIVISPSGKYNAVKL 200
3.74δ          SQPHTKPSVFVMKNGTNVACLVKEFYPKDIRINLVSSKKITEFDPAIVISPSGKYNAVKL 155
MAUδ           SQPHTKPSVFVMKNGTNVACLVKEFYPKDIRINLVSSKKITEFDPAIVISPSGKYNAVKL 179
CHAMδ          SQPHTKPSVFVMKNGTNVACLVKEFYPKDIRINLVSSKKITEFDPAIVISPSGKYNAVKL 201
PINδ           SQPHTKPSVFVMKNGTNVACLVKEFYPKDIRINLVSSKKITEFDPAIVISPSGKYNAVKL 207
δ1DAVID        SQPHTKPSVFVMKNGTNVACLVKEFYPKDIRINLVSSKKITEFDPAIVISPSGKYNAVKL 194
LESδ5          SQPHTKPSVFVMKNGTNVACLVKEFYPKDIRINLVSSKKITEFDPAIVISPSGKYNAVKL 204
δ3Nantes       SQPHTKPSVFVMKNGTNVACLVKEFYPKDIRINLVSSKKITEFDPAIVISPSGKYNAVKL 198
δ3clone26      SQPHTKPSVFVMKNGTNVACLVKEFYPKDIRINLVSSKKITEFDPAIVISPSGKYNAVKL 196
δ2Nantes       SQPHTKPSVFVMKNGTNVACLVKEFYPKDIRINLVSSKKITEFDPAIVISPSGKYNAVKL 224
               ************************************************************

1.06δ          GKYEDSNSVTCSVQHDNKTVHSTDFEVKTDSTDHVKPKETENTKQPSKSCHKPKAIVHTE 261
1.11δ          ------------------------------DHVKPKETENTKQPSKSCHKPKAIVHTE 229
1.36δ          GKYEDSNSVTCSVQHDNKTVHSTDFEVKTDSTDHVKPKETENTKQPSKSCHKPKAIVHTE 256
1.37δ          GKYEDSNSVTCSVQHDNKTVHSTDFEVKTDSTDHVKPKETENTKQPSKSCHKPKAIVHTE 266
3.17δ          GKYEDSNSVTCSVQHDNKTVHSTDFEVKTDSTDHVKPKETENTKQPSKSCHKPKAIVHTE 260
3.74δ          GKYEDSNSVTCSVQHDNKTVHSTDFEVKTDSTDHVKPKETENTKQPSKSCHKPKAIVHTE 215
MAUδ           GKYEDSNSVTCSVQHDNKTVHSTDFEVKTDSTDHVKPKETENTKQPSKSCHKPKAIVHTE 239
CHAMδ          GKYEDSNSVTCSVQHDNKTVHSTDFEVKTDSTDHVKPKETENTKQPSKSCHKPKAIVHTE 261
PINδ           GKYEDSNSVTCSVQHDNKTVHSTDFEVKTDSTDHVKPKETENTKQPSKSCHKPKAIVHTE 267
δ1DAVID        GKYEDSNSVTCSVQHDNKTVHSTDFEVKTDSTDHVKPKETENTKQPSKSCHKPKAIVHTE 254
LESδ5          GKYEDSNSVTCSVQHDNKTVHSTDFEVKTDSTDHVKPKETENTKQPSKSCHKPKAIVHTE 264
δ3Nantes       GKYEDSNSVTCSVQHDNKTVHSTDFEVKTDSTDHVKPKETENTKQPSKSCHKPKAIVHTE 258
δ3clone26      GKYEDSNSVTCSVQHDNKTVHSTDFEVKTDSTDHVKPKETENTKQPSKSCHKPKAIVHTE 256
δ2Nantes       GKYEDSNSVTCSVQHDNKTVHSTDFEVKTDSTDHVKPKETENTKQPSKSCHKPKAIVHTE 284
                                            ****************************

1.06δ          KVNMMSLTVLGLRMLFAKTVAVNFLLTAKLFFL         294
1.11δ          KVNMMSLTVLGLRMLFAKTVAVNFLLTAKLFFL         262
1.36δ          KVNMMSLTVLGLRMLFAKTVAVNFLLTAKLFFL         289
1.37δ          KVNMMSLTVLGLRMLFAKTVAVNFLLTAKLFFL         299
3.17δ          KVNMMSLTVLGLRMLFAKTVAVNFLLTAKLFFL         293
3.74δ          KVNMMSLTVLGLRMLFAKTVAVNFLLTAKLFFL         248
MAUδ           KVNMMSLTGSLHHILDAQKMVWNHR--------         264
CHAMδ          KVNMMSLTVLGLRMLFAKTVAVNFLLTAKLFFL         294
PINδ           KVNMMSLTVLGLRMLFAKTVAVNFLLTAKLFFL         300
δ1DAVID        KVNMMSLTVLGLRMLFAKTVAVNFLLTAKLFFL         287
LESδ5          KVNMMSLTVLGLRMLFAKTVAVNFLLTAKLFFL         297
δ3Nantes       KVNMMSLTVLGLRMLFAKTVAVNFLLTAKLFFL         291
δ3clone26      KVNMMSLTVLGLRMLFAKTVAVNFLLTAKLFFL         289
δ2Nantes       KVNMMSLTVLGLRMLFAKTVAVNFLLTAKLFFL         317
               ********    ::* *:.:. *.
```

Having verified the cDNA inserts, we ligated them into a TEEW vector, in which cDNA was under the control of the EF1α promoter, and used the ligation products to transform Endura competent cells. After selection and verification of newly transformed colonies, we produced high quantities of plasmids and used them to produce lentiviral particles by transient transfection of 293T packaging cells. As shown in Figure 4.30, J.RT3 cells after transduction expressed CD3 and γδ TCR, in stark contrast to not-transduced control (light blue). We next FACS-sorted double positive cells and cultured them to generate a reporter cell line. We were able to successfully generate three reporters, namely J.RT3_TCR-1.11, J.RT3_TCR-1.37 and J.RT3_TCR-3.74. Lentiviral particles were also generated for TCR-1.06 and TCR-1.36 but several rounds of transduction were not successful.

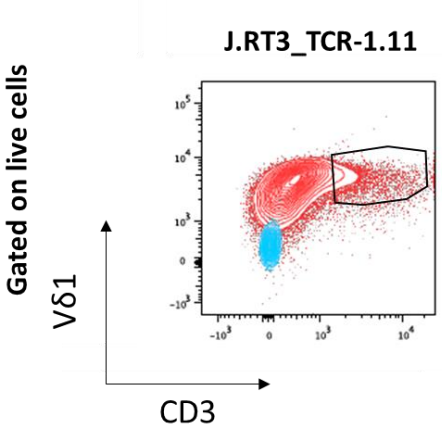

Figure 4.30 Example of a successful reporter transduction. J.RT3 cells after transduction expressed CD3 and γδ TCR in stark contrast to not-transduced control (light blue); double positive cells were FACS-sorted and cultured to generate a reporter cell line.

After generating the J.RT3_TCR reporters, we tested their reactivity capacity against several tumour target cell lines (Table 3.7). J.RT3_TCRs were incubated during 4 hours with the target cells in a 1:1 ratio and then analysed by FACS to assess CD69 expression as outcome of T cell activation. Plate bound α-CD3 was used as positive control for reporter activation. As shown in Figure 4.31, we did not detect any significant increase in CD69 median fluorescence intensity (MFI) after co-incubation with the tested AML cell lines. However, we observed a mild increase in CD69 MFI of all reporters after co-incubation with OCI-AML3. Plots are representative for *n* = 5 experiments and each histogram represents the average MFI value of the experimental conditions and controls (no target cell lines) ratio. The dashed red at 1 represents the control. We further tested the J.RT3_TCR-3.74 reactivity against other hematologic and solid tumour cell lines, but we did not identify any target inducing reporter activation (Figure 4.32). Plot is representative for *n* = 1 experiment.

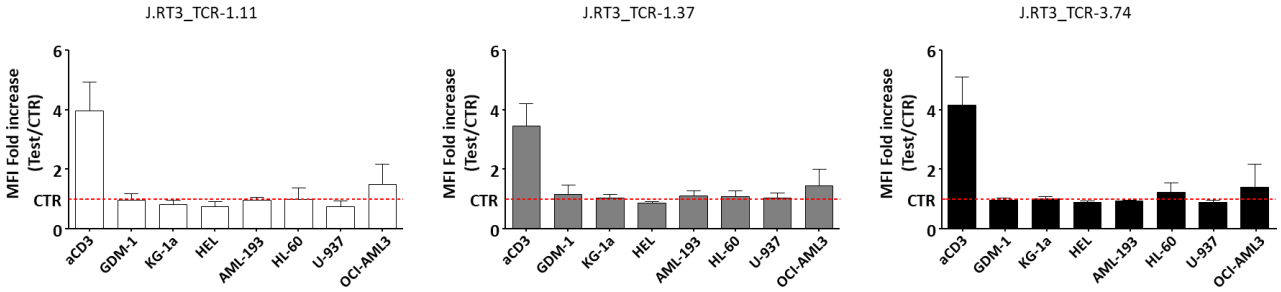

Figure 4.31 Reporter reactivity assay. J.RT3_TCRs were incubated during 4 hours with the target cells in a 1:1 ratio and then analysed by FACS to assess CD69 expression as outcome of T cell activation. Plate bound α-CD3 was used as positive control for reporter activation. Plots are representative for n = 5 experiments and each histogram represents the average MFI value of the experimental conditions and controls (no target cell lines) ratio. The dashed red at 1 represents the control.

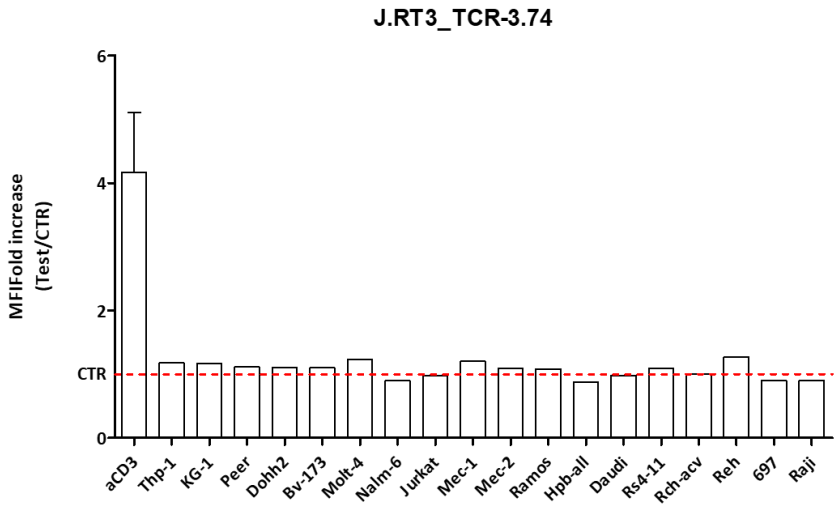

Figure 4.32 Additional J.RT3_TCR-3.74 reactivity assay. J.RT3_TCR-3.74 reactivity was assessed against other hematologic and solid tumour cell lines; no good target for reporter activation was identified. Plot is representative for n = 1 experiment.

Interestingly, in a subsequent series of experiments we serendipitously added an additional step consisting in pre-incubating the J.RT3_TCR reporter cells with α-CD3 monoclonal antibody (clone HIT3a) for 10', washing the α-CD3 in excess and co-incubating during 4 hours with the target cell lines in a 1:1 ratio. Again, the output was assessed in terms of CD69 MFI by FACS. Although the addition of a pre-activation step induced an increase in the basal CD69 MFI (Figure 4.33), we observed a further and robust increase in CD69 MFI of the JRT3.3_TCR-3.74 when co-cultured with the OCI-AML3 cell line in a pilot experiment (Figure 4.33).

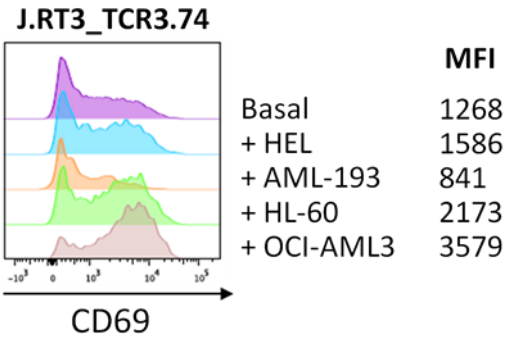

Figure 4.33 Pilot experiment with incubation the reporter with α-CD3. J.RT3_3.74 was incubated with α-CD3 (clone HIT3a) for 10', washed and co-incubated during 4 hours with the target cell lines in a 1:1 ratio. Output was assessed in terms of CD69 MFI by FACS.

To further evaluate this phenomenon, we repeated the new reactivity assay protocol including the JRT3_TCR-1.11 and JRT3_TCR-1.37 reporters and additional AML tumour cell targets (Figure 4.34). We observed that the addition of the α-CD3 stimulation induced approximately three-fold increase in the CD69 MFI values of the all the reporters compared to the control when these were co-incubated with the OCI-AML3 AML cell line. HL-60 was also inducing an increase in CD69 MFI but to a smaller extent (Figure 4.34A). Additionally, the increase in CD69 MFI was accompanied by a decrease in TCR expression as assessed by the percentage of $CD3^{+}V\delta1^{+}$ cells (Figure 4.34B).

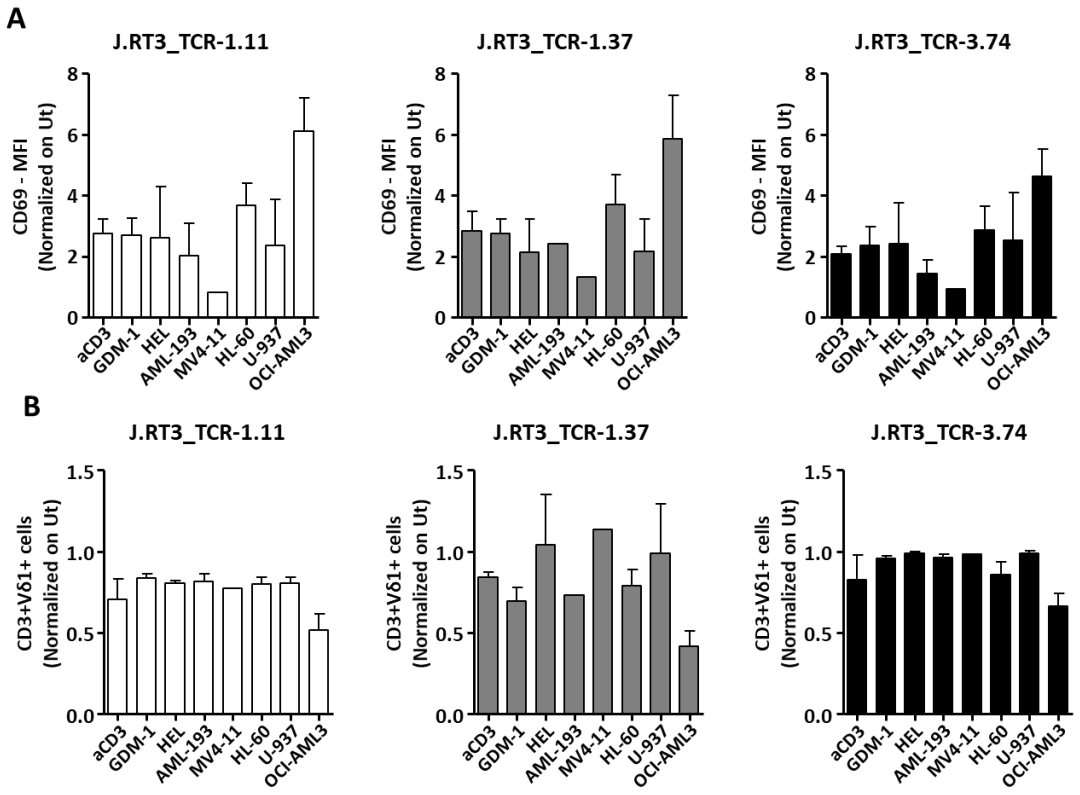

Figure 4.34 Reactivity assay following α-CD3 pre-incubation. J.RT3_TCR-1.11, -1.37 and -3.74 were incubated with α-CD3 (clone HIT3a) for 10', washed and co-incubated during 4 hours with the target cell lines in a 1:1 ratio. Output was assessed in terms of CD69 MFI and of CD3 and Vδ1 expression by FACS. Plot is representative for n = 4 experiments (mean + SD are indicated).

Additionally, we tested other tumour cell lines of hematologic (AML and not) origin as well as solid tumour cell lines, AML primary samples and healthy PBMC controls. Results are summarized in Figure 4.35.

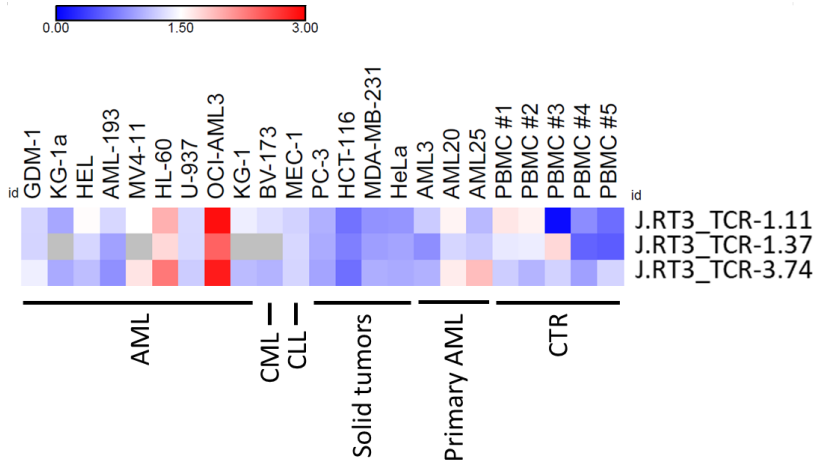

Figure 4.35 Reactivity assay heatmap for CD 69 MFI. J.RT3_TCR-1.11, -1.37 and -3.74 were incubated with α-CD3 (clone HIT3a) for 10', washed and co-incubated during 4 hours with the target cell lines in a 1:1 ratio. Ratio values (test condition over the control) are plotted in a colour scale where blue is associated with the smallest values and red to the highest (n = 3-5).

At this point, we decided to perform additional control experiments to evaluate the possibility that the increase in CD69 MFI was in fact due to an experimental artefact. We first demonstrated that the observed

induction of CD69 MFI after co-incubation with OCI-AML3 was dose-dependent by using α-CD3 dilutions (from 5µg/ml to 2.28ng/ml) during the pre-activation step of the J.RT3_reporters (Figure 4.36, left panel). Furthermore, we performed the reactivity assay after pre-incubating OCI-AML3 cells with a Fc receptor blocking reagent or with an Ig chain of the same type of the α-CD3 used for the reporter pre-activation (IgG2a). None of the two strategies were reducing the CD69 MFI induced after co-incubation (Figure 4.36, middle panel). Finally, we only observed activation of J.RT3_TCR reporters only after pre-activation with a specific α-CD3 clone, namely clone HIT3a. Despite bearing the same isotype of HIT3a antibody (IgG2a), clone OKT3 did not induce reporter activation.

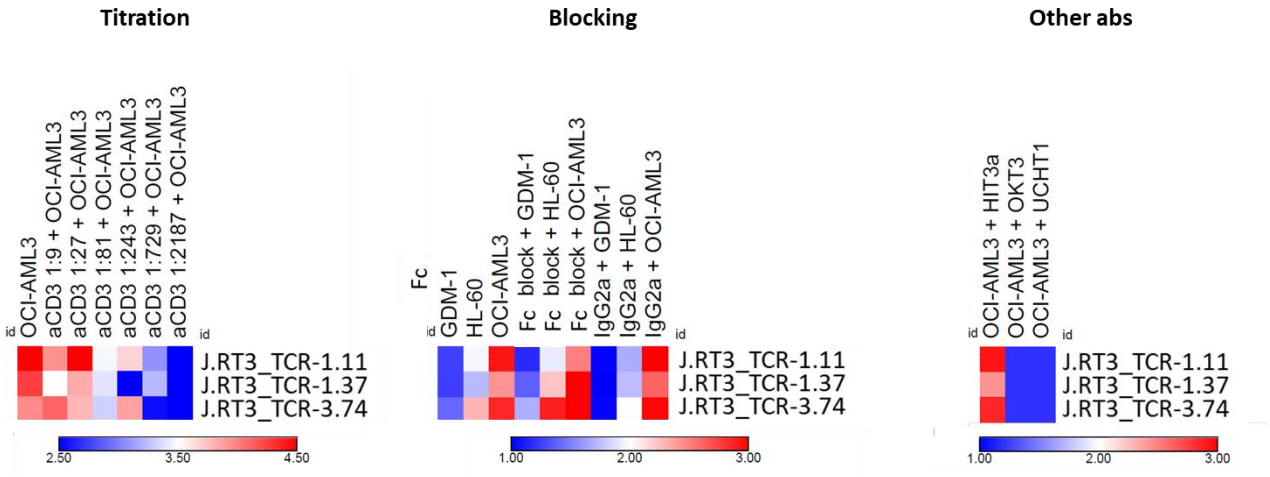

Figure 4.36 Reactivity assay experimental controls. Reporters were incubated with: dilutions of HIT3a (left), Fc block or IgG2a (middle), α-CD3 OKT3 or UCHT1 clones for 10'. Reporters cells were then washed and co-incubated during 4 hours with the target cell lines in a 1:1 ratio. Values are normalized for the untreated control (n =3; colour scale goes from the smallest value in blue to the highest in red).

To conclude, we also repeated the reactivity assays including in our experiments two TCR reporters (LES and MAU) and a target cell line (HT29) expressing their ligands. These lines were kindly provided by our collaborators in Bordeaux. As expected, CD69 MFI was not increased in JRT3_TCR-1.11, -1.37 and 3.74 when co-incubated with HT29, whereas LES and MAU reporters showed an increased CD69 MFI even in the absence of pre-stimulating α-CD3 antibody. Surprisingly, pre-activated LES and MAU reporters increased CD69 MFI when incubated with OCI-AML3 (Figure 4.37) even if their putative ligands are not expressed in this target cell line (Figure 4.38). These data raise the possibility that OCI-AML3 expresses a "pan-ligand" that reacts with multiple γδ TCRs (on their respective reporter lines).

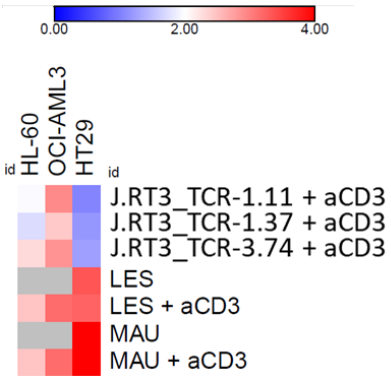

Figure 4.37 Addition of LES and MAU reporters to the reactivity assay. Reporters were incubated with HIT3a for 10', washed and co-incubated during 4 hours with the target cell lines in a 1:1 ratio. Values are normalized for the untreated control (n =3; colour scale goes from the smallest value in blue to the highest in red).

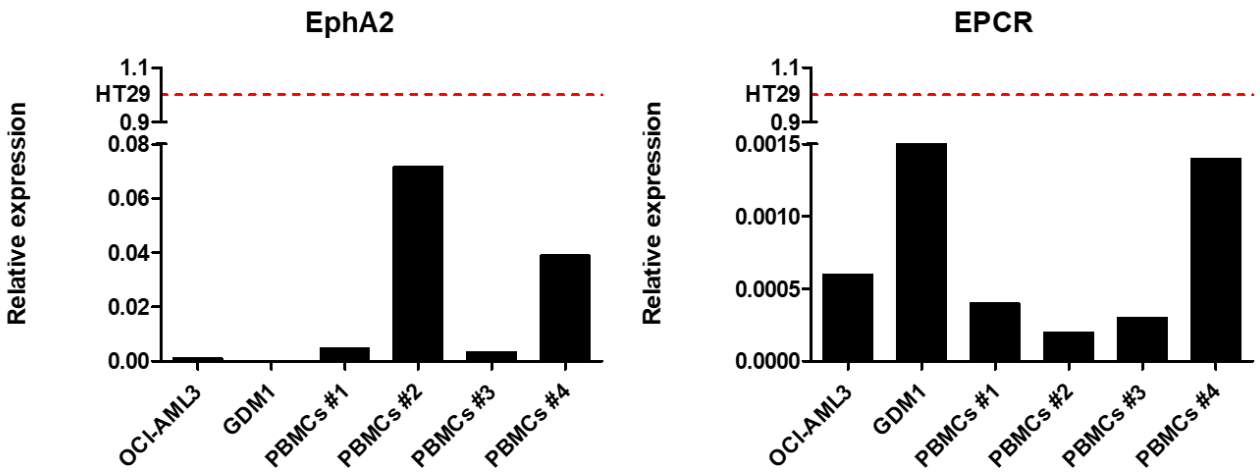

Figure 4.38 Eph2A and EPCR qPCR analysis. RNA was extracted from HT29, OCI-AML3, GDM1 and 4 healthy PB controls and the expression of Eph2A and EPCR was checked among these samples. Expression data are normalized to HT29 (red dashed line) used as positive control.

4.3.7 Conclusions

The identification of relevant tumour antigens recognized by Vδ1$^+$ T cells via their TCRVδ1 is not a trivial question, given that various other receptors, especially NK cell receptors, have been shown to be involved in tumour cell targeting *in vitro*[270]. In this study we successfully established and selected Vδ1$^+$ T-cell clones from healthy donors, cloned their TCRs into a J.RT3 line and thus generated TCR reporters with the aim of screening tumour cell lines for new Vδ1$^+$ TCR ligands.

Using *ex vivo* αβ-depleted PBMCs from HD#1-4, we were able to successfully replicate DOT cell expansion experimental results previously obtained in our laboratory[114]. The expansion method we used is indeed robust enough to allow Vδ1$^+$ T cells to become the dominant cell subset within 11 days of culture and continue to expand until day 21. At the end of expansion, we were able to enrich (>65%), expand (up to 2,300-fold) Vδ1$^+$ cells while observing a dramatic increase in the repertoire diversity; thus, DOT cells lost the oligoclonality of the Vδ1$^+$ peripheral blood repertoire, as highlighted by the contribution of the top 20 most frequent clones to the repertoire distribution (Figures 4.4 and 4.5) and by the increase in the intrasample diversity after the DOT-cell protocol (Table 4.3). Moreover, signs of previous immunological history of the donor, evaluated by CDR3 length distribution, were lost in the process (Figure 4.4). Furthermore, we were not able to predict whether a clonotype would be present in the final DOT-cell repertoire by looking at its frequency or abundance before expansion.

We generated Vδ1$^+$ clones using two methods: a limiting dilution and a single cell seeding approaches. In both strategies, cells were cultured for 21 days following the DOT cell expansion protocol and weekly providing irradiated feeders cells. Although we were able to establish clones using the limiting dilution approach, we selected the single cell seeding method, since it allowed us to save time and resources. After 21 days, we obtained enough cells to perform clone phenotypic and functional analyses, TCR Sanger sequencing and TCR molecular cloning of the selected clones. Given the limited availability of viable cells after clone expansion, we decided to test CD3^{hi}Vδ1^{hi} clones only against KG-1 AML cells. This target cell line, together with Kasumi-1, gave us the most reproducible results in terms of targeting and blocking experiments. Kasumi-1 was not selected because of its lower doubling time and difficulty in starting the culture. Interestingly, from our analysis there was no clear correlation between clone growth speed and NCR expression or between the expression of NCRs (NKp30 or NKp44) and the killing output, meaning that the recognition of targets by Vδ1$^+$ clones depends on the combination of several mechanisms (*i.e.* TCR, NKp30, NKp44, NKG2D). The role of NCRs is currently under investigation in other lines of research in the laboratory.

The extensive analysis of *ex vivo* and DOT-cell *TRG* and *TRD* repertoires was at the basis for the selection of Vδ1$^+$ clones. We selected a cohort of donors accordingly to the fraction of circulating Vδ1$^+$ T cells and we obtained data from their circulating Vδ1$^+$ T cell repertoires as well as data regarding the DOT cell repertoire products derived from their PB samples. Along with these analyses, we established single cell clones from each donor, with a clonal efficiency of approximately 25% that resulted in around 75 clones per donor. We aimed at identifying ligands for clones that could explain a bigger fraction of the Vδ1$^+$ T cell reactivity. To do so, we selected clones that were present in high frequencies in their repertoire of origin; were shared among several donors; and were able to kill the AML KG-1 cell line in a TCR-dependent manner. Our final selection was therefore composed of 8 clones: 1.37 δ chain accounted for 11.85% of HD#1 TRD repertoire and was found in the DOT repertoire of the same donor. Moreover, blocking the δ chain of the 1.37 clone with an α-Vδ1 TCR antibody (TCS1) reduced its ability of killing the KG-1 target cells by ~46% (Table 6.4), whereas the same intervention had almost no effect on clone 1.11 (~3% reduction). Clone 2.11 γ chain was present in low frequency in the *ex vivo* repertoire of the same donor and in the DOT repertoire of HD#1 (0.28% and 0.047% respectively). Clone 3.74 γ chain was highly conserved among *ex vivo* and DOT

repertoires of all donors with the exception of DOT sample generated from HD#3. The γ chain derived from clones 1.06 and 1.36 was highly shared among DOT repertoires of HD#2-4. Clone 3.17 γ chain was found as aa clonotype in the *ex vivo* repertoire of HD#1 and was detected in all the DOT repertoires. Finally, the δ chain derived from clone 2.18 constituted 37.84% of HD#2 *ex vivo* repertoire, 4.16% of HD#2 DOT repertoire and was found in HD#1 DOT repertoire (0.014%). Moreover, we also selected clone 1.36 because of a specific aminoacidic motif in its δ chain: indeed, this clone bears the that was previously described to be associated to clones that expanded in the clinical scenario of CMV infection[122]. Additionally, clone 3.74 was selected since its γ chain was previously found by our collaborators in an unrelated cord blood sample[48] and, therefore, could be defined as public γ chain sequence.

A possible criticism to our approach is the α-Vδ1 TCR antibody blockade, since it has been demonstrated that certain anti-γδTCR antibodies cause Fas-dependent apoptosis[334]. Thus, previous blocking assays reported in the literature may have overstated γδTCR involvement by assuming that decreased target death is due to TCR blockade, not realizing that a proportion of effector γδ T cells may have undergone apoptosis (effectively reducing the effector: target ratio). In this regard, a limitation of our study was not performing viability studies with the expanded clones upon incubation with anti-Vδ1 TCR mAb. Indeed, we used the samples for phenotypic and functional characterization, TCR chain Sanger sequencing and (as much cells as we could get) for the final molecular cloning. Therefore, it was not possible to evaluate the effect of the anti-Vδ1 blocking antibody (clone TSC-1) on the viability of each clone.

We were able to successfully generate three TCR reporters for the clones 1.11, 1.37 and 3.74. Although cloning and virus production of γ and δ chains from clones 1.06 and 1.36 were performed, several attempts of viral transduction on the J.RT3 cell line did not work, and we had no time for troubleshooting during the time frame of my PhD. With the generated J.RT3_TCR reporters, we tested them in coculture with several target cell lines of tumour origin. Since the J.RT3 is a mutant line derived from the E6-1 clone of Jurkat that lacks the β chain of the TCR, transducing functional TCRs allowed us to assess if the receptor was engaged in the recognition of target cell lines, through the measurement of CD69. Indeed, this protein is a well-known downstream for TCR dependent activation[335]. Moreover, this strategy was already successfully established and led our collaborators in Bordeaux to identify two γδ TCR ligands, namely EPCR[198] and Annexin 2A[199]. After generating J.RT3_TCR reporters and probing their functionality in terms of CD69 expression following CD3 stimulation, we assessed reporter reactivity against several target cell lines of tumour origin, with no success. Indeed, we did not find any cell line directly capable of inducing a strong CD69 upregulation in our reporters following direct TCR stimulation. Only thanks to the serendipitous short-term addition of anti-CD3 mAb (HIT3a) to the reporters before co-incubation with the target cells were we able to observe strong CD69 induction in the presence of OCI-AML3 target cells. We revised the protocol to change a fortuitous addition into a well-established experimental procedure, that included a reporter pre-stimulation step of 10' with 5μg/ml anti-CD3 (HIT3a) before co-incubation with the target cells. Interestingly, the pre-activation step was able to induce a strong increase in CD69 expression only when reporter cells were co-incubated with OCI-AML3 cells, with a milder effect after co-incubation with HL-60 cells.

We considered the possibility that these observations were an experimental artefact derived from the modified procedure, and thus devised a set of controls using OCI-AML3 and HL-60 as test conditions, and GDM-1 as negative control. We first assessed the effect of decreasing concentration of HIT3a antibody during the reporter pre-activation step on the final CD69 readout, going from the working dilution we used in the experiments to a final dilution of approximately 2ng/ml. CD69 upregulation was dose-dependent and led us to speculate about a fine modulation mechanism with rearrangement of extracellular proteins that remains to be investigated. Given the myeloid origin of the OCI-AML3 line, we also hypothesized that the antibody could act as a "bridge" between our reporters and the target cell lines, through binding of the Fab antigen binding site to the CD3 region (of the TCR complex on the reporters), and binding of the Fc portion

to Fc receptors (on OCI-AML3 cells). To test this hypothesis, we incubated the target cells with a Fc blocking reagent, consisting of a polyclonal mixture of anti-CD16, anti-CD32 and anti-CD64 antibodies, or with an IgG2a isotype control (the same heavy chain of HIT3a antibody). The results led us to exclude this hypothesis, since the pre-treatment of target cells with Fc blocking reagents did not interfere with the TCR engagement and CD69 upregulation. Finally, we decided to test other anti-CD3 antibody clones, specifically OKT3 and UCHT1, to assess if the effect was restricted to HIT3a. Indeed, only HIT3a pre-activated J.RT3_TCR reporters displayed an increase in CD69 expression after co-incubation with OCI-AML3. Of note, OKT3 bears the same isotype of HIT3a (IgG2a), but still did not induce CD69 upregulation after OCI-AML3 co-incubation, further supporting the exclusion the Fc receptor hypothesis.

Surprisingly, we observed that this effect was present in the three new reporters we generated, with no restriction in terms of CDR3 regions: although the chain usage was the same (Vγ9Vδ1), two of the reporters (1.11 and 1.37) were clonotypes for the γ chains, while the δ chains were not shared. Since the reporters might have been engaged by the same unknown ligand on OCI-AML3 cells, we decided to perform the reactivity assay using MAU and LES reporters (respectively Vγ9Vδ1 and Vγ4Vδ5 TCRs), already known to recognize specific ligands, namely EphA2 and EPCR[198]. As expected and described, LES and MAU reporters promptly recognized HT29 cells in the absence of anti-CD3 pre-treatment, whereas J.RT3_TCR-1.11, -1.37 and 3.74 did not. Moreover, LES and MAU were not activated in the presence of OCI-AML3, HL-60 or GDM-1, consistent with their lack of expression of EPCR and EphA2. However, when pre-incubated with HIT3a, both LES and MAU upregulated CD69 upon co-incubation with OCI-AML3. These unexpected data open two lines of research. On one hand, we need to understand how HIT3a is impacting the reactivity assay, considering potential conformational changes selectively induced by this antibody (and not other anti-CD3 clones) in the TCR complex of the reporters. On the other hand, the fact that OCI-AML3 cells were able to activate the five reporters independently of their γ and δ CDR3 regions (or chain usage) may indicate a "superantigen"-like recognition mechanism that requires further investigation beyond the time frame of this PhD thesis.

Superantigens are molecules of bacterial or viral origin capable of inducing strong and non-specific T cell activation thanks to their binding to the framework region between the CDR3 sequences in the variable region of the TCR[336,337]. Superantigens appear to interact with less restricted structural determinants of the TCR chain when compared to antigen-restricted responses and these molecules are therefore able to stimulate a larger proportion of the T cell repertoire (up to 30%). This mechanism may have been developed as immune-escape strategy: indeed, activating a big fraction of the T cell repertoire will consequentially lead to the dilution of the specific antigen-restricted T cells within a big portion of polyclonal and antigen-unrelated T cells. It is already known as well that γδ T cells (and especially Vγ9Vδ2$^-$ T cells) can proliferate in response to stimulation with staphylococcal enterotoxins (SEs) or mediate lysis of SE pulsed target cells. Proliferative responses have been found after stimulation with SEA, SEB and TSST. So far cytotoxic γδ T cell reactivity has only been found against the highly homologous enterotoxins SEA and SEE[258].

Based on these phenomena, we envisage a molecule expressed on the OCI-AML3 cell surface that could stimulate unrelated TCRs in an antigen-unspecific manner. We further hypothesize the need for HIT3a pre-activation to favor clustering of CD3-TCR complexes on the reporter surface and thus facilitate the reporter activation through the TCR. It is known from conventional T cells that TCR clustering promotes a conformational change needed to start the signalling cascade[338]. Indeed, the monovalent engagement of TCR by peptide-MHC or anti-TCR Fab fragments failed to transmit a conformational change to the cytoplasmic region of CD3ε, whereas bivalent and multivalent engagement did. This implies that TCR ligation *per se* is not sufficient to transmit structural alterations through the TCR heterodimer to the CD3 subunits: ligand binding generates induced-fit type changes only in the variable TCR regions at the ligand-binding interface, but no alterations at the distal portions of the heterodimer, which are connected to the

CD3 units. Additionally, unlike Fab fragments of antibodies against TCR, Fab fragments of the CD3 antibodies OKT3 and UCHT1 induced the conformational change by binding directly to CD3ε[338].

In sum, the data presented in this chapter currently supports a working model in which the HIT3a mAb pretreatment on our different reporter lines favors CD3-TCR complex clustering needed to recognize a "superantigen"-like molecule on the OCI-AML3 cell surface, with no involvement of the CDR3 region, and thereby overcoming the need of clonal-specific ligands. This line of research requires further investigation in a joint and continued effort between our laboratory and our collaborators'.

5 General discussion and future perspectives

Vδ1$^+$ lymphocytes are among the first T cells to develop in the human foetus and are the predominant γδ T cell subset in thymus and tissues after birth. During foetal life TRDV1 expression predominates between 15 and 16 weeks and together with TRDV2 are more strongly expressed than TRDV3 transcripts between 17 and 22 weeks. Only at 33 week gestation, the TRDV2 transcripts become predominant[339]. Vδ1$^+$ T cell generation increases later in gestation and, as consequence, Vδ1$^+$ T cells comprise the majority of the γδ repertoire in cord blood[48,49] and in paediatric thymus[142]. On the other hand, within the postnatal thymus, TRDV1 expression is predominant, with low expression of TRDV2. In turn, the post-birth γδ T cell output is mainly constituted by cells of the Vδ1$^+$ subset. However, contrarily to what might be expected from these statements, the most abundant γδ subset in adults is Vγ9δ2$^+$. The dramatic postnatal numerical expansion of Vγ9Vδ2$^+$ T cells likely occurs following microbial exposure, thanks their broad polyclonal responses to pAgs, with the Vγ9Vδ2$^+$ subset ultimately dominating the circulating γδ T cell repertoire during childhood.

With the advent of NGS technologies, new studies have provided new insights on Vδ1$^+$ T cell immunobiology. Previous studies in the literature[124], based on analyses of cord blood samples, showed that the TRDV1 repertoire is highly polyclonal and, consequently, unfocused, displaying a broad variety of Vγ chain pairings and no predominant CDR3 segments with a specific length. This is in stark contrast to Vγ9Vδ2 cells, which already includes prevalent public Vγ9-JγP clonotypes that will be present throughout life[52]. With our study, applying NGS to highly (FACS-)purified Vδ1$^+$ T cells from paediatric thymic samples, we contributed to the field providing a new layer of information about the TRGV and TRDV repertoires during early stages of human life. However, if our results confirmed what was described about the repertoires from cord blood samples, we also revealed unsuspected aspects of the rearranged and expressed (at the mRNA level) TRG and TRD repertoires of Vδ1$^+$ cells, with the presence of a big fraction (~20%) of Vδ2 sequences in the thymic TRD repertoire of all donors that we analysed and with the most abundant and frequent thymic clonotypes bearing TRDV2 sequences. In stark contrast to the TRDV repertoires from blood-derived Vδ1$^+$ cells, this large fraction of TRDV2 sequences in the thymic Vδ1$^+$ samples cannot be explained with contamination during the experimental procedures. Moreover, these TRDV2 sequences are predicted to be functional and do not include the common rearrangement with the VγJP segment, thus excluding a foetal or blood origin. At this point we can only speculate that the high amount of TRDV2 sequences could be linked to biallelic expression of δ-chains[309,317]. Although it has been reported that γδ T cells might be capable to express two functional TCR with different γ-chains[318], we rather assume that the second allele might be silenced post-transcriptionally. However, to address these open questions systematically it would require a rather challenging protein or mRNA analysis at the single-cell level (or derived clones). Thus, the hypothesis that there would necessarily be a Vδ2$^+$ single chain or heterodimer retained intracellularly, in order to allow the Vδ1$^+$ TCR to be uniquely expressed on the cell surface deserves future investigation.

From a more global standpoint, and as already described for total (unsorted) γδ thymocytes[312] and their αβ counterparts[319], our results showed that the thymic Vδ1$^+$ TCR repertoire has signatures of naïve repertoires[124], being unbiased and unfocused, with no skewing towards some clonotypes. Moreover, we also showed for the first time that Vδ1$^+$ thymocytes (as peripheral blood and cord blood Vδ1$^+$ T cells) display private TRDV repertoires, in contraposition to their TRGV counterparts that showed a fraction of common (shared among individuals) sequences[122,124]. Additional studies will be needed in order to understand whether the public TRG clonotypes are selected upon ligand encounter in the thymus; or simply the output of a favoured TCR rearrangement. This, in fact, is an open question also on the Vγ9-JPVδ2 rearrangement that is prevalent in foetal life[41].

Finally, besides showing new aspects of the TRDV1 thymocyte repertoire, our study qualified previous conclusions on the TCR repertoire of human thymic γδ T cells. Recently and for the first time, TRGV and TRDV repertoire diversity was recently during TCRγδ$^+$ T cell ontogeny and, specifically, in thymic samples[312]. Indeed, Kallemejin and colleagues demonstrated that thymic γδ$^+$ T cell repertoires (as well as cord blood-derived repertoires) showed a broad, diverse repertoire in samples with Gaussian CDR3-length distributions, in contrast to the more skewed repertoire in mature circulating TCRγδ$^+$ T cells in adult peripheral blood[312]. Critically, besides being in line with these findings, our results with the presence of an unexpected large fraction of TRDV2 sequences in Vδ1$^+$ thymocytes strongly advocates for the use of highly purified cell populations, ideally complemented by single-cell validation experiments, to avoid misinterpretations of NGS data in future studies.

A major goal of my thesis was to contribute to the identification of relevant tumour antigens recognized by Vδ1$^+$ T cells via their TCRVδ1, which remains a key question in the γδ T cell field[270]. We successfully established and selected Vδ1$^+$ T cell clones from healthy donors, cloned their TCRs into a J.RT3 line and thus generated TCR reporters in order to screen tumour cell lines for new Vδ1$^+$ TCR ligands, using a global methodology previously established by our collaborators in the Déchanet-Merville lab (Bordeaux, France).

The first set of reactivity assay screening did not result in any cell line that was able to activate our reporters. Only after the serendipitous addition of anti-CD3 (clone HIT3a) in culture, we designed a new protocol that included a pre-activation step prior to the co-incubation and that allowed our reporters to be activated by the OCI-AML3 cell line. We do not know what the pre-activation step induces, but we hypothesized that this step is necessary for the pre-clustering of CD3 molecules on the reporters. Further studies will be needed in this direction. Moreover, it was not possible to understand how the HIT3a antibody work in comparison to the other anti-CD3 clones (UCHT1 and OKT3) that we tested and that did not allow the reporters to recognize OCI-AML3. Indeed, there are no studies in the literature about the epitope recognized by HIT3a. In addition, we wanted to exclude the possibility of this being an experimental artefact due to the myeloid origin of OCI-AML3 and we thus performed several control experiments. In none of these, including the incubation of OCI-AML3 with IgG2a isotype or FcR blocking antibodies, we observed an alteration in the reactivity output of our reporters against OCI-AML3. Moreover, OCI-AML3 was able to activate also two unrelated reporters (LES and MAU, generated by our collaborators) after HIT3a pre-activation and even in the absence of their putative ligands. Indeed, OCI-AML3 does not express EphA2 and EPCR, ligands for the LES- and MAU-TCRs.

These evidences support our hypothesis that the HIT3a mAb pretreatment on our different reporter lines favors CD3-TCR complex clustering needed to recognize a “superantigen”-like molecule on the OCI-AML3 cell surface, with no involvement of the CDR3 region, and thereby overcoming the need of clonal-specific ligands. Interestingly, it has been recently demonstrated that a γδ TCR can directly interact with a ligand in a CDR3-independent manner. This was the case of the human Vγ4 chain whose HV4 region can recognize the CFG face of the amino-terminal IgV domain of BTNL3[340]. These findings suggested the presence of a conserved mechanism whereby the regulation of intestinal γδ IELs by BTNL proteins is mediated by an interacting chain coupled to a supporting chain that jointly determine biological activity. This might also be the case of the collaborative regulation of human PB γδ T cell responses to HMB-PP by BTN3A1 and BTN3A2. Further evidences emerged in this study showing that BTNL-responsive γδ IELs are diverse, expressing various TCRδ chains with diverse CDR3 regions. Indeed, clone-specific CDR3 regions could remain available to engage clonally restricted antigens, irrespective of the engagement of BTNL proteins. In this model, proposed by Hayday and colleagues, the γδ TCR has an intrinsic ability to use a discrete germline-encoded region to mediate innate, non-clonal responses to an endogenous agonist; and to use recombinase-dependent regions to mediate adaptive, clone-specific responses to diverse ligands. As such,

γδ T cells might use their TCRs to simultaneously engage agonists and clonally restricted ligands, potentially using HV4 to sense 'normal self' and the CDR1–CDR3 regions to sense 'stressed self'[340].

We envisage three possible approaches to identify the "superantigen"-like molecule expressed by OCI-AML3 cells – using bioinformatics, biochemistry and/ or genome-wide protein expression analysis. We have already started the design a bioinformatics approach to identify possible candidates by downloading RNA-seq data of OCI-AML3, HL-60 and GDM-1. We removed the genes that were not present in the OCI-AML3 and HL-60 datasets, we mapped the selected genes on Panther (http://www.pantherdb.org/) and made a selection for immune system related genes. At this point, we made a biased analysis selecting the genes expressed at higher levels in OCI-AML3, present in HL-60 at a lower level and absent or even lower in GDM-1 cells. We then selected genes encoding for membrane-localized proteins, obtaining a panel of 22 genes (Figure 5.1A-B). Although promising in terms of target prediction and reduction of the number of candidates, this approach needs to be further dissected and optimized in order to find more relevant candidates and proceed with knockout strategies.

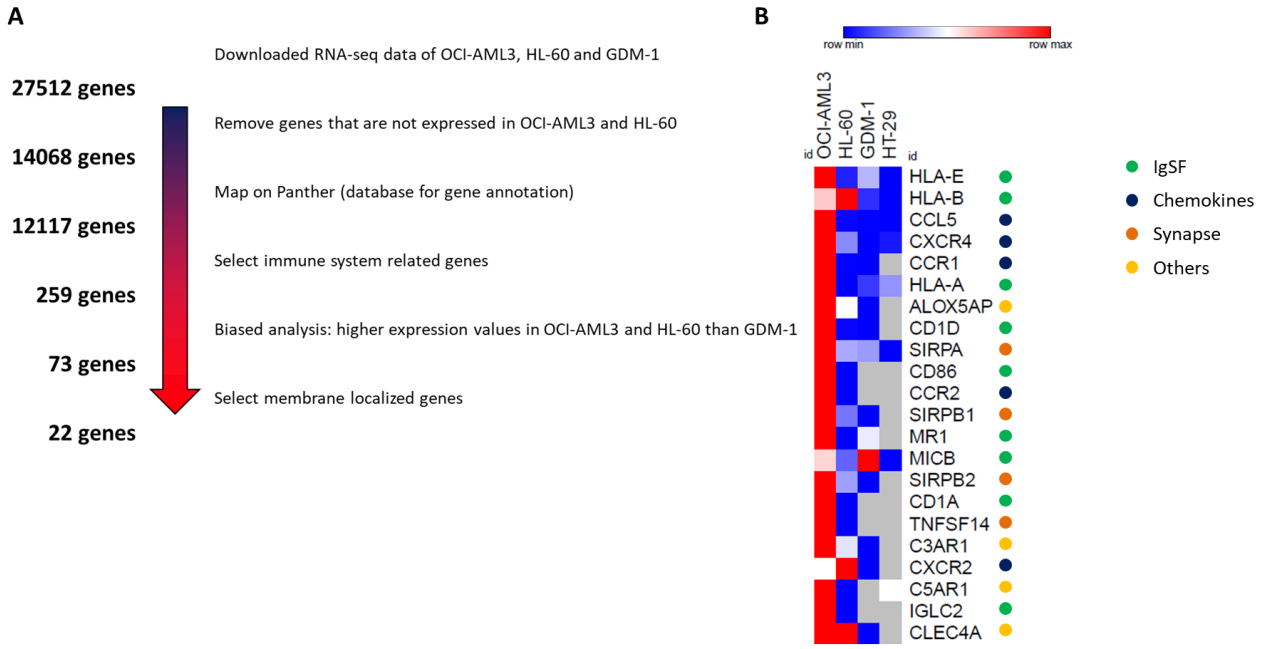

Figure 5.1 Bioinformatics approach to select candidates whose expression segregates with the reactivity (reporter) assays on tumour cell lines. (A) Starting from 27512 genes expressed in OCI-AML3, we identify a panel of 22 genes after removing genes that were present only in the GDM-1 dataset, that were not involved in immune system related mechanisms, that were highly expressed in GDM-1 and that were not encoding for membrane localized proteins. (B) The 22 genes are grouped by functions in: immunoglobulin super family genes (IgSF), chemokines, synaptic protein genes, others.

Another possible strategy to identify the potential "pan-ligand" present on OCI-AML3 cells relies on a biochemical approach as the one developed by our collaborators in the Déchanet-Merville lab (Bordeaux, franker). This method led already to the successful identification of EPCR[198] and Annexin A2[199] as ligands for specific γδ TCRs. The experimental procedure foresees the injection of the target cell line (OCI-AML3 in this case) without adjuvant into each footpad of the back legs of BALB/c mice, a boost in the same conditions 10 days later, and finally (at day 14) the collection of popliteal lymph nodes, B cell extraction and fusion with the mouse myeloma partner to generate hybridomas. After this step, hybridomas are grown until confluent and their supernatants assessed for neutralization of JRT3-OCI-AML3 reactivity. Hybridomas that secrete antibodies able to decrease or abrogate the reactivity are then cloned by limiting dilution, ending

with selection of a monoclonal antibody with robust neutralizing activity, which is used to immunoprecipitate the putative ligand on OCI-AML3 cells, followed by nLC-MS/MS analysis for its identification.

The last approach we envisage is based on a CRISPR/Cas9 genome-wide screening. CRISPR-Cas9 technology has significantly accelerated biological research, becoming routine in many laboratories. It is rapidly replacing conventional gene editing techniques and has high utility for both genome-wide and gene-focussed applications. Recently, the first individually cloned CRISPR-Cas9 genome wide arrayed sgRNA libraries covering 17,166 human genes at a complexity of 34,332 sgRNAs for the human genome has been described[341]. The libraries are arrayed in 96 micro-well plates and, in contrast to pooled libraries, allow the study of complex phenotypes. Given our interest, we would work using a cell surface protein library that targets 778 genes with up to 4 gRNA per gene target (pooled in a single well) for a total of 3,112 gRNAs (produced by ThermoFischer). This powerful tool would allow the generation of OCI-AML3 knockout lines in which the expression of a single membrane protein would be eliminated, one by one. These knockout lines would be used to test J.RT3_TCR reporter activation via CD69 upregulation.

These three approaches could theoretically contribute to the identification of the "pan-ligand" present on OCI-AML3 cells, which would be of great interest to the scientific community as it would represent a novel molecular mechanism underlying tumour cell recognition by γδ T cells, involving binding to the TCR but without occupying putative antigen-specific regions. It is thus captivating to think about a molecule expressed on the surface of tumour cells that can be recognized by the TCR independently from their CDR3 specificity, which would add further complexity to the model recently proposed by Hayday and colleagues[340].

Combining NGS TCR sequencing with single-cell TCR analyses and flow cytometric immunophenotyping can provide new insights into γδ T cell biology. Indeed, using combinations of these approaches, different Vδ1$^+$ T cell subsets in adult peripheral blood and cord blood samples have been described. Besides being unfocused, highly polyclonal and showing no biased in CDR3 length distribution, naïve Vδ1$^+$ cells were associated to the expression of multiple markers common to naïve T cells, including IL-7R, CD28, CD62L, and CCR7[124]. On the other hand, clonotypically expanded blood-derived Vδ1$^+$ T cells showed a differentiated effector CD27$^{lo/neg}$ phenotype, including expression of granzymes, perforin, and CX3CR1. Moreover, differentiated Vδ1$^+$ T cells may be involved in endothelial immunosurveillance, whereas naïve Vδ1$^+$ T cells were devoid of cytotoxic effector markers. These results from Willcox and colleagues[60,124,342] gave us some hints towards understanding the cellular dynamics upon DOT-cell expansion. Indeed, we found that the polyclonality of DOT-cell products, derived from oligoclonal *ex vivo* PB samples, stemmed from the preferential expansion of naïve CD27$^+$ Vδ1$^+$ T cells cells. Thus, the CDR3 distribution of DOT-cells resembles the Gaussian distribution typical of naïve repertoires like cord blood or thymus derived repertoires. On the other hand, the DOT-cell protocol enables the phenotypic maturation of these cells, allowing them to induce or increase the expression of several NKRs (including NKp30, NKp44, NKG2D and DNAM-1) and cytotoxicity functions (based on granzymes and perforin). Indeed, far from representing a pre-formed effector subset from birth, Vδ1$^+$ T cells are initially naïve in phenotype and feature an entirely unfocussed TCR repertoire; and their differentiation into effector lymphocytes is not an inevitable developmental process, but is linked to clonal amplification, in "adaptive-like" fashion.

Although other protocols to expand Vδ1$^+$ T cells have been described[160,161,306,343], none has achieved the yields and Vδ1$^+$ T cell enrichment of DOT-cell protocol while using clinical-grade reagents. Siegers and colleague developed in 2011 a protocol to expand Vδ1$^+$ and Vδ2$^+$ γδ T cells from peripheral blood, where

Vδ1$^+$ T cells were the predominant subset after 8-day of culture with Con A, a mitogen that binds to surface receptors on murine and human lymphocytes. At low doses, Con A is stimulatory, inducing cell growth; however, at higher doses it becomes toxic. This protocol required an initial stimulation with ConA followed by a continuous culturing in IL-2 and IL-4, producing cells with cytotoxic potential against B-CLL-derived cell lines[160,306,343]. Dokouhaki and colleagues' protocol was based on the use of cytokines and anti-CD3 antibody but led only to a maximum of 860-fold increase of total γδ with an increased fraction of Vδ1 T cells[344]. Finally, Deniger and colleagues developed an expansion protocol for polyclonal γδ T cells based on a clinical-grade artificial antigen-presenting cells (aAPC) derived from K562 tumour cells. The aAPC was used as irradiated feeders to activate and expand human γδ T cells to clinical scale; interestingly, the cellular product at the end of the expansion was constituted by polyclonal γδ T cells that demonstrated broad anti-tumour activities[212].

The DOT-cell expansion protocol was previously described in detail by Almeida and colleagues from our laboratory[114]. In stark contrast to the other methods, the DOT-cell protocol induced robust expression of the natural cytotoxicity receptors, NKp30 and NKp44, that synergized with the T cell receptor to mediate CLL targeting *in vitro*. Moreover, when transferred *in vivo*, DOT cells infiltrated tumours and peripheral organs, and persisted until the end of the analysis without showing signs of loss of function. Critically, DOT cells were capable of inhibiting tumour growth and preventing dissemination in xenograft models of CLL[114]. Importantly, even after almost 2 months in vivo, DOT TILs produced type I cytokines, IFNγ and TNFα, but no IL-17, which has been implicated in the promotion of tumour cell growth[162,310]. Also of note, the recovered DOT cells were 98% to 100% Vδ1$^+$ T cells (up from ∼65% in the initial inoculum), demonstrating that these constituted the active principle of the cellular therapy. In terms of safety, the absence of toxic effects in xenograft models is a promising indication of a favourable profile for DOT cells. However, xenograft murine models have important limitations for safety assessment, because the evaluation of cytokine release syndrome is not accurate in immunodeficient animals; and the absence of autoimmune side effects cannot be translated to human host tissues. These issues will need to be addressed in dose-escalation phase I clinical trials. Encouragingly, the clinical application of Vδ2$^+$ T cell based ACT has been reported to be free of any severe adverse effects[300].

In this thesis, we converged the properties and potential of DOT cells with the unmet immunotherapy needs of AML, thus aiming to purpose DOT cells specifically for AML treatment. Upon generating DOT cells, we found the cellular products to be composed of multiple clones with intrinsic capacity to target AML cells. Moreover, TCR blockade induced only a partial and variable reduction in the killing capacity of Vδ1$^+$ T cell clones, from 10% to 80% decrease, with most frequently a reduction of 30%, meaning that the remaining reactivity is likely mediated by natural cytotoxicity receptors[114,270,303], an hypothesis substantiated by the impact of knocking-down the NKp30 ligand, B7-H6. DOT cells also readily (within 3 hours) killed several AML cell lines and AML primary samples without targeting any normal leukocyte population (neither myeloid nor lymphoid) from the peripheral blood of healthy volunteers, including CD33$^+$ and CD123$^+$ myeloid progenitor cells targeted by the respective CAR-T cells, which cause the unwanted myeloablation[324,332].

Furthermore, we also assessed DOT cell tumoricidal function *in vivo*, in three xenograft mouse models of human AML (primary samples or cell lines, namely KG-1 and HEL). In all the tested models, DOT-cell treatment markedly reduced tumour burden and increased host survival, without any noticeable toxicity. However, the survival benefits herein obtained were smaller than the ones reported for CAR-T cells treatment of AML xenografts[331–333], although these models were biased to AML cell lines uniformly expressing the target antigens. Furthermore, and critically, xenografts cannot evaluate the toxicity of a strategy predicted to induce myeloablation in patients. Overall, we believe that the combined safety and efficacy profiles of DOT cells make them very attractive candidates for adoptive cell therapy of AML in the near future.

However, considering that the major therapeutic problem in AML at the present time is chemoresistance, which drives deadly relapses, we also asked whether DOT cells could target chemoresistant AML cells. Indeed, we demonstrated that DOT cells have the capacity of targeting AML cells previously treated with high doses of cytarabine plus doxorubicin for 72h, which led to >99% AML cell elimination. In light of this, and taking into account the highly polyclonal and multi-reactive DOT cell repertoire, we also questioned the ability of DOT cells to re-target AML cells "relapsing" after a first DOT cell treatment that also eliminated >99% tumour cells in 72h. Interestingly, DOT cells killed DOT-pre-treated AML cells as efficiently as non-treated controls, suggesting that DOT cell treatment did not select for a specific subset of DOT-resistant AML cells. Moreover, whereas chemotherapy selectively targeted approximately half of all barcoded AML single-cell lineages, DOT cells mostly preserved the clonal architecture of the AML population. These data collectively suggest that the breadth of AML targeting, based on many cytotoxic DOT cell clones, avoids the selection of resistant lineages and allows efficient re-treatment. Given the urgency of preventing the emergence of deadly refractory relapses, namely after standard chemotherapy, our work provides strong pre-clinical proof-of-concept for clinical application of DOT cells in AML treatment.

6 References

1 Hayday AC. γδ T Cells and the Lymphoid Stress-Surveillance Response. *Immunity* 2009; **31**: 184–196.

2 Janeway C jr, Medzhitov R. Innate immune recognition. *Annu Rev Immunol* 2002; **20**: 197–216.

3 Medzhitov R, Janeway C jr. Decoding the patterns of self and nonself by the innate immune system. *Science (80-)* 2002; **296**: 298–300.

4 Benoit M, Desnues B, Mege J. Macrophage polarization in bacterial infections. *J Immunol* 2008; **181**: 3733–9.

5 Medzhitov R, Janeway C jr. Innate immunity. *N Engl J Med* 2000; **343**: 338–44.

6 Kennedy A, DeLeo F. Neutrophil apoptosis and the resolution of infection. *Immunol Res* 2009; **43**: 25–61.

7 Biron C. More things in heaven and earth: defining innate and adaptive immunity. *Nat Immunol* 2010; **11**: 1080–2.

8 Cooper M, Colonna M, Yokoyama W. Hidden talents of natural killers: NK cells in innate and adaptive immunity. *EMBO Rep* 2009; **10**: 1103–10.

9 Medzhitov R, Janeway C jr. Innate immunity: impact on the adaptive immune response. *Curr Opin Immunol* 1997; **9**: 4–9.

10 Dranoff G. Cytokines in cancer pathogenesis and cancer therapy. *Nat Rev Cancer* 2004; **4**: 11–22.

11 Kondo M, Scherer D, King A, Manz M, Weissman I. Lymphocyte development from hematopoietic stem cells. *Curr Opin Genet Dev* 2001; **11**: 520–526.

12 Doulatov S, Notta F, Laurenti E, Dick J. Hematopoiesis: a human perspective. *Cell Stem Cell* 2012; **10**: 120–36.

13 Rothenberg E, Taghon T. Molecular genetics of T cell development. *Annu Rev Immunol* 2005; : 601–49.

14 Maillard I, Fang T, Pear W. Regulation of lymphoid development, differentiation, and function by the Notch pathway. *Annu Rev Immunol* 2005; : 945–74.

15 Sadlon T, Brown C, Bandara V, Hope C, Schjenken J, Pederson S *et al.* Unravelling the molecular basis for regulatory T-cell plasticity and loss of function in disease. *Clin Transl Immunol* 2018; **7**: e1011.

16 Schmidl C, Delacher M, Huehn J, Feuerer M. Epigenetic mechanisms regulating T-cell responses. *J Allergy Clin Immunol* 2018; **142**: 728–743.

17 Dong C, Martinez G. T cells: the usual subsets. *Nat Rev Immunol* 2015.https://www.nature.com/nri/posters/tcellsubsets/nri1009_tcellsubsets_poster.pdf.

18 Pardoll D, Fowlkes B, Bluestone J, Kruisbeek A, Maloy W, Coligan J *et al.* Differential expression of two distinct T-cell receptors during thymocyte development. *Nature* 1987; **326**: 79–81.

19 De Rosa SC, Andrus JP, Perfetto SP, Roederer M. Ontogeny of gamma delta T cells in humans. *J Immunol* 2004; **172**: 1637–1645.

20 Ribeiro ST, Ribot JC, Silva-Santos B. Five Layers of Receptor Signaling in γδ T-Cell Differentiation and Activation. *Front Immunol* 2015; **6**: 15.

21 Carding SR, Egan PJ. γδ T Cells: functional plasticity and heterogeneity. *Nat Rev Immunol* 2002; **2**:

336–345.

22 Janeway C jr, Travers P, Walport M, Shlomchik M. Immunobiology: The Immune System in Health and Disease. 2001.

23 Rock E, Sibbald P, Davis M, Chien Y. CDR3 length in antigen-specific immune receptors. *J Exp Med* 1994; **179**: 323–8.

24 Rock EP, Sibbald PR, Davis MM, Chien YH. CDR3 length in antigen-specific immune receptors. *J Exp Med* 1994; **179**: 323.

25 Scaviner D, Lefranc M. The human T cell receptor alpha variable (TRAV) genes. *Exp Clin Immunogenet* 2000; **17**: 83–96.

26 Folch G, Lefranc M. The human T cell receptor beta variable (TRBV) genes. *Exp Clin Immunogenet* 2000; **17**: 42–54.

27 Barbie V, Lefranc M. The human immunoglobulin kappa variable (IGKV) genes and joining (IGKJ) segments. *Exp Clin Immunogenet* 1998; **15**: 171–183.

28 Pallares N, Frippiat J, Giudicelli V, Lefranc M. The human immunoglobulin lambda variable (IGLV) genes and joining (IGLJ) segments. *Exp Clin Immunogenet* 1998; **15**: 8–18.

29 Pallares N, Lefebvre S, Contet V, Matsuda F, Lefranc MP. The human immunoglobulin heavy variable genes. *Exp Clin Immunogenet* 1999; **16**: 36–60.

30 Rabbitts TH, Lefranc MP, Stinson MA, Sims JE, Schroder J, Steinmetz M *et al.* The chromosomal location of T-cell receptor genes and a T cell rearranging gene: possible correlation with specific translocation in human T cell leukaemia. *Embo J* 1985; **4**: 1461–1465.

31 Bensmana M, Mattei M, Lefranc MP. Localization of the human T-cell receptor gamma locus (TCRG) to 7p14----p15 by in situ hybridization. *Cytogenet Cell Genet* 1991; **56**: 31–2.

32 Ghanem N, Soua Z, Zhang X, Zijun M, Zhiwei Y, Lefranc G *et al.* Polymorphism of the T-cell receptor gamma variable and constant region genes in a Chinese population. *Hum Genet* 1991; **86**: 450–6.

33 Lefranc MP, Lefranc G. *The T Cell Receptor Factsbook*. Academic Press, 2001.

34 Lefranc MP. Organization of the human T-cell receptor genes. *Eur Cytokine Netw* 1990; **1**: 121–30.

35 Thedrez A, Sabourin C, Gertner J, Devilder M, Allain-Maillet S, Fournié J *et al.* Self/non-self discrimination by human gammadelta T cells: simple solutions for a complex issue? *Immunol Rev* 2007; : 123–35.

36 Bassing C, Swat W, Alt F. The mechanism and regulation of chromosomal V(D)J recombination. *Cell* 2002; **109**: S45–S55.

37 Lafaille J, DeCloux A, Bonneville M, Takagaki Y, Tonegawa S. Junctional sequences of T cell receptor gamma delta genes: implications for gamma delta T cell lineages and for a novel intermediate of V-(D)-J joining. *Cell* 1989; **59**: 859–870.

38 Komori T, Okada A, Stewart V, Alt F. Lack of N regions in antigen receptor variable region genes of TdT-deficient lymphocytes. *Science (80-)* 1993; **261**: 1171–1175.

39 Lewis S. P nucleotide insertions and the resolution of hairpin DNA structures in mammalian cells. *Proc Natl Acad Sci U S A* 1994; **91**: 1332–1336.

40 Davis M, Bjorkman P. T-cell antigen receptor genes and T-cell recognition. *Nature* 1988; **334**: 395–402.

41 Willcox CR, Davey MS, Willcox BE. Development and Selection of the Human Vγ9Vδ2+ T-Cell Repertoire. *Front Immunol* 2018; **9**: 1501.

42 McVay L, Carding S. Extrathymic origin of human gamma delta T cells during fetal development. *J Immunol* 1996; **157**: 2873–82.

43 Morita C, Jin C, Sarikonda G, Wang H. Nonpeptide antigens, presentation mechanisms, and immunological memory of human Vgamma2Vdelta2 T cells: discriminating friend from foe through the recognition of prenyl pyrophosphate antigens. *Immunol Rev* 2007; **215**: 59–76.

44 Bukowski J, Morita C, Tanaka Y, Bloom B, Brenner M, Band H. V gamma 2V delta 2 TCR-dependent recognition of non-peptide antigens and Daudi cells analyzed by TCR gene transfer. *J Immunol* 1995; **154**: 998–1006.

45 Harly C, Guillaume Y, Nedellec S, Peigné C, Mönkkönen H, Li J *et al.* Key implication of CD277 / Butyrophilin-3 (BTN3A) in cellular stress sensing by a major human γ δ T cell subset Cassie-Marie. 2012; **3**: 1–3.

46 McVay L, Carding S, Bottomly K, Hayday A. Regulated expression and structure of T cell receptor γ/δ transcripts in human thymic ontogeny. *Embo J* 1991; **10**: 83–91.

47 Casorati G, De Libero G, Lanzavecchia A, Migone N. Molecular analysis of human γ/δ+ clones from thymus and peripheral blood. *J Exp Med* 1989; **170**: 1521–35.

48 Dimova T, Brouwer M, Gosselin F, Tassignon J, Leo O, Donner C *et al.* Effector Vγ9Vδ2 T cells dominate the human fetal γδ T-cell repertoire. *Proc Natl Acad Sci U S A* 2015; **112**: 556–565.

49 Morita C, Parker C, Brenner M, Band H. TCR usage and functional capabilities of human gamma delta T cells at birth. *J Immunol* 1994; **153**: 3979–88.

50 Ribot JC, Ribeiro ST, Correia D V, Sousa AE, Silva-Santos B. Human γδ Thymocytes Are Functionally Immature and Differentiate into Cytotoxic Type 1 Effector T Cells upon IL-2/IL-15 Signaling. *J Immunol* 2014; **192**: 2237–43.

51 Parker C, Groh V, Band H, Porcelli S, Morita C, Fabbi M *et al.* Evidence for extrathymic changes in the T cell receptor gamma/delta repertoire. *J Exp Med* 1990; **171**: 1597–612.

52 Willcox C, Davey M, Willcox B. Development and Selection of the Human Vγ9Vδ2+ T-Cell Repertoire. *Front Immunol* 2018; : 1501.

53 Davodeau F, Peyrat M, Hallet M, Gaschet J, Houde I, Vivien R *et al.* Close correlation between Daudi and mycobacterial antigen recognition by human gamma delta T cells and expression of V9JPC1 gamma/V2DJC delta-encoded T cell receptors. *J Immunol* 1993; **151**: 1214–23.

54 Davodeau F, Peyrat M, Hallet M, Houde I, Vie H, Bonneville M. Peripheral selection of antigen receptor junctional features in a major human gamma delta subset. *Eur J Immunol* 1993; **23**: 804–8.

55 Wang H, Fang Z, Morita C. Vgamma2Vdelta2 T Cell Receptor recognition of prenyl pyrophosphates is dependent on all CDRs. *J Immunol* 2010; **184**: 6209–22.

56 Delfau M, Hance A, Lecossier D, Vilmer E, Granchamp B. Restricted diversity of V gamma 9-JP rearrangements in unstimulated human gamma/delta T lymphocytes. *Eur J Immunol* 1992; **22**: 2437–43.

57 Caccamo N, Dieli F, Wesch D, Jomaa H, Eberl M. Sex-specific phenotypical and functional differences in peripheral human Vgamma9/Vdelta2 T cells. *J Leukoc Biol* 2006; **79**: 663–6.

58 Cairo C, Armstrong C, Cumming J, Deetz C, Tan M, Lu C *et al.* Impact of age, gender, and race on circulating γδ T cells. *Hum Immunol* 2010; **71**: 968–675.

59 Pauza C, Cairo C. Evolution and function of the TCR Vgamma9 chain repertoire: It's good to be public. *Cell Immunol* 2015; **296**: 22–30.

60 Davey M, Willcox C, Hunter S, Kasatskaya S, Remmerswaal E, Salim M *et al.* The human Vδ2+ T-cell compartment comprises distinct innate-like Vγ9+ and adaptive Vγ9- subsets. *Nat Commun* 2018; **9**: 1760.

61 Nielsen SCA, Boyd SD. Human adaptive immune receptor repertoire analysis-Past, present, and future. *Immunol Rev* 2018; **284**: 9–23.

62 Hozumi N, Tonegawa S. Evidence for somatic rearrangement of immunoglobulin genes coding for variable and constant regions. *Proc Natl Acad Sci U S A* 1976; **73**: 3628–32.

63 Matsuda F, Ishii K, Bourvagnet P, Kuma K, Hayashida H, Miyata T *et al.* The complete nucleotide sequence of the human immunoglobulin heavy chain variable region locus. *J Exp Med* 1998; **188**: 2152–62.

64 Tonegawa S. Somatic generation of antibody diversity. *Nature* 1983; **302**: 575–81.

65 Boyd S, Marshall E, Merker J, Maniar J, Zhang L, Sahaf B *et al.* Measurement and clinical monitoring of human lymphocyte clonality by massively parallel VDJ pyrosequencing. *Sci Transl Med* 2009; **1**: 12ra23.

66 Roskin K, Simchoni N, Liu Y, Lee J, Seo K, Hoh R *et al.* IgH sequences in common variable immune deficiency reveal altered B cell development and selection. *Sci Transl Med* 2015; **7**: 302ra135.

67 Yassai M, Naumov Y, Naumova E, Gorski J. A clonotype nomenclature for T cell receptors. *Immunogenetics* 2009; **61**: 493–502.

68 Pillai S, Gopalan V, Lam A. Review of sequencing platforms and their applications in phaeochromocytoma and paragangliomas. *Crit Rev Oncol Hematol* 2017; **116**: 58–67.

69 Alamyar E, Duroux P, Lefranc MP, Giudicelli V. IMGT(®) tools for the nucleotide analysis of immunoglobulin (IG) and T cell receptor (TR) V-(D)-J repertoires, polymorphisms, and IG mutations: IMGT/V-QUEST and IMGT/HighV-QUEST for NGS. *Methods Mol Biol* 2012; **882**: 569–604.

70 Ye J, Ma N, Madden T, Ostell J. IgBLAST: an immunoglobulin variable domain sequence analysis tool. *Nucleic Acids Res* 2013; : W34-40.

71 Bolotin D, Poslavsky S, Mitrophanov I, Shugay M, Mamedov I, Putintseva E *et al.* MiXCR: software for comprehensive adaptive immunity profiling. *Nat Methods* 2015; **12**: 380–1.

72 Benson D, Cavanaugh M, Clark K, Karsch-Mizrachi I, Lipman D, Ostell J *et al.* GenBank. *Nucleic Acids Res* 2013; : D36-42.

73 Shugay M, Bagaev D V., Turchaninova MA, Bolotin DA, Britanova O V., Putintseva E V. *et al.* VDJtools: Unifying Post-analysis of T Cell Receptor Repertoires. *PLoS Comput Biol* 2015; **11**: e1004503.

74 Nazarov VI, Pogorelyy M V., Komech EA, Zvyagin I V., Bolotin DA, Shugay M *et al.* tcR: An R package for T cell receptor repertoire advanced data analysis. *BMC Bioinformatics* 2015; **16**: 175.

75 Oksanen J, Blanchet F, Friendly M, Kindt R, Legendre P, McGlinn D *et al.* Vegan: community ecology package. R Package version 2.5-2. 2018.https://cran.r-project.org/package=vegan.

76 Tennekes M, Ellis P. treemap: Treemap Visualization. Version 2.4-2. 2017.https://cran.r-project.org/package=treemap.

77 Siegers GM, Swamy M, Fernández-Malavé E, Minguet S, Rathmann S, Guardo AC *et al.* Different composition of the human and the mouse γδ T cell receptor explains different phenotypes of CD3γ and CD3δ immunodeficiencies. *J Exp Med* 2007; **204**: 2537–2544.

78 Kuhns M, Badgandi H. Piecing together the family portrait of TCR-CD3 complexes. *Immunol Rev* 2012; **250**.

79 Tan Y, Manz B, Freedman T, Zhang C, Shokat K, Weiss A. Inhibition of the kinase Csk in thymocytes reveals a requirement for actin remodeling in the initiation of full TCR signaling. *Nat Immunol* 2014; **15**: 186–94.

80 Smith-Garvin J, Koretzky G, Jordan M. T cell activation. *Annu Rev Immunol* 2009; : 591–619.

81 Cipriani B, Knowles H, Chen L, Battistini L, Brosnan C. Involvement of classical and novel protein kinase C isoforms in the response of human Vγ9Vδ2 T cells to phosphate antigens. *J Immunol* 2002; **169**: 5761–70.

82 Correia D, d'Orey F, Cardoso B, Lança T, Grosso A, deBarros A *et al.* Highly Active Microbial Phosphoantigen Induces Rapid yet Sustained MEK/Erk- and PI-3K/Akt-Mediated Signal Transduction in Anti-Tumor Human γδ T-Cells. *PLoS One* 2009; **4**: e5657.

83 Nedellec S, Bonneville M, Scotet E. Human Vγ9Vδ2 T cells: from signals to functions. *Semin Immunol* 2010; **22**: 199–206.

84 Nedellec S, Sabourin C, Bonneville M, Scotet E. NKG2D costimulates human V gamma 9V delta 2 T cell antitumor cytotoxicity through protein kinase C theta-dependent modulation of early TCR-induced calcium and transduction signals. *J Immunol* 2010; **185**: 55–63.

85 Ribot J, deBarros A, Silva-Santos B. Searching for 'signal 2': costimulation requirements of γδ T cells. *Cell Mol Life Sci* 2011; **68**: 2345–55.

86 Ribot J, deBarros A, Mancio-Silva L, Pamplona A, Silva-Santos B. B7-CD28 costimulatory signals control the survival and proliferation of murine and human γδ T cells via IL-2 production. *J Immunol* 2012; **189**: 1202–8.

87 Lafont V, Liautard J, Gross A, Liautard J, Favero J. Tumor necrosis factor-alpha production is differently regulated in gamma delta and alpha beta human T lymphocytes. *J Biol Chem* 2000; **275**: 19282–7.

88 deBarros A, Chaves-Ferreira M, d'Orey F, Ribot J, Silva-Santos B. CD70-CD27 interactions provide survival and proliferative signals that regulate T cell receptor-driven activation of human γδ peripheral blood lymphocytes. *Eur J Immunol* 2011; **41**: 195–201.

89 Ferrarini M, Delfanti F, Gianolini M, Rizzi C, Alfano M, Lazzarin A *et al.* NF-kappa B modulates sensitivity to apoptosis, proinflammatory and migratory potential in short- versus long-term cultured human γδ lymphocytes. *J Immunol* 2008; **181**: 5857–64.

90 Biswas P, Rovere P, De Filippi C, Heltai S, Smith C, Dagna L *et al.* Engagement of CD30 shapes the secretion of cytokines by human gamma delta T cells. *Eur J Immunol* 2000; **30**: 2172–80.

91 Maniar A, Zhang X, Lin W, Gastman B, Pauza C, Strome S *et al.* Human gammadelta T lymphocytes induce robust NK cell-mediated antitumor cytotoxicity through CD137 engagement. *Blood* 2010; **116**: 1726–33.

92 Shao Z, Schwarz H. CD137 ligand, a member of the tumor necrosis factor family, regulates immune responses via reverse signal transduction. *J Leukoc Biol* 2011; **89**: 21–9.

93 Michel M, Pang D, Haque S, Potocnik A, Pennington D, Hayday A. Interleukin 7 (IL-7) selectively promotes mouse and human IL-17-producing γδ cells. *Proc Natl Acad Sci U S A* 2012; **109**: 17549–54.

94 Papotto P, Ribot J, Silva-Santos B. IL-17+ γδ T cells as kick-starters of inflammation. *Nat Immunol* 2017; **18**: 604–611.

95 Yamaguchi T, Suzuki Y, Katakura R, Ebina T, Yokoyama J, Fujimiya Y. Interleukin-15 effectively potentiates the in vitro tumor-specific activity and proliferation of peripheral blood gammadeltaT cells isolated from glioblastoma patients. *Cancer Immunol Immunother* 1998; **47**: 97–103.

96 Garcia V, Jullien D, Song M, Uyemura K, Shuai K, Morita C *et al.* IL-15 enhances the response of human gamma delta T cells to nonpeptide microbial antigens. *J Immunol* 1998; **160**: 4322–6.

97 Li H, Pauza C. HIV envelope-mediated, CCR5/α4β7-dependent killing of CD4-negative γδ T cells which are lost during progression to AIDS. *Blood* 2011; **118**: 5824–31.

98 Casetti R, Perretta G, Taglioni A, Mattei M, Colizzi V, Dieli F *et al.* Drug-induced expansion and differentiation of V gamma 9V delta 2 T cells in vivo: the role of exogenous IL-2. *J Immunol* 2005; **175**: 1593–8.

99 Li W, Kubo S, Okuda A, Yamamoto H, Ueda H, Tanaka T *et al.* Effect of IL-18 on expansion of gammadelta T cells stimulated by zoledronate and IL-2. *J Immunother* 2010; **33**: 287–96.

100 Tsuda J, Li W, Yamanishi H, Yamamoto H, Okuda A, Kubo S *et al.* Involvement of CD56brightCD11c+ cells in IL-18-mediated expansion of human γδ T cells. *J Immunol* 2011; **186**: 2003–12.

101 Thedrez A, Harly C, Morice A, Salot S, Bonneville M, Scotet E. IL-21-mediated potentiation of antitumor cytolytic and proinflammatory responses of human V gamma 9V delta 2 T cells for adoptive immunotherapy. *J Immunol* 2009; **182**: 3423–31.

102 Moens E, Brouwer M, Dimova T, Goldman M, Willems F, Vermijlen D. IL-23R and TCR signaling drives the generation of neonatal Vgamma9Vdelta2 T cells expressing high levels of cytotoxic mediators and producing IFN-gamma and IL-17. *J Leukoc Biol* 2011; **89**: 743–52.

103 Caccamo N, La Mendola C, Orlando V, Meraviglia S, Todaro M, Stassi G *et al.* Differentiation, phenotype, and function of interleukin-17-producing human Vγ9Vδ2 T cells. *Blood* 2011; **118**: 129–38.

104 Ness-Schwickerath K, Jin C, Morita C. Cytokine requirements for the differentiation and expansion of IL-17A- and IL-22-producing human Vgamma2Vdelta2 T cells. *J Immunol* 2010; **184**: 7268–80.

105 Bansal R, Mackay C, Moser B, Eberl M. IL-21 enhances the potential of human γδ T cells to provide B-cell help. *Eur J Immunol* 2012; **42**: 110–9.

106 Caccamo N, Todaro M, La Manna M, Sireci G, Stassi G, Dieli F. IL-21 regulates the differentiation of a human γδ T cell subset equipped with B cell helper activity. *PLoS One* 2012; **7**: e41940.

107 Gasser S, Orsuliic S, Brown E, Raulet D. The DNA damage pathway regulates innate immune system ligands of the NKG2D receptor. *Nature* 2005; **436**: 1186–90.

108 Champsaur M, Lanier L. Effect of NKG2D ligand expression on host immune responses. *Immunol Rev* 2010; **235**: 237–85.

109 Correia D, Lopes A, Silva-Santos B. Tumor cell recognition by γδ T lymphocytes: T-cell receptor vs. NK-cell receptors. *Oncoimmunology* 2013; **2**: e22892.

110 Das H, Groh V, Kujil C, Sugita M, Morita C, Spies T *et al.* MICA engagement by human Vgamma2Vdelta2 T cells enhances their antigen-dependent effector function. *Immunity* 2001; **15**: 83–93.

111 Rincon-Orozco B, Kunzmann V, Wrobel P, Kabelitz D, Steinle A, Hermann T. Activation of V gamma 9V delta 2 T cells by NKG2D. *J Immunol* 2005; **175**: 2144–51.

112 Lança T, Correia D, Moita C, Raguel H, Neves-Costa A, Ferreira C *et al.* The MHC class Ib protein ULBP1 is a nonredundant determinant of leukemia/lymphoma susceptibility to gammadelta T-cell

cytotoxicity. *Blood* 2010; **115**: 2407–11.

113 Toutirais O, Cabillic F, Le Friec G, Salot S, Loyer P, Le Gallo M *et al.* DNAX accessory molecule-1 (CD226) promotes human hepatocellular carcinoma cell lysis by Vgamma9Vdelta2 T cells. *Eur J Immunol* 2009; **39**: 1361–8.

114 Almeida AR, Correia D V., Fernandes-Platzgummer A, Silva CL da, Silva MG da, Anjos DR *et al.* Delta One T cells for immunotherapy of chronic lymphocytic leukemia: clinical-grade expansion/differentiation and preclinical proof-of-concept. *Clin Cancer Res* 2016; **22**: 5795–5804.

115 Iwasaki M, Tanaka Y, Kobayashi H, Murata-Hirai K, Miyabe H, Sugie T *et al.* Expression and function of PD-1 in human γδ T cells that recognize phosphoantigens. *Eur J Immunol* 2011; **41**: 345–55.

116 Kulpa D, Lawani M, Cooper A, Peretz Y, Aslers J, Sékaly R. PD-1 coinhibitory signals: the link between pathogenesis and protection. *Semin Immunol* 2013; **25**: 219–27.

117 Pedoeem A, Azoulay-Alfaquter I, Strazza M, Silverman G, Mor A. Programmed death-1 pathway in cancer and autoimmunity. *Clin Immunol* 2014; **153**: 145–52.

118 McGrath M, Najafian N. The role of coinhibitory signaling pathways in transplantation and tolerance. *Front Immunol* 2012; : 47.

119 Gertner-Dardenne J, Fauriat C, Orlanducci F, Thibult M, Pastor S, Fitzgibbon J *et al.* The co-receptor BTLA negatively regulates human Vγ9Vδ2 T-cell proliferation: a potential way of immune escape for lymphoma cells. *Blood* 2013; **122**: 922–31.

120 Morris GP, Allen PM. How the TCR balances sensitivity and specificity for the recognition of self and pathogens. *Nat Immunol* 2012; **13**: 121–128.

121 Pitard V, Roumanes D, Lafarge X, Couzi L, Garrigue I, Lafon M *et al.* Long-term expansion of effector/memory Vδ2- γδ T cells is a specific blood signature of CMV infection. *Blood* 2008; **112**: 1317–24.

122 Ravens S, Schultze-Florey C, Raha S, Sandrock I, Drenker M, Oberdorfer L *et al.* Human γδ T cells are quickly reconstituted after stem-cell transplantation and show adaptive clonal expansion in response to viral infection. *Nat Immunol* 2017; **18**: 393–401.

123 Hunter S, Willcox C, Davey M, Kasatskaya S. Human liver infiltrating γδ T cells are composed of clonally expanded circulating and tissue-resident populations. *J Hepatol* 2018. doi:10.1016/j.jhep.2018.05.007.

124 Davey MS, Willcox CR, Joyce SP, Ladell K, Kasatskaya SA, Mclaren JE *et al.* Clonal selection in the human Vδ1 T cell repertoire indicates γδ TCR-dependent adaptive immune surveillance. *Nat Commun* 2017; **8**: 14760.

125 Jackson KJL, Kidd MJ, Wang Y, Collins AM. The shape of the lymphocyte receptor repertoire: Lessons from the B cell receptor. *Front Immunol* 2013; **4**: 263.

126 Ciofani M, Knowles G, Wiest D, van Boehmer H, Zúñiga-Pflücker J. Stage-specific and differential notch dependency at the alphabeta and gammadelta T lineage bifurcation. *Immunity* 2006; **25**: 105–16.

127 Ciofani M, Zúñiga-Pflücker J. Determining γδ versus αß T cell development. *Nat Rev Immunol* 2010; **10**: 657–63.

128 Ishida I, Verbeek S, Bonneville M, Itohara S, Berns A, Tonegawa S. T-cell receptor gamma delta and gamma transgenic mice suggest a role of a gamma gene silencer in the generation of alpha beta T cells. *Proc Natl Acad Sci U S A* 1990; **87**: 3067–71.

129 Bonneville M, Ishida I, Mombaerts P, Katsuki M, Verbeek S, Berns A *et al.* Blockage of alpha beta T-cell development by TCR gamma delta transgenes. *Nature* 1989; **342**: 931–4.

130 Kreslavsky T, Garbe A, Krueger A, von Boehmer H. T cell receptor-instructed alphabeta versus gammadelta lineage commitment revealed by single-cell analysis. *J Exp Med* 2008; **205**: 1173–86.

131 Wong G, Zúñiga-Pflücker J. Gammadelta and alphabeta T cell lineage choice: resolution by a stronger sense of being. *Semin Immunol* 2010; **22**: 228–36.

132 Terrence K, Pavlovich C, Matechak E, Fowlkes B. Premature expression of T cell receptor (TCR)alphabeta suppresses TCRgammadelta gene rearrangement but permits development of gammadelta lineage T cells. *J Exp Med* 2000; **192**: 537–48.

133 Haks M, Lefebvre J, Lauritsen J, Carleton M, Rhodes M, Miyazaki T *et al.* Attenuation of gammadeltaTCR signaling efficiently diverts thymocytes to the alphabeta lineage. *Immunity* 2005; **22**: 595–606.

134 Hayes S, Love P. Distinct structure and signaling potential of the gamma delta TCR complex. *Immunity* 2002; **16**: 827–38.

135 Hayes S, Li L, Love P. TCR signal strength influences alphabeta/gammadelta lineage fate. *Immunity* 2005; **22**: 583–93.

136 Lauritsen J, Wong G, Lee S, Lefebvre J, Ciofani M, Rhodes M *et al.* Marked induction of the helix-loop-helix protein Id3 promotes the gammadelta T cell fate and renders their functional maturation Notch independent. *Immunity* 2009; **31**: 565–75.

137 Takeuchi A, Yamasaki S, Takase K, Nakatsu F, Arase H, Onodera M *et al.* E2A and HEB activate the pre-TCR alpha promoter during immature T cell development. *J Immunol* 2001; **167**: 2157–63.

138 Mahtani-Patching J, Neves J, Pang D, Stoenchev K, Aguirre-Blanco A, Silva-Santos B *et al.* PreTCR and TCRγδ signal initiation in thymocyte progenitors does not require domains implicated in receptor oligomerization. *Sci Signal* 2011; **4**: ra47.

139 Kreslavsky T, von Boehmer H. gammadeltaTCR ligands and lineage commitment. *2010* 22AD; **4**.

140 Zarin P, Wong G, Mohtashami M, Wiest D, Zúñiga-Pflücker J. Enforcement of γδ-lineage commitment by the pre-T-cell receptor in precursors with weak γδ-TCR signals. *Proc Natl Acad Sci U S A* 2014; **111**: 5658–63.

141 Zarin P, Chen E, In T, Anderson M, Zúñiga-Pflücker J. Gamma delta T-cell differentiation and effector function programming, TCR signal strength, when and how much? *Cell Immunol* 2015; **296**: 70–5.

142 Ribot JC, Ribeiro ST, Correia D V., Sousa AE, Silva-Santos B. Human thymocytes are functionally immature and differentiate into cytotoxic type 1 effector T cells upon IL-2/IL-15 signaling. *J Immunol* 2014; **192**: 2237–2243.

143 Gibbons D, Hague S, Silberzahn T, Hamilton K, Langford C, Ellis P *et al.* Neonates harbour highly active gammadelta T cells with selective impairments in preterm infants. *Eur J Immunol* 2009; **39**: 1794–806.

144 Dieli F, Poccia F, Lipp M, Sireci G, Caccamo N, Di Sano C *et al.* Differentiation of Effector/Memory Vδ2 T Cells and Migratory Routes in Lymph Nodes or Inflammatory Sites. *J Exp Med* 2003; **198**: 391–7.

145 Cheng C, Wang B, Gao L, Liu J, Chen X, Huang H *et al.* Next generation sequencing reveals changes of the γδ T cell receptor repertoires in patients with pulmonary tuberculosis. *Sci Rep* 2018; **8**: 3956.

146 Déchanet J, Merville P, Lim A, Retière C, Pitard V, Lafarge X *et al.* Implication of γδ T cells in the

human immune response to cytomegalovirus. *J Clin Invest* 1999; **103**: 1437–1449.

147 Déchanet J, Merville P, Berge F, Bone-mane G, Taupin J, Michel P *et al.* Major expansion of gammadelta T lymphocytes following cytomegalovirus infection in kidney allograft recipients. *J Infect Dis* 1999; **179**: 1–8.

148 Hinz T, Wesch D, Friese K, Reckziegel A, Arden B, Kabelitz D. T cell receptor gamma delta repertoire in HIV-1-infected individuals. *Eur J Immunol* 1994; **24**: 3044–9.

149 Knight A, Madrigal A, Grace S, Sivakumaran J, Kottaridis P, Mackinnon S *et al.* The role of Vδ2-negative γδ T cells during cytomegalovirus reactivation in recipients of allogeneic stem cell transplantation. *Blood* 2010; **116**: 2164–72.

150 Bonneville M, O'Brien RL, Born WK. γδ T cell effector functions: a blend of innate programming and acquired plasticity. *Nat Rev Immunol* 2010; **10**: 467–478.

151 Gomes A, Martin D, Silva-Santos B. Targeting γδ T lymphocytes for cancer immunotherapy: from novel mechanistic insight to clinical application. *Cancer Res* 2010; **70**: 10024–7.

152 Korematsu S, Tanaka Y, Nagakura T, Minato N, Izumi T. Human gammadelta T cells modulate the mite allergen-specific T-helper type 2-skewed immunity. *Clin Exp Allergy* 2007; **1681**–**7**.

153 Rei M, Pennington D, Silva-Santos B. The emerging Protumor role of γδ T lymphocytes: implications for cancer immunotherapy. *Cancer Res* 2015; **75**: 798–802.

154 Duault C, Betous D, Bezombes C, Roga S, Cayrol C, Girard J *et al.* IL-33-expanded human Vγ9Vδ2 T cells have anti-lymphoma effect in a mouse tumor model. *Eur J Immunol* 2017; **47**: 2137–2141.

155 Born W, Jin N, Aydintug M, Wands J, French J, Roark C *et al.* γδ T Lymphocytes—Selectable Cells Within the Innate System? *J Clin Immunol* 2007; **27**: 133–44.

156 Jameson J, Havran WL. Skin γδ T-cell functions in homeostasis and wound healing. *Immunol Rev* 2007; **215**: 114–122.

157 Moser B, Eberl M. gammadelta T cells: novel initiators of adaptive immunity. *Immunol Rev* 2007; : 89–102.

158 Gentles A, Newman A, Liu C, Bratman S, Feng W, Kim D *et al.* The prognostic landscape of genes and infiltrating immune cells across human cancers. *Nat Med* 2015; **21**: 938–945.

159 Di Carlo E, Bocca P, Emionite L, Cilli M, Cipollone G, Morandi F *et al.* Mechanisms of the antitumor activity of human Vγ9Vδ2 T cells in combination with zoledronic acid in a preclinical model of neuroblastoma. *Mol Ther* 2013; **21**: 1034–43.

160 Siegers G, Dhamko H, Wang X, Mathieson A, Kosaka Y, Felizardo T *et al.* Human Vδ1 γδ T cells expanded from peripheral blood exhibit specific cytotoxicity against B-cell chronic lymphocytic leukemia-derived cells. *Cytotherapy* 2011; **13**: 753–64.

161 Siegers GM, Lamb LS. Cytotoxic and Regulatory Properties of Circulating Vδ1+ γδ T Cells: A New Player on the Cell Therapy Field? *Mol Ther* 2014; **22**: 1416–1422.

162 Wu P, Wu D, Ni C, Ye J, Chen W, Hu G *et al.* γδT17 cells promote the accumulation and expansion of myeloid-derived suppressor cells in human colorectal cancer. *Immunity* 2014; **40**: 785–800.

163 Lafont V, Sanchez F, Laprevotte E, Michaud H-A, Gros L, Eliaou J-F *et al.* Plasticity of γδ T Cells: Impact on the Anti-Tumor Response. *Front Immunol* 2014; **5**: 622.

164 Lo Presti E, Dieli F, Meraviglia S. Tumor-Infiltrating γδ T Lymphocytes: Pathogenic Role, Clinical Significance, and Differential Programing in the Tumor Microenvironment. *Front Immunol* 2014; **5**: 607.

165 Zhao Y, Niu C, Cui J. Gamma-delta (γδ) T cells: friend or foe in cancer development? *J Transl Med* 2018; **16**: 3.

166 Niu C, Jin H, Li M, Xu J, Xu D, Hu J *et al.* In vitro analysis of the proliferative capacity and cytotoxic effects of ex vivo induced natural killer cells, cytokine-induced killer cells, and gamma-delta T cells. *BMC Immunol* 2015; : 61.

167 Alexander A, Maniar A, Cumming J, Hebbeler A, Schulze D, Gastman B *et al.* Isopentenyl pyrophosphate-activated CD56+ {gamma}{delta} T lymphocytes display potent antitumor activity toward human squamous cell carcinoma. *Clin Cancer Res* 2008; **14**: 4232–40.

168 Viey E, Fromont G, Escudier B, Morel Y, Da Rocha S, Chouaib S *et al.* Phosphostim-activated gamma delta T cells kill autologous metastatic renal cell carcinoma. *J Immunol* 2005; **174**: 1338–47.

169 Todaro M, D'Asaro M, Caccamo N, Iovino F, Francipane MG, Meraviglia S *et al.* Efficient killing of human colon cancer stem cells by gammadelta T lymphocytes. *J Immunol* 2009; **182**: 7287–96.

170 Dieli F, Vermijlen D, Fulfaro F, Caccamo N, Meraviglia S, Cicero G *et al.* Targeting human {gamma}delta} T cells with zoledronate and interleukin-2 for immunotherapy of hormone-refractory prostate cancer. *Cancer Res* 2007; **67**: 7450–7.

171 Fisher J, Yan M, Heuijerjans J, Carter L, Abolhassani A, Frosch J *et al.* Neuroblastoma killing properties of Vδ2 and Vδ2-negative γδT cells following expansion by artificial antigen-presenting cells. *Clin Cancer Res* 2014; **20**: 5720–32.

172 Couzi L, Pitard V, Sicard X, Garrigue I, Hawchar O, Merville P *et al.* Antibody-dependent anti-cytomegalovirus activity of human γδ T cells expressing CD16 (FcγRIIIa). *Blood* 2012; **119**: 1418–27.

173 Ramstead A, Jutila M. Complex role of γδ T-cell-derived cytokines and growth factors in cancer. *J Interf Cytokine Res* 2012; **32**: 563–9.

174 Gao Y, Yang W, Pan M, Scully E, Girardi M, Augenlicht L *et al.* Gamma delta T cells provide an early source of interferon gamma in tumor immunity. *J Exp Med* 2003; **198**: 433–42.

175 Li H, Luo K, Pauza C. TNF-alpha is a positive regulatory factor for human Vgamma2 Vdelta2 T cells. *J Immunol* 2008; **181**: 7137–7.

176 Muto M, Baghdadi M, Maekawa R, Wada H, Seino K. Myeloid molecular characteristics of human γδ T cells support their acquisition of tumor antigen-presenting capacity. *Cancer Immunol Immunother* 2015; **64**: 941–9.

177 Brandes M, Willimann K, Moser B. Professional antigen-presentation function by human gammadelta T Cells. *Science (80-)* 2005; **309**: 264–8.

178 Van Acker H, Anguille S, Van Tendeloo V, Lion E. Empowering gamma delta T cells with antitumor immunity by dendritic cell-based immunotherapy. *Oncoimmunology* 2015; **4**: e1021538.

179 Wakita D, Sumida K, Iwakura Y, Nishikawa H, Ohkuro T, Chamoto K *et al.* Tumor-infiltrating IL-17-producing gammadelta T cells support the progression of tumor by promoting angiogenesis. *Eur J Immunol* 2010; **40**: 1297–37.

180 Patil R, Shah S, Shrikhande S, Goel M, Dikshit R, Chiplunkar S. IL17 producing γδT cells induce angiogenesis and are associated with poor survival in gallbladder cancer patients. *Int J Cancer* 2016; **139**: 869–81.

181 Li J, Liu J, Mao X, Tang Q, Lu H. IL-7 receptor blockade inhibits IL-17-producing γδ cells and suppresses melanoma development. *Inflammation* 2014; **37**: 1444–52.

182 Welte T, Zhang X. Interleukin-17 Could Promote Breast Cancer Progression at Several Stages of the

Disease. *Mediat Inflamm* 2015; : 804347.

183 Sabbione F, Gabelloni M, Ernst G, Gori M, Salamone G, Oleastro M *et al.* Neutrophils suppress γδ T-cell function. *Eur J Immunol* 2014; **44**: 819–30.

184 Kalyan S, Chandrasekaran V, Quabius E, Lindhorst T, Kabelitz D. Neutrophil uptake of nitrogen-bisphosphonates leads to the suppression of human peripheral blood γδ T cells. *Cell Mol Life Sci* 2014; **71**: 2335–46.

185 Kobayashi H, Tanaka Y. γδ T Cell Immunotherapy-A Review. *Pharm* 2015; **8**: 40–61.

186 Peng G, Wang HY, Peng W, Kiniwa Y, Seo KH, Wang RF. Tumor-Infiltrating γδ T Cells Suppress T and Dendritic Cell Function via Mechanisms Controlled by a Unique Toll-like Receptor Signaling Pathway. *Immunity* 2007; **27**: 334–348.

187 Daley D, Zambirinis C, Seifert L, Akkad N, Mohan N, Werba N *et al.* γδ T Cells Support Pancreatic Oncogenesis by Restraining αβ T Cell Activation. *Cell* 2016; **166**: 1485–1499.

188 Tanaka Y, Morita C, Tanaka Y, Nieves E, Brenner M, Bloom B. Natural and synthetic non-peptide antigens recognized by human gamma delta T cells. *Nature* 1995; **375**: 155–8.

189 Weintraub B, Jackson M, Hedrick S. Gamma delta T cells can recognize nonclassical MHC in the absence of conventional antigenic peptides. *J Immunol* 1994; **153**: 3051–8.

190 Fisch P, Oettel K, Fudim N, Surfus J, Malkovsky M, Sondel P. MHC-unrestricted cytotoxic and proliferative responses of two distinct human gamma/delta T cell subsets to Daudi cells. *J Immunol* 1992; **148**: 2315–23.

191 Morita C, Beckman E, Bukowski J, Tanaka Y, Band H, Bloom B *et al.* Direct presentation of nonpeptide prenyl pyrophosphate antigens to human gamma delta T cells. *Immunity* 1995; **3**: 495–507.

192 Jomaa H, Feurle J, Luhs K, Kunzmann V, Tony H, Herderich M *et al.* Vγ9/Vδ2 T cell activation induced by bacterial low molecular mass compounds depends on the 1-deoxy-D-xylulose 5-phosphate pathway of isoprenoid biosynthesis. *FEMS Immunol Med Microbiol* 1999; **25**: 371–8.

193 Fisch P, Malkovsky M, Kovats S, Sturm E, Braakman E, Klein B *et al.* Recognition by human V gamma 9/V delta 2 T cells of a GroEL homolog on Daudi Burkitt's lymphoma cells. *Science (80-)* 1990; **250**: 1269–73.

194 Kaur I, Voss S, Gupta R, Schell K, Fisch P, Sondel P. Human peripheral gamma delta T cells recognize hsp60 molecules on Daudi Burkitt's lymphoma cells. *J Immunol* 1993; **150**: 2046–55.

195 Laad A, Thomas M, Fakih A, Chiplunkar S. Human gamma delta T cells recognize heat shock protein-60 on oral tumor cells. *Int J Cancer* 1999; **80**: 709–14.

196 Chen H, He X, Wang Z, Wu D, Zhang H, Xu C *et al.* Identification of human T cell receptor gammadelta-recognized epitopes/proteins via CDR3delta peptide-based immunobiochemical strategy. *J Biol Chem* 2008; **283**: 12528–37.

197 Scotet E, Martinez L, Grant E, Barbaras R, Jeno P, Guiraud M *et al.* Tumor recognition following Vgamma9Vdelta2 T cell receptor interactions with a surface F1-ATPase-related structure and apolipoprotein A-I. *Immunity* 2005; **22**: 71–80.

198 Willcox CR, Pitard V, Netzer S, Couzi L, Salim M, Silberzahn T *et al.* Cytomegalovirus and tumor stress surveillance by binding of a human γδ T cell antigen receptor to endothelial protein C receptor. *Nat Immunol* 2012; **13**: 872–879.

199 Marlin R, Pappalardo A, Kaminski H, Willcox CR, Pitard V, Netzer S. Sensing of cell stress by human

γδ TCR-dependent recognition of annexin A2. *Proc Natl Acad Sci U S A* 2017. doi:10.1073/pnas.1621052114.

200 Steinle A, Li P, Morris D, Groh V, Lanier L, Strong R *et al.* Interactions of human NKG2D with its ligands MICA, MICB, and homologs of the mouse RAE-1 protein family. *Immunogenetics* 2001; **53**: 279–87.

201 Bauer S, Groh V, Wu J, Steinle A, Phillips J, Lanier L *et al.* Activation of NK cells and T cells by NKG2D, a receptor for stress-inducible MICA. *Science (80-)* 1999; **285**: 727–9.

202 Groh V, Rhinehart R, Secrist H, Bauer S, Grabstein K, Spies T. Broad tumor-associated expression and recognition by tumor-derived gamma delta T cells of MICA and MICB. *Proc Natl Acad Sci U S A* 1999; **96**: 6879–84.

203 Wu J, Groh V, Spies T. T cell antigen receptor engagement and specificity in the recognition of stress-inducible MHC class I-related chains by human epithelial gamma delta T cells. *J Immunol* 2002; **169**: 1236–40.

204 Groh V, Steinle A, Bauer S, Spies T. Recognition of stress-induced MHC molecules by intestinal epithelial gammadelta T cells. *Sci 1998* 1998; **279**: 1737–40.

205 Catellani S, Poggi A, Bruzzone A, Dadati P, Ravetti JL, Gobbi M *et al.* Expansion of Vδ1 T lymphocytes producing IL-4 in low-grade non-Hodgkin lymphomas expressing UL-16 – binding proteins patients with NHL with increased circulat-. 2007; **109**: 2078–2086.

206 Poggi A, Venturino C, Catellani S, Clavio M, Miglino M, Gobbi M *et al.* Vδ1 T lymphocytes from B-CLL patients recognize ULBP3 expressed on leukemic B cells and up-regulated by trans-retinoic acid. *Cancer Res* 2004; **64**: 9172–9179.

207 Kong Y, Cao W, Xi X, Ma C, Cui L, He W. The NKG2D ligand ULBP4 binds to TCRgamma9/delta2 and induces cytotoxicity to tumor cells through both TCRgammadelta and NKG2D. *Blood* 2009; **114**: 310–7.

208 Wrobel P, Shojaei H, Schittek B, Gieseler F, Wollenberg B, Kalthoff H *et al.* Lysis of a broad range of epithelial tumour cells by human gamma delta T cells: involvement of NKG2D ligands and T-cell receptor- versus NKG2D-dependent recognition. *Scand J Immunol* 2007; **66**: 320–8.

209 Mami-Chouaib F, Del Porto P, Delorme D, Hercend T. Further evidence for a gamma/delta T cell receptor-mediated TCT.1/CD48 recognition. *J Immunol* 1991; **147**: 2864–7.

210 Dai Y, Chen H, Mo C, Cui L, He W. Ectopically expressed human tumor biomarker MutS homologue 2 is a novel endogenous ligand that is recognized by human γδ T cells to induce innate anti-tumor/virus immunity. *J Biol Chem* 2012; **287**: 16812–9.

211 Gertner-Dardenne J, Castellano R, Mamessier E, Garbit S, Kochbati E, Etienne A *et al.* Human Vγ9Vδ2 T cells specifically recognize and kill acute myeloid leukemic blasts. *J Immunol* 2012; **188**: 4701–8.

212 Deniger D, Maiti S, Mi T, Switzer K, Ramachandran V, Hurton L *et al.* Activating and propagating polyclonal gamma delta T cells with broad specificity for malignancies. *Clin Cancer Res* 2014; **20**: 5708–19.

213 Knight A, Mackinnon S, Lowdell M. Human Vdelta1 gamma-delta T cells exert potent specific cytotoxicity against primary multiple myeloma cells. *Cytotherapy* 2012; **14**: 1110–8.

214 Todaro M, Orlando V, Cicero G, Caccamo N, Meraviglia S, Stassi G *et al.* Chemotherapy sensitizes colon cancer initiating cells to Vγ9Vδ2 T cell-mediated cytotoxicity. *PLoS One* 2013; **8**: e65145.

215 Niu C, Jin H, Li M, Zhu S, Zhou L, Jin F *et al.* Low-dose bortezomib increases the expression of NKG2D and DNAM-1 ligands and enhances induced NK and γδ T cell-mediated lysis in multiple myeloma.

Oncotarget 2017; **8**: 5954–5964.

216 Chitadze G, Lettau M, Luecke S, Wang T, Jannsen O, Furst D *et al.* NKG2D- and T-cell receptor-dependent lysis of malignant glioma cell lines by human γδ T cells: Modulation by temozolomide and A disintegrin and metalloproteases 10 and 17 inhibitors. *Oncoimmunology* 2016; **5**: e1093276.

217 Peipp M, Wesch D, Oberg H, Lutz S, Muskulus A, van de Winkel J *et al.* CD20-Specific Immunoligands Engaging NKG2D Enhance γδ T Cell-Mediated Lysis of Lymphoma Cells. *Scand J Immunol* 2017; **86**: 196–206.

218 Panchamoorthy G, McLean J, Modlin R, Morita C, Ishikawa S, Brenner M *et al.* A predominance of the T cell receptor V gamma 2/V delta 2 subset in human mycobacteria-responsive T cells suggests germline gene encoded recognition. *J Immunol* 1991; **147**: 3360–9.

219 Kabelitz D, Bender A, Prospero T, Wesselborg S, Janssen O, Pechhold K. The primary response of human gamma/delta + T cells to Mycobacterium tuberculosis is restricted to V gamma 9-bearing cells. *J Exp Med* 1991; **173**: 1331–8.

220 Chen Z. Protective immune responses of major Vγ2Vδ2 T-cell subset in M. tuberculosis infection. *Curr Opin Immunol* 2016; : 105–112.

221 Martino A, Casetti R, Sacchi A, Poccia F. Central memory Vgamma9Vdelta2 T lymphocytes primed and expanded by bacillus Calmette-Guérin-infected dendritic cells kill mycobacterial-infected monocytes. *J Immunol* 2997; **179**: 3057–64.

222 Pechhold K, Wesch D, Schondelmaier S, Kabelitz D. Primary activation of V gamma 9-expressing gamma delta T cells by Mycobacterium tuberculosis. Requirement for Th1-type CD4 T cell help and inhibition by IL-10. *J Immunol* 1994; **152**: 4984–92.

223 Li B, Bassiri H, Rossman M, Kramer P, Eyuboglu A, Torres M *et al.* Involvement of the Fas/Fas ligand pathway in activation-induced cell death of mycobacteria-reactive human gamma delta T cells: a mechanism for the loss of gamma delta T cells in patients with pulmonary tuberculosis. *J Immunol* 1998; **161**: 1558–67.

224 Young J, Goodall J, Beacock-Sharp H, Gaston J. Human gamma delta T-cell recognition of Yersinia enterocolitica. *Immunology* 1997; **91**: 503–10.

225 Barisa M, Kramer A, Majani Y, Moulding D, Saraiva L, Bajaj-Elliott M *et al.* E. coli promotes human Vγ9Vδ2 T cell transition from cytokine-producing bactericidal effectors to professional phagocytic killers in a TCR-dependent manner. *Sci Rep* 2017; **7**: 2805.

226 Hara T, Mizuno Y, Takaki K, Takada H, Akeda H, Aoki T *et al.* Predominant activation and expansion of V gamma 9-bearing gamma delta T cells in vivo as well as in vitro in Salmonella infection. *J Clin Invest* 1992; **90**: 204–10.

227 Munk M, Elser C, Kaufmann S. Human γ/δ T-cell response to Listeria monocytogenes protein components in vitro. *Immunology* 1996; **87**: 230–235.

228 Jouen-Beades F, Paris E, Dieulois C, Lemeland J, Barre-Dezelus V, Marret S *et al.* In vivo and in vitro activation and expansion of gammadelta T cells during Listeria monocytogenes infection in humans. *Infect Immun* 1997; **65**: 4267–72.

229 Morita C, Mariuzza R, Brenner M. Antigen recognition by human gamma delta T cells: pattern recognition by the adaptive immune system. *Springer Semin Immunopathol* 2000; **22**: 191–217.

230 Lafarge X, Merville P, Cazin M, Berge F, Potaux L, Moreau J *et al.* Cytomegalovirus Infection in Transplant Recipients Resolves When Circulating γδ T Lymphocytes Expand, Suggesting a Protective Antiviral Role. *J Infect Dis* 2001; **184**: 533–541.

231 Sciammas R, Bluestone J. TCRgammadelta cells and viruses. *Microbes Infect* 1999; **1**: 203–12.

232 Enders P, Yin C, Martini F, Evans P, Propp N, Poccia F *et al.* HIV-mediated gammadelta T cell depletion is specific for Vgamma2+ cells expressing the Jgamma1.2 segment. *AIDS Res Hum Retroviruses* 2003; **19**: 21–9.

233 Cumming J, Cairo C, Armstrong C, Davis C, Pauza C. Impacts of HIV infection on Vgamma2Vdelta2 T cell phenotype and function: a mechanism for reduced tumor immunity in AIDS. *J Leukoc Biol* 2008; **84**: 371–9.

234 Par G, Rukavina D, Podack E, Horanvi M, Szekers-Barthò J, Hegedus G *et al.* Decrease in CD3-negative-CD8dim(+) and Vdelta2/Vgamma9 TcR+ peripheral blood lymphocyte counts, low perforin expression and the impairment of natural killer cell activity is associated with chronic hepatitis C virus infection. *J Hepatol* 2002; **37**: 514–22.

235 Agrati C, Nisii C, Oliva A, D'Offizi G, Montesano C, Pucillo L *et al.* Lymphocyte distribution and intrahepatic compartmentalization during HCV infection: a main role for MHC-unrestricted T cells. *Arch Immunol Exp* 2002; **50**: 307–16.

236 Agrati C, D'Offizi G, Narciso P, Abrignani S, Ippolito G, Colizzi V *et al.* Vdelta1 T lymphocytes expressing a Th1 phenotype are the major gammadelta T cell subset infiltrating the liver of HCV-infected persons. *Mol Med* 2001; **7**: 11–9.

237 Sathar M, York D, Gouws E, Coutsoudis A, Coovadia H. GB virus type C coinfection in HIV-infected African mothers and their infants, KwaZulu Natal, South Africa. *Clin Infect Dis* 2004; **38**: 405–9.

238 Maccario R, Revello M, Comoli P, Montagna D, Locatelli F, Gerna G. HLA-unrestricted killing of HSV-1-infected mononuclear cells. Involvement of either gamma/delta+ or alpha/beta+ human cytotoxic T lymphocytes. *J Immunol* 1993; **150**: 1437–45.

239 De Paoli P, Gennari D, Martelli P, Cavarzerani V, Comoretto R, Santini G. Gamma delta T cell receptor-bearing lymphocytes during Epstein-Barr virus infection. *J Infect Dis* 1990; **161**: 1013–6.

240 Yasukawa M, Inatsuki A, Yakushijin Y, Kobayashi Y. Human T-cell leukemia virus type I(HTLV-I) infection of T cells bearing T-cell receptor gamma delta: effects of HTLV-I infection on cytotoxicity. *Int J Cancer* 1992; **50**: 431–7.

241 Furukawa S, Sasai K, Matsubara J, Yabuta K, Hiramatsu K, Yamamoto J *et al.* Increase in T cells expressing the gamma/delta receptor and CD4+CD8+ double-positive T cells in primary immunodeficiency complicated by human T-cell lymphotropic virus type I infection. *Blood* 1992; **80**: 3253–5.

242 Sing G, Butterworth L, Chen X, Bryant A, Cooksley G. Composition of peripheral blood lymphocyte populations during different stages of chronic infection with hepatitis B virus. *J Viral Hepat* 1998; **5**: 83–93.

243 Cimini E, Viola D, Cabeza-Cabrerizo M, Romanelli A, Tumino N, Sacchi A *et al.* Different features of Vδ2 T and NK cells in fatal and non-fatal human Ebola infections. *PLoS Negl Trop Dis* 2017; **11**: e0005645.

244 De Weerd W, Twilhaar W, Kimpen J. T cell subset analysis in peripheral blood of children with RSV bronchiolitis. *Scand J Infect Dis* 1998; **30**: 77–80.

245 Aoyagi M, Shimojo N, Sekine K, Nishimuta T, Kohno Y. Respiratory syncytial virus infection suppresses IFN-gamma production of gammadelta T cells. *Clin Exp Immunol* 2003; **131**: 312–7.

246 Bieback K, Breer C, Nanan R, ter Meulen V, Schneider-Schaulies S. Expansion of human gamma/delta T cells in vitro is differentially regulated by the measles virus glycoproteins. *J Gen Virol* 2003; **84**:

1179–88.

247 Ho M, Webster H, Tongtawe P, Pattanapanyasat K, Weidanz W. Increased gamma delta T cells in acute Plasmodium falciparum malaria. *Immunol Lett* 1990; **25**: 139–41.

248 Roussilhon C, Agrapart M, Ballet J, Bensussan A. T lymphocytes bearing the gamma delta T cell receptor in patients with acute Plasmodium falciparum malaria. *J Infect Dis* 1990; **162**: 283–5.

249 Elloso M, van der Heyde H, vande Waa J, Manning D, Weidanz W. Inhibition of Plasmodium falciparum in vitro by human gamma delta T cells. *J Immunol* 1994; **153**: 1187–94.

250 Goodier M, Lundgvist C, Hammarstrom M, Troye-Blomberg M, Langhorne J. Cytokine profiles for human V gamma 9+ T cells stimulated by Plasmodium falciparum. *Parasite Immunol* 1996; **17**: 413–23.

251 Hensmann M, Kwiatkowski D. Cellular basis of early cytokine response to Plasmodium falciparum. *Infect Immun* 2001; **69**: 2364–71.

252 Burk M, Carena I, Donda A, Mariana F, Mori L, De Libero G. Functional inactivation in the whole population of human V gamma 9/V delta 2 T lymphocytes induced by a nonpeptidic antagonist. *J Exp Med* 1997; **185**: 91–7.

253 De Libero G. Sentinel function of broadly reactive human gamma delta T cells. *Immunol Today* 1997; **18**: 22–26.

254 Hintz M, Reichenberg A, Altincicek B, Bahr U, Gschwind R, Kollas A *et al.* Identification of (E)-4-hydroxy-3-methyl-but-2-enyl pyrophosphate as a major activator for human gammadelta T cells in Escherichia coli. *FEBS Lett* 2001; **509**: 317–22.

255 Eberl M, Hintz M, Reichenberg A, Kollas A, Wiesner J, Jomaa H. Microbial isoprenoid biosynthesis and human gammadelta T cell activation. *FEBS Lett* 2003; **544**: 4–10.

256 Marx S, Wesch D, Kabelitz D. Activation of human gamma delta T cells by Mycobacterium tuberculosis and Daudi lymphoma cells: differential regulatory effect of IL-10 and IL-12. *J Immunol* 1997; **158**: 2842–8.

257 Kurup S, Harty J. γδ T cells and immunity to human malaria in endemic regions. *Ann Transl Med* 2015; : S22.

258 Rust C, Koning F. γδ T cell reactivity towards bacterial superantigens. *Semin Immunol* 1993; **5**: 41–46.

259 Xi X, Han X, Li L, Zhao Z. Identification of a new tuberculosis antigen recognized by γδ T cell receptor. *Clin Vaccine Immunol* 2013; **20**: 530–9.

260 Xi X, Zhang X, Wang B, Wang J, Huang H, Cui L *et al.* A novel strategy to screen Bacillus Calmette-Guérin protein antigen recognized by γδ TCR. *PLoS One* 2011; **6**: e18809.

261 Sciammas R, Bluestone J. HSV-1 glycoprotein I-reactive TCR gamma delta cells directly recognize the peptide backbone in a conformationally dependent manner. *J Immunol* 1998; **161**: 5187–92.

262 Dai Y, Liu H, Liu Y, Zhang Y, He W. EBV transformation induces overexpression of hMSH2/3/6 on B lymphocytes and enhances γδT-cell-mediated cytotoxicity via TCR and NKG2D. *Immunology* 2018; **Epub ahead**.

263 Russano A, Bassotti G, Agea E, Bistoni O, Mazzocchi A, Morelli A *et al.* CD1-Restricted Recognition of Exogenous and Self-Lipid Antigens by Duodenal γδ+ T Lymphocytes. *J Immunol* 2007; **178**: 3620–6.

264 Uldrich AP, Le Nours J, Pellicci DG, Gherardin N a, McPherson KG, Lim RT *et al.* CD1d-lipid antigen recognition by the γδ TCR. *Nat Immunol* 2013; **14**: 1137–45.

265 Luoma AM, Castro CD, Mayassi T, Bembinster LA, Bai L, Picard D *et al.* Crystal structure of Vδ1 T cell receptor in complex with CD1d-sulfatide shows MHC-like recognition of a self-lipid by human γδ T cells. *Immunity* 2013; **39**: 1032–42.

266 Bessoles S, Ni M, Garcia-Jimenez S, Sanchez F, Lafont V. Role of NKG2D and its ligands in the anti-infectious activity of Vγ9Vδ2 T cells against intracellular bacteria. *Eur J Immunol* 2011; **41**: 1619–28.

267 Fausther-Bovendo H, Wauguier N, Cherfils-Vicini J, Cremer I, Debré P, Vieillard V. NKG2C is a major triggering receptor involved in the Vδ1 T cell-mediated cytotoxicity against HIV-infected CD4 T cells. *AIDS* 2008; **22**: 217–26.

268 Hudspeth K, Fogli M, Correia D, Mikulak J, Roberto A, Della Bella S *et al.* Engagement of NKp30 on Vδ1 T-cells induces the production of CCL3, CCL4 and CCL5 and suppresses HIV-1 replication. *Blood* 2012; **119**: 4013–6.

269 Lu Y, Li Z, Ma C, Wang H, Zheng J, Cui L *et al.* The interaction of influenza H5N1 viral hemagglutinin with sialic acid receptors leads to the activation of human γδ T cells. *Cell Mol Immunol* 2013; **10**: 463–70.

270 Simões A, Di Lorenzo B, Silva-Santos B. Molecular determinants of target cell recognition by human γδ T cells. *Front Immunol* 2018; **9**: 929.

271 De Libero G, Casorati G, Giachino C, Carbonara C, Migone N, Matzinger P *et al.* Selection by two powerful antigens may account for the presence of the major population of human peripheral gamma/delta T cells. *J Exp Med* 1991; **173**: 1311–22.

272 Pfeffer K, Schoel B, Gulle H, Kaufmann S, Wagner H. Primary responses of human T cells to mycobacteria: a frequent set of gamma/delta T cells are stimulated by protease-resistant ligands. *Eur J Immunol* 1990; **20**: 1175–9.

273 Bukowski J, Morita C, Band H, Brenner M. Crucial role of TCR gamma chain junctional region in prenyl pyrophosphate antigen recognition by gamma delta T cells. *J Immunol* 1998; **161**: 286–93.

274 Amslinger S, Hecht S, Rohdich F, Eisenreich W, Adam P, Bacher A *et al.* Stimulation of Vgamma9/Vdelta2 T-lymphocyte proliferation by the isoprenoid precursor, (E)-1-hydroxy-2-methyl-but-2-enyl 4-diphosphate. *Immunobiology* 2007; **212**: 47–55.

275 Chen Z. Multifunctional immune responses of HMBPP-specific Vγ2Vδ2 T cells in M. tuberculosis and other infections. *Cell Mol Immunol* 2013; **10**: 58–64.

276 Kunzmann V, Bauer E, Feurle J, Weissinger F, Tony H, Wilhelm M. Stimulation of gammadelta T cells by aminobisphosphonates and induction of antiplasma cell activity in multiple myeloma. *Blood* 2000; **96**: 384–92.

277 Wilhelm M, Kunzmann V, Eckstein S, Reimer P, Weissinger F, Ruediger T *et al.* Gammadelta T cells for immune therapy of patients with lymphoid malignancies. *Blood* 2003; **102**: 200–6.

278 Das H, Wang L, Kamath A, Bukowski J. Vgamma2Vdelta2 T-cell receptor-mediated recognition of aminobisphosphonates. *Blood* 2001; **98**: 1616–8.

279 Thompson K, Rogers M. Statins prevent bisphosphonate-induced gamma,delta-T-cell proliferation and activation in vitro. *J Bone Min Res* 2004; **19**: 278–88.

280 Vavassori S, Kumar A, Wan GS, Ramanjaneyulu GS, Cavallari M, El Daker S *et al.* Butyrophilin 3A1 binds phosphorylated antigens and stimulates human γδ T cells. *Nat Immunol* 2013; **14**: 908–16.

281 Sandstrom A, Peigné C-M, Léger A, Crooks JE, Konczak F, Gesnel M-C *et al.* The intracellular B30.2 domain of butyrophilin 3A1 binds phosphoantigens to mediate activation of human Vγ9Vδ2 T cells. *Immunity* 2014; **40**: 490–500.

282 Peigné C, Léger A, MC G, Konczak F, Olive D, Bonneville M *et al.* The Juxtamembrane Domain of Butyrophilin BTN3A1 Controls Phosphoantigen-Mediated Activation of Human Vγ9Vδ2 T Cells. *J Immunol* 2017; **198**: 4228–4234.

283 Gu S, Sachleben J, Boughter C, Nawrocka W, Borowska M, Tarrasch J *et al.* Phosphoantigen-induced conformational change of butyrophilin 3A1 (BTN3A1) and its implication on Vγ9Vδ2 T cell activation. *Proc Natl Acad Sci U S A* 2017; **114**: E7311-20.

284 Sebestyen Z, Scheper W, Vyborova A, Gu S, Rychnavska Z, Schiffler M *et al.* RhoB Mediates Phosphoantigen Recognition by Vγ9Vδ2 T Cell Receptor. *Cell Rep* 2016; **15**: 1973–85.

285 Inman B, Frigola X, Harris K, Kuntz S, Lohse C, Leibovich B *et al.* Questionable relevance of gamma delta T lymphocytes in renal cell carcinoma. *J Immunol* 2008; **180**: 3578–84.

286 Viey E, Lucas C, Romagne F, Escudier B, Chouaib S, Caignard A. Chemokine receptors expression and migration potential of tumor-infiltrating and peripheral-expanded Vgamma9Vdelta2 T cells from renal cell carcinoma patients. *J Immunol* 2008; **31**: 313–23.

287 Viey E, Laplace C, Escudier B. Peripheral gammadelta T-lymphocytes as an innovative tool in immunotherapy for metastatic renal cell carcinoma. *Expert Rev Anticancer Ther* 2005; **5**: 973–86.

288 Zheng B, Ng S, Chua D, Sham J, Kwong D, Lam C *et al.* Peripheral gamma delta T-cell deficit in nasopharyngeal carcinoma. *Int J Cancer* 2002; **99**: 213–7.

289 Bialasiewicz A, Ma J, Richard G. Alpha/beta- and gamma/delta TCR(+) lymphocyte infiltration in necrotising choroidal melanomas. *Br J Ophtalmol* 1999; **83**: 1069–73.

290 Ke Y, Kapp L, Kapp J. Inhibition of tumor rejection by gammadelta T cells and IL-10. *Cell Immunol* 2003; **221**: 107–14.

291 Kunzmann V, Jomaa H, Feurle J, Bauer E, Herderich M, Wilhelm M. Stimulation of γδ T cells by aminobisphosphonates used in treatment of bone disorders. *Blood* 1997; **90**: 575 abstract.

292 Kunzmann V, Bauer E, Wilhelm M. Gamma/delta T-cell stimulation by pamidronate. *N Engl J Med* 1999; **340**: 737–8.

293 Sakamoto M, Nakajima J, Murakawa T, Fukami T, Yoshida Y, Murayama T *et al.* Adoptive immunotherapy for advanced non-small cell lung cancer using zoledronate-expanded γδTcells: a phase I clinical study. *J Immunother* 2011; **34**: 202–11.

294 Qaqish A, Huang D, Chen C, Zhang Z, Wang R, Li S *et al.* Adoptive Transfer of Phosphoantigen-Specific γδ T Cell Subset Attenuates Mycobacterium tuberculosis Infection in Nonhuman Primates. *J Immunol* 2017; **198**: 4753–4763.

295 Fisher JP, Heuijerjans J, Yan M, Gustafsson K, Anderson J. γδ T cells for cancer immunotherapy: A systematic review of clinical trials. *Oncoimmunology* 2014; **3**: e27572.

296 Fournié J, Sicard H, Poupot M, Bezombes C, Blanc A, Romagne F *et al.* What lessons can be learned from γδ T cell-based cancer immunotherapy trials? *Cell Mol Immunol* 2013; **10**: 35–41.

297 Mateusz L, Cole DK, Sewel AK. The promise of γδ T cells and the γδ T cell receptor for cancer immunotherapy. *Cell Mol Immunol* 2015; **12**.

298 Zou C, Zhao P, Xiao Z, Han X, Fu F, Fu L. γδ T cells in cancer immunotherapy. *Oncotarget* 2017; **8**: 8900–8909.

299 Vantourout P, Hayday A. Six-of-the-best: unique contributions of γδ T cells to immunology. *Nat Rev Immunol* 2013; **13**: 88–100.

300 Bennouna J, Bompas E, Neidhardt E, Rolland F, Philip I, Galea C *et al.* Phase-I study of Innacell

gammadelta, an autologous cell-therapy product highly enriched in gamma9delta2 T lymphocytes, in combination with IL-2, in patients with metastatic renal cell carcinoma. *Cancer Immunol Immunother* 57AD; **11**.

301 Lamb LJ, Henslee-Downey P, Parrish R, Thompson J, Lee C, Gee A. Increased frequency of TCR gamma delta + T cells in disease-free survivors following T cell-depleted, partially mismatched, related donor bone marrow transplantation for leukemia. *J Hematother* 1996; **5**: 503–9.

302 Godder K, Henslee-Downey P, Mehta J, Park B, Chiang K, Abhyankar S *et al.* Long term disease-free survival in acute leukemia patients recovering with increased γδ T cells after partially mismatched related donor bone marrow transplantation. *Bone Marrow Transplant* 2007; **39**: 751–757.

303 Correia D, Fogli M, Hudspeth K, Gomes Da Silva M, Mavilio D, Silva-Santos B. Differentiation of human peripheral blood Vδ1+ T cells expressing the natural cytotoxicity receptor NKp30 for recognition of lymphoid leukemia cells. *Blood* 2011; **118**: 992–1001.

304 Tang Q, Grzywacz B, Wang H, Kataria N, Cao Q, Wagner J *et al.* Umbilical cord blood T cells express multiple natural cytotoxicity receptors after IL-15 stimulation, but only NKp30 is functional. *J Immunol* 2008; **181**: 4507–15.

305 Correia M, Cardoso E, Pereira C, Neves R, Uhrberg M, Arosa F. Hepatocytes and IL-15: a favorable microenvironment for T cell survival and CD8+ T cell differentiation. *J Immunol* 2009; **185**: 6149–59.

306 Siegers G, Ribot E, Keating A, Foster P. Extensive expansion of primary human gamma delta T cells generates cytotoxic effector memory cells that can be labeled with Feraheme for cellular MRI. *Cancer Immunol Immunother* 2013; **62**: 571–83.

307 Caiado F, Maia-Silva D, Jardim C, Carvalho T, Reforço C, Faria R *et al.* Hypomethylating agents prevent chemoresistance in acute myeloid leukemia relapses by suppressing leukemia-initiating single-cell lineages. *Press*.

308 Trainor K, Morley A. Cloning of lymphocytes from whole blood by limiting dilution. *J Immunol Methods* 1983; **65**: 369–372.

309 Brady B, Steinel N, Bassing C. Antigen receptor allelic exclusion: an update and reappraisal. *J Immunol* 2010; **185**: 3801–8.

310 Silva-Santos B, Serre K, Norell H. γδ T cells in cancer. *Nat Rev Immunol* 2015; **15**: 683–91.

311 Luoma AM, Castro CD, Adams EJ. γδ T cell surveillance via CD1 molecules. *Trends Immunol* 2014; **35**: 613–621.

312 Kallemeijn MJ, Kavelaars FG, van der Klift MY, Wolvers-Tettero ILM, Valk PJM, van Dongen JJM *et al.* Next-generation sequencing analysis of the human TCRγδ+ T-cell repertoire reveals shifts in Vγ- and Vδ-usage in memory populations upon aging. *Front Immunol* 2018; **9**: 448.

313 Cheng C, Wang B, Gao L, Liu J, Chen X, Huang H *et al.* Next generation sequencing reveals changes of the γδ T cell receptor repertoires in patients with pulmonary tuberculosis. *Sci Rep* 2018; **8**: 3956.

314 Li B, Li T, Pignon JC, Wang B, Wang J, Shukla SA *et al.* Landscape of tumor-infiltrating T cell repertoire of human cancers. *Nat Genet* 2016; **48**: 725–32.

315 Di Lorenzo B, Ravens S, Silva-Santos B. Vδ1+ human thymocyte sequencing. NCBI Seq. Read Arch. 2018; : http://identifiers.org/ncbi/insdc.sra:SRP164910.

316 Di Lorenzo B, Tieppo P, Ravens S, Prinz I, Vermijlen D, Silva-Santos B. HTS data of human gamma and delta repertoires from peripheral blood, DOT and naive vs differentiated V delta 1 T cells. NCBI Seq. Read Arch. 2018; : http://identifiers.org/ncbi/insdc.sra:SRP162140.

317 Sleckman B, Khor B, Monroe R, Alt F. Assembly of productive T cell receptor delta variable region genes exhibits allelic inclusion. *J Exp Med* 1998; **188**: 4165–71.

318 Davodeau F, Peyrat M, Houde I, Hallet M, De Libero G, Vié H *et al.* Surface expression of two distinct functional antigen receptors on human gamma delta T cells. *Science (80-)* 1993; **260**: 1800–2.

319 Vanhanen R, Heikkilä N, Aggarwal K, Hamm D, Tarkkila H, Pätilä T *et al.* T cell receptor diversity in the human thymus. *Mol Immunol* 2016; **76**: 116–122.

320 Visser O, Trama A, Maynadié M, Stiller C, Marcos-Gragera R, De Angelis R *et al.* Incidence, survival and prevalence of myeloid malignancies in Europe. *Eur J Cancer* 2012; **48**: 3257–3266.

321 Kadia TM, Ravandi F, Cortes J, Kantarjian H. New drugs in Acute Myeloid Leukemia (AML). *Ann Oncol* 2016; **27**: 770–8.

322 Wei AH, Tiong IS. Midostaurin, enasidenib, CPX-351, gemtuzumab ozogamicin, and venetoclax bring new hope to AML. *Blood* 2017; **130**: 2469–2474.

323 Bross PF, Beitz J, Chen G, Chen XH, Duffy E, Kieffer L *et al.* Approval summary: gemtuzumab ozogamicin in relapsed acute myeloid leukemia. *Clin Cancer Res* 2001; **7**: 1490–1496.

324 Tasian S. Acute myeloid leukemia chimeric antigen receptor T-cell immunotherapy: how far up the road have we traveled? *Ther Adv Hematol* 2018; **9**: 135–148.

325 Garson O, Hagemeijer A, Sakurai M, Reeves B, Swansbury G, Williams G *et al.* Cytogenetic studies of 103 patients with acute myelogenous leukemia in relapse. *Cancer Genet Cytogenet* 1989; **40**: 187–202.

326 Testa J, Mintz U, Rowley J, Vardiman J, Golomb H. Evolution of karyotypes in acute nonlymphocytic leukemia. *Cancer Res* 1979; **39**: 3619–27.

327 Ding L, Ley T, Larson D, Miller C, Koboldt D, Welch J *et al.* Clonal evolution in relapsed acute myeloid leukaemia revealed by whole-genome sequencing. *Nature* 2012; **481**: 506–510.

328 Przepiorka D, Deisseroth A, Farrell A. Acute Myeloid Leukemia Response Measures Other Than Complete Remission. *J Clin Oncol* 2015; **33**: 3675–3676.

329 Di Tullio A, Rouault-Pierre K, Abarrategi A, Mian S, Grey W, Gribben J *et al.* The combination of CHK1 inhibitor with G-CSF overrides cytarabine resistance in human acute myeloid leukemia. *Nat Commun* 2017; **8**: 1679.

330 June C, O'Connor R, Kawalekar O, Ghassemi S, Milone M. CAR T cell immunotherapy for human cancer. *Science (80-)* 2018; **359**: 1361–1365.

331 Mardiros A, Dos Santos C, McDonald T, Brown C, Wang X, Budde L *et al.* T cells expressing CD123-specific chimeric antigen receptors exhibit specific cytolytic effector functions and antitumor effects against human acute myeloid leukemia. *Blood* 2013; **122**: 3138–48.

332 Gill S, Tasian S, Ruella M, Shestova O, Li Y, Porter D *et al.* Preclinical targeting of human acute myeloid leukemia and myeloablation using chimeric antigen receptor-modified T cells. *Blood* 2014; **123**: 2343–54.

333 Petrov J, Wada M, Pinz K, Yan L, Chen K, Shuai X *et al.* Compound CAR T-cells as a double-pronged approach for treating acute myeloid leukemia. *Leukemia* 2018; **32**: 13171326.

334 Dutta I, Postovit L, Siegers G. Apoptosis Induced via Gamma Delta T Cell Antigen Receptor "Blocking" Antibodies: A Cautionary Tale. *Front Immunol* 2017; **8**: fimmu.2017.00776.

335 Sancho D, Gomez M, Sanchez-Madrid F. CD69 is an immunoregulatory molecule induced following activation. *Trends Immunol* 2005; **26**: 136–140.

336 Buonpane R, Moza B, Sundberg E, Kranz D. Characterization of T Cell Receptors Engineered for High Affinity Against Toxic Shock Syndrome Toxin-1. *J Mol Biol* 2005; **353**: 308–21.

337 Brouillard J, Gunther S, Varma A, Gryski I, Herfst C, Rahman A *et al.* Crystal structure of the streptococcal superantigen SpeI and functional role of a novel loop domain in T cell activation by group V superantigens. *J Mol Biol* 2007; **367**: 925–34.

338 Minguet S, Swamy M, Alarcón B, Luescher I, Schamel W. Full Activation of the T Cell Receptor Requires Both Clustering and Conformational Changes at CD3. *Immunity* 2007; **26**: 43–54.

339 McVay LD, Jaswal SS, Kennedy C, Hayday A, Carding SR. The generation of human gammadelta T cell repertoires during fetal development. *J Immunol* 1998; **160**: 5851–60.

340 Melandri D, Zlatareva I, Chaleil R, Dart R, Chancellor A, Nussbaumer O *et al.* The γδTCR combines innate immunity with adaptive immunity by utilizing spatially distinct regions for agonist selection and antigen responsiveness. *Nat Immunol* 2018; **19**: 1352–1365.

341 Metzakopian E, Strong A, Iyer V, Hodgkins A, Tzelepis K, Antunes L *et al.* Enhancing the genome editing toolbox: genome wide CRISPR arrayed libraries. *Sci Rep* 2017; **7**: 2244.

342 Davey M, Willcox C, Baker A, Hunter S, Willcox B. Recasting Human Vδ1 Lymphocytes in an Adaptive Role. *Trends Immunol* 2018; **39**: 446–459.

343 Siegers G, Felizardo T, Mathieson A, Kosaka Y, Wang X, Medin J *et al.* Anti-leukemia activity of in vitro-expanded human gamma delta T cells in a xenogeneic Ph+ leukemia model. *PLoS One* 2011; **6**: e16700.

344 Dokouhaki P, Han M, Joe B, Li M, Johnston M, Tsao M *et al.* Adoptive immunotherapy of cancer using ex vivo expanded human gammadelta T cells: A new approach. *Cancer Lett* 2010; **297**: 126–36.

7 Published manuscripts

Cellular & Molecular Immunology (2017) 14, 733–735

www.nature.com/cmi

RESEARCH HIGHLIGHT

Peripheral clonal selection shapes the human γδ T-cell repertoire

Biagio Di Lorenzo[1,2], Julie Déchanet-Merville[3,4] and Bruno Silva-Santos[1,4]

Cellular & Molecular Immunology (2017) **14**, 733–735; doi:10.1038/cmi.2017.51; published online 7 August 2017

γδ T cells are often placed at the interface between innate and adaptive immunity. These cells share T-cell receptor (TCR) rearrangements and memory functions[1] in common with their αβ T-cell counterparts but differ in terms of their response kinetics and mechanisms of target recognition (Figure 1). Indeed, γδ T cells provide fast responses against infected or transformed cells in a major histocompatibility complex-independent manner, thus participating in the first line of defense, which gives the organism time to mount antigen-specific αβ T-cell responses.[2] Although the four TCR loci were discovered and characterized almost simultaneously,[3] our knowledge of the mechanisms underlying γδ T-cell responses remains insufficient. However, an increasing amount of evidence has demonstrated that γδ T cells recognize self-antigens on the surface of target cells; the expression of these self-antigens is known or expected to increase upon stress, infection or transformation in a TCR-dependent manner, making them an attractive source for cell-based immunotherapies.[4] This response is noted in the case of BTN3A associated with phosphoantigens,[5] lipid-presenting CD1 molecules,[6] endotelial protein C receptor[7] and Annexin A2.[8] However, these molecules constitute only a small fraction of the ligands recognized by γδ T cells. In addition, the mechanism by which the γδ TCR repertoire is shaped under physiological conditions and how (much) it changes in response to pathogenic challenge remain poorly understood.

In a recent issue of *Nature Immunology*,[9] Ravens and colleagues analyzed the largest available cohort of γδ T-cell repertoires, including more than 2×10^7 rearranged TCR sequences. This prospective longitudinal cohort study was possible thanks to recent technical advances in the comprehensive analysis of TCR repertoires using next-generation sequencing. Moreover, this study was designed to monitor the regeneration of T cell receptor gamma and delta repertoires in allogeneic hematopoietic stem cell transplantation (alloHSCT) patients over 180 days. The study also included not only blood samples from alloHSCT patients who experienced cytomegalovirus (CMV) reactivation, which is a major complication of transplantation associated with γδ T-cell expansion,[10] but also cord blood samples as important controls to provide information on the ontogeny and dynamics of the γδ T-cell repertoire.

The newly published data confirmed that the human adult blood γδ TCR repertoire is dominated by the usage of Vγ9 and Vδ2 TCR chains with high prevalence of the Vγ9–Jγ1.2 Vδ2 rearrangement.[11] However, the cord blood control group exhibited a less pronounced bias toward Vγ9 and Vδ2 and an increase in Vγ2, Vγ3, Vγ4, Vγ5, Vδ1, Vδ3 and Vδ5 chain usage, confirming the previously reported preponderance of Vγ9-negative γδ T cells in neonates.[1] This finding indicates that the bias toward Vγ9Vδ2 rearrangements is driven by postnatal proliferation likely in response to pathogen-derived phosphoantigens, which are well established and specific agonists of Vγ9Vδ2 TCR.[12]

Consistent with these findings, the 20 most abundant clones of the analyzed adult samples constituted ~40% of the repertoire. Conversely, the 20 most abundant clones in cord blood represented only ~10–20% of the entire repertoire. In addition to the reduction in diversity observed with age, Raven and colleagues pinpointed clear differences between the γ and δ chain repertoires. Greater clonal diversity was observed in rearranged T cell receptor delta genes in both cord blood and adult samples.

[1]Instituto de Medicina Molecular, Faculdade de Medicina, Universidade de Lisboa, 1649-028 Lisbon, Portugal; [2]Instituto Superior Tecnico, Universidade de Lisboa, 1649-028 Lisbon, Portugal and [3]ImmunoConcept, CNRS UMR 5164, Equipe Labelisée Ligue Contre le Cancer, University of Bordeaux, F-33000 Bordeaux, France
[4]These authors contributed equally to this work.
Correspondence: Dr J Déchanet-Merville, PhD, ImmunoConcept, CNRS UMR 5164, University of Bordeaux, Bordeaux F-33000, France or Professor B Silva-Santos, PhD, Instituto de Medicina Molecular, Faculdade de Medicina, Universidade de Lisboa, Av Prof Egas Moniz, Lisbon 1649-028, Portugal.
E-mail: Julie.dechanet-merville@u-bordeaux.fr or bssantos@medicina.ulisboa.pt
Received: 25 May 2017; Accepted: 30 May 2017

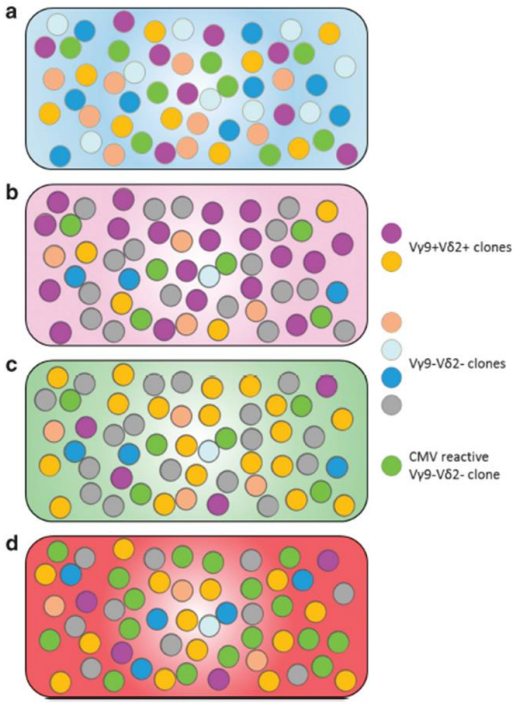

Figure 1 Graphical representation of the dynamics of the human γδ T-cell repertoire. (**a**) Prenatal generation of γδ T cells is unfocused and unbiased. At birth, the human γδ repertoire in blood is variable, exhibiting Vγ2, Vγ3, Vγ4, Vγ5, Vδ1, Vδ3 and Vδ5 chain usage and no bias toward Vγ9 and Vδ2. (**b**) Up to 40% of the adult repertoire is composed of the 20 most abundant clones. The focus toward the Vγ9Vδ2 chain rearrangement (purple circles) is driven by postnatal proliferation in response to pathogen- or tumor-derived phosphoantigens. (**c**) AlloHSCT strongly perturbs the adult γδ repertoire. However, 60 days after alloHSCT, the repertoire is fully reconstituted and qualitatively comparable to the host repertoires before transplantation but displays very different clonotypes compared with the donor. (**d**) CMV reactivation occurs 25–60 days after alloHSCT. The γδ T-cell repertoire recovery observed in alloHSCT is perturbed by the proliferation of a few, mainly Vγ9–Vδ2, clones that comprise 20–75% of the repertoire.

Moreover, unrelated donors (cord blood or adult) shared TCRγ chain sequences (interestingly only Vγ9JP sequences in adults), making them 'public'. By contrast,
TCRδ chain repertoires were mostly 'private', especially in the Vδ2$^-$ T-cell compartment. These results are consistent with the long, variable lengths of TCRδ CDR3 compared with the short, constrained TCRγ CDR3, in addition to the presence of three D gene segments in the TCRδ locus that are absent from the TCRγ locus.[13] Beyond these insights into the γδ TCR repertoire ontogeny, Ravens and colleagues also documented that established adult γδ T-cell repertoires are stable over time (within a window of 90 days) if no major immunological events, such as alloHSCT or CMV reactivation, occur. Strikingly, even after alloHSCT, stable γδ T-cell repertoires were rapidly reconstituted between 30 and 60 days after transplantation in the absence of CMV reactivation. The new repertoires after transplantation were qualitatively comparable to the host repertoires before transplantation but displayed very different clonotypes compared with both the donor and host repertoires, indicating that the new repertoires were successfully generated from the donor stem cells and differentiated *de novo* in the host thymus. Whether the γδ T-cell population either recognizes the same ligands and thus restores functionally similar clones or the clones are randomly selected remains to be established.

In the examined cohort, CMV reactivation occurred between 25 and 60 days after transplantation. The γδ T-cell repertoire recovery observed in 10 alloHSCT patients undergoing CMV reactivation was perturbed by a massive proliferation of a few individual clones that comprised 20–75% of the repertoire, with an important variability among patients. These results hence provide interesting details of the previously reported oligoclonal expansion of non-Vγ9Vδ2 γδ T cells responding to CMV in humans[10,14] and mice.[15,16] These clones expressed different Vδ and Vγ chains of diverse clonotypes; thus, their nucleotide (and amino acid) sequences were not shared among different donors, indicating that CMV reactivation did not induce the clonal expansion of public clones. Nevertheless, several Vδ1$^+$ clones shared substantial homology in the CDR3 region, including a common amino-acid sequence composed of a tryptophan, glycin and isoleucine (WGI) preceded by one or more tyrosine(s). Interestingly, a similar amino-acid sequence was found in the CDR3 of Vδ1$^+$ γδ T cells responding to CMV in kidney transplant recipients,[10] suggesting structural constraints for recognition of CMV-related antigens by these TCRs. Single-cell analysis of TCRs further allowed studies of Vγ and Vδ chain pairing and confirmed clonal expansion of non-Vγ9Vδ2 γδ T cells of different clonotypes that can express diverse Vγ and Vδ pairings.

These findings strengthen the idea that non-Vγ9Vδ2 γδ T cells undergo continuous and extra-thymic selection of a few TCR clonotypes, thus making their repertoire oligoclonal. Similar to Vγ9Vδ2$^+$ γδ T cells, the presence of ligands for some specific non-Vγ9Vδ2 γδ T cells in the periphery would be responsible for this selection and skewing. Unfortunately, the majority of these ligands remain unknown, but

this study raises the interesting issue of the diversity of the antigens recognized by such impressively selected and expanded non-Vγ9Vδ2 γδ T cell clones. Does CMV infection generate as many antigens as the different private γδ TCRs or are a limited number of antigens recognized by many different γδ TCRs, as is the case for CMV-derived peptides recognized by αβ TCRs? The localization of these antigens is also an important issue to address for these populations of non-Vγ9Vδ2 γδ T cells normally residing in tissues. Nevertheless, this study demonstrated that less numerous clones undergo strong clonal selection and expansion when challenged, as in the case of CMV reactivation, which aligns human non-Vγ9Vδ2 γδ T cells with adaptive immunity. Previous data supporting peripheral selection and oligoclonal expansion were derived from the recognition of endotelial protein C receptor by a γδ T cell clone (named LES) bearing a Vγ4Vδ5 TCR.[7] This LES clone represented ~25% of the circulating T cells in the patient in which it was found.

This evidence highlights how the γδ T-cell subset mounts an adaptive-like immune response that is independent of canonical major histocompatibility complex presentation but relies on clonal expansion of reactive clones. However, what these reactive clones recognize remains unclear. Some reports suggest that these targets are self-proteins (related or not to major histocompatibility complex) whose expression, membrane localization or tertiary structure is modified in response to cellular stress, such as transformation and bacterial or viral infection. These clones arise from an unfocused repertoire that becomes more focused and more public throughout life (for Vγ9Vδ2 γδ T cells). Adult γδ T-cell repertoires contained variable numbers of highly proliferative oligoclonal sequences, whereas neonatal γδ T-cell repertoires were more diverse and less focused. Each individual γδ T-cell repertoire thus represents a singular individual immunological history. This TCR repertoire skewing allows γδ T cells to be rapidly, but specifically, generated, thereby blurring the boundaries between innate and adaptive immunity.

CONFLICT OF INTEREST

The authors declare no conflict of interest.

ACKNOWLEDGEMENTS

We thank Fundação para a Ciência e Tecnologia (PD/BD/105880/2014 to BDL; and PTDC/DTP-PIC/4931/2014 to BS-S) and the Ligue Contre le Cancer and Fondation pour la Recherche Médicale (to JD-M) for funding.

1 De Rosa SC, Andrus JP, Perfetto SP, Mantovani JJ, Herzenberg LA, Herzenberg LA *et al.* Ontogeny of gamma delta T cells in humans. *J Immunol* 2004; **172**: 1637–1645.
2 Carding SR, Egan PJ. γδ T Cells: functional plasticity and heterogeneity. *Nat Rev Immunol* 2002; **2**: 336–345.
3 Pardoll DM, Fowlkes BJ, Bluestone JA, Kruisbeek A, Maloy WL, Coligan JE *et al.* Differential expression of two distinct T-cell receptors during thymocyte development. *Nature* 1987; **326**: 79–81.
4 Legut M, Cole DK, Sewell AK. The promise of γδ T cells and the γδ T cell receptor for cancer immunotherapy. *Cell Mol Immunol* 2015; **12**: 656–668.
5 Harly C, Guillaume Y, Nedellec S, Peigné CM, Mönkkönen H, Mönkkönen J *et al.* Key implication of CD277/butyrophilin-3 (BTN3A) in cellular stress sensing by a major human γδ T-cell subset. *Blood* 2012; **120**: 2269–2279.
6 Luoma AM, Castro CD, Mayassi T, Bembinster LA, Bai L, Picard D *et al.* Crystal structure of Vδ1 T cell receptor in complex with CD1d-sulfatide shows MHC-like recognition of a self-lipid by human γδ T cells. *Immunity* 2013; **39**: 1032–1042.
7 Willcox CR, Pitard V, Netzer S, Couzi L, Salim M, Silberzahn T *et al.* Cytomegalovirus and tumor stress surveillance by binding of a human γδ T cell antigen receptor to endothelial protein C receptor. *Nat Immunol* 2012; **13**: 872–879.
8 Marlin R, Pappalardo A, Kaminski H, Willcox CR, Pitard V, Netzer S *et al.* Sensing of cell stress by human γδ TCR-dependent recognition of annexin A2. *Proc Natl Acad Sci USA* 2017; **114**: 3163–3168.
9 Ravens S, Schultze-Florey C, Raha S, Sandrock I, Drenker M, Oberdörfer L *et al.* Human γδ T cells are quickly reconstituted after stem-cell transplantation and show adaptive clonal expansion in response to viral infection. *Nat Immunol* 2017; **18**: 393–401.
10 Déchanet J, Merville P, Lim A, Retière C, Pitard V, Lafarge X *et al.* Implication of gammadelta T cells in the human immune response to cytomegalovirus. *J Clin Invest* 1999; **103**: 1437–1449.
11 Triebel F, Faure F, Graziani M, Jitsukawa S, Lefranc MP, Hercend T. A unique V-J-C-rearranged gene encodes a gamma protein expressed on the majority of CD3+ T cell receptor-alpha/beta- circulating lymphocytes. *J Exp Med* 1988; **167**: 694–699.
12 Constant P, Davodeau F, Peyrat MA, Poquet Y, Puzo G, Bonneville M *et al.* Stimulation of human gamma Delta T cells by nonpeptidic mycobacterial ligands. *Science* 1994; **264**: 267–270.
13 Rock EP, Sibbald PR, Davis MM, Chien YH. CDR3 length in antigen-specific immune receptors. *J Exp Med* 1994; **179**: 323–328.
14 Vermijlen D, Brouwer M, Donner C, Liesnard C, Tackoen M, Van Rysselberge M *et al.* Human cytomegalovirus elicits fetal γδ T cell responses in utero. *J Exp Med* 2010; **207**: 807–821.
15 Sell S, Dietz M, Schneider A, Holtappels R, Mach M, Winkler TH. Control of murine cytomegalovirus infection by γδ T cells. *PLoS Pathog* 2015; **11**: e1004481.
16 Khairallah C, Netzer S, Villacreces A, Juzan M, Rousseau B, Dulanto S *et al.* γδ T cells confer protection against murine cytomegalovirus (MCMV). *PLoS Pathog* 2015; **11**: e1004702.

frontiers in Immunology

MINI REVIEW
published: 27 April 2018
doi: 10.3389/fimmu.2018.00929

Molecular Determinants of Target Cell Recognition by Human γδ T Cells

André E. Simões[1†], Biagio Di Lorenzo[1,2†] and Bruno Silva-Santos[1]*

[1] Faculdade de Medicina, Instituto de Medicina Molecular, Universidade de Lisboa, Lisbon, Portugal, [2] Instituto Superior Técnico, Universidade de Lisboa, Lisbon, Portugal

The unique capabilities of gamma-delta (γδ) T cells to recognize cells under stressed conditions, particularly infected or transformed cells, and killing them or regulating the immune response against them, paved the way to the development of promising therapeutic strategies for cancer and infectious diseases. From a mechanistic standpoint, numerous studies have unveiled a remarkable flexibility of γδ T cells in employing their T cell receptor and/or NK cell receptors for target cell recognition, even if the relevant ligands often remain uncertain. Here, we review the accumulated knowledge on the diverse mechanisms of target cell recognition by γδ T cells, focusing on human γδ T cells, to provide an integrated perspective of their therapeutic potential in cancer and infectious diseases.

Keywords: gamma-delta T cell, T cell receptor, NK cell receptor, NKG2D, tumor immunology

OPEN ACCESS

Edited by:
Kenth Gustafsson,
University College London,
United Kingdom

Reviewed by:
Tom Taghon,
Ghent University, Belgium
David L. Wiest,
Fox Chase Cancer Center,
United States

****Correspondence:***
Bruno Silva-Santos
bssantos@medicina.ulisboa.pt

[†]These authors have contributed equally to this work.

Specialty section:
This article was submitted to T Cell Biology, a section of the journal Frontiers in Immunology

Received: *01 March 2018*
Accepted: *16 April 2018*
Published: *27 April 2018*

Citation:
Simões AE, Di Lorenzo B and Silva-Santos B (2018) Molecular Determinants of Target Cell Recognition by Human γδ T Cells. Front. Immunol. 9:929. doi: 10.3389/fimmu.2018.00929

INTRODUCTION

More than three decades after the discovery of gamma-delta (γδ) T cells (1), the research community is still missing a compelling picture about their mechanisms of activation and target cell recognition. Despite the relatively small abundance of γδ T cells in the human blood, it is clear that this lymphocyte population plays an important role at the interface between the innate and the adaptive immune systems. These cells share T cell receptor (TCR) rearrangements and memory functions (2) with their αβ T cell counterparts, but differ in their response kinetics and mechanisms of target cell recognition. Thus, γδ T cell activation is typically independent of antigen presentation by major histocompatibility complex (MHC) molecules. Furthermore, γδ T cells bear a plethora of NK cell receptors (NKRs) on their surface, which allow for very fast responses against infected or transformed cells (3), thus contributing to a first line of defense that precedes antigen-specific αβ T-cell responses (4).

Unlike αβ T cells, there is little evidence of thymic negative selection of self-reactive γδ T cells. Vγ9Vδ2 T cells, which constitute the major (60–95%) γδ T cell subtype in humans, seemingly expand in the periphery in response to microbial or stress-induced phosphorylated antigens (2) while displaying preferential Vγ9-JP TCR rearrangements (5). Other human γδ T cell subsets, namely Vδ1$^+$ and Vδ3$^+$ T cells that are highly reactive to cytomegalovirus (CMV) infection (6), display TCR repertoires biased toward sequences recognizing CMV-infected cells (7). But while Vγ9Vδ2 TCR recognition has been well characterized and discussed (5, 8), it remains less clear how other γδ T cell subsets are activated to participate in lymphoid stress surveillance (9).

The purpose of this review is to discuss the current knowledge on target cell recognition by human γδ T cells (**Table 1**), emphasizing the role of the TCR as well as NKRs and their ligands, in the context of cancer and infectious diseases.

TUMOR CELL RECOGNITION

Early research on the molecular mechanisms of γδ T cell recognition in the 1990s led to the realization of its unusual independence of peptide processing and MHC-restricted presentation, in marked contrast with αβ T lymphocytes (42–44). One of the first lines of evidence came from non-peptidic

TABLE 1 | Tumor- or infected cell-associated ligands recognized by gamma-delta (γδ) T cells.

Ligand	Receptor	γδ subset	Infection/cancer	Reference
CD1 proteins + endogenous or exogenous lipids	T cell receptor (TCR)	Duodenal	Infection	(10, 11)
BTN3A1 + phosphoantigens	TCR	Vγ9Vδ2	Infection	(5)
Endothelial protein C receptor	TCR	Vγ4Vδ5	Both	(12)
Annexin A2	TCR	Vγ8Vδ3	Both	(13)
Heat shock protein 60	TCR		Both	(14–17)
F1-ATPase	TCR		Cancer	(18)
SEA and SEE	TCR		Infection	(19)
OXYS	TCR		Infection	(20)
DXS2	TCR		Infection	(21)
Glycoprotein I	TCR		Infection	(21)
MSH2	TCR		Both	(14, 22)
	NKG2D			(22)
HLA-E	NKG2C		Infection	(23)
HA	Sialic acid receptor		Infection	(24)
CD48	2B4		Cancer	(25–27)
MICA/MICB	TCR	Vδ1	Both	(28–30)
	NKG2D			(29–32)
MICA	NKG2D	Vγ9Vδ2	Cancer	(33)
UL16 binding protein (ULBP)1	NKG2D	Vγ9Vδ2	Cancer	(34)
ULBP2	NKG2D	Vδ1	Cancer	(35, 36)
ULBP3	NKG2D	Vδ1	Cancer	(35–37)
ULBP4	TCR and NKG2D	Vδ2	Cancer	(38)
?	NKp30	Vδ1	Both	(39, 40)
PVR/Nectin-2	DNAX accessory molecule 1	Vγ9Vδ2	Cancer	(41)

"?" means undescribed/unknown in the referenced studies.

prenyl pyrophosphates ["phosphoantigens" (PAg)] recognized by Vγ9Vδ2 TCRs (45, 46). Initially, bacteria and parasites were shown to produce strong PAg agonists for Vγ9Vδ2 TCRs (47), but later it became clear that these could also be activated by weaker agonists, such as isopentenyl pyrophosphate (IPP) and dimethylallyl pyrophosphate, that are natural intermediates of the mevalonate pathway of isoprenoid and steroid synthesis in eukaryotic cells (48). Importantly, the dysregulation of the mevalonate pathway in some tumor cells allows for the accumulation of these (weaker) PAgs, thus promoting Vγ9Vδ2 TCR-mediated recognition (49). Furthermore, treatment with zoledronate or pamidronate (which are approved drugs) was shown to be very effective at inducing the accumulation of intracellular PAgs like IPP, and thus potentiate TCR-dependent Vγ9Vδ2 T cell cytotoxicity against tumor cell targets, including cancer stem cells (50).

A key recent breakthrough was the discovery of butyrophilin-related proteins, especially BTN3A1, as major molecular determinants of Vγ9Vδ2TCR-mediated recognition of PAgs, even if the underlying mechanism has gathered some controversy. A model supporting extracellular PAg presentation to the Vγ9Vδ2 T cell (in a MHC-like manner) was first proposed, with biophysical and structural data in support (51). However, following reports demonstrated that PAgs interact directly with the intracellular B30.2 domain of BTN3A1 through a positively charged surface pocket; and that charge reversal of pocket residues abrogates PAg binding and Vγ9Vδ2 T cell activation, with no detectable association with the extracellular domain of BTN3A1 (13, 52, 53). More recently, it has been shown that changes in the juxtamembrane domain of BTN3A1, which is located close to the start of the B30.2 domain, induced marked alterations in Vγ9Vδ2 T cell reactivity, thus highlighting the importance of the intracellular domain for the correct Vγ9Vδ2 T cell function and activation (54). Because of its location between the intracellular and the extracellular domains, the B30.2 domain seems critical in translating the pAg-induced conformational change of BTN3A1 from the inside to the outside of the target cells (55, 56).

Besides sensing PAgs, γδ T cells seemingly recognize transformed cells through proteins that are expressed at the cell surface in a stress-induced manner. Some examples are typically endogenous proteins, such heat shock protein 60 (14–17) or FI-ATPase (18), that can be ectopically expressed on the cell membrane upon transformation and recognized by Vγ9Vδ2 TCRs to promote tumor cell lysis. More recently, endothelial protein C receptor (EPCR), which acts on the coagulation cascade, was shown to be exposed on the cell surface during transformation and recognized by a non-Vδ2 (Vγ4Vδ5) TCR (12). Similarly, Annexin A2, expressed on tumor cells in response to increasing quantities of reactive oxygen species, engaged directly with a Vγ8Vδ3 TCR (13). The identification of these rather different ligands highlights the complexity of tumor cell recognition *via* γδ TCRs. This notwithstanding, it is clear that γδ T cells also rely on "NK-like" mechanisms for tumor cell recognition, using receptors such as 2B4 and NKG2D, originally thought to be specific to NK cells.

The first indication of an NK-like recognition mechanism was unveiled upon the ability of stimulated murine γδ T cells to recognize CD48 (25, 26), a well-known 2B4 ligand, suggested to work as an accessory molecule that strengthens effector–target interactions (27). Surprisingly, only the $2B4^+$ γδ T cells were able to develop non-MHC-restricted cytotoxicity against lymphoma cells (57, 58). Although 2B4 is also expressed on activated human γδ T cells, its relevance is still unclear as 2B4 engagement failed to promote proliferation or cytokine production (59).

Much more consensual is the role of NKG2D, which is widely expressed not only in NK cells but also in most γδ and some αβ

T cells (31, 60, 61). In human γδ T cells, both Vδ1$^+$ and Vδ2$^+$ subsets, NKG2D was shown to be responsible for recognition of tumor cells expressing MHC class I chain-related (MIC) A/B (28, 29, 31–33, 62) or UL16 binding protein (ULBP) 1/2/3/4 (34–38, 50, 63) ligands. In fact, human carcinoma samples from lung, breast, kidney, ovary, and prostate cancers expressing MICA or MICB presented higher levels of infiltrating Vδ1$^+$ T cells, which in turn were able to target and kill autologous and heterologous tumor cells (25, 59). Our group's work revealed that ULBP1 was particularly important for leukemia and lymphoma cell recognition by PAg-activated Vγ9Vδ2 T cells (34). Notwithstanding, one should note the relevance of a synergistic TCR engagement for an efficient cytotoxic response (37, 38). In fact, some works suggested that MIC or ULBP recognition by γδ T cells is not only restricted to NKG2D but also involves the γδ TCR (26, 31). A similar recognition pattern was also observed against human MutS homolog 2 (hMSH2) ectopically expressed in epithelial tumor cell lines. Both TCRγδ and NKG2D were able to interact with hMSH2 and contribute to Vδ2$^+$ γδ T cell-mediated cytotoxicity and interferon γ (IFN-γ) production (14, 22).

Besides 2B4 and NKG2D, DNAX accessory molecule 1 (DNAM-1) was also shown to be widely expressed in Vδ1$^+$, Vδ2$^+$, and Vδ1$^-$Vδ2$^-$ γδ T cell subsets (64); and masking DNAM-1 on γδ T cells significantly inhibited tumor cell killing (64, 65). DNAM-1-dependent γδ T cell recognition was reported for hepatocellular carcinoma (41), acute (65) and chronic (64) myeloid leukemia, and multiple myeloma (66) cell lines. More specifically, Vγ9Vδ2 T cells were shown to use DNAM-1 to interact with Nectin-2 and PVR that are widely expressed in the tumor cell targets (41, 65). Curiously, PVR engagement potentiated γδ T cell cytotoxicity, whereas Nectin-2 blocking did not affect it (41). Tumor targets that expressed both DNAM-1 and NKG2D ligands were able to engage both receptors on γδ T cells, having a synergistic effect on their cytolytic activity (41, 64, 66). Moreover, therapeutic strategies that enhanced the expression of NKG2D or DNAM-1 ligands, such as MICA/B and ULBP1/2, or Nectin-2 and PVR, respectively, potentiated γδ T cell recognition of colon cancer, glioblastoma, multiple myeloma, and lymphoma cells (67–70).

From a therapeutic perspective, γδ T cell recognition of tumor cells may also rely on the induced expression of natural cytotoxicity receptors (NCRs) that recognize a distinct set of tumor-associated ligands, such as B7-H6 or BAT3 (71). Thus, our group has shown that NKp30 and NKp44 can be reproducibly induced *in vitro* in Vδ1$^+$ (but not Vδ2$^+$) γδ T cells (39). A very mild expression of NKp44 on expanded γδ T cells had been reported before (72); and shown to contribute γδ T cell cytotoxicity against myeloma cells (61). In our studies, we observed not only a robust expression of NKp44 but also NKp30, in Vδ1$^+$ T cells activated with TCR agonists and IL-15 (or IL-2); and both receptors enhanced γδ T cytotoxicity against tumor target cells (39, 73). Among the various known ligands for NCRs, it is still unclear which are most relevant for NCR$^+$ Vδ1$^+$ T cell recognition of tumor cells. While the NKp30 ligand, B7-H6, is an obvious candidate (74), a very recent report identified an unanticipated ligand for NKp44 in the form of platelet-derived growth factor (PDGF)-DD (75), known for its capacity to promote of tumor cell proliferation, epithelial–mesenchymal transition, and angiogenesis. PDGF-DD ligation to NKp44 enhanced IFN-γ and TNF-α secretion (by NK cells), which in turn induced tumor cell growth arrest (75). Additional investigation will be needed to elucidate the relative importance of NCR, NKG2D, DNAM-1, or TCR ligands in tumor cell recognition by γδ T cells, aiming to maximize their potential in cancer immunotherapy.

INFECTED CELL RECOGNITION

Multiple lines of evidence since the late 1980s have shown that γδ T cells display strong activities against bacteria, including *Mycobacterium tuberculosis* (76–81); parasites, such as *Plasmodium falciparum* (82–86); and viruses (87, 88), most notably CMV (89–91).

Vγ9Vδ2 T cells can be specifically and potently activated by PAgs like (E)-4-hydroxy-3-methyl-but-2-enyl pyrophosphate, an intermediate of the 2-C-methyl-D-erythritol 4-phosphate pathway employed by eubacteria and apicomplexan protozoa but not by eukaryotes (48, 92, 93). This likely underlies the striking expansions of Vγ9Vδ2 T cells in individuals infected with *M. tuberculosis* (76–81) or *P. falciparum* (83). Besides PAgs, several other molecules of microbial origin have been proposed as γδ T cell antigens accounting for the specific recognition of infected cells. These candidates include the bacterial superantigens SEA (and to a lesser extent SEE) (19); OXYS and DXS2, two mycobacterial proteins found to activate γδ T cells from BCG-infected human subjects but not from healthy donors (20, 21); and HSV-1 glycoprotein I, specifically recognized by a Vγ1.2Vδ8 TCR independently from antigen processing and MHC presentation (20, 21).

Subsequent reports demonstrated that γδ T cells also recognize stress antigens of cellular origin, either in antibody-like or antigen-presentation-like fashion. γδ T cells can indeed directly recognize stress proteins like hMSH2, a nuclear protein ectopically expressed on the cell surface of different epithelial tumor cells and induced by EBV transformation (22); and Annexin A2 whose expression was induced by CMV infection and recognized specifically by a Vγ8Vδ3 T cell clone (13). On the other hand, γδ T cells can recognize nonpolymorphic MHC-like (class Ib) proteins presenting lipids, such as CD1 proteins, in a similar way to other unconventional T cells like NKT or MAIT cells (11, 94–96). In particular, a subpopulation of Vδ1$^+$ T cells has been clearly shown to bind CD1d loaded with the self-lipid sulfatide (97) but any concrete link to the recognition of infected (or transformed) cells remains to be established. Of note, another CD1-like protein, EPCR, was shown to bind directly (independently of lipid cargo) the TCR of a Vγ4Vδ5 T cell clone (expanded from a CMV$^+$ individual), thus allowing it to recognize endothelial cells infected with CMV (12).

In addition to the TCR, γδ T cells can also use NKG2D to recognize cells infected with various viruses and intracellular bacteria (32, 98–102). More specifically, the stress-inducible molecule, MICA, was induced on the surface of dendritic and epithelial cells by *M. tuberculosis* infection *in vitro* and *in vivo*; and its binding to NKG2D, substantially enhanced the TCR-dependent Vγ9Vδ2 T cell response to PAgs (28). Furthermore, in the case of *Brucella*, ULBP1 was the main NKG2D ligand upregulated on infected macrophages, and its engagement promoted Vγ9Vδ2 T cell cytotoxicity and cytokine production, which contributed to the inhibition of bacterium development (100).

A few other receptors have implicated in γδ T cell recognition of infected cells. Thus, another NKR, NKG2C, constitutively expressed on Vδ1$^+$ T cells, induced a cytolytic response against HIV-infected CD4$^+$ T cells expressing its ligand, HLA-E (23). On the other hand, we found that NKp30 can also play an important role in HIV-1 infection upon its induced expression in Vδ1$^+$ T cells; NKp30 ligation triggered the production of CCL3, CCL4, and CCL5 chemokines that suppressed the replication of a CCR5 tropic strain of HIV-1 (40). Finally, in the case of avian influenza (H5N1), γδ T cells were reported to use sialic acid receptors for the recognition of viral hemagglutinin (24). To understand how different microorganisms may elicit distinct pathways of γδ T cell recognition of pathogen-associated or stress-induced antigens remains a challenge for future research.

CONCLUDING REMARKS

In contrast with the well-established paradigm of MHC-restricted recognition of peptides by conventional αβ T cells, or even MHC class Ib-dependent recognition of lipids by unconventional αβ T cells, the molecular mechanisms of target cell recognition by γδ T cells remain poorly understood. A notable exception is the BTN3A1-mediated sensing of PAgs by Vγ9Vδ2 T cells, which underlies their responses to tumors and infections like TB or malaria. For most other γδ T cell subsets, however, TCR specificities are either unknown, not generalizable or of unclear physiological relevance. Therefore, the identification of relevant, non-Vγ9Vδ2 TCR ligands remains a major challenge in the γδ T cell field.

On the other hand, while NKRs are also clearly involved in γδ T cell recognition of tumor or infected cells, we still lack appropriate understanding how the multiple signals derived from all the expressed NKRs are integrated, also with those coming from the TCR itself. This likely depends on the relative expression levels of the various putative NKR and TCR ligands in each target cell, which adds significant complexity to the process of γδ T cell recognition.

The broad spectrum of MHC-unrestricted recognition of infected or transformed cells by γδ T makes them attractive candidates for adoptive cell therapy (ACT). All clinical trials have thus far concentrated on Vγ9Vδ2 T cells, probably due to their relative abundance in the peripheral blood and especially the availability of FDA-approved drugs, such as zoledronate and pamidronate, that allow their activation and expansion *in vivo* (103). Vγ9Vδ2 ACT has shown promising pre-clinical results against TB (104) and has already been tested in various cancer clinical trials [reviewed in Ref. (105)] that documented its safety and some (albeit still sub-optimal) efficacy (106–108). This could be maybe explained by Vγ9Vδ2 T cell susceptibility to exhaustion and activation-induced cell death (AICD). Nonetheless, improvements in Vγ9Vδ2 ACT protocols may still increase their efficacy, as indicated by some studies with exogenous provision of IL-2, importantly without the need for lymphodepleting preconditioning (109, 110). As for Vδ1$^+$ γδ T cells, they are less susceptible to AICD and exhaustion when compared to Vγ9Vδ2 T cells (111). However, no clinical trial has yet focused on this γδ T cell subset, mostly due to the lack of clinical-grade protocols allowing their successful expansion. Importantly, we have recently developed a clinical-grade process to effectively expand Vδ1$^+$ T cells while also inducing NCR (and augmenting NKG2D) expression; and established the proof-of-concept in leukemia xenograft models (73). We further anticipate NCR$^+$ Vδ1$^+$ ACT to be a promising therapeutic strategy also for solid tumors and chronic viral infections.

AUTHOR CONTRIBUTIONS

AS, BL, and BS-S conceived and wrote the manuscript. AS and BL contributed equally to the manuscript.

FUNDING

We acknowledge funding from Fundação para a Ciência e a Tecnologia (PTDC/DTP-PIC/4931/2014 to BS-S; and PD/BD/105880/2014 to BL). This publication was sponsored by LISBOA-01-0145-FEDER-007391, project cofunded by FEDER, through POR Lisboa 2020—Programa Operacional Regional de Lisboa, PORTUGAL 2020, and Fundação para a Ciência e a Tecnologia.

REFERENCES

1. Pardoll DM, Fowlkes BJ, Bluestone JA, Kruisbeek A, Maloy WL, Coligan JE, et al. Differential expression of two distinct T-cell receptors during thymocyte development. *Nature* (1987) 326:79–82. doi:10.1038/326079a0
2. De Rosa SC, Andrus JP, Perfetto SP, Mantovani JJ, Herzenberg LA, Roederer M. Ontogeny of T cells in humans. *J Immunol* (2004) 172:1637–45. doi:10.4049/jimmunol.172.3.1637
3. Ribeiro ST, Ribot JC, Silva-Santos B. Five layers of receptor signaling in γδ T-cell differentiation and activation. *Front Immunol* (2015) 6:15. doi:10.3389/fimmu.2015.00015
4. Carding SR, Egan PJ. γδ T cells: functional plasticity and heterogeneity. *Nat Rev Immunol* (2002) 2:336–45. doi:10.1038/nri797
5. Karunakaran MM, Herrmann T. The Vγ9Vδ2 T cell antigen receptor and butyrophilin-3 A1: models of interaction, the possibility of co-evolution, and the case of dendritic epidermal T cells. *Front Immunol* (2014) 5:648. doi:10.3389/fimmu.2014.00648
6. Khairallah C, Déchanet-Merville J, Capone M. γδ T cell-mediated immunity to cytomegalovirus infection. *Front Immunol* (2017) 8:105. doi:10.3389/fimmu.2017.00105
7. Ravens S, Schultze-Florey C, Raha S, Sandrock I, Drenker M, Oberdörfer L, et al. Human γδ T cells are quickly reconstituted after stem-cell transplantation and show adaptive clonal expansion in response to viral infection. *Nat Immunol* (2017) 18:393–401. doi:10.1038/ni.3686
8. Gu S, Nawrocka W, Adams EJ. Sensing of pyrophosphate metabolites by Vγ9Vδ2 T cells. *Front Immunol* (2015) 5:688. doi:10.3389/fimmu.2014.00688
9. Hayday AC. γδ T cells and the lymphoid stress-surveillance response. *Immunity* (2009) 31:184–96. doi:10.1016/j.immuni.2009.08.006
10. Sieling PA, Jullien D, Dahlem M, Tedder TF, Rea TH, Modlin RL, et al. CD1 expression by dendritic cells in human leprosy lesions: correlation with effective host immunity. *J Immunol* (1999) 162:1851–8.
11. Russano AM, Bassotti G, Agea E, Bistoni O, Mazzocchi A, Morelli A, et al. CD1-restricted recognition of exogenous and self-lipid antigens by duodenal γδ+ T lymphocytes. *J Immunol* (2007) 178:3620–6. doi:10.4049/jimmunol.178.6.3620
12. Willcox CR, Pitard V, Netzer S, Couzi L, Salim M, Silberzahn T, et al. Cytomegalovirus and tumor stress surveillance by binding of a human γδ T cell antigen receptor to endothelial protein C receptor. *Nat Immunol* (2012) 13:872–9. doi:10.1038/ni.2394

13. Marlin R, Pappalardo A, Kaminski H, Willcox CR, Pitard V, Netzer S, et al. Sensing of cell stress by human γδ TCR-dependent recognition of annexin A2. *Proc Natl Acad Sci U S A* (2017) 114:3163–8. doi:10.1073/pnas.1621052114
14. Chen H, He X, Wang Z, Wu D, Zhang H, Xu C, et al. Identification of human T cell receptor γδ-recognized epitopes/proteins via CDR3δ peptide-based immunobiochemical strategy. *J Biol Chem* (2008) 283:12528–37. doi:10.1074/jbc.M708067200
15. Laad AD, Thomas ML, Fakih AR, Chiplunkar SV. Human gamma delta T cells recognize heat shock protein-60 on oral tumor cells. *Int J Cancer* (1999) 80:709–14. doi:10.1002/(SICI)1097-0215(19990301)80:5<709::AID-IJC14>3.0.CO;2-R
16. Kaur I, Voss SD, Gupta RS, Schell K, Fisch P, Sondel PM. Human peripheral gamma delta T cells recognize hsp60 molecules on Daudi Burkitt's lymphoma cells. *J Immunol* (1993) 150:2046–55.
17. Fisch P, Malkovsky M, Kovats S, Sturm E, Braakman E, Klein BS, et al. Recognition by human V gamma 9/V delta 2 T cells of a GroEL homolog on Daudi Burkitt's lymphoma cells. *Science* (1990) 250:1269–73. doi:10.1126/science.1978758
18. Scotet E, Martinez LO, Grant E, Barbaras R, Jenö P, Guiraud M, et al. Tumor recognition following Vγ9Vδ2 T cell receptor interactions with a surface F1-ATPase-related structure and apolipoprotein A-I. *Immunity* (2005) 22:71–80. doi:10.1016/j.immuni.2004.11.012
19. Rust C, Koning F. γδ T cell reactivity towards bacterial superantigens. *Semin Immunol* (1993) 5:41–6. doi:10.1006/smim.1993.1006
20. Xi XY, Zhang XY, Wang B, Wang J, Huang H, Cui LX, et al. A novel strategy to screen bacillus Calmette-Guérin protein antigen recognized by γδ TCR. *PLoS One* (2011) 6:e18809. doi:10.1371/journal.pone.0018809
21. Xi X, Han X, Li L, Zhao Z. Identification of a new tuberculosis antigen recognized by γδ T cell receptor. *Clin Vaccine Immunol* (2013) 20:530–9. doi:10.1128/CVI.00584-12
22. Dai Y, Chen H, Mo C, Cui L, He W. Ectopically expressed human tumor biomarker MutS homologue 2 is a novel endogenous ligand that is recognized by human γδ T cells to induce innate anti-tumor/virus immunity. *J Biol Chem* (2012) 287:16812–9. doi:10.1074/jbc.M111.327650
23. Fausther-Bovendo H, Wauquier N, Cherfils-Vicini J, Cremer I, Debré P, Vieillard V. NKG2C is a major triggering receptor involved in the Vδ1 T cell-mediated cytotoxicity against HIV-infected CD4 T cells. *AIDS* (2008) 22:217–26. doi:10.1097/QAD.0b013e3282f46e7c
24. Lu Y, Li Z, Ma C, Wang H, Zheng J, Cui L, et al. The interaction of influenza H5N1 viral hemagglutinin with sialic acid receptors leads to the activation of human γδ T cells. *Cell Mol Immunol* (2013) 10:463–70. doi:10.1038/cmi.2013.26
25. Mami-Chouaib F, Miossec C, Del Porto P, Flament C, Triebel F, Hercend T. T cell target 1 (TCT.1): a novel target molecule for human non-major histocompatibility complex-restricted T lymphocytes. *J Exp Med* (1990) 172:1071–82. doi:10.1084/jem.172.4.1071
26. Mami-Chouaib F, Del Porto P, Delorme D, Hercend T. Further evidence for a gamma/delta T cell receptor-mediated TCT.1/CD48 recognition. *J Immunol* (1991) 147:2864–7.
27. Flament C, Bellagha K, Rosenthal-Allieri A, Chouaib S, Mami-Chouaib F. CD48 may serve as an accessory molecule for the activation of a subset of human γ/δ T cells. *Hum Immunol* (1996) 46:82–92. doi:10.1016/0198-8859(96)00010-9
28. Groh V, Steinle A, Bauer S, Spies T. Recognition of stress-induced MHC molecules by intestinal epithelial γδ T cells. *Science* (1998) 279:1737–40. doi:10.1126/science.279.5357.1737
29. Wu J, Groh V, Spies T. T cell antigen receptor engagement and specificity in the recognition of stress-inducible MHC class I-related chains by human epithelial gamma delta T cells. *J Immunol* (2002) 169:1236–40. doi:10.4049/jimmunol.169.3.1236
30. Xu B, Pizarro JC, Holmes MA, McBeth C, Groh V, Spies T, et al. Crystal structure of a T-cell receptor specific for the human MHC class I homolog MICA. *Proc Natl Acad Sci U S A* (2011) 108:2414–9. doi:10.1073/pnas.1015433108
31. Bauer S, Groh V, Wu J, Steinle A, Phillips JH, Lanier LL, et al. Activation of NK cells and T cells by NKG2D, a receptor for stress-inducible MICA. *Science* (1999) 285:727–9. doi:10.1126/science.285.5428.727
32. Das H, Groh V, Kuijl C, Sugita M, Morita CT, Spies T, et al. MICA engagement by human Vgamma2Vdelta2 T cells enhances their antigen-dependent effector function. *Immunity* (2001) 15:83–93. doi:10.1016/S1074-7613(01)00168-6
33. Lu J, Das M, Kanji S, Aggarwal R, Joseph M, Ray A, et al. Induction of ATM/ATR pathway combined with Vγ2Vδ2 T cells enhances cytotoxicity of ovarian cancer cells. *Biochim Biophys Acta* (2014) 1842:1071–9. doi:10.1016/j.bbadis.2014.04.003
34. Lança T, Correia DV, Moita CF, Raquel H, Neves-Costa A, Ferreira C, et al. The MHC class Ib protein ULBP1 is a nonredundant determinant of leukemia/lymphoma susceptibility to γδ T-cell cytotoxicity. *Blood* (2010) 115:2407–11. doi:10.1182/blood-2009-08-237123
35. Catellani S, Poggi A, Bruzzone A, Dadati P, Ravetti JL, Gobbi M, et al. Expansion of Vδ1 T lymphocytes producing IL-4 in low-grade non-Hodgkin lymphomas expressing UL-16-binding proteins. *Blood* (2007) 109:2078–85. doi:10.1182/blood-2006-06-028985
36. Bryant NL, Gillespie GY, Lopez RD, Markert JM, Cloud GA, Langford CP, et al. Preclinical evaluation of ex vivo expanded/activated gammadelta T cells for immunotherapy of glioblastoma multiforme. *J Neurooncol* (2011) 101:179–88. doi:10.1007/s11060-010-0245-2
37. Poggi A, Venturino C, Catellani S, Clavio M, Miglino M, Gobbi M, et al. Vδ1 T lymphocytes from B-CLL patients recognize ULBP3 expressed on leukemic B cells and up-regulated by trans-retinoic acid. *Cancer Res* (2004) 64:9172–9. doi:10.1158/0008-5472.CAN-04-2417
38. Kong Y, Cao W, Xi X, Ma C, Cui L, He W. The NKG2D ligand ULBP4 binds to TCRγ9/δ2 and induces cytotoxicity to tumor cells through both TCRγδ and NKG2D. *Blood* (2009) 114:310–7. doi:10.1182/blood-2008-12-196287
39. Correia DV, Fogli M, Hudspeth K, Gomes Da Silva M, Mavilio D, Silva-Santos B. Differentiation of human peripheral blood Vδ1+ T cells expressing the natural cytotoxicity receptor NKp30 for recognition of lymphoid leukemia cells. *Blood* (2011) 118:992–1001. doi:10.1182/blood-2011-02-339135
40. Hudspeth K, Fogli M, Correia DV, Mikulak J, Roberto A, Della S, et al. Engagement of NKp30 on Vδ1 T-cells induces the production of CCL3, CCL4 and CCL5 and suppresses HIV-1 replication. *Blood* (2012) 119:4013–6. doi:10.1182/blood-2011-11-390153
41. Toutirais O, Cabillic F, Le Friec G, Salot S, Loyer P, Le Gallo M, et al. DNAX accessory molecule-1 (CD226) promotes human hepatocellular carcinoma cell lysis by Vγ9Vδ2 T cells. *Eur J Immunol* (2009) 39:1361–8. doi:10.1002/eji.200838409
42. Sturm E, Braakman E, Fisch P, Vreugdenhil RJ, Sondel P, Bolhuis RL. Human V gamma 9-V delta 2 T cell receptor-gamma delta lymphocytes show specificity to Daudi Burkitt's lymphoma cells. *J Immunol* (1990) 145:3202–8.
43. Fisch P, Oettel K, Fudim N, Surfus JE, Malkovsky M, Sondel PM. MHC-unrestricted cytotoxic and proliferative responses of two distinct human gamma/delta T cell subsets to Daudi cells. *J Immunol* (1992) 148:2315–23.
44. Weintraub BC, Jackson MR, Hedrick SM. Gamma delta T cells can recognize nonclassical MHC in the absence of conventional antigenic peptides. *J Immunol* (1994) 153:3051–8.
45. Tanaka Y, Morita CT, Tanaka Y, Nieves E, Brenner MB, Bloom BR. Natural and synthetic non-peptide antigens recognized by human gamma delta T cells. *Nature* (1995) 375:155–8. doi:10.1038/375155a0
46. Morita CT, Beckman EM, Bukowski JF, Tanaka Y, Band H, Bloom BR, et al. Direct presentation of nonpeptide prenyl pyrophosphate antigens to human γδ T cells. *Immunity* (1995) 3:495–507. doi:10.1016/1074-7613(95)90178-7
47. Jomaa H, Feurle J, Lühs K, Kunzmann V, Tony HP, Herderich M, et al. Vγ9/Vδ2 T cell activation induced by bacterial low molecular mass compounds depends on the 1-deoxy-D-xylulose 5-phosphate pathway of isoprenoid biosynthesis. *FEMS Immunol Med Microbiol* (1999) 25:371–8. doi:10.1016/S0928-8244(99)00110-8
48. Thedrez A, Sabourin C, Gertner J, Devilder MC, Allain-Maillet S, Fournie JJ, et al. Self/non-self discrimination by human gammadelta T cells: simple solutions for a complex issue? *Immunol Rev* (2007) 215:123–35. doi:10.1111/j.1600-065X.2006.00468.x
49. Gober H-J, Kistowska M, Angman L, Jenö P, Mori L, De Libero G. Human T cell receptor gammadelta cells recognize endogenous mevalonate metabolites in tumor cells. *J Exp Med* (2003) 197:163–8. doi:10.1084/jem.20021500
50. Todaro M, D'Asaro M, Caccamo N, Iovino F, Francipane MG, Meraviglia S, et al. Efficient killing of human colon cancer stem cells by gammadelta T lymphocytes. *J Immunol* (2009) 182:7287–96. doi:10.4049/jimmunol.0804288

51. Vavassori S, Kumar A, Wan GS, Ramanjaneyulu GS, Cavallari M, El Daker S, et al. Butyrophilin 3A1 binds phosphorylated antigens and stimulates human γδ T cells. *Nat Immunol* (2013) 14:908–16. doi:10.1038/ni.2665
52. Harly C, Guillaume Y, Nedellec S, Peigné CM, Mönkkönen H, Mönkkönen J, et al. Key implication of CD277/butyrophilin-3 (BTN3A) in cellular stress sensing by a major human γδ T-cell subset. *Blood* (2012) 120:2269–79. doi:10.1182/blood-2012-05-430470
53. Sandstrom A, Peigné CM, Léger A, Crooks J, Konczak F, Gesnel MC, et al. The intracellular B30.2 domain of butyrophilin 3A1 binds phosphoantigens to mediate activation of human Vγ9Vδ2T cells. *Immunity* (2014) 40: 490–500. doi:10.1016/j.immuni.2014.03.003
54. Peigné C-M, Léger A, Gesnel M-C, Konczak F, Olive D, Bonneville M, et al. The juxtamembrane domain of butyrophilin BTN3A1 controls phosphoantigen-mediated activation of human Vγ9Vδ2 T cells. *J Immunol* (2017) 198:4228–34. doi:10.4049/jimmunol.1601910
55. Gu S, Sachleben JR, Boughter CT, Nawrocka WI, Borowska MT, Tarrasch JT, et al. Phosphoantigen-induced conformational change of butyrophilin 3A1 (BTN3A1) and its implication on Vγ9Vδ2 T cell activation. *Proc Natl Acad Sci U S A* (2017) 114:E7311–20. doi:10.1073/pnas.1707547114
56. Sebestyen Z, Scheper W, Vyborova A, Gu S, Rychnavska Z, Schiffler M, et al. RhoB mediates phosphoantigen recognition by Vγ9Vδ2 T cell receptor. *Cell Rep* (2016) 15:1973–85. doi:10.1016/j.celrep.2016.04.081
57. Garni-Wagner BA, Purohit A, Mathew PA, Bennett M, Kumar V. A novel function-associated molecule related to non-MHC-restricted cytotoxicity mediated by activated natural killer cells and T cells. *J Immunol* (1993) 151:60–70.
58. Schuhmachers G, Ariizumi K, Mathew PA, Bennett M, Kumar Y, Takashima A. Activation of murine epidermal γδ T cells through surface 2B4. *Eur J Immunol* (1995) 25:1117–20. doi:10.1002/eji.1830250440
59. Nakajima H, Cella M, Langen H, Friedlein A, Colonna M. Activating interactions in human NK cell recognition: the role of 2B4-CD48. *Eur J Immunol* (1999) 29:1676–83. doi:10.1002/(SICI)1521-4141(199905)29:05<1676::AID-IMMU1676>3.0.CO;2-Y
60. Steinle A, Li P, Morris DL, Groh V, Lanier LL, Strong RK, et al. Interactions of human NKG2D with its ligands MICA, MICB, and homologs of the mouse RAE-1 protein family. *Immunogenetics* (2001) 53:279–87. doi:10.1007/s002510100325
61. Von Lilienfeld-Toal M, Nattermann J, Feldmann G, Sievers E, Frank S, Strehl J, et al. Activated γδ T cells express the natural cytotoxicity receptor natural killer p44 and show cytotoxic activity against myeloma cells. *Clin Exp Immunol* (2006) 144:528–33. doi:10.1111/j.1365-2249.2006.03078.x
62. Groh V, Rhinehart R, Secrist H, Bauer S, Grabstein KH, Spies T. Broad tumor-associated expression and recognition by tumor-derived gamma delta T cells of MICA and MICB. *Proc Natl Acad Sci U S A* (1999) 96: 6879–84. doi:10.1073/pnas.96.12.6879
63. Wrobel P, Shojaei H, Schittek B, Gieseler F, Wollenberg B, Kalthoff H, et al. Lysis of a broad range of epithelial tumour cells by human γδ T cells: involvement of NKG2D ligands and T-cell receptor- versus NKG2D-dependent recognition. *Scand J Immunol* (2007) 66:320–8. doi:10.1111/j.1365-3083.2007.01963.x
64. Deniger DC, Maiti SN, Mi T, Switzer KC, Ramachandran V, Hurton LV, et al. Activating and propagating polyclonal gamma delta T cells with broad specificity for malignancies. *Clin Cancer Res* (2014) 20:5708–19. doi:10.1158/1078-0432.CCR-13-3451
65. Gertner-dardenne J, Castellano R, Mamessier E, Garbit S, Kochbati E, Etienne A, et al. Human Vγ9Vδ2 T cells specifically recognize and kill acute myeloid leukemic blasts. *J Immunol* (2012) 188:4701–8. doi:10.4049/jimmunol.1103710
66. Knight A, MacKinnon S, Lowdell MW. Human Vdelta1 gamma-delta T cells exert potent specific cytotoxicity against primary multiple myeloma cells. *Cytotherapy* (2012) 14:1110–8. doi:10.3109/14653249.2012.700766
67. Chitadze G, Lettau M, Luecke S, Wang T, Janssen O, Fürst D, et al. NKG2D- and T-cell receptor-dependent lysis of malignant glioma cell lines by human γδ T cells: modulation by temozolomide and A disintegrin and metalloproteases 10 and 17 inhibitors. *Oncoimmunology* (2016) 5:e1093276. doi:10.1080/2162402X.2015.1093276
68. Niu C, Jin H, Li M, Zhu S, Zhou L, Jin F, et al. Low-dose bortezomib increases the expression of NKG2D and DNAM-1 ligands and enhances induced NK and γδ T cell-mediated lysis in multiple myeloma. *Oncotarget* (2016) 8:5954–64. doi:10.18632/oncotarget.13979
69. Peipp M, Wesch D, Oberg HH, Lutz S, Muskulus A, van de Winkel JGJ, et al. CD20-specific immunoligands engaging NKG2D enhance γδ T cell-mediated lysis of lymphoma cells. *Scand J Immunol* (2017) 86:196–206. doi:10.1111/sji.12581
70. Todaro M, Orlando V, Cicero G, Caccamo N, Meraviglia S, Stassi G, et al. Chemotherapy sensitizes colon cancer initiating cells to Vγ9Vδ2 T cell-mediated cytotoxicity. *PLoS One* (2013) 8:e65145. doi:10.1371/journal.pone.0065145
71. Hudspeth K, Silva-Santos B, Mavilio D. Natural cytotoxicity receptors: broader expression patterns and functions in innate and adaptive immune cells. *Front Immunol* (2013) 4:69. doi:10.3389/fimmu.2013.00069
72. Cantoni C, Bottino C, Vitale M, Pessino A, Augugliaro R, Malaspina A, et al. NKp44, a triggering receptor involved in tumor cell lysis by activated human natural killer cells, is a novel member of the immunoglobulin superfamily. *J Exp Med* (1999) 189:787–95. doi:10.1084/jem.189.5.787
73. Almeida AR, Correia DV, Fernandes-Platzgummer A, Da Silva CL, Da Silva MG, Anjos DR, et al. Delta one T cells for immunotherapy of chronic lymphocytic leukemia: clinical-grade expansion/differentiation and preclinical proof of concept. *Clin Cancer Res* (2016) 22:5795–804. doi:10.1158/1078-0432.CCR-16-0597
74. Brandt CS, Baratin M, Yi EC, Kennedy J, Gao Z, Fox B, et al. The B7 family member B7-H6 is a tumor cell ligand for the activating natural killer cell receptor NKp30 in humans. *J Exp Med* (2009) 206:1495–503. doi:10.1084/jem.20090681
75. Barrow AD, Edeling MA, Trifonov V, Luo J, Goyal P, Bohl B, et al. Natural killer cells control tumor growth by sensing a growth factor. *Cell* (2018) 172:534–48.e19. doi:10.1016/j.cell.2017.11.037
76. Young JL, Goodall JC, Beacock-Sharp H, Gaston JS. Human gamma delta T-cell recognition of *Yersinia enterocolitica*. *Immunology* (1997) 91:503–10. doi:10.1046/j.1365-2567.1997.00289.x
77. Barisa M, Kramer AM, Majani Y, Moulding D, Saraiva L, Bajaj-Elliott M, et al. *E. coli* promotes human Vγ9Vδ2 T cell transition from cytokine-producing bactericidal effectors to professional phagocytic killers in a TCR-dependent manner. *Sci Rep* (2017) 7:1–12. doi:10.1038/s41598-017-02886-8
78. Hara T, Mizuno Y, Takaki K, Takada H, Akeda H, Aoki T, et al. Predominant activation and expansion of V gamma 9-bearing gamma delta T cells in vivo as well as in vitro in *Salmonella* infection. *J Clin Invest* (1992) 90:204–10. doi:10.1172/JCI115837
79. Munk ME, Elser C, Kaufmann SHE. Human γ/δ T-cell response to *Listeria monocytogenes* protein components in vitro. *Immunology* (1996) 230:230–5. doi:10.1046/j.1365-2567.1996.470549.x
80. Marx S, Wesch D, Kabelitz D. Activation of human gamma delta T cells by *Mycobacterium tuberculosis* and Daudi lymphoma cells: differential regulatory effect of IL-10 and IL-12. *J Immunol* (1997) 158:2842–8.
81. Chen ZW. Protective immune responses of major Vγ2Vδ2 T-cell subset in *M. tuberculosis* infection. *Curr Opin Immunol* (2016) 42:105–12. doi:10.1016/j.coi.2016.06.005
82. Hara T, Ohashi S, Yamashita Y, Abe T, Hisaeda H, Himeno K, et al. Human V delta 2+ gamma delta T-cell tolerance to foreign antigens of *Toxoplasma gondii*. *Proc Natl Acad Sci U S A* (1996) 93:5136–40. doi:10.1073/pnas.93.10.5136
83. Kurup SP, Harty JT. γδ T cells and immunity to human malaria in endemic regions. *Ann Transl Med* (2015) 3:S22. doi:10.3978/j.issn.2305-5839.2015.02.22
84. Russo DM, Armitage RJ, Barral-Netto M, Barral A, Grabstein KH, Reed SG. Antigen-reactive gamma delta T cells in human leishmaniasis. *J Immunol* (1993) 151:3712–8.
85. Elloso MM, van der Heyde HC, vande Waa JA, Manning DD, Weidanz WP. Inhibition of *Plasmodium falciparum* in vitro by human gamma delta T cells. *J Immunol* (1994) 153:1187–94.
86. Giulia C, Loizon S, Guenot M, Mocan I, Halary F, De Saint-Basile G, et al. Control of *Plasmodium falciparum* erythrocytic cycle: γδ T cells target the red blood cell-invasive merozoites. *Blood* (2011) 118:6952–62. doi:10.1182/blood-2011-08-376111
87. Poccia F, Agrati C, Martini F, Capobianchi MR, Wallace M, Malkovsky M. Antiviral reactivities of γδ T cells. *Microbes Infect* (2005) 7:518–28. doi:10.1016/j.micinf.2004.12.009
88. Cimini E, Viola D, Cabeza-Cabrerizo M, Romanelli A, Tumino N, Sacchi A, et al. Different features of Vδ2 T and NK cells in fatal and non-fatal human

Ebola infections. *PLoS Negl Trop Dis* (2017) 11:e0005645. doi:10.1371/journal.pntd.0005645
89. Knight A, Madrigal AJ, Grace S, Sivakumaran J, Kottaridis P, Mackinnon S, et al. The role of Vδ2-negative γδ T cells during cytomegalovirus reactivation in recipients of allogeneic stem cell transplantation. *Blood* (2010) 116:2164–72. doi:10.1182/blood-2010-01-255166
90. Pitard V, Roumanes D, Lafarge X, Couzi L, Garrigue I, Lafon ME, et al. Long-term expansion of effector/memory V{delta}2-{gamma}-{delta} T cells is a specific blood signature of CMV infection. *Blood* (2008) 112:1317–24. doi:10.1182/blood-2008-01-136713
91. Lafarge X, Merville P, Cazin MC, Bergé F, Potaux L, Moreau JF, et al. Cytomegalovirus infection in transplant recipients resolves when circulating gammadelta T lymphocytes expand, suggesting a protective antiviral role. *J Infect Dis* (2001) 184:533–41. doi:10.1086/322843
92. Eberl M, Hintz M, Reichenberg A, Kollas AK, Wiesner J, Jomaa H. Microbial isoprenoid biosynthesis and human γδ T cell activation. *FEBS Lett* (2003) 544:4–10. doi:10.1016/S0014-5793(03)00483-6
93. Hintz M, Reichenberg A, Altincicek B, Bahr U, Gschwind RM, Kollas AK, et al. Identification of (E)-4-hydroxy-3-methyl-but-2-enyl pyrophosphate as a major activator for human γδ T cells in *Escherichia coli*. *FEBS Lett* (2001) 509:317–22. doi:10.1016/S0014-5793(01)03191-X
94. Gao Y, Williams AP. Role of innate T cells in anti-bacterial immunity. *Front Immunol* (2015) 6:302. doi:10.3389/fimmu.2015.00302
95. Pellicci DG, Uldrich AP, Le Nours J, Ross F, Chabrol E, Eckle SB, et al. The molecular bases of delta/alphabeta T cell-mediated antigen recognition. *J Exp Med* (2014) 211:2599–615. doi:10.1084/jem.20141764
96. Uldrich AP, Le Nours J, Pellicci DG, Gherardin NA, Mcpherson KG, Lim RT, et al. CD1d-lipid antigen recognition by the γδ TCR. *Nat Immunol* (2013) 14:1137–45. doi:10.1038/ni.2713
97. Luoma AM, Castro CD, Mayassi T, Bembinster LA, Bai L, Picard D, et al. Crystal structure of Vδ1 T cell receptor in complex with CD1d-sulfatide shows MHC-like recognition of a self-lipid by human γδ T cells. *Immunity* (2013) 39:1032–42. doi:10.1016/j.immuni.2013.11.001
98. Agrati C, D'Offizi G, Narciso P, Abrignani S, Ippolito G, Colizzi V, et al. Vdelta1 T lymphocytes expressing a Th1 phenotype are the major gammadelta T cell subset infiltrating the liver of HCV-infected persons. *Mol Med* (2001) 7:11–9.
99. Li H, Xiang Z, Feng T, Li J, Liu Y, Fan Y, et al. Human Vγ9Vδ2-T cells efficiently kill influenza virus-infected lung alveolar epithelial cells. *Cell Mol Immunol* (2013) 10:159–64. doi:10.1038/cmi.2012.70
100. Bessoles S, Ni M, Garcia-Jimenez S, Sanchez F, Lafont V. Role of NKG2D and its ligands in the anti-infectious activity of Vγ9Vδ2 T cells against intracellular bacteria. *Eur J Immunol* (2011) 41:1619–28. doi:10.1002/eji.201041230
101. Bieback K, Breer C, Nanan R, Ter Meulen V, Schneider-Schaulies S. Expansion of human gamma/delta T cells in vitro is differentially regulated by the measles virus glycoproteins. *J Gen Virol* (2003) 84:1179–88. doi:10.1099/vir.0.19027-0
102. Knight A, Arnouk H, Britt W, Gillespie GY, Cloud GA, Harkins L, et al. CMV-independent lysis of glioblastoma by ex vivo expanded/activated Vδ1+ γδ T cells. *PLoS One* (2013) 8:e68729. doi:10.1371/journal.pone.0068729
103. Kunzmann V, Bauer E, Wilhelm M. γ/δ T-cell stimulation by pamidronate. *N Engl J Med* (1999) 340:737–8. doi:10.1056/NEJM199903043400914
104. Qaqish A, Huang D, Chen CY, Zhang Z, Wang R, Li S, et al. Adoptive transfer of phosphoantigen-specific γδ T cell subset attenuates mycobacterium tuberculosis infection in nonhuman primates. *J Immunol* (2017) 198:4753–63. doi:10.4049/jimmunol.1602019
105. Fisher JP, Heuijerjans J, Yan M, Gustafsson K, Anderson J. γδ T cells for cancer immunotherapy. *Oncoimmunology* (2014) 3:e27572. doi:10.4161/onci.27572
106. Fournié JJ, Sicard H, Poupot M, Bezombes C, Blanc A, Romagné F, et al. What lessons can be learned from γδ T cell-based cancer immunotherapy trials? *Cell Mol Immunol* (2013) 10:35–41. doi:10.1038/cmi.2012.39
107. Legut M, Cole DK, Sewell AK. The promise of γδT cells and the γδT cell receptor for cancer immunotherapy. *Cell Mol Immunol* (2015) 12:656–8. doi:10.1038/cmi.2015.28
108. Zou C, Zhao P, Xiao Z, Han X, Fu F, Fu L. γδ T cells in cancer immunotherapy. *Oncotarget* (2017) 8:8900–9. doi:10.18632/oncotarget.13051
109. Nakajima J, Murakawa T, Fukami T, Goto S, Kaneko T, Yoshida Y, et al. A phase I study of adoptive immunotherapy for recurrent non-small-cell lung cancer patients with autologous γδ T cells. *Eur J Cardiothorac Surg* (2010) 37:1191–7. doi:10.1016/j.ejcts.2009.11.051
110. Izumi T, Kondo M, Takahashi T, Fujieda N, Kondo A, Tamura N, et al. Ex vivo characterization of γδ T-cell repertoire in patients after adoptive transfer of Vγ9Vδ2 T cells expressing the interleukin-2 receptor β-chain and the common γ-chain. *Cytotherapy* (2013) 15:481–91. doi:10.1016/j.jcyt.2012.12.004
111. Siegers GM, Lamb LS. Cytotoxic and regulatory properties of circulating Vδ1+ γδ t cells: a new player on the cell therapy field? *Mol Ther* (2014) 22:1416–22. doi:10.1038/mt.2014.104

Conflict of Interest Statement: BS-S is a co-founder and shareholder of Lymphact—Lymphocyte Activation Technologies S.A. The other authors declare that the research was conducted in the absence of any commercial or financial relationships that could be construed as a potential conflict of interest.

Published OnlineFirst March 20, 2019; DOI: 10.1158/2326-6066.CIR-18-0647

Priority Brief

Cancer Immunology Research

Broad Cytotoxic Targeting of Acute Myeloid Leukemia by Polyclonal Delta One T Cells

Biagio Di Lorenzo[1,2], André E. Simões[1,3], Francisco Caiado[1], Paola Tieppo[4], Daniel V. Correia[1,5], Tânia Carvalho[1], Maria Gomes da Silva[6], Julie Déchanet-Merville[7], Ton N. Schumacher[8], Immo Prinz[9], Haakan Norell[1], Sarina Ravens[9], David Vermijlen[4], and Bruno Silva-Santos[1]

Abstract

Acute myeloid leukemia (AML) remains a clinical challenge due to frequent chemotherapy resistance and deadly relapses. We are exploring the immunotherapeutic potential of peripheral blood Vδ1$^+$ T cells, which associate with improved long-term survival of stem-cell transplant recipients but have not yet been applied as adoptive cell therapy. Using our clinical-grade protocol for expansion and differentiation of "Delta One T" (DOT) cells, we found DOT cells to be highly cytotoxic against AML primary samples and cell lines, including cells selected for resistance to standard chemotherapy. Unlike chemotherapy, DOT-cell targeting did not select for outgrowth of specific AML lineages, suggesting a broad recognition domain, an outcome that was consistent with the polyclonality of the DOT-cell T-cell receptor (TCR) repertoire. However, AML reactivity was only slightly impaired upon Vδ1$^+$ TCR antibody blockade, whereas it was strongly dependent on expression of the NKp30 ligand, B7-H6. In contrast, DOT cells did not show reactivity against normal leukocytes, including CD33$^+$ or CD123$^+$ myeloid cells. Adoptive transfer of DOT cells *in vivo* reduced AML load in the blood and target organs of multiple human AML xenograft models and significantly prolonged host survival without detectable toxicity, thus providing proof-of-concept for DOT-cell application in AML treatment.

Introduction

Acute myeloid leukemia (AML) has a dismal (10%) survival rate among the elderly (age 65 or older), mostly due to resistance to standard treatment. Available treatment consists of a combination of cytarabine with an anthracyclin drug, which although effective at inducing complete remissions, ultimately selects for chemoresistant clones that drive refractory relapses (1, 2). Promising alternatives to chemotherapy are targeted therapies (1, 3) and upcoming immunotherapies (2), especially chimeric antigen receptor (CAR) T-cell transfer, which has been successful against in B-cell malignancies (4). However, CARs have proved difficult to implement in AML due to on-target effects on vital healthy myeloid progenitor cells that express the target antigens CD33 and CD123 (2). We focused here on *ex vivo* differentiated Vδ1$^+$ T (Delta One T, or "DOT") cells that rely on physiologic receptors, namely T-cell receptor (TCR) and natural cytotoxicity receptors (NCR) such as NKp30 and NKp44, to distinguish the transformed from healthy cells (5–7). DOT cells are derived from peripheral blood Vδ1$^+$ γδ T cells, the *in vivo* expansion of which correlated with enhanced long-term disease-free survival of patients with leukemia who received allogeneic hematopoietic stem cell transplantation (8).

Although the clinical manipulation of Vδ1$^+$ γδ T cells has been hindered by their relatively low abundance (<0.5%) among peripheral blood lymphocytes, we have devised a clinical-grade protocol to expand and differentiate large numbers of DOT-cells endowed with antitumor cytotoxicity (5, 6). Our 3-week protocol achieves >1,000-fold expansions of Vδ1$^+$ γδ T cells. During the first stage, the synergistic action of TCR and IL4 stimulation is critical for large expansion yields. The second stage focuses on the IL15-dependent differentiation of antitumor DOT-cell effectors endowed with NCR expression (6). Seeing the convergence between the properties of DOT cells with the unmet immunotherapy needs of AML, in this study, we aimed to refine DOT cells for use in treatment of AML.

Materials and Methods

Ethics statement

Primary AML cells were obtained from the peripheral blood of patients at first presentation, after informed consent and institutional review board approval. The study was conducted in accordance with the Declaration of Helsinki.

[1]Instituto de Medicina Molecular João Lobo Antunes, Faculdade de Medicina, Universidade de Lisboa, Lisbon, Portugal. [2]Instituto Superior Técnico, Universidade de Lisboa, Lisbon, Portugal. [3]Lymphact – Lymphocyte Activation Technologies S.A., Coimbra, Portugal. [4]Department of Pharmacotherapy and Pharmaceutics, Institute for Medical Immunology, Université Libre de Bruxelles, Brussels, Belgium. [5]GammaDelta Therapeutics, London, United Kingdom. [6]Instituto Português de Oncologia – Francisco Gentil, Lisbon, Portugal. [7]Immunoconcept, CNRS UMR 5164, Université de Bordeaux, Bordeaux, France. [8]Netherlands Cancer Institute, Amsterdam, the Netherlands. [9]Hannover Medical School, Hannover, Germany.

Note: Supplementary data for this article are available at Cancer Immunology Research Online (http://cancerimmunolres.aacrjournals.org/).

Corresponding Author: Bruno Silva-Santos, Instituto de Medicina Molecular João Lobo Antunes, Avenida Prof. Egas Moniz, 1649-028 Lisboa 1649-028, Portugal. Phone: 3519-1453-8335; Fax: 3512-1798-5142; E-mail: bssantos@medicina.ulisboa.pt

doi: 10.1158/2326-6066.CIR-18-0647

Published OnlineFirst March 20, 2019; DOI: 10.1158/2326-6066.CIR-18-0647

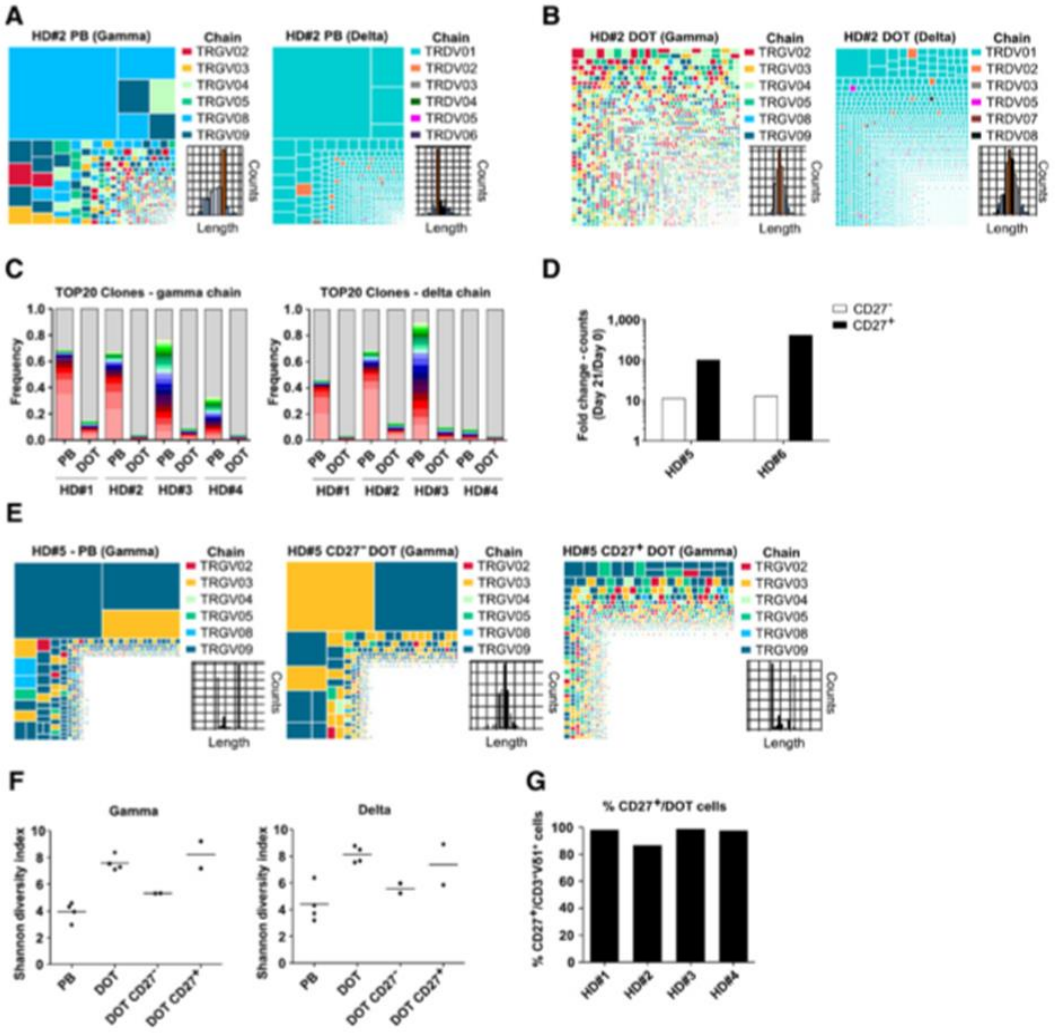

Figure 1.

DOT cells display higher clonal diversity than *ex vivo* Vδ1$^+$ T cells. Graphical representation of *TRGV* (left) and *TRDV* (right) repertoires and CDR3 length (number of nucleotides) distribution of FACS-sorted Vδ1$^+$ T cells from peripheral blood/PB (**A**); or DOT-cell products (**B**; see also Supplementary Fig. S2A–S2C). Each square represents a different clonotype (with distinct nucleotide sequence), its area is proportional to the relative abundance in the sample; and the color groups the clonotypes by chains. **C,** Contribution of the top 20 clones to the overall Vδ1$^+$ TCR repertoire of each sample (HD1–4, healthy donors 1 to 4). **D,** Fold expansion of presorted CD27$^-$ versus CD27$^+$ Vδ1$^+$ T cells after 21 days with the DOT-cell protocol (HD5–6, healthy donors 5 and 6). **E,** Graphical representation of *TRGV* repertoire and CDR3 length distribution (as in **A–B**) for CD27$^-$ versus CD27$^+$ Vδ1$^+$ T cells cultured for 21 days with the DOT-cell protocol (see also Supplementary Fig. S3). **F,** Shannon indices for intrasample variability of *TRGV* and *TRDV* repertoires from **A–B** and **E**. **G,** Percentage of CD27$^+$ cells upon expansion with the DOT-cell protocol. Data in this Figure are derived from 6 independent healthy donors.

Mice

NOD SCID $\gamma_c^{-/-}$ (NSG), NOD SCID $\gamma_c^{-/-}$ SGM3 (NSGS), and NOD Rag1$^{-/-}$ $\gamma_c^{-/-}$ SGM3 (NRGS) mice were obtained from the Jackson Laboratories. Age and sex-matched mice were randomly distributed among the different groups. Disease development was followed through weekly bleedings (in intrabone marrow models) and disease end-point is achieved upon first indication of back leg decreased mobility. All animal procedures were performed in accordance to national guidelines from the Direção Geral de Veterinária and approved by the Animal Ethics Committee of Instituto de Medicina Molecular João Lobo Antunes (Lisboa, Portugal).

Published OnlineFirst March 20, 2019; DOI: 10.1158/2326-6066.CIR-18-0647

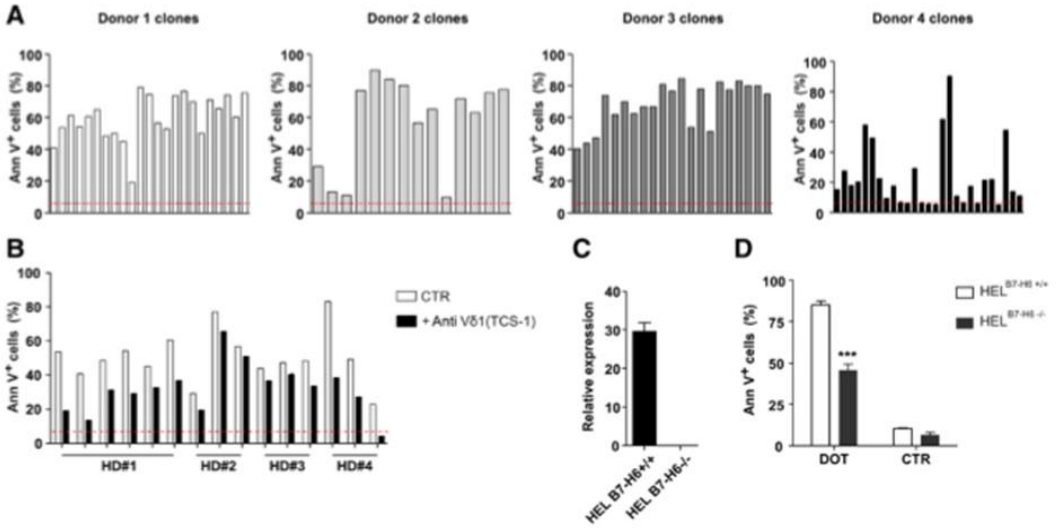

Figure 2.

Clonal DOT-cell reactivity against AML cells. **A** and **B,** *In vitro* killing of AML KG-1 cells by DOT-cell clones generated from single Vδ1$^+$ T cells sorted from healthy donors. Cells were coincubated for 3 hours at 10:1 (E:T) ratio and then analyzed by Annexin V staining (percentage of positive events among prelabeled KG-1 cells). Each bar represents killing of KG-1 cells upon coincubation with individual clones. Dashed red line represents the mean basal tumor cell death (without DOT cells). In **B,** either anti-Vδ1$^+$ TCR-specific mAb or isotype control was added to the cultures. Shown are the clones where the blockade led to clearer reduction in KG-1 targeting. Data represent the average of two technical replicates and are derived from 4 independent healthy donors (HD). **C,** Real-time PCR assessing B7-H6 mRNA in parental (B7-H6$^{+/+}$) and CRISPR/Cas9-manipulated (B7-H6$^{-/-}$) AML HEL cell lines. **D,** *In vitro* killing of B7-H6$^{+/+}$ or B7-H6$^{-/-}$ AML HEL cells by bulk DOT cells produced from 3 healthy donors (tested in technical duplicates). Cells were coincubated for 3 hours at 10:1 (E:T) ratio and then analyzed by Annexin V staining (shown are percentages of positive events among prelabeled HEL cells). Indicated are mean + SEM (***, $P < 0.001$).

DOT-cell production and TCR repertoire analysis

DOT cells were produced from peripheral blood of healthy donors, cultured for 21 days as previously detailed (6). In brief, MACS-sorted γδ T cells were resuspended in serum-free culture medium (OpTmizer-CTS) supplemented with 5% autologous plasma and 2 mmol/L L-glutamine (Thermo Fisher Scientific). Animal-free human cytokines rIL4 (100 ng/mL), rIFNγ (70 ng/mL), rIL21 (7 ng/mL), and rIL1β (15 ng/mL; all from PeproTech), and a soluble mAb to CD3 (clone OKT-3, 70 ng/mL; BioXcell), were added to the medium. Cells were incubated at 37°C and 5% CO_2. Every 5–6 days, old medium was removed and replaced with fresh medium supplemented with cytokines, including rIL15 (70 ng/mL), IFNγ (30 ng/mL), and anti-CD3 (1 μg/mL).

For *TRGV* and *TRDV* repertoire analysis, Vδ1$^+$ T cells were FACS-sorted either from the initial blood sample (*ex vivo*); or from the final (3-week culture) DOT-cell product. Next-generation sequencing was performed as described previously (9, 10). The software for data analysis is described in Supplementary Table S1.

For DOT-cell clone generation, CD3$^+$ TCRVδ1$^+$ TCRVδ2$^-$ single cells were FACS-sorted into 96-wells/plates; and cultured for 21 days using the DOT-cell protocol in the presence of (weekly renewed) 10^4 irradiated autologous peripheral blood mononuclear cells (feeders).

AML cell targeting *in vitro* and *in vivo*

AML cell lines (THP-1, HEL, AML-193, MV4-11, HL-60, U-937, OCI-AML3, Kasumi-1, and KG-1) were obtained from and authenticated by the German Resource Center for Biologic Material (DSMZ); and used at passages p3–p8. Lentiviral barcoding of AML cells was performed and analyzed as detailed previously (11). For *in vitro* targeting, AML cell lines or primary samples were coincubated with DOT cells for 3 hours; and stained with Annexin V, as detailed previously (6). For *in vivo* targeting, three xenograft hAML models were established as represented in Supplementary Fig. S5A–S5C. The patient-derived xenograft (intratibial injection) was described previously (12). Tumor burden was assessed by staining with antihuman CD45 (HI30) and CD33 (P67.6). Flow cytometry acquisition was performed on a LSR Fortessa (BD Biosciences) and data was analyzed with FlowJo X software (Tree Star).

CRISPR/Cas9 Knockout

Guide RNAs (gRNA1: CACCGTTCCGGACCACCGTTATAAC; gRNA2: CACCGCGGCTCTGATCCAATATGAT) were designed to target the genomic sequence of B7-H6 in two areas close to the promoter. gRNAs were inserted into a plasmid containing the sequence codifying for Cas9 enzyme and transfected by electroporation in HEL cells. Successful single-cell knockout clones were confirmed by qRT-PCR (forward primer: CACAGGGAACAGTCCAGCTT; reverse primer TGATCCAGCAACAATCTGCT, performed as described previously; ref. 5).

Statistical analysis

Performed using GraphPad Prism software. All data expressed as mean ± SEM. Comparisons of two groups by Student *t* test; and more than two groups by ANOVA test with Dunnet post test.

Published OnlineFirst March 20, 2019; DOI: 10.1158/2326-6066.CIR-18-0647

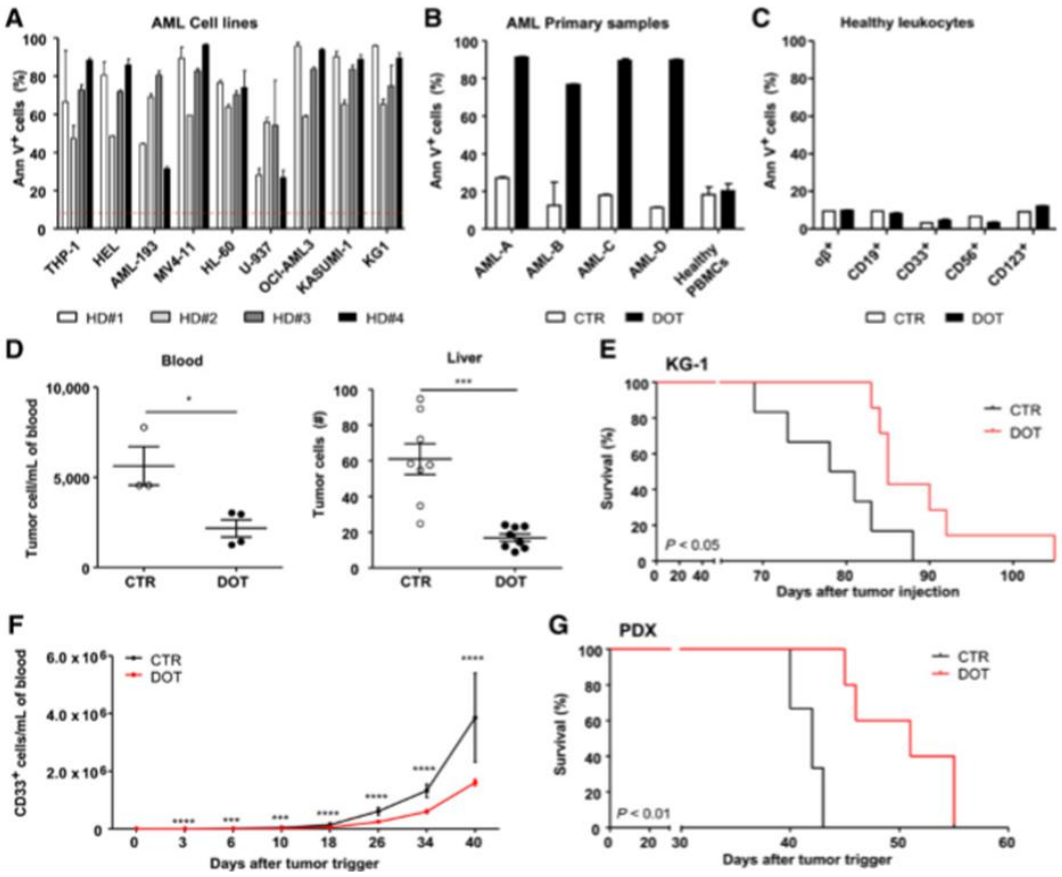

Figure 3.

DOT cells target multiple AML cell types but not healthy leukocytes. *In vitro* killing assays with DOT cells produced from 3–4 healthy donors, coincubated for 3 hours at 10:1 (E:T) ratio with the indicated AML cell lines (**A**), primary AML samples (**B**), or normal leukocyte populations FACS-sorted from the peripheral blood (**C**). In **A**, the dashed red line represents the mean basal tumor cell death; and in **B**, CTR refers also to tumor cells alone (without DOT cells). Experiments were performed with technical triplicates. *In vivo* AML targeting by DOT cells. DOT cells (3 injections of 2×10^7 cells, see Supplementary Fig. S5A–S5C) were transferred to NSG mice ($n = 6$ CTR, 7 DOT-treated mice) preinjected with KG-1 AML cells (**D–E**); or NSGS mice ($n = 5$ CTR, 5 DOT-treated mice) bearing primary AML cells (**F–G**; patient-derived xenograft, PDX). Tumor burden was assessed in the blood and liver one week after the last DOT-cell transfer (**D**); or through weekly bleedings (**F**). Indicated are mean + SEM, *, $P < 0.05$; ***, $P < 0.001$; ****, $P < 0.0001$. Animals were sacrificed when advanced disease symptoms (such as back leg paralysis) were observed. Survival curves are presented in panels E ($P < 0.05$) and G ($P < 0.01$).

Animal survival comparisons performed using log-rank (Mantel–Cox) test.

Data sharing

The TCR repertoire NGS data have been deposited with links to BioProject accession number PRJNA491919 in the NCBI BioProject database (https://www.ncbi.nlm.nih.gov/bioproject/); the sample list is available as Supplementary Table S2.

Results and Discussion

We are interested in developing a Vδ1$^+$ γδ T cell–based adoptive cell therapy for cancer (5, 6). Here, we initially characterized the DOT-cell product upon expansion of αβ-depleted peripheral blood mononuclear cells with the established DOT-cell protocol (6). We analyzed Vδ1$^+$ T-cell percentages and amounts along with NCR expression over time (Supplementary Fig. S1A–S1F). Because reports described the clonal expansion and focusing of the adult peripheral blood Vδ1$^+$ T-cell repertoire (13), likely driven by common pathogens such as CMV (10), we analyzed the effect of the DOT-cell expansion on the TCR repertoire. We performed next-generation sequencing of the CDR3 regions in *TRGV* and *TRDV* genes, before and after the cells were 3 weeks in culture. We found DOT-cells to be highly polyclonal and devoid of dominant clones, in contrast to *ex vivo* Vδ1$^+$ T cells from all donors analyzed (Fig. 1A and B; Supplementary Fig. S2A–S2C).

Published OnlineFirst March 20, 2019; DOI: 10.1158/2326-6066.CIR-18-0647

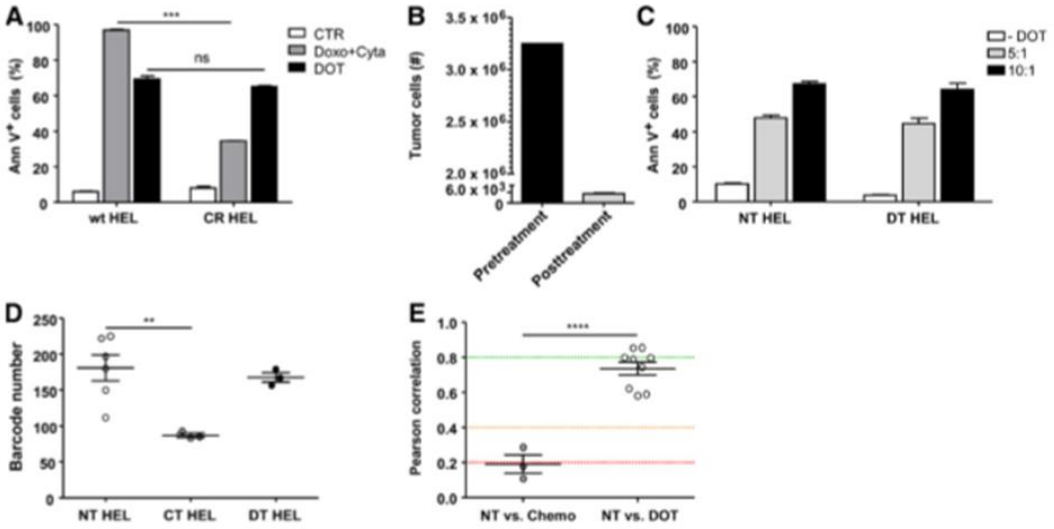

Figure 4.

DOT cells (re-)target chemotherapy-resistant AML. Comparison of the *in vitro* anti-AML activity of DOT cells and standard chemotherapy. **A,** DOT cells and standard AML chemotherapy (doxorubicin plus cytarabine) protocols were tested against chemotherapy-naïve (wild type, wt) or chemo-relapsed (CR, regrown after >99% HEL cell elimination) AML cells. Shown are the percentages of Annexin V$^+$ HEL cells after 3 hours of treatment. **B,** Number of AML HEL cells before and after 72 hours of treatment with DOT cells (at 5:1 E:T ratio). Surviving cells (<1%) were resorted and allowed to regrow, thus generating the DOT-treated (DT) samples of (**C–E**). **C,** DOT cells were coincubated for 3 hours with nontreated (NT) or previously DOT-treated (DT) AML HEL cells at 5:1 or 10:1 (E:T) ratios. Shown are the percentages of Annexin V$^+$ HEL cells. **D,** Number of barcoded AML single-cell lineages in non-treated (NT), chemotherapy-treated (CT), or DOT-treated (DT) AML HEL cells. **E,** Pearson correlation for distribution of barcoded AML single-cell lineages between different treatments. Red, yellow, and green dashed lines represent low, medium, and high correlations, respectively. Indicated are mean + SEM (**, $P < 0.01$; ***, $P < 0.001$; ****, $P < 0.0001$).

This was illustrated by the contribution of the top 20 expanded clones to the overall Vδ1$^+$ TCR repertoire. Although these 20 clones represented >60% in the peripheral blood, they accounted for less than 10% in the DOT-cell products (Fig. 1C). Moreover, few clonotypes (especially for *TRDV*) were shared between those identified *ex vivo* and in DOT cells (Supplementary Table S3). We next aimed to better understand the basis for the diversification of the DOT-cell repertoire. Given the previous association of CD27 downregulation with preexpanded/differentiated Vδ1$^+$ T cells (13), we compared the TCR clonality of DOT cells produced from presorted CD27$^-$ versus CD27$^+$ subsets, which displayed distinct proliferation capacities under the DOT-cell protocol (Fig. 1D). We found that the generation of diverse DOT cells was restricted to CD27$^+$ precursors (Fig. 1E and F; Supplementary Fig. S3A). Taking into account that CD27$^+$ cells typically represent only a small fraction of *ex vivo* Vδ1$^+$ T cells (Supplementary Fig. S3B), these data suggest that the DOT-cell protocol preferentially expands naïve-like CD27$^+$ Vδ1$^+$ T cells with a diverse TCR repertoire at the expense of preexpanded and terminally differentiated CD27$^-$ Vδ1$^+$ T cells. In support of this, the DOT-cell population (generated from bulk Vδ1$^+$ T cells) was largely composed of CD27$^+$ cells (Fig. 1G). DOT-cell products originated from presorted CD27$^+$ cells expressed NKp30 and were highly cytotoxic against KG-1 AML cells (Supplementary Fig. S3C and S3D).

To assess the functional relevance of DOT-cell polyclonality, we generated clones from single-cell sorted Vδ1$^+$ T cells, expanded/differentiated using an adapted DOT-cell protocol including the addition of feeder cells. We tested their cytotoxicity against the AML cell line KG-1 (Fig. 2A). We found the majority of clones (from different donors) to be efficient at inducing apoptosis of KG-1 cells upon short (3-hour) coincubation *in vitro* (Fig. 2A). These results show that DOT-cell products are composed of multiple clones with intrinsic capacity to target AML cells. To functionally test whether the TCR is involved in this reactivity, we performed the killing assay in the presence of a Vδ1$^+$ TCR–specific blocking mAb (or isotype control), and observed only a mild reduction in KG-1 cell targeting across a number of clones from different donors (Fig. 2B). At this stage, we hypothesized that most of the reactivity was mediated by natural cytotoxicity receptors (5–7), particularly NKp30 (Supplementary Fig. S1F). In fact, DOT-cell cytotoxicity was significantly decreased upon CRISPR/Cas9-mediated knockout (at the population level) of the best established tumor-associated NKp30 ligand, B7-H6, in target AML cells (Fig. 2C and D).

To further evaluate the anti-AML activity, we tested bulk DOT-cell products (from multiple donors) against various other AML cell lines as well as primary samples obtained from patients at diagnosis. In all cases, DOT cells readily (within 3 hours) killed AML cells *in vitro* (Fig. 3A and B), in similar fashion to what was reported for CAR-T cells (14–16), and unlike *ex vivo* Vδ1$^+$ T cells (Supplementary Fig. S4A). DOT-cell cytotoxicity associated with increased degranulation and expression of perforin and granzyme B upon tumor cell recognition (Supplementary Fig. S4B and S4C). DOT cells did not target any normal leukocyte population (myeloid or lymphoid)

from the peripheral blood of healthy volunteers (Fig. 3C), including $CD33^+$ and $CD123^+$ myeloid progenitor cells, whose on-target depletion by the respective CAR-T cells is known to be responsible for the unwanted myeloablation (2, 15).

To test DOT cells against AML *in vivo*, we established various independent xenograft models of AML (Supplementary Fig. S5A–S5C). Both in AML cell line models (Fig. 3D and E; Supplementary Fig. S5C) and in two patient-derived xenografts (Fig. 3F and G; Supplementary Fig. S5D and S5E), DOT-cell treatment reduced tumor burden and increased host survival, without noticeable toxicity. Although CAR-T cells have been reported to produce bigger survival benefits in AML xenografts (14–16), these models were biased to AML cell lines uniformly expressing the target antigens. On the other hand, the toxicity of a strategy predicted to induce myeloablation in patients cannot be evaluated with the use of xenografts. Overall, we believe that the combined safety and efficacy profiles of DOT cells make them candidates for adoptive cell therapy of AML in the future.

Chemoresistance drives deadly relapses in the context of AML therapies. We next asked whether DOT cells could target chemoresistant AML cells. For that purpose, we treated AML cells with cytarabine plus doxorubicin for 72 hours, which led to >99% tumor cell elimination, allowed the surviving cells to regrow, then treated the culture with chemotherapy or DOT cells. Although the cytotoxic efficacy of chemotherapy was reduced, the targeting efficacy of DOT cells was unaffected (Fig. 4A), demonstrating the superior capacity of DOT cells to target chemoresistant AML cells. In light of this, and taking into account the polyclonal and multireactive DOT-cell repertoire (Fig. 1A–C), we also questioned the ability of DOT cells to retarget AML cells following a first DOT-cell treatment that eliminated >99% tumor cells in 72 hours (Fig. 4B). Thus, we FACS-sorted the remaining approximately 0.1% of AML cells present at 72 hours and allowed the cell culture to regrow before retreatment with DOT cells. DOT cells killed DOT-pretreated AML cells as efficiently as nontreated controls (Fig. 4C), suggesting that DOT-cell treatment did not select for a specific subset of DOT-resistant AML cells. To track the AML clonal dynamics upon therapeutic (DOT cells or chemotherapy) pressure, we tagged single AML cells with cellular barcodes (noncoding DNA sequences that can be tracked by NGS; ref. 11). Although chemotherapy selectively targeted approximately half of all the barcoded AML single-cell lineages, DOT cells preserved the clonal architecture of the AML population (Fig. 4D and E). These data collectively suggest that the breadth of AML targeting by cytotoxic DOT cells avoids the selection of resistant lineages and allows efficient retreatment. Emergence of refractory relapses after chemotherapy needs to be prevented. Our work thus provides preclinical proof-of-concept for clinical application of DOT cells in AML treatment.

Disclosure of Potential Conflicts of Interest

D.V. Correia has ownership interest in GammaDelta Therapeutics; B. Silva-Santos reports receiving commercial research funding from, has ownership interest in, and is a consultant/advisory board member for GammaDelta Therapeutics. No potential conflicts of interest were disclosed by the other authors.

Authors' Contributions

Conception and design: B.D. Lorenzo, A.E. Simões, H. Norell, D. Vermijlen, B. Silva-Santos

Development of methodology: B.D. Lorenzo, A.E. Simões, F. Caiado, D.V. Correia, T. Carvalho, M.G. da Silva, J. Dechanet-Merville, T.N. Schumacher, I. Prinz

Acquisition of data (provided animals, acquired and managed patients, provided facilities, etc.): B.D. Lorenzo, A.E. Simões, F. Caiado, P. Tieppo, S. Ravens

Analysis and interpretation of data (e.g., statistical analysis, biostatistics, computational analysis): B.D. Lorenzo, A.E. Simões, F. Caiado, D. Vermijlen

Writing, review, and/or revision of the manuscript: B.D. Lorenzo, A.E. Simões, B. Silva-Santos

Administrative, technical, or material support (i.e., reporting or organizing data, constructing databases): B.D. Lorenzo, A.E. Simões

Study supervision: B. Silva-Santos

Acknowledgments

Our work was funded by Fundação para a Ciência e Tecnologia (PTDC/DTP-PIC/4931/2014 to B. Silva-Santos; PD/BD/105880/2014 to B.D. Lorenzo; BPD/85947/2012 to D.V. Correia); Lymphact S.A. (upon investment from Portugal Capital Ventures, S.A, and Busy Angels SCR); GammaDelta Therapeutics (sponsored research agreement to B. Silva-Santos); and Télévie-FNRS (7.4555.14F to D. Vermijlen). We also acknowledge UID/BIM/50005/2019, project funded by Fundação para a Ciência e a Tecnologia (FCT)/Ministério da Ciência, Tecnologia e Ensino Superior (MCTES) through Fundos do Orçamento de Estado; and LISBOA-01-0145-FEDER-016394, project cofounded by FEDER, through POR Lisboa 2020 - Programa Operacional Regional de Lisboa, PORTUGAL 2020, and Fundação para a Ciência e a Tecnologia.

We thank Inês Barbosa (Instituto Português de Oncologia, Lisboa, Portugal) for help with provision of primary AML samples; Miguel Marques Antunes, Diogo Conduto, Simão Rocha, and Teresa F. Mendes for technical help; Diogo R. Anjos and Natacha G. Sousa for administrative support; and the Animal and Flow Cytometry facilities of iMM-JLA for technical assistance.

Received September 19, 2018; revised December 12, 2018; accepted January 30, 2019; published first March 20, 2019.

References

1. Wei AH, Tiong IS. Midostaurin, enasidenib, CPX-351, gemtuzumab ozogamicin, and venetoclax bring new hope to AML. Blood 2017;130:2469–74.
2. Tasian S. Acute myeloid leukemia chimeric antigen receptor T-cell immunotherapy: how far up the road have we traveled? Ther Adv Hematol 2018;9:135–48.
3. Di Tullio A, Rouault-Pierre K, Abarrategi A, Mian S, Grey W, Gribben J, et al. The combination of CHK1 inhibitor with G-CSF overrides cytarabine resistance in human acute myeloid leukemia. Nat Commun 2017;8:1679.
4. June C, O'Connor R, Kawalekar O, Ghassemi S, Milone M. CAR T cell immunotherapy for human cancer. Science 2018;359:1361–5.
5. Correia D, Fogli M, Hudspeth K, Gomes Da Silva M, Mavilio D, Silva-Santos B. Differentiation of human peripheral blood Vδ1+ T cells expressing the natural cytotoxicity receptor NKp30 for recognition of lymphoid leukemia cells. Blood 2011;118:992–1001.
6. Almeida AR, Correia DV, Fernandes-Platzgummer A, da Silva CL, da Silva MG, Anjos DR, et al. Delta One T cells for immunotherapy of chronic lymphocytic leukemia: clinical-grade expansion/differentiation and preclinical proof-of-concept. Clin Cancer Res 2016;22:5795–804.
7. Simões A, Di Lorenzo B, Silva-Santos B. Molecular determinants of target cell recognition by human γδ T cells. Front Immunol 2018;9:929.
8. Godder K, Henslee-Downey P, Mehta J, Park B, Chiang K, Abhyankar S, et al. Long term disease-free survival in acute leukemia patients recovering with increased γδ T cells after partially mismatched related donor bone marrow transplantation. Bone Marrow Transplant 2007;39:751–7.
9. Verstichel G, Vermijlen D, Martens L, Goetgeluk G, Brouwer M, Thiault N, et al. The checkpoint for agonist selection precedes conventional selection in human thymus. Sci Immunol 2017;2:pii:eaah4232.
10. Ravens S, Schultze-Florey C, Raha S, Sandrock I, Drenker M, Oberdorfer L, et al. Human γδ T cells are quickly reconstituted after stem-cell

Published OnlineFirst March 20, 2019; DOI: 10.1158/2326-6066.CIR-18-0647

transplantation and show adaptive clonal expansion in response to viral infection. Nat Immunol 2017;18:393–401.
11. Naik SH, Perié L, Swart E, Gerlach C, Van Rooij N, De Boer RJ, et al. Diverse and heritable lineage imprinting of early haematopoietic progenitors. Nature 2013;496:229–32.
12. Nobrega-Pereira S, Caiado F, Carvalho T, Matias I, Graça G, Gonçalves LG, et al. VEGFR2–mediated reprogramming of mitochondrial metabolism regulates the sensitivity of acute myeloid leukemia to chemotherapy. Cancer Res 2018;78:731–41.
13. Davey MS, Willcox CR, Joyce SP, Ladell K, Kasatskaya SA, Mclaren JE, et al. Clonal selection in the human Vδ1 T cell repertoire indicates γδ TCR-dependent adaptive immune surveillance. Nat Commun 2017;8:14760.
14. Mardiros A, Dos Santos C, McDonald T, Brown C, Wang X, Budde L, et al. T cells expressing CD123-specific chimeric antigen receptors exhibit specific cytolytic effector functions and antitumor effects against human acute myeloid leukemia. Blood 2013;122:3138–48.
15. Gill S, Tasian S, Ruella M, Shestova O, Li Y, Porter D, et al. Preclinical targeting of human acute myeloid leukemia and myeloablation using chimeric antigen receptor-modified T cells. Blood 2014;123:2343–54.
16. Petrov J, Wada M, Pinz K, Yan L, Chen K, Shuai X, et al. Compound CAR T-cells as a double-pronged approach for treating acute myeloid leukemia. Leukemia 2018;32:13171326.